



THE UNIVERSITY *of* EDINBURGH

This thesis has been submitted in fulfilment of the requirements for a postgraduate degree (e.g. PhD, MPhil, DClinPsychol) at the University of Edinburgh. Please note the following terms and conditions of use:

This work is protected by copyright and other intellectual property rights, which are retained by the thesis author, unless otherwise stated.

A copy can be downloaded for personal non-commercial research or study, without prior permission or charge.

This thesis cannot be reproduced or quoted extensively from without first obtaining permission in writing from the author.

The content must not be changed in any way or sold commercially in any format or medium without the formal permission of the author.

When referring to this work, full bibliographic details including the author, title, awarding institution and date of the thesis must be given.

**New approaches for the analysis of
dyestuffs in historical textiles by liquid
chromatography and desorption
electrospray ionisation (DESI) mass
spectrometry: applications to Renaissance
embroideries and late nineteenth century
textiles**

Edith Sandström



THE UNIVERSITY
of EDINBURGH

A thesis submitted for the degree of
Doctor of Philosophy

The University of Edinburgh

2022

Declaration

This thesis is submitted in part fulfilment of the requirement for the degree of Doctor of Philosophy at the University of Edinburgh. Unless otherwise stated, the work described in this thesis is original and has not been submitted previously in whole, or in part for any degree or qualification at this, or any other university. In accordance with the dissertation regulations as specified by The University of Edinburgh, this thesis does not exceed 100,000 words in length.

Edith Sandström

December 2022

Major components of Chapter 3 and Chapter 5 have been published in:

E. Sandström, H. Wyld, C. L. Mackay, L. G. Troalen, A. N. Hulme, *Anal. Methods*, 2021, **13**, 4220–4227, <https://doi.org/10.1039/D1AY01151K>.

E. Sandström, C. Vettorazzo, C. L. Mackay, L. G. Troalen, A. N. Hulme, *Anal. Chem.*, 2023, **95**, 4846–4854, <https://doi.org/10.1021/acs.analchem.2c03281>.

Acknowledgements

First of all, I would like to express my gratitude to my supervisors Alison Hulme, Lore Troalen, Helen Wyld and Logan Mackay for all their support over these years. Alison, your constant encouragement and attitude to work and life is inspiring. I am grateful for your steadfast guidance and belief in my abilities. Lore, without your support and knowledge, I would not have learned nearly as much about object analysis or life itself. I hope you know how grateful I am for all your advice and help. Thank you to Helen who opened up a whole new world of appreciation for textiles and textile production. Your helpful attitude and generous sharing of knowledge have contributed to what most likely is a lifelong obsession with lace knitting. Finally, a huge thank you to Logan whose limitless thinking and ideas have taught me to think outside-the-box. Thank you for always having time to discuss problems and making me feel like an engineer.

I thank the AHRC CDP for the funding that has allowed me to undertake this work and gained access to an active network of other interdisciplinary students that understand the particular struggles of working at the interface of science and the humanities. I also thank Chanté St Clair Inglis for allowing me access to the amazing collections at National Museums Scotland, Andrea Cop for help with the financial side and Lynn McLean and Danielle Connolly for helping with sampling and any conservation questions I might have. I am grateful to all the staff at the National Museums Collection Centre for always being so helpful and happy to talk. Similarly, my thanks go to all support staff in the school of chemistry and beyond whose hard work has made everyday life run smoothly.

I would also like to thank the members of the Hulme group, past and present, for being so welcoming, always happy to discuss any issue and letting me steal some consumables. I especially thank Craig Steven, Maria-Eleni Kouridaki, Ander Maguregui Villalobos, Ellen Poot, Manasa Ravindra Punaha, Ektoras Yiannakas, honorary Hulme group member Johanna Rademacher and covid bubble buddies Katie Grant and Alex Martin for all the fun times, both in and out of the lab. These years would not have been nearly as good without you. Thank you for allowing me to force you to celebrate midsommar every year!

I have also had the honour of being the daily supervisor of some wonderful students over the years, so a particular thanks to James Weatherill, Milda Lebedytė and Chiara Vettorazzo. I am certain you will go on to do amazing things and please know that I will claim all the credit for your success.

Lastly, I would like to thank my friends and family, especially my parents Lotta and Åke, for their unwavering support and encouragement. It is a privilege to know that I will always have people to fall back on regardless of circumstance and I would not be who I am without you. I dedicate this work to my sisters, Agnes and Ellen, with whom I face this world.

Abstract

The analysis of historical dyestuffs plays a central role in the understanding of the socioeconomic context of textile production while also informing strategies for the display and preservation of museum objects. Chapter 1 presents a summary of the most important dyes and fibres together with analytical challenges unique to the field of historical dye analysis. The main analytical techniques used in the field, including both invasive and non-invasive as well as destructive and non-destructive techniques are also discussed. Emphasis is given to the need for the development of more reliable, efficient, and ideally minimally or non-invasive analytical approaches for historical dye analysis.

The material and methods used are shown in Chapter 2 while the high-throughput, small-scale sample preparation method and short analytical time UHPLC-PDA method developed are described in Chapter 3. The entire workflow from extraction, filtration, drying and reconstitution strategies as well as the UHPLC-PDA separation were evaluated using nine flavonoid and anthraquinone chromophores. The method was applied to a set of 85 reference samples covering 12 dye sources and a case study of the wedding tartan of Flora MacDonald from the West Highland Museum.

In Chapter 4, the workflow is applied to important examples of Scottish and English embroideries dated from the mid-16th to early 18th centuries housed at National Museums Scotland (NMS). The significance of the collection is contextualised through discussion of embroidery in Tudor and Stuart Scotland and England. The analysis of 26 objects spanning from professional clothing to domestic furnishings show that similar materials was accessible to all types of embroiderers. The range of dyestuffs identified; from locally sourced lichens to imported cochineal demonstrate that embroidery was already by the 16th century, a craft dependent on global trade. The study also showcases the efficiency of the method applied to over 250 samples.

The development of non-invasive, minimally destructive desorption electrospray ionisation (DESI) mass spectrometry for the field of dye analysis is presented in Chapter 5. The design and construction of the source are outlined, alongside optimisation of geometric parameters using silk and wool samples dyed with rhodamine B. The feasibility of the application of DESI-MS to textile analysis was evaluated on natural and early synthetic dye references and successfully applied to the study of late 19th century historical samples.

Lay Abstract

The scientific study of our cultural heritage is an important and challenging field as the need for the analysis of objects needs to be balanced with the need to preserve the objects for future generations. This is especially true for fragile objects such as textiles, which are of particular interest to the dye analysis field. The analysis of dyestuffs in historical textiles gives information on the raw material and manufacturing processes available to the society of production as well as its global trade relations. Identifying and understanding the dyes used in objects are also important from a museum perspective to inform strategies of conservation and display.

In this project, new analytical approaches that reduces the physical impact on the objects have been developed and applied to a collection of Renaissance embroideries from the National Museums Scotland and an early synthetic dye reference book from 1893. The first method developed was a sample preparation workflow requiring up to ten times less sample than conventional methods. This workflow was used to characterise the dyes in a collection of Scottish and English embroideries, showing the global aspect of these domestic objects.

The second method developed required no sample to be removed from the objects and instead relied on direct analysis of the object. The constructed method has previously been used in other analytical fields, but this is the first time it is successfully introduced in dye analysis.

Abbreviations

ACN	Acetonitrile	
APCI	Atmospheric pressure chemical ionisation	
ASAP	Atmospheric-pressure solids analysis probe	
AU	Arbitrary units	
DART	Direct analysis in real time	
DESI	Desorption electrospray ionisation	
DMSO	Dimethyl sulfoxide	
ESI	Electrospray ionisation	
FA	Formic acid	
FORS	Fibre optics reflectance spectroscopy	
FT-ICR	Fourier transform ion cyclotron resonance	
HPLC	High performance liquid chromatography	
LC	Liquid chromatography	
LoD	Limit of detection	
LoQ	Limit of quantification MS	Mass spectrometry
MeOH	Methanol	
MODHT	Monitoring of Damage in Historic Tapestries	
NMS	National Museums Scotland	
OA	Oxalic acid	
PDA	Photo diode array	
SERS	Surface-enhanced Raman spectroscopy	
UHPLC	Ultra-high performance liquid chromatography	

Table of Contents

Declaration	II
Acknowledgements	III
Abstract	V
Lay Abstract	VI
Abbreviations	VII
Chapter 1 Introduction	1
1.1 Historical dye analysis	1
1.2 Material considered in this work	2
1.2.1 Textile culture in Renaissance Scotland and England.....	2
1.2.2 The synthetic dye revolution	2
1.3 The process of textile dyeing	3
1.3.1 Proteinaceous substrates	4
1.3.2 Cellulosic substrates	7
1.4 Common natural dyestuffs.....	8
1.4.1 Direct dyes.....	8
1.4.2 Mordant dyes	11
1.4.2.1 Flavonoids.....	12
1.4.2.2 Anthraquinones	13
1.4.2.3 Homoisoflavonoids	16
1.4.2.4 Tannins	17
1.4.3 Vat dyes	18
1.5 Early synthetic dyes	20
1.5.1 Azo dyes.....	20
1.5.2 Di- and triphenylmethane dyes	21
1.5.3 Nitro, xanthene and thiazine dyes.....	21
1.6 Common analytical challenges in historical dye analysis	22
1.6.1 Complex dye mixtures	22
1.6.2 Photodegradation	23
1.7 Analytical approaches for historical dye analysis	24
1.7.1 Non-invasive techniques.....	24
1.7.2 Invasive techniques	25
1.8 Knowledge gaps and project aims	26
1.9 References.....	26
Chapter 2 Materials and Methods	35
2.1 Instrumentation.....	35

2.1.1 Sample preparation workflow	35
2.1.2 Liquid chromatography	35
2.1.3 Mass spectrometry	35
2.1.4 Software	36
2.2 Materials.....	36
2.2.1 Sample preparation workflow.....	36
2.2.2 Standard mixture 1	37
2.2.3 Natural dye references.....	37
2.2.4 Synthetic dye references	38
2.2.5 Historical samples.....	38
2.3 Methods	38
2.3.1 Extraction.....	38
2.3.2 Filtration.....	39
2.3.3 Drying and reconstitution	39
2.3.4 UHPLC-PDA method	39
2.3.5 Gradient optimisation.....	39
2.3.6 Chromatographic peak integration	40
2.3.7 Calibration curves	40
2.3.8 Limit of detection and limit of quantification.....	40
2.3.9 Dyeing of lichen references	40
2.3.10 Parameter optimisation of DESI method on rhodamine B ink.....	41
2.3.11 Parameter optimisation of DESI method on rhodamine dyed silk and wool cloth	42
2.3.12 Parameter optimisation of DESI method on natural dyestuffs	43
2.3.13 Dyeing of early synthetic dye references.....	43
2.3.14 Application of DESI method to reference and historical samples	43
Chapter 3 Small-scale sample preparation workflow and UHPLC method development	45
3.1 Aims	45
3.2 Introduction	45
3.2.1 Current sample preparation methods for UHPLC dye analysis	46
3.2.2 Overview of the sample preparation method developed for UHPLC dye analysis	47
3.3 Extraction step.....	48
3.3.1 Extraction step optimisation	50
3.4 Filtration step.....	57
3.4.1 Filtration step optimisation	58

3.4.2 Filtration step evaluation	60
3.5 Drying and reconstitution step	62
3.6 Liquid chromatography	64
3.6.1 Retention	65
3.6.2 Selectivity	66
3.6.3 Efficiency	66
3.6.4 HPLC vs UHPLC	67
3.7 UHPLC method development	68
3.8 UHPLC method evaluation	70
3.8.1 Repeatability and resolution factors	70
3.8.2 Linearity and calibration curves	72
3.8.3 Limit of detection and limit of qualification	73
3.9 Application of workflow	74
3.9.1 Application to natural dye references	74
3.9.2 Flora MacDonald wedding tartan	77
3.10 Conclusion	80
3.11 References	82
Chapter 4 Dye analysis of a 16th and 17th centuries embroidery collection at National Museums Scotland	85
4.1 Aims	85
4.2 Introduction	85
4.3 The collection at National Museums Scotland (NMS)	87
4.4 Embroidered clothing	88
4.4.1 Blackwork	88
4.4.2 Stomachers	89
4.4.3 Coifs	91
4.4.4 Inspired by Nature	92
4.5 Embroidered furnishings	92
4.5.1 Larger furnishings	93
4.5.2 Biblical imagery	95
4.5.3 Pictures and book covers	97
4.6 Sampling strategy	101
4.7 UHPLC-PDA analysis of the NMS embroidery collection	103
4.8 Yellow and green	104
4.8.1 Weld (<i>Reseda luteola</i> L.)	104
4.9 Black and brown	108

4.9.1 Tannins (mainly <i>Quercus infectoria</i> L. and <i>Rhus</i> spp.).....	108
4.9.2 Young fustic (<i>Cotinus coggygria</i> Scop) and old fustic (<i>Maclura tinctoria</i> L.)	110
4.10 Blue, grey and purple	113
4.10.1 Indigo (<i>Indigofera</i> spp.) and woad (<i>Isatic tinctoria</i> L.).....	115
4.10.2 Saxon blue.....	115
4.10.3 Lichen purple	117
4.11 Red, orange and pink	118
4.11.1 Madder (<i>Rubiaceae</i> spp.)	118
4.11.2 Soluble redwood (<i>Caesalpinia</i> spp.).....	123
4.11.3 Cochineal (<i>Coccoidea</i> superfamily).....	125
4.11.4 Safflower (<i>Carthamus tinctorius</i> L.).....	129
4.12 The global dye trade and the NMS collection	132
4.13 Conclusion	133
4.14 References.....	135
Chapter 5 Construction and application of a desorption electrospray ionisation (DESI) source for historical dye analysis	140
5.1 Aims	140
5.2 Introduction	140
5.3 Ambient mass spectrometry	141
5.3.1 Direct analysis in real time mass spectrometry (DART-MS).....	142
5.3.2 Atmospheric-pressure solids analysis probe mass spectrometry (ASAP- MS).....	143
5.4 Desorption electrospray ionisation (DESI)	144
5.4.1 Desorption and ionisation mechanisms.....	144
5.4.2 DESI source geometry.....	147
5.4.3 Fourier Transform Ion Cyclotron Resonance (FT-ICR).....	148
5.5 Design and construction of DESI source	149
5.5.1 xy stage	150
5.5.2 Sprayer holder set-up and mass spectrometer inlet.....	151
5.6 Optimisation of DESI source.....	155
5.6.1 Initial qualitative geometry parameter trials on rhodamine B ink on glass	155
5.6.2 Parameter optimisation on silk and wool samples dyed with rhodamine B	157
5.6.3 Sprayer solvent system.....	160
5.6.4 Sprayer angle	163

5.6.5 Background contaminants	167
5.7 DESI-MS analysis of natural dyes	168
5.7.1 Plant material.....	168
5.7.2 Dyed references	170
5.8 DESI-MS analysis of early synthetic dyes.....	172
5.9 Application of DESI-MS analysis to historical dye samples.....	178
5.9.1 Lehne’s handbook (1893)	178
5.9.2 DESI-MS-MS investigation of historical triphenylmethane dyes	182
5.10 Conclusion	185
5.11 References.....	186
Chapter 6 Summary and Future Work.....	190
Appendices.....	194
A1 Sample preparation workflow and UHPLC-PDA method specifications.....	194
A2 Sampled objects and sample locations	198
A3 Collected samples and identified dye sources.....	209
A4 DESI-MS solvent spot and shape of tested solvent systems.....	263
A5 DESI-MS spectra of early synthetic and historical dyes.....	264

Chapter 1 Introduction

1.1 Historical dye analysis

Historical dye analysis is the scientific field under the wider umbrella of heritage science which is concerned with the characterisation and understanding of colourants found in cultural objects. An increased knowledge of the dyestuffs used in objects not only gives an indication of the regional access to trade relations, manufacturing processes and technological advancements, it can also help to suggest a date of production or the presence of a forgery. Another important aspect of historical dye analysis is to provide scientific information to support strategies and policies for long-term preservation of collections, including conservation, display and object rotation approaches.¹⁻⁴

Before the mid-19th century, dyes were obtained from a large variety of sources from the plant and animal kingdom, including roots, berries, flowers, bark, leaves, heartwood, lichens, mushrooms, shellfish, and insects. The range of dye sources results in dye molecules showing a wide range of chemical structures and application practices.²⁻⁶ The material which was dyed could also vary, from the common textile fibres such as silk, wool, linen, and cotton, to more uncommon material such as leather,⁷ barkcloth⁸⁻¹⁰ and porcupine quills.¹¹ Many dyes could also be transformed to pigments and used in easel and mural paintings.¹²⁻¹⁴

The complexity of the dye molecules, application processes and substrates used in textile dyeing results in the need for a variety of analytical techniques to be employed.^{15,16} The techniques can be invasive, such as liquid chromatography (LC) and mass spectrometry (MS), which require a sample to be physically removed from the object. Non-invasive methods, such as fibre optics reflectance spectroscopy (FORS) or Raman spectroscopy, has no physical impact on the object but cannot obtain the same level of information as invasive techniques.¹⁷ The analytical techniques used may also be destructive or non-destructive, resulting in the sample being consumed during analysis or not. The choice of analytical approach in the analysis of heritage objects thus requires careful consideration and relies on the continuous development of less invasive methods that can still produce comprehensive data.

The main aim of this work was to develop such minimally to non-invasive methods for dye analysis with focus on LC and MS approaches. Emphasis was put on the need for more reproducible datasets and ambient analytical techniques in dye analysis. The secondary aim was to apply these methods to a collection of Renaissance embroideries and a 19th century dye reference book to investigate the limitations of the developed techniques and explore what dye analysis can add to the understanding of these objects.

1.2 Material considered in this work

1.2.1 Textile culture in Renaissance Scotland and England

Textiles played an important role in 16th and 17th centuries Scotland and England.¹⁸ Beyond their basic function as clothes providing warmth to all social classes, they were also used to display the wealth and power of the nobility as garments, embroideries, and tapestries.^{19–21} The textile industry has always been one of the main drivers for global trade relations²² and its importance in Renaissance Scotland and England can be seen in the emergence of the wool industry during the 17th century as arguably the first capitalistic industry in the Western world.¹⁸

European expansion during the colonial age resulted in increased economic prosperity of European countries and a great influx of goods and designs to Europe. This led to many families gaining the time and resources to keep women at home instead of having them work for wages. Domestic textile production, in particular decorative textile production such as embroidery, knitting and lace making, have often been the responsibility of women; thus, the study of textiles is an important avenue for examining history from a female perspective.²³

An embroidery collection from the National Museums Scotland (NMS) spanning from mid-16th to early 18th centuries was studied in this project. The collection contains a variety of materials, designs, and objects, including both domestic and professional productions of clothing and furnishings pieces. The study of such a diverse collection contributes to a better understanding of Scottish and English embroidery production and global trade relations during the Renaissance.

1.2.2 The synthetic dye revolution

In 1856, the young student William H. Perkin experimented in his home laboratory trying to make quinine and accidentally discovered mauveine – the first synthetic

dye.²⁴ 'Semi-synthetic' dyes such as picric acid (1771) and Saxon blue (1743) were used to some extent in the textile industry before this great discovery, but natural dyes dominated.²⁵

The industrial revolution resulted in the production of coal-tar derivatives in need of purposes.²⁶ The timely discovery of a synthetic route to mauveine based on such a derivative, aniline, inspired a surge of organic chemistry research with focus on dye synthesis. The number of synthetic dyes invented exploded during the latter half of the 19th century and almost 1000 synthetic dyestuffs were commercially available by the turn of the 20th century.²⁷ The synthetic dye revolution affected all aspects of modern life, from fashion²⁸ to the boom in chemical industry and the advancement of chemical theory.²⁶ Thus, the study of early synthetic dyes reflects an increasingly transitional period in history.

In this study, a book from 1893 attempting to summarise the most important commercially available dyestuffs was analysed. The book is written by Adolf Lehne, a prominent German dye chemist active in various official and academic roles related to the synthetic dye field from 1880 to 1925.²⁹ Lehne collected 324 dyestuffs divided by chemical structure into 16 dye families. The book includes commercial names, dyeing details and one or more dyed sample(s) of each dyestuff presented. It therefore provides authentic, naturally degraded reference samples of early synthetic dyes, making it an important source for understanding original synthetic routes and degradation pathways.

1.3 The process of textile dyeing

Textile dyeing is an ancient art found in all cultures in history. The earliest archaeological evidence of coloured fibres are 30,000-year-old flax fibres found at Zudana Cave, Georgia³⁰ showing that textile dyeing is likely to be as old as textile production itself. Dyeing includes complicated chemical processes dependent on the dye source and substrate used which were well-established long before chemistry emerged as a scientific field in the 19th century.^{3,4} Many of the technical processes that were intuitively and empirically determined throughout history have been found to correspond closely to the differences in the chemical composition of the dye sources.^{3,4}

The textile production process includes, in its most basic form, fibre collection, spinning of the yarns and weaving of the cloth.³¹ The fibres can be dyed before the

yarns are spun or after the cloth is woven, but commonly the spun hanks of yarn are dyed before weaving the cloth. The most common fibres dyed in Europe throughout history were silk and wool, which both are proteinaceous fibres of animal origin. Cellulosic fibres, such as linen and cotton, were not as efficiently dyed until technological advancements and the introduction of synthetic dyes in the 19th century.³

There are traditionally three types of dyeing techniques which depends on the dyestuff and colour desired: direct dyeing, mordant dyeing and vat dyeing.^{3,6} Direct dyeing is the simplest dyeing technique, and it merely involves soaking or boiling the dye plant in water before the fibres are immersed in the resulting dyebath. The presence of polar groups in direct dyes encourages intermolecular forces between the dye molecule and the substrate.

Fairly few natural dye sources are direct dyes and instead most require the addition of a metal salt, known as a mordant, to fix the dyestuff to the fibre. The textile can be mordanted in a separate bath before dyeing or the mordant can be added to the same dyebath as the dyestuff or applied as an after-treatment. The addition of the mordant complex with the dye molecule and substrate, resulting in a stronger chemical interaction compared to direct dyes and increasing the lightfastness of the colour.³

The last dyeing technique, known as vat dyeing, is particular to indigoid-containing dyestuffs such as indigo and shellfish purple. The chromophores in these dyes are insoluble in their coloured form and therefore need to undergo reduction in an alkaline bath to dissolve and impregnate the fibres. They are then oxidised in the air into their insoluble, coloured form when adsorbed on the fibres, dyeing the cloth. Vat dyes do not form any covalent bonds with the fibres so abrasion of the dye might occur.³²

1.3.1 Proteinaceous substrates

Wool and silk were the main fibres for textiles in Western Europe until the slave plantations in North America and the industrial revolution reduced the price and increased the supply of cotton during the 19th century. Wool production was a widespread domestic industry in most of Western Europe, and one of the most important exports of Renaissance England. It has been estimated that by the end of the 17th century, a third of English exports was woollen goods.¹⁸

Wool was appreciated for its warmth and was cheap in comparison to other textiles due to its coarser feel and domestic production which made it available to all social

classes.³³ In contrast, silk was considered a luxury item due to its lustre, softness, and affinity for dyes and because it had to be imported to England and Scotland. Silk was initially imported from China, where its production had been known since the 3rd millennium BC. After the Byzantine empire successfully managed to smuggle live silkworm eggs out of China in 552 AD, silk could be imported from closer regions.³⁴ During the Renaissance, the Italian city states had become the major silk producing centres of Europe.³⁵

Wool is a natural fibre that consists of mainly two types of cells, the cortical and the cuticle cells. The cuticle cells form scales surrounding the cortical cells. Wool consists of approximately 97 % keratinous material which is characterised by a relatively high percentage of sulfur-containing amino acid residues. Keratin proteins form α -helices as secondary structures and these are wound around each other forming fibrils that are combined into fibres (Fig 1.1).³⁶ Keratins possess high mechanical strength due to the large number of disulfide bridges created. Higher percentage of sulfur-containing amino acids (cysteine or methionine) in the polypeptide sequence therefore results in higher stiffness of the final fibre (e.g nails – high sulfur). The variation in sulfur content is dependent on multiple parameters including breed of sheep, diet and climate.^{37,38}

changes in environment, acidity, and basicity.³¹ It is also prone to degrade by photo-oxidation or enzymatic attack. It is receptive to most dyes and as such, it is widely used in embroidery, both as the ground and the threads.^{40,41}

Both wool and silk are dyed by electrostatical interactions of the amino and carboxyl groups on the amino acid and similar groups on the dye or mordant molecule. $\pi - \pi$ interactions between the aromatic amino acids (phenylalanine, tyrosine, tryptophan) and the often polyphenolic dye/mordant molecules have also been suggested to contribute to the strength of the fibre-dye/mordant system.⁴² The strength of these interactions is dependent on multiple variables, including number of sulfonate groups and polarity of the dye molecule/mordant.

1.3.2 Cellulosic substrates

Cotton and linen are the main plant sources of fibre substrates. Cotton, both natural and synthetic, is the main fibre used in the modern world. Before the slave trade facilitated cheap cotton from the Americas, it was imported from India. Before the 19th century, most cotton and linen cloth were bleached but undyed and usually worn as undergarments.²² Both are based on cellulose, which is a linear polymer of β -D-glucopyranose with 1,4- glycosidic bonds (Fig 1.3).^{41,42}

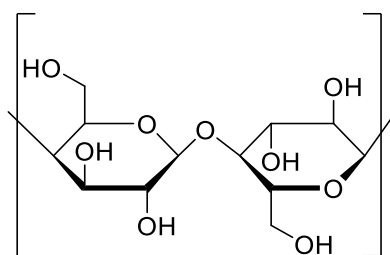


Figure 1.3: Monomer of cellulose (β -D-glucopyranose with 1,4- glycosidic bonds).

The flat, tightly packed crystalline structure of cellulosic fibres results in the electrostatic and $\pi - \pi$ interactions most natural dyes rely on for fibre-dye/mordant system formation is less efficient. The lower affinity of natural dyes to cellulose fibres compared to proteinaceous ones, were likely the reason for the low quantity of cellulose cloth dyed historically. However, modern synthetic dyes show great lightfastness on cellulosic cloth.⁴²

1.4 Common natural dyestuffs

1.4.1 Direct dyes

Direct dyes contain polar functional groups oriented so they can favourably interact with polar groups on the fibre, meaning that they can be applied directly onto the textile without any fixing agents.^{3,5} Their solubility and weak chemical interactions between dye molecule and fibre, mean that direct dyes often have a poor lightfastness, but they were still used during the Renaissance. Safflower, and orchil are examples of direct dyes that are known to have been used historically in Europe.^{3,4,43}

Orchil dyes are obtained from lichens and can give purple, yellow, and brown colours depending on the lichen species and dyeing process.⁶ Important lichen species for purple orchil dyes are *Rocella tinctoria* D.C., *Rocella fuciformis* D.C., *Pertusaria dealbescens* Erichs., and *Orchrolechia tartarea* L. The latter was the main lichen used for the production of cudbear, an important Scottish purple dyestuff that was manufactured on an industrial scale 1758 – 1851. The common species used for yellow and brown colours, also known as crotal dyes, are *Parmelia saxatilis* L. and *Parmelia omphalodes* L.⁴³

Lichen purples were used as an alternative to more expensive dye sources such as shellfish purple. The low lightfastness of the dyestuff made it cheap, and its use was prohibited in some cloth-producing centres. The use of lichen purple in objects therefore reflect lower-quality textile production.^{4,43,44}

The production of purple lichen dye is complex by comparison to the production of crotal dyes, as lichens do not naturally contain the purple phenoxazone chromophores, known as orceins **(1)**.^{3,6,43,45} Instead, a chemical pre-treatment of the depside **(2)** and depsidone **(3)** components naturally present in lichens is required. The molecules **(2)** and **(3)** are hydrolysed to orsellic acid **(4)** during fermentation in an alkaline solution, traditionally urine. Compound **(4)** then undergo decarboxylation to form orsinol **(5)** which gives various orcein **(1)** derivatives after a sequence of condensation reactions (Fig 1.4). The orcein derivatives are closely related and give similar UV-vis spectra so MS methods are required for confident assignment.^{46–48}

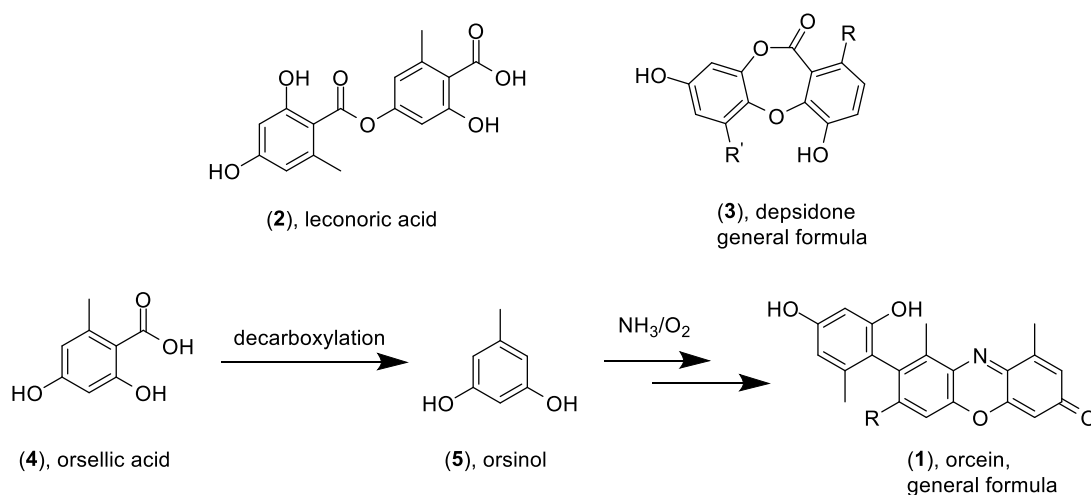


Figure 1.4: Molecular structures of intermediates in the production of purple lichen chromophores, orceins (1).

Brown and yellow crotaI dyes are more lightfast in comparison to the purple lichen dyes and are obtained by simply boiling the lichen in water (alternatively stale urine) for several hours before the cloth is added. The colour is said to come from the depside atranorin (6) and the depsidones salazinic (7) and lobaric (8) acid (Fig 1.5).⁴³

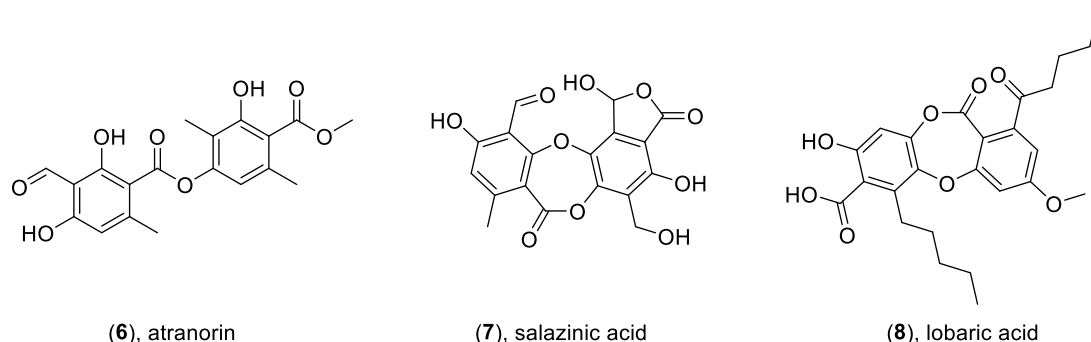


Figure 1.5: Molecular structures of chromophores of crotaI lichen dyes.

Safflower is another direct dye that requires chemical pre-treatment before application to fibres. The safflower petals contain both water-soluble yellow and red chromophores that require an alkaline bath for extraction. Dyeing with safflower red must therefore be preceded by multiple washings to remove the yellow dye.⁴⁹

The washing step was labour intensive and according to a dye treatise from 1763, it normally it took a man two days to thoroughly wash 30 kg of flowers.³ Safflower red was more common in Asian^{50–52} and Coptic⁵³ textiles than European, although it has been characterised in a few European objects as well.^{11,54,55} The use of safflower yellow as a dye was rare, and has not yet been found on European textiles and only

one document from China has reportedly mentioned the use of safflower as a source of yellow.⁵⁶

The main chromophore in safflower red, carthamin (**9**) (Fig 1.6), is insoluble in water at neutral pH so the washing step is followed by turning the dyebath alkaline. The fibres are introduced into the dyebath and the solution is then acidified to complete the dyeing process.^{3,4}

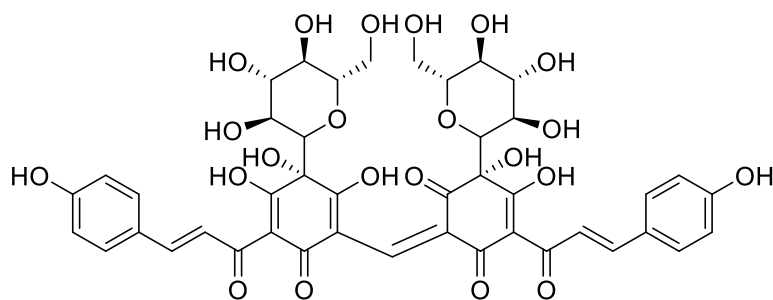
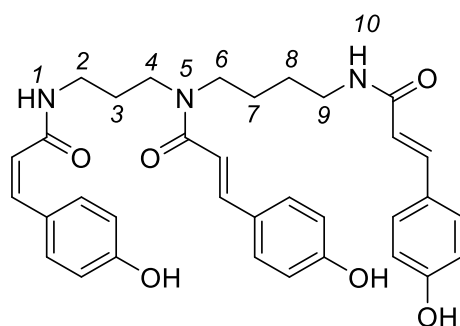


Figure 1.6: Molecular structure of carthamin (**9**).

Safflower red gives an attractive soft pink colour with low lightfastness, and carthamin is often degraded in textiles dyed with safflower red. Markers assigned Ct1-4 (**10 - 13**) (Fig 1.7) are instead commonly used to identify the presence of safflower red, as these have been shown to be resistant to both photodegradation as well as acid hydrolysis extraction.^{49,57} The molecular structure of these four and an additional two related markers (Ct5 (**14**), Ct6 (**15**)) for safflower red have recently been proposed by Lech *et al* (Fig 1.7).⁵⁸

Safflower has been cultivated across Anatolia, Egypt, Southeast Asia, and Europe and it has been found in Asian and European textiles despite its low lightfastness. Safflower red is more commonly found in Asian textiles, however, it has been identified in English tapestries and embroideries from the Renaissance^{59,60} suggesting its use in Renaissance Europe on a small scale. It is a dye tied to tradition as it is the traditional red to dye the Japanese flag and it was the dye still used for the red tape tying British government documents together up until the 20th century.^{3,58}



- (10) ZZZ isomer ($N^1 = Z, N^5 = Z, N^{10} = Z$)
 (11) - (14) Mixture of ZZE, ZEZ, EZZ, ZEE, EZE, EEZ isomers
 (15) EEE isomer ($N^1 = E, N^5 = E, N^{10} = E$)

Figure 1.7: Proposed molecular structures of the isomeric ct1-ct4 markers for safflower red.⁵⁸

1.4.2 Mordant dyes

In comparison to direct dyes, mordant dyes generally are more lightfast due to the complex formed between the metal ion, dye molecule and fibre (Fig 1.8).^{3,4} The choice of mordant and application method influence the final hue, with Fe salts (often FeSO_4) saddening colours, Cu salts (often CuSO_4) tinting green or yellow blue and Cr salts (often $\text{K}_2\text{Cr}_2\text{O}_7$) heightening orange and brown colours.^{3,43}

The use of Al salts (often alum: $\text{KAl}(\text{SO}_4)_2 \cdot 12\text{H}_2\text{O}$) results in no major colour change and were often the main mordant used.³ Alum can be extracted from alum shales and Scotland had to import alum mainly from England and the Low Countries before alum shale mining started in the 1800s. There is also a clubmoss (*Lycopodium complanatum* L.) native to Scotland and Scandinavia that naturally accumulates aluminium and was thus used as a mordant in this region. All flavonoid, anthraquinone and neoflavonoid dyes are mordant dyes.^{6,43}

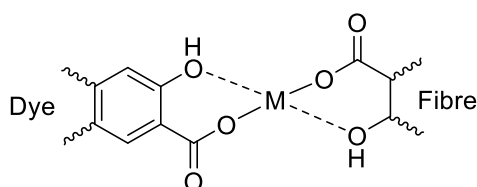


Figure 1.8: Generic schematic of dye-metal-fibre complex.

1.4.2.1 Flavonoids

Most yellow dyes are derivatives of flavonoids. This group can be further divided into structural sub-groups, mainly flavones (**16**), flavonols (**17**) or isoflavones (**18**) (Fig 1.8). In contrast to indigoids and anthraquinones, which have specific geographical sources and have been trade commodities since antiquity, flavonoid compounds are present mainly as glycosides in many plants throughout the world. Flavonoid dyes were therefore often locally produced, and identification of the dyestuff can give valuable information about potential object provenance.^{61–63} Recently, strategies using the glycoside : aglycone ratio of samples has been used for species identification, which requires the preservation of the glycosidic flavonoid form. Such investigations thus require less acidic conditions of extraction during sample.⁶⁴

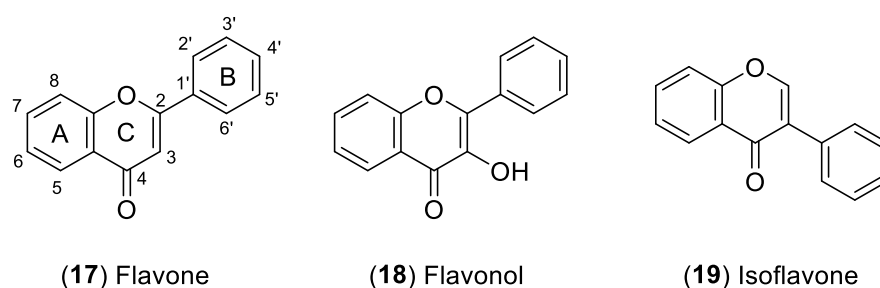


Figure 1.9: General molecular structure of flavones (**16**), flavonols (**17**) and isoflavone (**18**).

Common flavonoid dye sources in Renaissance Europe were weld (*Reseda luteola* L.), dyer's green weed (*Genista tinctoria* L.), and young fustic (*Rhus cotinus* L.).^{60,61,65} After the Spanish colonisation of South America, importation of old fustic (*Maclura tinctoria* L.) containing flavonols became increasingly popular.³

Weld mainly contains the flavones luteolin, apigenin and the *O*-methylated compound chrysoeriol and is fairly easy to cultivate even in cold climates.^{6,66} It gives a bright yellow colour with relatively good lightfastness, which probably explains the long popularity of the dye source in Europe.^{3,43} There is evidence for weld being used on the continent since pre-historic times and it continued to be one of the main sources of yellow in Europe until the introduction of synthetic dyes in mid-19th century.⁶³ Due to the ease of cultivation of weld across Europe, much weld was sourced domestically and large areas in every country was designated to its farming.^{3,4}

Dyer's greenweed was also a domestic source of yellow and the main chromophore is genistein, an isoflavone.⁶¹ It was regarded as a lower quality dye compared to weld

but its use in tapestries is well-documented.^{11,61,65} It was often used to dye cloth green in combination with a blue dye source.^{3,4}

Young fustic is obtained from the heartwood or inner bark of *Cotinus coggygria* Scop. (also known as *Rhus cotinus* L.) and it has been used for textile dyeing in Europe since antiquity. Textiles dyed with young fustic has been found to contain the main chromophores fisetin (**7**) and sulfuretin (**8**) and other flavonoids such as myricetin and quercetin.^{3,4,65} Valianou *et al.*⁶⁷ identified 11 compounds as well as ellagic acid in the dye source of young fustic.

Both old and young fustic give a more orange colour and are less lightfast than other yellow sources such as weld.⁴ The poorer quality of the dyestuff and the large quantity of colorant obtained from each harvested tree meant that old and young fustic were a less expensive alternative to other yellows and was often used when the purity of yellow was not important.³ Its poor lightfastness resulted in it often being banned to be used in high-quality textiles.⁴ Consequently, it was often used to dye the fibre core of gilt metal thread and in combination with other dyestuffs as the yellow source for colours such as brown and orange.^{3,11,65}

The phenolic moieties and carbonyl group of flavonoid compounds makes flavonoid-based dyes one of the more fugitive ones.^{3,65} Flavones (**16**) shows greater lightfastness compared to flavonols (**17**) and stronger colour than isoflavones (**18**). This has been related to the proximity of the -OH group and carbonyl on the C-ring for flavonols.⁶⁸⁻⁷⁰

1.4.2.2 Anthraquinones

Anthraquinone derivatives (Fig. 1.9) are abundant in nature and can be found in both plants and insects. The anthraquinone structure is stable against photooxidative fading and can give all shades of reds, from vibrant crimson to softer oranges and pinks, depending on their source, processing method and mordant. Common sources for anthraquinone dyes are the roots of different Rubiaceae species and coccid insect species.³

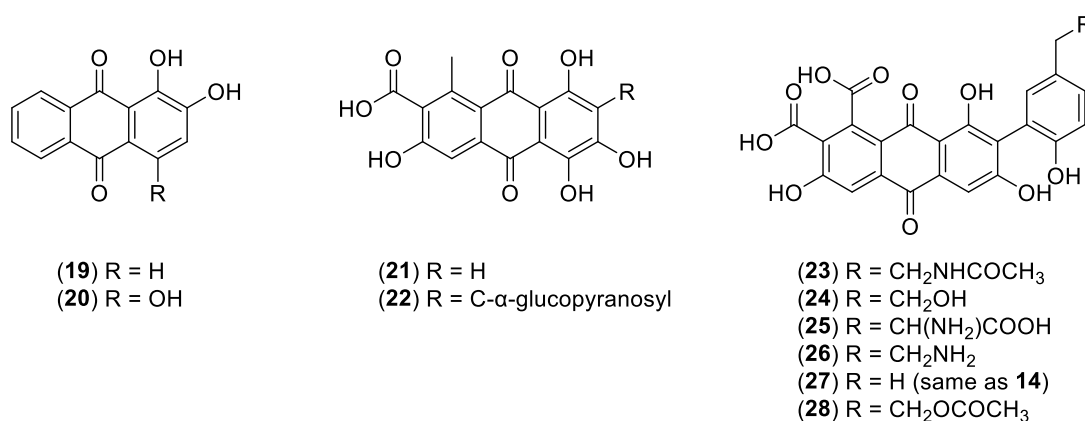


Figure 1.10: Anthraquinone molecular structures of common dyestuffs.

The main species of the Rubiaceae family historically used as a dye source in Europe was madder, (*Rubia tinctorum* L.). Other species such as munjeet (*Rubia cordifolia* L.) and *Rubia akane* were also used, but they were more common in Asian textiles.⁷¹ Munjeet was prominently used in India and *Rubia akane* was typically used in Japan.^{3,72} *Rubia* is one of three main genera of Rubiaceae plants used for dyeing red, the others being *Galium* and *Morinda*.⁴

All Rubiaceae plants contain multiple anthraquinone molecules and their glycosidic counterparts, which vary depending on the species, age and environment of the plant used as well as the preparation of the roots and dye bath conditions.^{3,4,71,73–76} Additionally, the analytical protocol followed (Section 3.3) also affects the anthraquinone content observed.^{74,77,78} The effect of these variables is difficult to predict which makes it complicated to determine the species used.

Ruberythric acid (**19**) and lucidin primeveroside (**20**) have been reported in high concentrations in cultivated madder (*Rubia tinctorum* L.) roots,^{76,79–82} but is not present to the same extent in textile samples dyed with *Rubia tinctorum* L.^{74,77,78} Deglycosylation of ruberythric acid (**19**) into alizarin (**24**) and lucidin primeveroside (**20**) into lucidin have been shown to occur enzymatically when the roots are macerated in warm water or boiled before dyeing.^{74,75,83} A strongly acidic extraction method⁸⁴ will also result in deglycosylation as well as induce the decarboxylation of various other anthraquinones present in *Rubia tinctorum* L. including munjistin (**21**) and pseudopurpurin (**23**).^{74,77,78}

Thus, the most abundant chromophores in textiles samples dyed with *Rubia tinctorum* L. are not the glycosidic compounds present in the plant but alizarin (**24**) and purpurin (**25**).^{3,71,73,74} Munjistin (**21**), xanthopurpurin (**22**), pseudopurpurin (**23**) and

nordamnacanthal have also been reported.^{74,77,78} Lucidin is often not identified^{73,74} as it has been suggested to be oxidised to nordamnacanthal *in planta*.^{75,79} Textile samples dyed with wild madder (*Rubia peregrina* L.) and lady's bedstraw (*Galium verum* L.) have shown low to no presence of alizarin^{74,77,84} but high purpurin, munjistin, pseudopurpurin and rubiadin. Japanese madder (*Rubia akane* L.) has shown to contain the marker 6-hydroxyrubiadin,^{74,77,84} making it possible to differentiate these species uses from the use of *Rubia tinctorum* L.⁷⁴

Insect red dyes were one of the most valued dyestuffs due to the labour-intensive cultivation and processing and the lightfast crimson colours obtained. Insects from the Coccoidea superfamily were used to obtain three insect red dyes: kermes from *Kermes vermilio* P., lac dye from *Kerria lacca* Kerr and cochineal from three insect species: *Dactylopius coccus* C., *Porphyrophora polonica* L., and *Porphyrophora hamelii* Brandt.⁸⁵ The main chromophore in kermes dye is kermesic acid (**21**) and cochineal dye contains carminic acid (**22**). Laccaic acid A – F (**23** - **28**) are the main chromophores present in lac dyes (Fig 1.9).

Kermes, lac, and cochineal from *Porphyrophora polonica* L. (Polish cochineal) and *Porphyrophora hamelii* Brandt (Armenian cochineal) were used in Europe and Asia from pre-historic times.^{3,85} The Spanish conquest of South America introduced Mexican cochineal (*Dactylopius coccus* L) to the European market in 1521²² which soon became the main source of insect red. Mexican cochineal contains a higher concentration of carminic acid (**22**) compared to Polish and Armenian cochineal, resulting in stronger colours and less dyestuff required per mass of fibre.

The popularity and cost of Mexican cochineal dye made the dyestuff one of the most important exports for Spain.^{22,86} The cultural importance of insect red dye as a luxury good can be understood by its frequent use by monarchs and nobility as well as the strict and successful Spanish monopoly on Mexican cochineal to the aggravation of other European countries. The brilliant red colours and the laborious production process added to the cost and appreciation of this dye source.^{3,4,22,86}

Cochineal can be produced from three types of insects, *Porphyrophora hamelii* Brandt (Armenian cochineal), *Porphyrophora polonica* L. (Polish cochineal) and *Dactylopius coccus* C. (Mexican or American cochineal).^{3,87,88} Mexican cochineal was introduced to the European market by the Spanish in 1521 and due to its higher dye content, it soon became the main source for cochineal red and the most profitable export for Spain after silver.^{22,86}

Cochineal dye contain a complex mixture of anthraquinones with the main chromophore obtained from all three insects being carminic acid (**32**).^{3,4,85,89} Many minor chromophores are also present,⁹⁰ with the main ones being dcII (**31**), dcIV (**33**), dcVII (**34**), kermesic (**35**) and flavokermesic (**36**) acid^{3,4,85,91,92} (Table 4.9). Wouters and Verhecken proposed an approach based on the dcII (**31**) and flavokermesic + kermesic acid (**35 + 36**) content to distinguish between the species.⁹¹ The reliability of this approach has been questioned however,⁸⁸ mainly due to the natural variability of the marker compounds depending on the developmental stage of the insect as well as the frequent co-elution of dcII with carminic acid and the effect of strong acid extraction. Instead, multivariate approaches, such as principal component analysis (PCA)⁸⁸ and partial-least squares discriminant analysis (PLS-DA),⁹³ has been shown to be a more reliable alternative for species identification.

1.4.2.3 Homoisoflavonoids

Soluble redwood dye sources, also referred to as brazilwoods, contain homoisoflavonoids which can be extracted from the heartwood by soaking in water. Multiple *Caesalpinia* species have been used as a source of the dye chromophores, with the main one being *Caesalpinia sappan* L. Currently there are no analytical methods to distinguish between redwood species. The naturally occurring homoisoflavonoid in redwoods is brazilin (**29**), which needs to be oxidised to produce the main chromophore brazilein (**30**) (Fig 1.10).^{3,4,6}

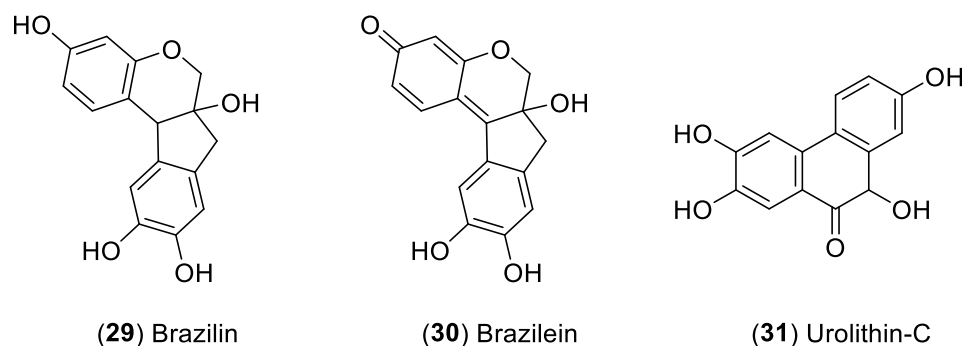


Figure 1.11: molecular structures of brazilin (**29**), brazilein (**30**) and urolithin-C (**31**).

Despite the poor lightfastness in comparison to madder and cochineal, the popularity of soluble redwoods can be explained by the quantity of dyestuff per mass of wood, the ease of transportation and the attractive pinkish reds that can be achieved using the dyestuff. The affordability of soluble redwood dyes resulted in it being used

extensively as a red source for orange and brown colours, but it was also used on its own.^{3,65,94}

Redwood was imported to Europe from eastern Asia until the colonisation of the Americas which led to a large influx of the dye source from South America. The country Brazil was even named after the dyestuff brazilwood, which shows the importance of the dyestuff trade historically, as well as the excess of soluble redwoods that was found in South America.³

The fast degradation of brazilin and brazilin in textile samples makes it necessary to use a marker for the identification of a redwood dyes source (Fig 1.10). The marker is unique to soluble redwoods, although not species specific. It was recently identified as urolithin-C.⁹⁴

1.4.2.4 Tannins

Tannins are polymeric polyphenolic compounds widely distributed in the plant kingdom.^{3,4} They can be classified as either hydrolysable (gallotannins and ellagitannins) or condensed tannins, also known as proanthocyanidins (flavan-3-ol oligomers and polymers, also known as catechin or epicatechin polymers). Hydrolysable tannins are usually found in large polymeric networks connected through ester bonds with monosaccharides.

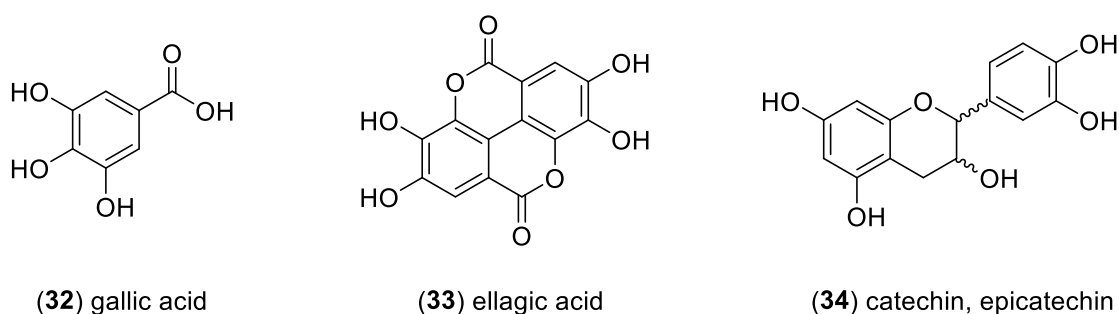


Figure 1.12: Molecular structures of gallic acid monomer (32), ellagic acid monomer (33) and catechin, epicatechin monomer (34).

Common sources of tannins are oak galls formed from the buds of *Quercus infectoria* L. after the infestation of an insect (*Cynips* spp.), sumac trees (*Rhus* spp. L.) and alder trees *Alnus* spp. L.). Unfortunately, current analytical techniques cannot differentiate between tannin sources with confidence.^{3,4,6}

Tannins could be used as a mordant dye for black and brown colours, but they could also act as a mordant or additive to the dyeing of other colours.^{3,6} The tanning step in

the production of leather is reliant on the use of tannins, a process which can be traced back to 5th century BC.⁹⁵

Another use of tannins was in iron gall ink, which was the main black ink used in the West from the Middle Ages to the 19th century. The degradation of iron-tannin complexes is well-known and a large issue for the preservation of manuscripts written in iron gall ink and tannin dyed textiles with iron mordants.^{3,96–99} Tannins were also used in the weighting process of silk fibres after degumming.⁴⁰ The versatility in the use of tannins means that it is common to find traces of them in more than only brown and black textile samples.

1.4.3 Vat dyes

Vat dyes are characterised by their insolubility in aqueous solvents, so they need to be reduced to impregnate the fabric and then oxidised into its coloured form. Blue and purple indigoid dyes, such as indigo from the indigo plant (*Indigofera tinctoria* L.) and woad (*Isatis tinctoria* L.), as well as shellfish purple from molluscs (*Bolinus brandaris* L. and *Hexapilus trunculus* L.), require vat dyeing. Colonial expansion and increased global trade during the 17th century resulted in a great influx of *Indigofera tinctoria* L. onto the European market which almost completely outcompeted the domestic woad production.^{3,32} Their chemical structures (Fig 1.13) make them compatible with all fibres and their high adsorption within the textile structure makes them very lightfast. Both indigo and woad contain the same main chromophores responsible for the blue colour although indigo is seen as a higher quality dye source due to its higher dye content.^{3,4,32}

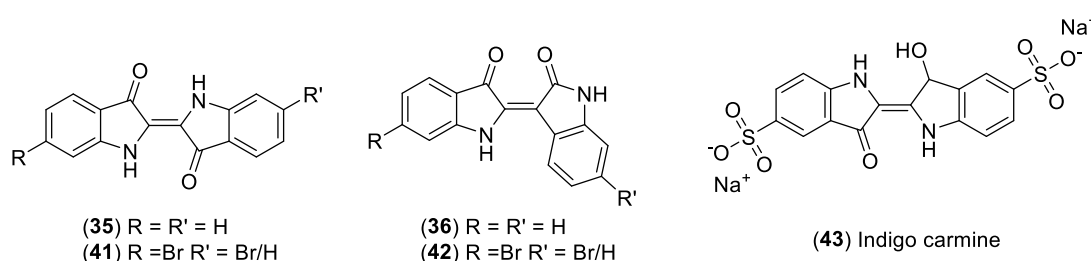


Figure 1.13: Molecular structures of indigotin (35) and indirubin (36), their brominated structures (41, 42) and indigo carmine (43).

The main chromophores of indigo are indigotin (35) and indirubin (36) which are not present naturally in the plants but must be produced through a laborious extraction process (Fig 1.12) including enzymatic hydrolysis of the naturally occurring indoxyl

glycosides (**37**, **38**) to indoxyl (**39**). Upon oxidation (**39**) is converted to 'leuco-indigo' (**40**) and then to indigotin (**35**). A side reaction producing indirubin (**36**) can occur during fermentation, giving more reddish blues.

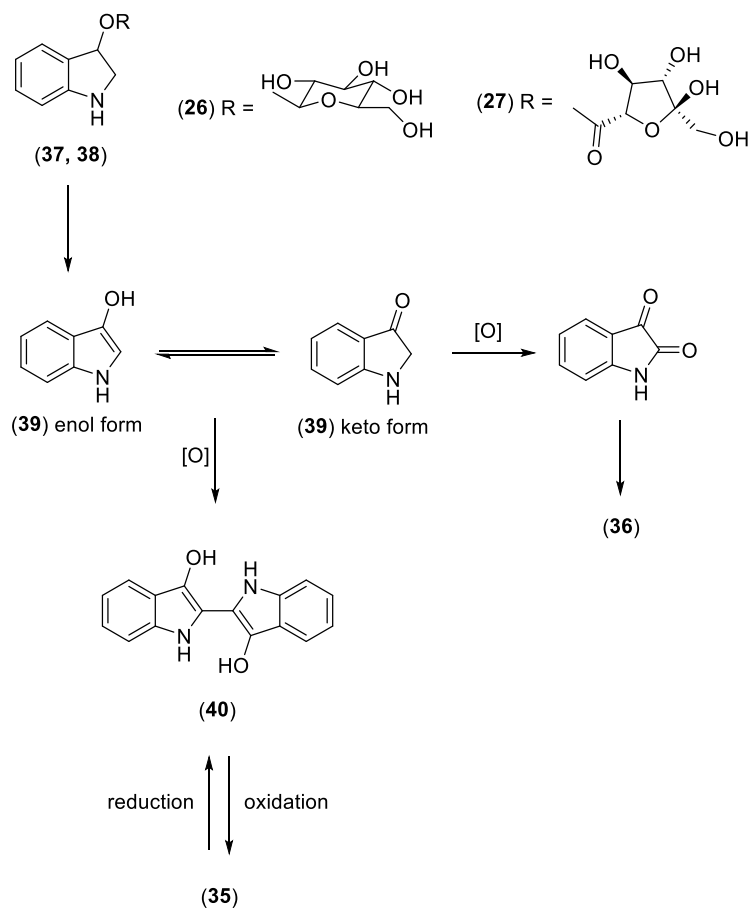


Figure 1.14: Molecular structures of intermediates of the production of indigotin (**24**) and indirubin (**25**).

The main chromophores in shellfish purple are (di-)brominated indigoids (**41**) and indirubins (**42**), which give the textile a rich purple colour (Fig 1.11). The long and complex process required to produce the colour from the precursors present in the molluscs together with the huge quantity of snails required for the production of a few grams of purple dye, made shellfish purple incredibly expensive. Thus, purple has historically been used mainly by royalty and as a symbol for wealth and power. The historical implication of purple may also have been one of the factors of the huge success of the first synthetic dyestuff, mauveine (Section 1.5).

Saxon blue was one of the first 'semi-synthetic' dyes, known as such since it was produced by the sulfonation of indigo using H_2SO_4 to indigo disulfonic acid, also known as indigo carmine (**43**) (Fig 1.11). The dyestuff was invented in 1743 by the

German Johann Christian Barth and was patented in England 1748. The addition of the sulfate groups made the dye water-soluble and thus textiles could be dyed blue without the need for vat dyeing, simplifying the process. However, the increased water-solubility gave it low wash- and lightfastness, resulting in Saxon blue being seen as a low quality and cheap dyestuff. The natural variety thus dominated the indigo market until synthetic routes to indigotin were invented at the end of 19th century.¹⁰⁰

1.5 Early synthetic dyes

The development of a wide variety of synthetic dyestuffs closely followed Perkin's discovery of mauve in 1856,²⁷ and this group of dyes are known as early synthetic dyes, coal-tar dyes or aniline dyes.¹⁰¹ The study of these dyes is made complicated by the confused nomenclature, as many dyes were given different commercial names depending on country, the same dyestuff could have multiple names due to wrong characterisation of the structure, and chemically different molecules could have similar names.¹⁰² Additionally, early synthetic dyes can be classified either based on chemical structure or application.⁴² Some of the main dye families classified by structure is presented below.

1.5.1 Azo dyes

The first azo dye, Bismarck brown, was synthesised by Peter Griess in 1858 and it is the most important synthetic dye group used today. It accounts for around 60 – 70 % of all dyestuffs used across modern industries.¹⁰³

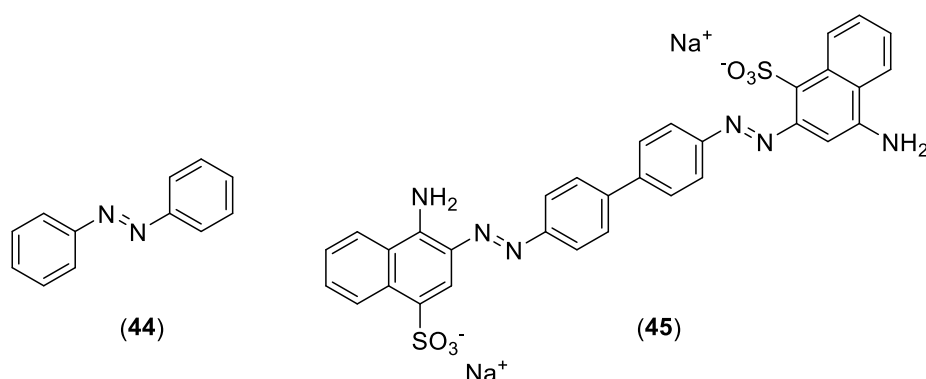


Figure 1.15: Generic monoazo dye structure (44) and the structure of Congo red (45) as an example of a diazo dye.

Azo dyes have the common structure feature of an azo group (-N=N-) which usually links two aromatic ring systems (fig 1.15). Mono-, di- or triazo dyes exist and the first

diazo dye was Congo red, invented in 1884.¹⁰⁴ Many azo dyes act as pH indicators.^{104,105} Despite their wide use, they do pose a health and environmental risk so many studies focus on the degradation of azo dyes, particularly with the help of bacteria and microbes.^{103,106–109}

1.5.2 Di- and triphenylmethane dyes

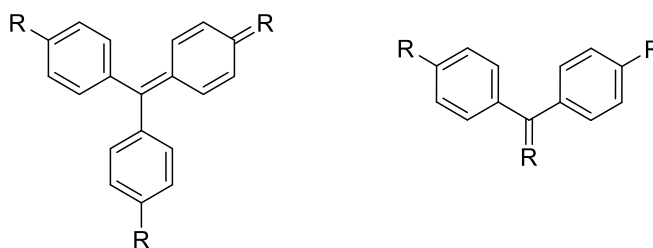


Figure 1.16: Generic structures of tri- and diphenylmethane dyes. The R groups are often -NR₂ groups. Methylation at the meta-position of the benzene ring can also occur.

The first triphenylmethane (dye synthesised was fuchsine by Verguin in 1859.¹¹⁰ The synthetic route was found by oxidation of crude aniline with tin (IV) chloride and the di- and triphenylmethane dyes were immediately popular due to their intense and broad range of colours.¹¹¹ They show poor lightfastness, and their degradation has been thoroughly studied.^{112–116} Known degradation pathways for these dyes are N-demethylation, photooxidative cleavage of the central C-phenyl bond and photoreduction of an excited state dye cation to a leuco-dye form by addition of an electron.¹¹²

1.5.3 Nitro, xanthene and thiazine dyes

The nitro dye picric acid was arguably the first synthetic dye as it was invented in 1771.¹¹⁷ However, it was never commercially successful due to its poor dyeing properties, toxicity and explosive properties. Only a few synthetic dyes are classed as nitro dyes, and they provide bright yellow, orange and red shades. They were never as important commercially as the other dye classes but they can be found in historical objects.¹⁰³

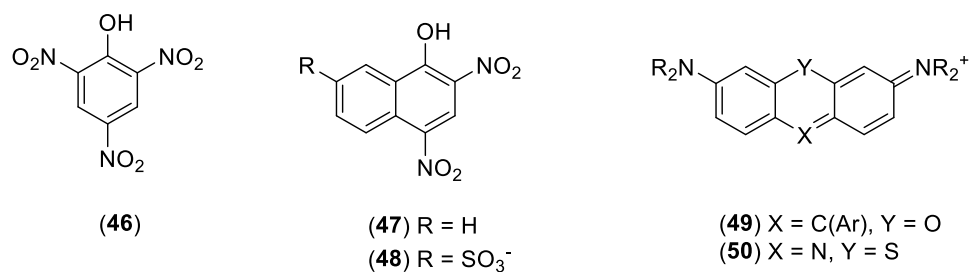


Figure 1.17: (46) = picric acid, (47) = Martius yellow and (48) = naphthol yellow S are all examples of nitro dyes. The general structure of xanthene (49) and thiazine (50) are also shown.

Xanthene and thiazines give strong, bright colours and were, and still are, commercially successful compounds.^{42,103} Xanthenes, such as rhodamine, fluorescein and eosin, are particularly important in biology as stains and fluorescent probes.¹¹⁸ However, they have been found to be environmentally harmful and carcinogenic so studies focussing on their systemic removal from water streams have grown in importance recently.^{119–121}

1.6 Common analytical challenges in historical dye analysis

The limited sample sizes available from historical textiles combined with the often low concentration of dyestuffs and presence of multiple dye sources and degradation products makes dye analysis a challenging field.^{2,5} Additionally, ethical considerations when investigating culturally significant objects needs to be understood and justified.¹²² Non-invasive techniques that do not need a sample have grown in popularity in recent years due to these concerns but they cannot achieve similar levels of information as invasive techniques.¹⁷ Thus, these challenges require careful consideration and the development of sensitive analytical techniques and protocols.

1.6.1 Complex dye mixtures

Complexity is introduced in the dye samples at multiple stages before analysis. Natural dye sources often contain multiple chromophores that are present in different ratios depending on soil composition, age of plant and time of harvest, any pre-treatments and dyebath conditions.^{64,73} The dye composition is further complicated by photodegradation and the history of the object; location of display, storage environment and conservation treatments all affect the obtained analytical result.¹²² Finally, the sample preparation and analytical technique employed will also influence the final result.^{123,124}

Early synthetic dye samples show variability based on the synthetic route and starting material used.¹²⁵ Many early synthetic dyes thought of as pure compounds has been found to be mixtures of chromophores. For example, mauveine from Perkin's lab was found to contain more than thirteen related methyl derivatives.^{126–128}

Samples of early synthetic dyes are similar to natural dye samples made increasingly more complex by object history and the analytical approach employed. Additionally, many textiles dyed with either natural or synthetic dyes use more than one dye to achieve the desired shade of colour, adding another layer of complexity to the data interpretation.

The mixture of dye components commonly found in historical samples is one of the main advantages of invasive chromatographic methods as separation of a complex mixture often is required for full understanding of the sample. When utilising an invasive method, the previous mentioned challenges including low dye content, small sample sizes and ethical considerations grow in size.

1.6.2 Photodegradation

One of the main concerns for museum collections is the photodegradation of dyestuff. The rate of degradation of dye compounds upon exposure to light is dependent on the molecular structure, type of fibre and the use of mordant. It can also be altered by environmental factors such as irradiation wavelength, temperature, and relative humidity. Typically, natural and early synthetic dyes show fast rates of photodegradation in comparison to modern synthetic dyes.^{68,129} Additionally, the fibre substrate in itself is also known to degrade over time, such as the yellowing of wool over time which has been attributed to the oxidation of tryptophan residues.⁶⁸

One of the main natural dyes of concern is flavonoids. The common observation of grass and trees looking blue in Renaissance tapestries is a good example of the faster rate of photodegradation of flavonoid dyes compared to indigoids. Originally, the designs were green, obtained by the overdyeing of indigoids with flavonoids.¹³⁰ The phenolic moieties and carbonyl group of flavonoid compounds, particularly the proximity of the -OH group and carbonyl on the C-ring for flavonols^{68–70} have been found to be the reason for the fugitive nature of flavonoids.^{3,65}

Early synthetic dyes were also prone to photodegradation, shown in the often short popularity of commercial dyes.²⁷ For example, mauveine was almost completely replaced by the mid-1860s due to its rapid discolouration.^{24,131} Triphenylmethane dyes

have also been shown to have a fast rate of degradation upon exposure to light. The main pathway for these dyes have been shown to be de-alkylation.^{114,116,117}

The presence of products from photodegradation together with the usually complex dye matrix discussed above, makes it important to develop sensitive analytical methods. Additionally, it is a large and important area of research to better understand likely degradation pathways and products to inform conservation strategies to be able to preserve these objects for future generations.

1.7 Analytical approaches for historical dye analysis

1.7.1 Non-invasive techniques

When no physical sample is removed from an object, the technique is defined as non-invasive.^{15,16} Spectroscopic techniques, such as fibre optic reflectance spectroscopy (FORS),¹³² hyperspectral or multispectral imaging,¹³³ and Raman spectroscopy¹³⁴ are non-invasive and also non-destructive, meaning that no physical alteration of the object occurs.

FORS uses a fibre optic probe to illuminate the object and the reflected light is collected to produce a reflectance spectrum. Comparison of the spectrum to reference material allows dye identification.¹³² FORS has been successfully incorporated into the dye analysis field and used to study anthraquinones,^{80,135} Chinese textiles¹³⁶ and lake pigments¹³⁷ but the resolution is limited by the probe, as it does not allow the analysis of very thin areas of colour. It can also be difficult to differentiate between dye sources using FORS data, particularly yellow dyes.¹³⁶ Overdyeing and complex dye mixtures complicates the interpretation of FORS data, and models based on references need to be developed for data interpretation.^{135,137}

Hyperspectral imaging uses different wavelengths of light to map the photoluminescence and reflective characteristics of surfaces which can be used for dye identification.¹³³ Hyperspectral imaging has mainly been used for paintings¹³⁸ and manuscripts¹³⁹ but has been introduced into textile analysis particularly as an important tool for the guided sampling of historical objects.¹⁴⁰

Raman spectroscopy has been a long-established technique in the field of heritage science, particularly for paintings.^{13,132} The micro-invasive surface-enhanced Raman spectroscopy (SERS) is particularly popular in the study of textiles, but it requires a sample.^{46,47,141}

Non-invasive techniques have the obvious advantage of having no, to minimal, physical impact on the object investigated. This makes the analysis of extremely fragile and/or culturally important objects possible when it would not be ethical to collect a sample. They also have a large advantage when it comes to ease of use and analysis of environmental or large cultural heritage such as cave paintings.¹⁴²

The main disadvantage of non-invasive spectroscopic techniques is their low selectivity in comparison to invasive approaches. The complex dye mixtures present often makes data interpretation difficult and complex processing is required to simplify the spectra.¹³⁵ Many dye sources have similar responses, meaning that the level of information obtained from invasive approaches cannot be reached.¹⁷

1.7.2 Invasive techniques

The main invasive analytical techniques used in dye analysis are liquid chromatography (LC) (Section 3.6) and mass spectrometry (MS) (Section 5.2).^{3,5} LC is commonly combined with UV-visible spectrometry, such as photo diode array (PDA) or MS detection and it is useful in simplifying the often complex dye mixtures present.¹²² Combined with mild extraction methods (Section 3.3), the information gained from LC investigations are unparalleled to any of the other techniques used in dye analysis.^{5,16} LC-PDA and LC-MS have been used to study minor components present for species identification,^{62,74,88,90} degradation processes^{67,72,143} and identification of unknown dye markers.^{49,94}

The simplification of complex dye mixtures upon separation using liquid chromatography and the high selectivity and sensitivity of a mass spectrometric approach makes these invasive techniques highly informative in comparison to non-invasive techniques. The main disadvantage is the need for sampling, which reduces its applicability to many objects which are either too fragile or too significant culturally. Non-invasive although micro-destructive techniques, such as ambient MS approaches may reduce the sample size needed while preserving the level of information gained from the analysis.¹⁴⁴ Often a combination of preliminary non-invasive techniques, guiding sampling for invasive techniques if required is utilised and seen as a good compromise.^{12,140,145,146}

1.8 Knowledge gaps and project aims

The dye analysis field requires the continuous development of new analytical approaches that reduce the physical impact of analysis on the objects whilst gaining maximum information. This concern is amplified when working with more fragile objects, such as historical textiles, where sampling often is impossible without threatening the structural integrity of the object.

The development of such methods was the central focus of this study and two main approaches have been developed. The first method is a sample preparation workflow requiring reduced sample sizes for minimally invasive and micro-destructive chromatographic and mass spectrometric analysis without reducing the level of information gained (Chapter 3). The second approach developed is the application of the non-invasive, but micro-destructive, ambient mass spectrometric technique of desorption electrospray ionisation mass spectrometry (DESI-MS) to historical dyestuffs (Chapter 5).

Both of these approaches were successfully applied to historical samples. A collection of Scottish and English embroideries from mid-16th to early 18th centuries housed in National Museums Scotland (NMS) was analysed using the chromatographic workflow developed in this thesis (Chapter 4). The DESI-MS assembly was successfully used to investigate synthetic dyes with focus on an early synthetic dye reference book from 1893 (Chapter 5). The techniques developed and applied in this work will hopefully benefit the dye analysis field and ultimately help preserve cultural heritage objects for future generations while increasing the understanding of our past.

1.9 References

- 1 Analytical Methods Committee, AMCTB No. 101, *Anal. Methods*, 2021, **13**, 558–562.
- 2 W. Nowik, in *Elsevier Reference Module in Chemistry, Molecular Sciences and Chemical Engineering*, ed. J. Reedijk, Elsevier Inc., Waltham, 2013.
- 3 D. Cardon, *Natural Dyes: Sources, Traditions, Technology & Science*, Archetype Books, London, 2007.
- 4 J. H. Hofenk de Graaff, *Colourful Past*, Archetype Books, London, 2007.
- 5 V. Pauk, P. Barták and K. Lemr, *J. Sep. Sci.*, 2014, **37**, 3393–3410.
- 6 E. S. B. Ferreira, A. N. Hulme, H. McNab and A. Quye, *Chem. Soc. Rev.*, 2004, **33**,

329–336.

- 7 L. G. Troalen, L. Robinet, J. Weatherill, S. Heu-thao, A. N. Hulme, C. L. Mackay and E. Blouet, *ICOM-CC*, 2021, 1–8.
- 8 D. Tamburini, C. R. Cartwright, M. Melchiorre Di Crescenzo and G. Rayner, *Archaeol. Anthropol. Sci.*, 2019, **11**, 3121–3141.
- 9 M. J. Smith and A. Macken, *JCMS*, 2020, **18**, 1–10.
- 10 T. H. Flowers, M. J. Smith and J. Brunton, *Herit. Sci.*, 2019, 1–15.
- 11 L. G. Troalen, PhD Thesis, the University of Edinburgh, 2013.
- 12 M. Veneno, P. Nabais, V. Otero, A. Clemente, M. C. Oliveira and M. J. Melo, *Heritage*, 2021, **4**, 422–436.
- 13 I. Karapanagiotis, E. Minopoulou, L. Valianou, S. Daniilia and Y. Chryssoulakis, *Anal. Chim. Acta*, 2009, **647**, 231–242.
- 14 J. Kirby, M. Spring and C. Higgitt, *Natl. Gall. Tech. Bull.*, 2007, **28**, 69–95.
- 15 I. Degano, E. Ribechini, F. Modugno and M. P. Colombini, *Appl. Spectrosc. Rev.*, 2009, **44**, 363–410.
- 16 M. Shahid, J. Wertz, I. Degano, M. Aceto, M. I. Khan and A. Quye, *Anal. Chim. Acta*, 2019, **1083**, 58–87.
- 17 M. Gulmini, A. Idone, E. Diana, D. Gastaldi, D. Vaudan and M. Aceto, *Dye. Pigment.*, 2013, **98**, 136–145.
- 18 A. Clark, *Working lives of women in the 17th century*, Routledge, London, 2nd Edition, 1919.
- 19 G. Wingfield Digby, *Elizabethan Embroidery*, Faber and Faber, London, 1963.
- 20 J. Reiss, *English Embroidery from the Metropolitan Museum of Art, 1580-1700: 'Twixt Art and Nature*, Metropolitan Museum of Art, New York, NY, 2008, vol. 7.
- 21 H. Wyld, *The Art of Tapestry*, Bloomsbury Publishing, London, 2022.
- 22 A. Peck, Ed., *Interwoven globe: the worldwide textile trade, 1500-1800*, Metropolitan Museum of Art, New York, NY, 2013.
- 23 L. M. Poggemoeller, MA Thesis, University of Missouri-Kansas City, 2015.
- 24 A. Dronsfield and J. Edmonds, *The transition from natural to synthetic dyes*, John Edmonds, Little Chalfont, 2001.

- 25 R. D. Welham, *J Soc Dye Colour*, 1963, **79**, 146–152.
- 26 R. E. Rose, *J. Chem. Educ.*, 1926, **3**, 973–1132.
- 27 E. Hagan and J. Poulin, *Herit. Sci.*, 2021, 1–14.
- 28 V. Forster, S. Vettese Forster and R. M. Christie, *J. Int. Colour Assoc.*, 2013, 1–17.
- 29 O. Stolberg-Wernigerode, *Neue deutsche Biographie [New German biography]*, Duncker & Humblot, Berlin, 1985.
- 30 E. Kvavadze, O. Bar-Yosef, A. Belfer-Cohen, E. Boaretto, N. Jakeli, Z. Matskevich and T. Meshveliani, *Science*, 2009, **325**, 1359.
- 31 M. I. Tobler-Rohr, *Handbook of Sustainable Textile Production*, Woodhead Publishing, Sawston, Cambridge, 2011.
- 32 J. Balfour-Paul, *Indigo*, British Museum Press, London, 1998.
- 33 M. L. Ryder, *Sheep and man*, Duckworth, London, 1983.
- 34 D. Jacoby, *Dumbart. Oaks Pap.*, 2004, **58**, 197–240.
- 35 V. Hansen, *The Silk Road: A New History*, Oxford University Press, Oxford, 2012.
- 36 B. Wang, W. Yang, J. McKittrick and M. A. Meyers, *Prog. Mater. Sci.*, 2016, **76**, 229–318.
- 37 C. Popescu and H. Höcker, *Chem. Soc. Rev.*, 2007, **36**, 1282–1291.
- 38 R. Kozłowski and M. Mackiewicz-Talarczyk, Eds., *Handbook of Natural Fibres Volume 1: Types, Properties and Factors Affecting Breeding and Cultivation*, Woodhead Publishing, Sawston, Cambridge, 2nd edn.
- 39 M. Clark, *Handbook of Textile and Industrial Dyeing*, Woodhead Publishing, Sawston, Cambridge, 2011.
- 40 M. Hacke, *Stud. Conserv.*, 2008, **53**, 3–15.
- 41 K. M. Babu, in *Textiles and Fashion*, Elsevier Ltd, Amsterdam, 2015, pp. 57–78.
- 42 M. Clark, *Handbook of Textile and Industrial Dyeing: Principles, Processes and Types of Dyes - vol II*, Woodhead Publishing, Sawston, Cambridge, 2011, vol. 1.
- 43 S. Grierson, *The colour cauldron*, Mrs. S. Grierson, Perth, 1986.
- 44 H. Wyld, *West 86th*, **19**, 231–254.
- 45 L. J. Rather, S. Jameel, S. A. Ganie and K. A. Bhat, *Handb. Renew. Mater. Color. Finish.*, 2018, 103–114.

- 46 B. Doherty, F. Gabrieli, C. Clementi, D. Cardon, A. Sgamellotti, B. Brunetti and C. Miliani, *J. Raman Spectrosc.*, 2014, **45**, 723–729.
- 47 I. Serafini, L. Lombardi, C. Fasolato, M. Sergi, F. Di Ottavio, F. Sciubba, C. Montesano, M. Guiso, R. Costanza, L. Nucci, R. Curini, P. Postorino, M. Bruno and A. Bianco, *Nat. Prod. Res.*, 2019, **33**, 1040–1051.
- 48 J. Alcántara-García and M. Nix, *Herit. Sci.*, 2018, **6**, 1–15.
- 49 J. Wouters, C. M. Grzywacz and A. Claro, *Stud. Conserv.*, 2010, **55**, 186–203.
- 50 D. Tamburini, C. R. Cartwright, M. Pullan and H. Vickers, *Archaeol. Anthropol. Sci.*, 2019, **11**, 1221–1239.
- 51 D. Tamburini, *Dye. Pigment.*, 2019, **163**, 454–474.
- 52 N. Shibayama, M. Wypyski and E. Gagliardi-Mangilli, *Herit. Sci.*, 2015, **3**, 12.
- 53 D. Tamburini, J. Dyer, P. Davit, M. Aceto, V. Turina, M. Borla, M. Vandenbeusch and M. Gulmini, *Molecules*, 2019, **24**, 1–18.
- 54 R. Costantini, I. Vanden Berghe and F. C. Izzo, *J. Cult. Herit.*, 2019, **38**, 37–45.
- 55 I. Degano, J. J. Łucejko and M. P. Colombini, *J. Cult. Herit.*, 2011, **12**, 295–299.
- 56 J. Han, PhD Thesis, University of Glasgow, 2016.
- 57 D. Mantzouris, I. Karapanagiotis and C. Panayiotou, *Microchem. J.*, 2014, **115**, 78–85.
- 58 K. Lech, J. Nawała and S. Popiel, *J. Am. Soc. Mass Spectrom.*, 2021, **32**, 2552–2566.
- 59 E. Sandström, H. Wyld, C. L. Mackay, L. G. Troalen and A. N. Hulme, *Anal. Methods*, 2021, **13**, 4220–4227.
- 60 L. G. Troalen and A. N. Hulme, in *Tapestries from the Burrell Collection*, eds. E. Cleland and L. Karafel, 2017, pp. 46–51.
- 61 L. G. Troalen, A. S. Phillips, D. A. Peggie, P. E. Barran and A. N. Hulme, *Anal. Methods*, 2014, **6**, 8915–8923.
- 62 D. A. Peggie, A. N. Hulme, H. McNab and A. Quye, *Microchim. Acta*, 2008, **162**, 371–380.
- 63 K. Grömer, *The Art of Prehistoric Textile Making*, 2016.
- 64 C. Mouri and R. Laursen, *J. Chromatogr. A*, 2011, **1218**, 7325–7330.

- 65 D. A. Peggie, PhD Thesis, University of Edinburgh, 2006.
- 66 A. Villela, E. J. C. van der Klift, E. S. G. M. Mattheussens, G. C. H. Derksen, H. Zuilhof and T. A. van Beek, *J. Chromatogr. A*, 2011, **1218**, 8544–8550.
- 67 L. Valianou, K. Stathopoulou, I. Karapanagiotis, P. Magiatis, E. Pavlidou, A. L. Skaltsounis and Y. Chryssoulakis, *Anal. Bioanal. Chem.*, 2009, **394**, 871–882.
- 68 H. Chaaban, I. Ioannou, C. Paris, C. Charbonnel and M. Ghoul, *J. Photochem. Photobiol. A Chem.*, 2017, **336**, 131–139.
- 69 Š. Ramešová, R. Sokolová, I. Degano, J. Bulíčková, J. Žabka and M. Gál, *Anal. Bioanal. Chem.*, 2012, **402**, 975–982.
- 70 G. J. Smith, S. J. Thomsen, K. R. Markham, C. Andary and D. Cardon, *J. Photochem. Photobiol. A Chem.*, 2000, **136**, 87–91.
- 71 V. Daniels, T. Devière, M. Hacke and C. Higgitt, *Tech. Res. Bull.*, 2014, **8**, 13–28.
- 72 R. S. Blackburn, *Color. Technol.*, 2017, **133**, 449–462.
- 73 R. S. Blackburn, *Color. Technol.*, 2017, **133**, 449–462.
- 74 C. Mouri and R. Laursen, *Microchim. Acta*, 2012, **179**, 105–113.
- 75 G. C. H. Derksen, M. Naayer, T. A. van Beek, A. Capelle, I. K. Haaksman, H. A. van Doren and Æ. de Groot, *Phytochem. Anal.*, 2003, **14**, 137–144.
- 76 R. Singh, Geetanjali and S. M. S. Chauhan, *Chem. Biodivers.*, 2004, **1**, 1241–1264.
- 77 L. Ford, R. L. Henderson, C. M. Rayner and R. S. Blackburn, *J. Chromatogr. A*, 2017, **1487**, 36–46.
- 78 X. Zhang and R. A. Laursen, *Anal. Chem.*, 2005, **77**, 2022–2025.
- 79 G. C. H. Derksen, PhD Thesis, Wageningen University, 2001.
- 80 R. L. Henderson, PhD Thesis, University of Leeds, 2013.
- 81 G. Cuoco, C. Mathe, P. Archier, F. Chemat and C. Vieillescazes, *Ultrason. Sonochem.*, 2009, **16**, 75–82.
- 82 I. Boldizsár, Z. Szucs, Z. Füzfaí and I. Molnár-Perl, *J. Chromatogr. A*, 2006, **1133**, 259–274.
- 83 Hill and Richter, *Nature*, 1936, **628**, 1936.
- 84 J. Wouters, *Stud. Conserv.*, 1985, **30**, 119–128.
- 85 C. J. Cooksey, *Biotech. Histochem.*, 2018, **94**, 100–107.

- 86 C. M. Salinas, in *Global History and New Polycentric Approaches*, eds. M. Perez Garcia and L. De Sousa, Palgrave Macmillan, Singapore, 2018, pp. 255–273.
- 87 A. Serrano, Master Thesis, Universidade de Lisboa, 2010.
- 88 A. Serrano, M. M. Sousa, J. Hallett, J. A. Lopes and M. C. Oliveira, *Anal. Bioanal. Chem.*, 2011, **401**, 735–743.
- 89 E. Rosenberg, *Anal. Bioanal. Chem.*, 2008, **391**, 33–57.
- 90 K. Lech and M. Jarosz, *Anal. Bioanal. Chem.*, 2016, **408**, 3349–3358.
- 91 J. Wouters and A. Verhecken, *Annls Soc. ent. Fr.*, 1989, **25**, 393–410.
- 92 K. Stathopoulou, L. Valianou, A. L. Skaltsounis, I. Karapanagiotis and P. Magiatis, *Anal. Chim. Acta*, 2013, **804**, 264–272.
- 93 A. Serrano, A. van den Doel, M. van Bommel, J. Hallett, I. Joosten and K. J. Van den Berg, *Anal. Chim. Acta*, 2015, **897**, 116–127.
- 94 D. A. Peggie, J. Kirby, J. Poulin, W. Genuit, J. Romanuka, D. F. Wills, A. De Simone and A. N. Hulme, *Anal. Methods*, 2018, **10**, 617–623.
- 95 C. Van Driel-Murray, in *The Oxford Handbook of Engineering and Technology in the Classical World*, ed. J. P. Oleson, Oxford University Press, Oxford, 2012.
- 96 M. A. Lutui, F. Gilard and M. Sablier, *J. Mass Spectrom.*, 2008, **43**, 1123–1131.
- 97 J. Kolar, A. Štolfa, M. Strlič, M. Pompe, B. Pihlar, M. Budnar, J. Simčič and B. Reissland, *Anal. Chim. Acta*, 2006, **555**, 167–174.
- 98 I. Degano, M. Mattonai, F. Sabatini and M. P. Colombini, *Molecules*, 2019, **24**, 2318.
- 99 H. Wilson, C. Carr and M. Hacke, *Chem. Cent. J.*, 2012, **6**, 1–13.
- 100 M. De Keijzer, M. R. Van Bommel, R. Hofmann-De Keijzer, R. Knaller and E. Oberhumer, *Stud. Conserv.*, 2012, **57:sup1**, S87–S95.
- 101 J. C. Barnett, *Stud. Conserv.*, 2007, **52**, 67–77.
- 102 D. Tamburini, C. M. Shimada and B. McCarthy, *Dye. Pigment.*, 2021, **190**, 109286.
- 103 R. M. Christie, *Colour Chemistry*, Royal Society of Chemistry, Cambridge, 2015, 2nd edn.
- 104 C. J. Cooksey, *Biotech. Histochem.*, 2014, **89**, 384–387.
- 105 M. Štastná, M. Trávníček and K. Šlais, *Electrophoresis*, 2005, **26**, 53–59.
- 106 A. C. R. Ngo and D. Tischler, *Int. J. Environ. Res. Public Health*, 2022, **19**, 4740.

- 107 N. P. Shetti, S. J. Malode, R. S. Malladi, S. L. Nargund, S. S. Shukla and T. M. Aminabhavi, *Microchem. J.*, 2019, **146**, 387–392.
- 108 M. Solís, A. Solís, H. I. Pérez, N. Manjarrez and M. Flores, *Process Biochem.*, 2012, **47**, 1723–1748.
- 109 R. G. Saratale, G. D. Saratale, J. S. Chang and S. P. Govindwar, *J. Taiwan Inst. Chem. Eng.*, 2011, **42**, 138–157.
- 110 C. J. Cooksey and A. T. Dronsfield, *Biotech. Histochem.*, 2015, **90**, 288–293.
- 111 J. Fabian, in *Light absorption of Organic Colorants*, Springer Verlag, Heidelberg, 1980, pp. 137–138.
- 112 C. Weyermann, D. Kirsch, C. Costa Vera and B. Spengler, *J. Forensic Sci.*, 2009, **54**, 339–345.
- 113 C. Weyermann, D. Kirsch, C. Costa-Vera and B. Spengler, *Am. Soc. Mass Spectrom.*, 2006, **17**, 297–306.
- 114 D. Confortin, H. Neevel, M. Brustolon, L. Franco, A. J. Kettelarij, R. M. Williams and M. R. Van Bommel, *J. Phys. Conf. Ser.*, 2010, **231**, 012011.
- 115 G. Favaro, D. Confortin, P. Pastore and M. Brustolon, *J. Mass Spectrom.*, 2012, **47**, 1660–1670.
- 116 C. G. Kumar, P. Mongolla, J. Joseph and V. U. Maheshwara, *Process Biochem.*, 2012, **47**, 1388–1394.
- 117 K. Lech, E. Wilicka, J. Witowska-Jarosz and M. Jarosz, *J. Mass Spectrom.*, 2013, **48**, 141–147.
- 118 C. J. Cooksey, *Biotech. Histochem.*, 2016, **91**, 71–76.
- 119 R. Nagaraja, N. Kottam, C. R. Girija and B. M. Nagabhushana, *Powder Technol.*, 2012, **215–216**, 91–97.
- 120 M. Sundararajan, V. Sailaja, L. John Kennedy and J. Judith Vijaya, *Ceram. Int.*, 2017, **43**, 540–548.
- 121 S. Y. Lee, D. Kang, S. Jeong, H. T. Do and J. H. Kim, *ACS Omega*, 2020, **5**, 4233–4241.
- 122 I. Degano and J. La Nasa, *Top. Curr. Chem.*, 2016, **374**, 263–290.
- 123 A. Manhita, T. Ferreira, A. Candeias and C. B. Dias, *Anal Bioanal Chem*, 2011, **400**, 1501–1514.

- 124 J. Wouters, C. M. Grzywacz and A. Claro, *Stud. Conserv.*, 2011, **56**, 231–249.
- 125 C. S. da Costa Nogueira Souto, Master Thesis, Universidade de Lisboa, 2010.
- 126 M. M. Sousa, M. J. Melo, A. J. Parola, P. J. T. Morris, H. S. Rzepa, J. S. Seixas and D. Melo, *Chem. Eur. J.*, 2008, **14**, 8507–8513.
- 127 J. S. De Melo, S. Takato, M. Sousa, M. J. Melo and A. J. Parola, *Chem. Commun.*, 2007, 2624–2626.
- 128 O. Meth-Cohn and M. Smith, *J. Chem. Soc. Perkin Trans I*, 1994, 5–7.
- 129 E. Hagan, I. Castro-Soto, M. Breault and J. Poulin, *Herit. Sci.*, 2022, **10**, 1–11.
- 130 A. Quye, K. Hallett and C. Herrero Carretero, *Wrought in Gold and Silk: Preserving the Art of Historic Tapestries*, NMS Enterprises Limited, Edinburgh, 2009.
- 131 M. J. Plater, *J. Chem. Res.*, 2015, **39**, 251–259.
- 132 M. Bacci, *Sensors Actuators B. Chem.*, 1995, **29**, 190–196.
- 133 M. Kubik, in *Physical techniques in the study of Art, Archaeology and Cultural Heritage, Volume 2*, eds. D. Creagh and D. Bradley, Elsevier B.V., Amsterdam, 2007.
- 134 B. Doherty, C. Miliani, I. Vanden Berghe, A. Sgamellotti and B. G. Brunetti, *J. Raman Spectrosc.*, 2008, **39**, 638–645.
- 135 C. Chavanne, L. G. Troalen, I. B. Fronty, P. Buléon and P. Walter, *Anal. Chem.*, 2022, **94**, 7674–7682.
- 136 D. Tamburini and J. Dyer, *Dye. Pigment.*, 2019, **162**, 494–511.
- 137 C. Miguel, W. Jacobs, C. B. Dias, A. Manhita, T. Ferreira, A. F. Conde and A. Candeias, *Eur. J. Sci. Theol.*, 2020, **16**, 151–164.
- 138 C. Cucci, J. K. Delaney and M. Picollo, *Acc. Chem. Res.*, 2016, **49**, 2070–2079.
- 139 P. Ricciardi, J. K. Delaney, L. Glinsman, M. Thoury, M. Facini and E. R. de la Rie, *O3A Opt. Arts, Archit. Archaeol. II*, 2009, **7391**, 739106.
- 140 J. Dyer, D. Tamburini, E. R. O'Connell and A. Harrison, *PLoS One*, 2018, **13**, e0204699.
- 141 M. Aceto, A. Arrais, F. Marsano, A. Agostino, G. Fenoglio, A. Idone and M. Gulmini, *Spectrochim. Acta - Part A Mol. Biomol. Spectrosc.*, 2015, **142**, 159–168.
- 142 M. Olivares, K. Castro, M. S. Corchón, D. Gárate, X. Murelaga, A. Sarmiento and N. Etxebarria, *J. Archaeol. Sci.*, 2013, **40**, 1354–1360.

- 143 D. Tamburini, J. Dyer and I. Bonaduce, *Sci. Rep.*, 2017, **7**, 1–15.
- 144 M. Z. Huang, C. H. Yuan, S. C. Cheng, Y. T. Cho and J. Shiea, *Annu. Rev. Anal. Chem.*, 2010, **3**, 43–65.
- 145 L. Arberet, F. Pottier, A. Michelin, W. Nowik, L. Bellot-Gurlet and C. Andraud, *Analyst*, 2021, **146**, 2520–2530.
- 146 P. Nabais, J. Oliveira, F. Pina, N. Teixeira, V. De Freitas, N. F. Brás, A. Clemente, M. Rangel, A. M. S. Silva and M. J. Melo, *Sci. Adv.*, 2020, **6**, 1–9.

Chapter 2 Materials and Methods

2.1 Instrumentation

2.1.1 Sample preparation workflow

Extraction was carried out using a Stuart Block heater (SBH2000D) with a 96 well plate aluminium insert. Filtration was carried out using a Thermo Scientific Megafuge 8 centrifuge and M10 Microplate swinging bucket rotor.

2.1.2 Liquid chromatography (UHPLC-PDA)

UHPLC-PDA analysis was performed using a Waters Acquity UPLC™ system comprising of the Waters Binary Gradient Manager with Waters Sample Manager incorporating a Waters Column Heater with sample detection by a Waters PDA detector (210 – 800 nm). Data were collected by Waters Empower 3 (Waters, Milford, MA, USA) and processed with Origin 9.5 (OriginLab, Northampton, MA, USA).

2.1.3 Mass spectrometry (DESI-FT-ICR-MS)

The mass spectrometer used for all DESI-MS experiments was a Bruker Solarix 7T FT-ICR-MS using Compass HyStar 5.1 (Bruker Daltonik GmbH, Billerica, MA, USA). A stainless-steel nozzle (90 × 0.4 mm (length × i.d.), tightened around the MS capillary using a metal spring, was attached to the MS inlet. Initial data processing was conducted using Compass DataAnalysis 5.0 (Bruker Daltonik GmbH, Billerica, MA, USA).

The DESI stage was made of stainless steel covered with an acrylic sheet (9 × 14 × 0.3 cm, $l \times w \times d$), mounted onto two perpendicular stepping motors. The construction was attached with double-sided adhesive tape to a lab jack. An Arduino-compatible board (EleksMaker EleksMana V5.2) controlled via LaserGRBL (v4.6.0) using G-code and a desktop computer was attached to the stepping rotors.

The 3-D printed parts of the built DESI source were designed using Fusion360 (Autodesk, San Rafael, CA, USA) and 3-D printed in polylactic acid (PLA) using an Ultimaker 2 3D printer (Ultimaker B.V., Utrecht, The Netherlands). The DESI source design included x-, y- and z-axis positioners (WPI Inc. Kite Manual Micromanipulator) and a rotation mount (THORLABS RP01 Manual Rotation Stage). A space for a remotely controlled camera (ESP32-CAM) was also incorporated into the design.

2.1.4 Software

Statistical analysis and construction of figures were performed using GraphPad Prism 9.3.1 (GraphPad software, LLC, San Diego, CA, USA), Origin 9.5 (OriginLab, Northampton, MA, USA), ImageJ (Rasband, W. S., U. S. National Institutes of Health, Bethesda, MA, USA) and Microsoft 365 2020 (Microsoft, Redmond, WA, USA).

Waters Empower 3 (Waters, Milford, MA, USA) was used to collect and process the chromatographic data.

Fusion360 (Autodesk, San Rafael, CA, USA), LaserGRBL (v4.6.0) and Ultimaker 2 3D printer (Ultimaker B.V., Utrecht, The Netherlands) were used in the design and construction of the DESI source.

Compass HyStar 5.1 (Bruker Daltonik GmbH, Billerica, MA, USA) and Compass DataAnalysis 5.0 (Bruker Daltonik GmbH, Billerica, MA, USA) were used to collect and process the mass spectrometry data.

2.2 Materials

2.2.1 Sample preparation workflow

Well plates (AB-2800, Thermo Scientific), filter plates (350 μ l, 0.2 μ m WWPTFE, Acroprep Adv, Pall corporation), 96 well plate silicone sealing mats (Starlab) and Zone-free™ Sealing Films for 96 well plates were used.

2.2.2 Standard mixture 1

The eight flavonoids and one anthraquinone used in standard mixture 1 were all purchased from Extrasynthese. Solvent used was MeOH:H₂O 1:1 v/v.

Compound number	Chromophore	Stock solution concentration ($\times 10^{-5}$ M)
1	Fisetin	6.99
2	Sulfuretin	7.78
3	Luteolin	6.99
4	Genistein	7.41
5	Apigenin	7.41
6	Chrysoeriol	7.00
7	Diosmetin	7.33
8	Alizarin	8.75
9	Prunetin	7.04

This stock solution was diluted by factors of 2, 4, 8, 20, 40 and 200 for all the concentrations used in the UHPLC-PDA method evaluation.

2.2.3 Natural dye references

Dyed silk and wool reference samples from the COST G8 project “Non-destructive testing and analysis of museum objects” (FP5)¹ and the Monitoring of Damage to Historic Tapestries project (MODHT) (FP5, EC contract number EVK4-CT-2001-00048)^{2,3} were used as part of the evaluation of the sample preparation and UHPLC-PDA methods. References previously dyed in-house at NMS scientific lab were also used to build the reference database.

Luteolin reference standard was purchased from Fluorochem Ltd, Hadfield, UK and dried weld plant was purchased from George Weil & Sons, Guildford, UK. Purpurin and alizarin reference standard were obtained from Sigma Aldrich Inc., St. Louis, MO, USA and turmeric root and powder were purchased locally

Two types of lichen were collected locally and used to dye reference silk and wool cloth from the MODHT project.

2.2.4 Early synthetic dye references

Undyed, degummed, unmordanted silk (2-ply, 66 Tex, thread count 43 cm⁻²) and undyed, washed, unmordanted wool cloth (3-ply, 158 Tex, thread count 36 cm⁻²) from the Monitoring of Damage to Historic Tapestries project (MODHT) (FP5, EC contract number EVK4-CT-2001-00048)^{3,4} and undyed cotton cloth locally purchased (thread count 32 cm⁻²) were used as reference cloths.

Rhodamine B, aniline yellow, congo red, crocein scarlet 7B, disperse orange III, methyl red, orange II sodium salt, ponceau 3R, ponceau S, xylidine ponceau, auramine O, brilliant green, light green SF yellowish, methyl green, malachite green, naphthol yellow S, eosin Y and fluorescein were obtained from Sigma Aldrich Inc., St. Louis, MO, USA. Methylene blue, basic fuchsin, methyl violet 2B and Martius yellow were purchased from Fluorochem Ltd, Hadfield, UK.

Permanent pen with rhodamine B ink was purchased from Staedtler.

2.2.5 Historical samples

Four samples from the wedding tartan of Flora MacDonald (WHM.1961.02) from the West Highland Museum, Fort William were collected by dress historian Jo Watson.

270 samples from 26 embroideries dated 1550 – 1720 from the National Museums Scotland were collected by Edith Sandström and Helen Wyld. Accession numbers of the objects stated in Table 4.1.

12 sample swatches in the 1893 edition of *Tabellarische Übersicht über die künstliche organischen Farbstoffe und ihre Anwendung in Färberei und Zeugdruck [Tabular overview of the synthetic organic dyestuffs and their use in dyeing and printing]* by Adolf Lehne were analysed. The book was obtained from the private collection of Dr Lore Troalen.

2.3 Methods

2.3.1 Extraction

Weighed samples (typically 0.01 – 0.2 mg ± 0.005 mg) were placed on a 96 well plate. 50 µL MeOH:CH₃COCH₃:H₂O:C₂H₂O₄ (oxalic acid, OA) (1 M aq) (30:30:40:1 v/v/v/v) was added to each sample and the well plate covered with a silicone cover. The well plate was heated on a heat block at 60 °C for 30 min and left to cool to room

temperature. The samples were then pipetted into a filtration plate. For samples suspected to contain indigoid dyestuffs, a second extraction was performed; 25 μL DMSO was added to each well and the well plate covered with a silicone cover. The well plate was heated on a heat block at 80 $^{\circ}\text{C}$ for 15 min and left to cool to room temperature before the DMSO solvent was transferred to a second filtration plate.

2.3.2 Filtration

Following oxalic acid extraction: The filtration plate was placed over a receiving 96 well plate and the set-up centrifuged at 1500 rpm (300 $\times g$) for 5 min. The samples were washed with 25 μL MeOH:H₂O 1:1 v/v twice and centrifuged at 1500 rpm (300 $\times g$) for 5 min after each wash.

Following DMSO extraction: The filtration plate was placed over a receiving 96 well plate and the set-up centrifuged at 1500 rpm (300 $\times g$) for 7.5 min. The samples were then covered with sealing film and either analysed immediately or stored in the fridge until analysis.

2.3.3 Drying and reconstitution

The receiving plate with the filtered OA extracts was placed in a desiccator over P₂O₅ and dried completely (ca 2-3 h). The extracts were then reconstituted using 25 μL MeOH:H₂O 1:1 v/v + 0.1 % CHOOH (formic acid, FA) or MeOH:H₂O 1:3 v/v before analysis.

2.3.4 UHPLC-PDA method

The UHPLC method developed used a Cortex BEH C18 1.6 μm column, 90 \AA , 75 \times 2.1 mm (length \times i.d.) with an in-line filter. The total run time was 13.92 min at a flow rate of 400 $\mu\text{L min}^{-1}$ and the column was maintained at 45 \pm 1 $^{\circ}\text{C}$. A binary solvent system was used; A = H₂O + 0.05 % FA and B = MeOH + 0.05 % FA. The elution program was isocratic for 1.17 min (77A:23B) then a linear gradient from 1.17 min to 10.92 min (10A:90B) before recovery of the initial conditions over 0.5 min and equilibration over 2.5 min.

2.3.5 Gradient optimisation

Acquity column calculator transfer programme (Waters, Milford, MA, USA) was used to transfer the gradient from Method developed by Dr Lore Troalen⁵ to the gradient used in Section 2.3.4.

2.3.6 Chromatographic peak integration

All chromatographic integration was done using ApexTrack™ integration algorithm developed by Waters® as part of the Empower 3® software. The start parameter was set at 0.30 min and the end parameter at 9.00 min. Lutoff % and Touchdown% were both set at 0.5 %. AutoPeak width and AutoThreshold were used as default for the peak detection except in instances when known chromophores were investigated. In those cases, the smallest peak of interest was used as the minimum peak width and threshold.

2.3.7 Calibration curves

Triplicates of standard mixture 1 at five different concentrations (20, 10, 5, 1, 0.5 µg mL⁻¹) were used for the calibration curves. The peak area was found by automatic integration of the chromatograms at 254 nm by Waters Empower 2 software and the graphs were plotted in Microsoft Excel 2019.

2.3.8 Limit of detection (LoD) and limit of quantification (LoQ)

The limit of detection (LoD) and limit of quantification (LoQ) was calculated by the signal-to-noise-method. The noise for each component in standard mixture 1 was defined as the average signal obtained in blank samples (n = 3) around the retention time (± 0.25 min) of each analytical peak.

LoD and LoQ were calculated using the slopes (S) of the calibration curves and the baseline noise (s) at the time of elution of each chromophore. LoD was defined as the signal being 3.3 times larger than the background noise (Equation 2.1), and LoQ as the signal being 10 times larger (Equation 2.2).

$$LoD = \frac{3.3 \times s}{S} \quad \text{Equation 2.1}$$

$$LoQ = \frac{10 \times s}{S} \quad \text{Equation 2.2}$$

s = baseline noise, S = slope of calibration curve of compound.

2.3.9 Dyeing of lichen references

The two lichens collected were separated, washed and boiled in 100 mL deionised H₂O for 30 min. The temperature was reduced to 80 °C and the lichen left in the dyebath whilst dyeing. A silk sample (1 cm²) was added to the dyebath left at 80 °C

and dyed for 30 min before the silk sample was removed and rinsed in cold, deionised water. The same dyebath and procedure were used to dye a wool sample (1 cm²) except the wool sample was pre-wetted in deionised H₂O for 10 min before dyeing.

2.3.10 Parameter optimisation of DESI method on rhodamine B ink

The rhodamine B ink was applied on a clean glass slide directly before analysis. Time of analysis differed between 5 min and 10 min depending on the distance of the geometrical parameter tested.

DESI parameter	Value used for analysis
Sweep excitation energy	15 %
Skimmer voltage	15 V
Source temperature	200 °C
Sprayer capillary voltage	3.5 kV
Dry gas flow	3.9 bar
Accumulation	2.0 s
Time-of-flight (ToF)	0.6 ms
Flow rate	300 µl h ⁻¹
Sprayer angle, α	26°
Solvent	3:1 v/v ACN:H ₂ O + 0.1 % FA

2.3.11 Parameter optimisation of DESI method on rhodamine B dyed silk and wool cloth

Rhodamine B samples were dyed as outlined in 2.3.13. The same process as in Section 2.3.10 was followed for optimisation of the geometrical parameters using the parameters tabulated below.

DESI parameter	Value used for analysis
Sweep excitation energy	15 %
Skimmer voltage	15 V
Source temperature	200 °C
Sprayer capillary voltage	3.5 kV
Dry gas flow	3.9 bar
Accumulation	1.5 s
Time-of-flight (ToF)	0.6 ms
Flow rate	750 $\mu\text{l h}^{-1}$
Sprayer angle, α	26°
Solvent	3:1 v/v ACN:H ₂ O + 0.1 % FA

Investigation of the mass spectrometer parameters used the parameters tabulated below and the same process as 2.3.10.

DESI parameter	Value used for analysis
Sweep excitation energy	15 %
Skimmer voltage	15 V
Source temperature	200 °C
Sprayer capillary voltage	3.5 kV
Dry gas flow	3.9 bar
Accumulation	1.5 s
Time-of-flight (ToF)	0.6 ms
Flow rate	750 $\mu\text{l h}^{-1}$
Sprayer angle, α	26°
Solvent	3:1 v/v ACN:H ₂ O + 0.1 % FA
Sprayer – MS inlet distance, d_x	5 – 7 mm
Sprayer – MS inlet offset, d_y	< 0.5 mm
MS inlet – sample height, k	< 1 mm
Sprayer to sample height, h	1 – 2 mm

2.3.12 Parameter optimisation of DESI method on natural dyestuffs

Parameters outlined below were used for DESI analysis of natural dyestuff references. The sample was wetted for one minute and spectra recorded for two minutes. A new spot on the same dyed sample was used for each analysis.

DESI parameter	Value used for analysis
Sweep excitation energy	15 %
Skimmer voltage	15 V
Source temperature	200 °C
Sprayer capillary voltage	4.5 kV
Dry gas flow	3.9 bar
Accumulation	1.5 s
Time-of-flight (ToF)	0.4 ms
Flow rate	750 $\mu\text{l h}^{-1}$
Sprayer angle, α	26°
Solvent	ACN
Sprayer – MS inlet distance, d_x	5 – 7 mm
Sprayer – MS inlet offset, d_y	< 0.5 mm
MS inlet – sample height, k	< 1 mm
Sprayer to sample height, h	2 mm \pm 0.5 mm

2.3.13 Dyeing of early synthetic dye references

100 mg \pm 0.005 mg of each reference dyestuff were dissolved in 7.5 mL deionised H₂O and the dyebaths were heated to 75 °C before 100 mg \pm 0.005 mg (ca. 1 cm²) silk cloth (Section 2.2.4) was added. The dyebaths were kept at 75 °C for 15 min before the silk samples were removed and rinsed at least twice with cold, deionised water and left to dry completely. The same dyebaths were used to dye the wool samples (150 mg \pm 0.005 mg, ca 1 cm²) following the same procedure except the wool samples were pre-wetted in deionised H₂O for 10 min before dyeing.

2.3.14 Application of DESI method to reference and historical samples

Parameters outlined below were used for DESI analysis of reference and historical early synthetic dyestuff. The spot was wetted for one minute before spectra were recorded for one minute. New spot on the same dyed sample used for each analysis.

DESI parameter positive mode	Value used for analysis
Sweep excitation energy	15 %
Skimmer voltage	15 V
Source temperature	200 °C
Sprayer capillary voltage	4.5 kV
Dry gas flow	3.9 bar
Accumulation	1.5 s
Time-of-flight (ToF)	Analyte dependent
Flow rate	750 $\mu\text{l h}^{-1}$
Sprayer angle, α	35°
Solvent	3:1 v/v ACN:H ₂ O
Sprayer – MS inlet distance, d_x	5 – 7 mm
Sprayer – MS inlet offset, d_y	< 0.5 mm
MS inlet – sample height, k	< 1 mm
Sprayer to sample height, h	2 mm \pm 0.5 mm

DESI parameter negative mode	Value used for analysis
Sweep excitation energy	15 %
Skimmer voltage	15 V
Source temperature	200 °C
Sprayer capillary voltage	4.2 kV
Dry gas flow	3.9 bar
Accumulation	1.5 s
Time-of-flight (ToF)	Analyte dependent
Flow rate	750 $\mu\text{l h}^{-1}$
Sprayer angle, α	35°
Solvent	3:1 v/v ACN:H ₂ O
Sprayer – MS inlet distance, d_x	5 – 7 mm
Sprayer – MS inlet offset, d_y	< 0.5 mm
MS inlet – sample height, k	< 1 mm
Sprayer to sample height, h	2 mm \pm 0.5 mm

Chapter 3 Small-scale sample preparation workflow and UHPLC method development

3.1 Aims

The aim of this investigation was to develop a sample preparation method that requires less sample and increases time and resource efficiency. Two areas were developed to reach this aim: a parallel sample preparation workflow to enhance the replication and reproducibility of data sets in the dye analysis field; and a more efficient chromatographic method to reduce the analytical time for a larger number of samples from sampling to result.

3.2 Introduction

The need to minimise the sample size required for reliable analysis is not a unique challenge for heritage science, but it is arguably one of the most important aspects for the field to consider. The scientific questions asked in heritage science often revolve around culturally important artefacts, making it vital to limit the physical sampling required to make sure the artefact remains accessible for generations to come. This issue is amplified when working with more fragile objects, such as historical textiles, where sampling often is impossible without threatening the structural integrity of the object. When sampling is possible, the resulting datasets are often non-reproducible, as the samples are often too small or too few for replicate analysis.

Both invasive and non-invasive techniques are in use in dye analysis (Section 1.7). The invasive and destructive technique of liquid chromatography (LC) is one of the main techniques used in heritage science due to its sensitivity and the ability to couple to multiple detectors such as photodiode arrays (PDA) and mass spectrometers (MS).^{1,2} The considerable advantage of being able to separate the often complex mixtures present in dye samples outweighs the disadvantage of LC analysis requiring sampling. Therefore, one main way to improve LC analysis is to develop sample preparation methods requiring less sample for the same analytical quality.

Common sample preparation workflows are both labour- and resource-intensive, relying heavily on the preparation and analysis of individual samples (Fig 3.1).³⁻⁷ Adopting a more high-throughput approach would thus not only decrease the

introduced random error but also make the analysis more environmentally friendly. Additionally, making larger and more reproducible data sets more common is important for the use of modern statistical analysis approaches, such as multivariate data analysis and principal component analysis, in the dye analysis field. Some studies utilising these methods have been published in recent years, but these are still relatively uncommon.⁸⁻¹⁰

3.2.1 Current sample preparation methods for UHPLC dye analysis

Sample preparation methods for LC and MS dye analysis follow a set of fundamental steps:^{2,11} extraction of the dye molecule from the fibre or mordant, filtration, drying and reconstitution (Fig 3.1).

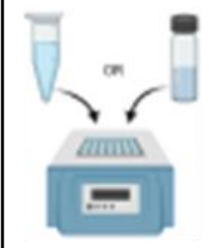
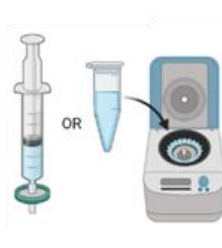
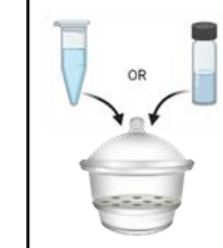
	Extraction	Filtration	Drying + reconstitution
			
(i) ³	Unstoppered test tubes	Centrifugation and supernatant collection	Desiccator over silica gel/NaOH
(ii) ⁴	Open 1.7 ml conical microcentrifuge tubes	Centrifugation and Supernatant collection	Desiccator over NaOH pellets
(iii) ⁵	1.5 ml microcentrifuge tubes	Centrifugation/supernatant collection/syringe filtration	Desiccator over NaOH pellets
(iv) ⁶	1.5 ml glass vials	0.45 µm PTFE filter	Desiccator
(v) ⁷	2 ml glass vials	Centrifugation + 0.45 µm PTFE filter	Freeze drier

Figure 3.1: Comparison of sample preparation methods used in dye analysis.³⁻⁷ Figure reproduced from E. Sandström *et al.*¹² with permission from the Royal Society of Chemistry.

The extraction step induces chemical transformations as it involves breaking bonds between the dye molecule and fibre. Thus, the choice of extraction method and solvent has a large impact on the compounds seen in the analysis (Section 3.3). Most workflows extract the samples by adding a volume of extraction solvent to the fibres present in individual test tubes, microcentrifuge tubes or glass vials before heating them to accelerate the bond breaking (Fig 3.1).³⁻⁷

The filtration step is necessary to remove any solid contaminants that can damage analytical instruments. This step determines the minimum sample size possible as it

inherently involves a loss in volume (Section 3.4). Commonly, the filtration in dye analysis is done by pipetting the sample extract into syringes with attached filters and filtering into a second vial. Another common way is to centrifuge the samples and collect the supernatant. A syringe filtration can follow if necessary. Treating samples individually in this way introduces a high random error as it relies on the repeatability of the analyst.³⁻⁷

The drying and reconstitution step is often done in a desiccator or freeze dryer. After drying, samples are reconstituted in a decreased volume of solvent to increase the concentration of the sample before analysis. The efficiency and repeatability of the drying step is therefore dependent on the solubility of the dyestuffs and the initial concentration.³⁻⁷

Utilising a workflow based on the individual treatment of samples across these steps not only increases the labour and resources needed but also increases the random error within a sample set, resulting in less reproducible datasets. The development of a more systematic approach with low volume loss and less manual steps would therefore not only result in smaller sample sizes needed but also increase data replication.

3.2.2 Overview of the sample preparation method developed for UHPLC dye analysis

The developed sample preparation workflow (Fig 3.2) is based on 96 well plates and filtration by centrifugation, inspired by workflows already implemented in biology and forensic science.¹³⁻¹⁷

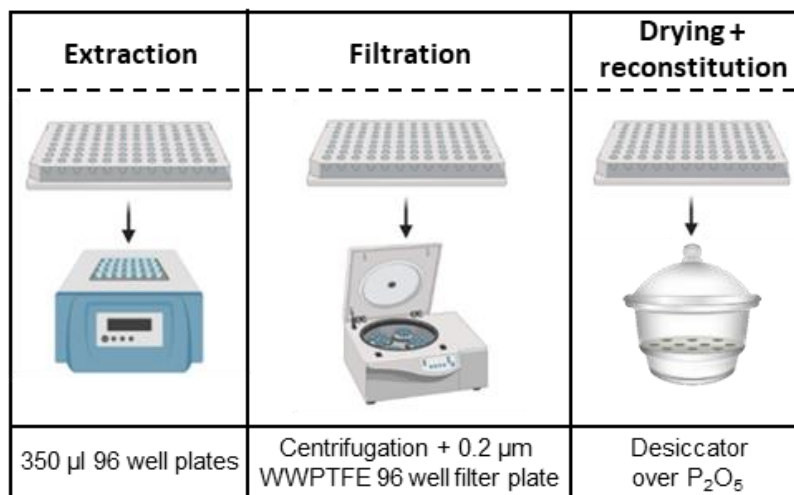


Figure 3.2: Sample preparation workflow developed. Figure reproduced from E. Sandström *et al.*¹² with permission from the Royal Society of Chemistry.

All samples are put on the same well plate, the extraction solvent added, and the wells covered with a silicone cover before the well plate is heated (Section 3.3). The only manual transfer follows the extraction when the dye extracts are pipetted into the filtration well plate. The filtration well plate is placed on top of a collection plate and the set-up centrifuged (Section 3.4). The collection plate is dried in a desiccator and the samples are reconstituted in their wells before analysis (Section 3.5).

The sample preparation workflow was evaluated using seven concentrations (0.1 – 20 μ g mL⁻¹) of standard mixture 1 (Section 2.2.2) and silk and wool reference samples dyed with natural dyestuffs from the MODHT project (Section 2.2.3). The reproducibility of each step needed to be investigated so the aims of requiring less sample, reducing the introduced error and make it possible to prepare up to 96 samples simultaneously could be reached.

3.3 Extraction step

The choice of extraction solvent has a large influence on the overall quality of the analysis as the successful cleavage of bonds to the substrate or mordant influences what compounds are detected.^{2,11,18} The large variety in chemistry and methods of application of dyestuffs result in multiple variables that are needed to be taken into consideration for a successful analysis, mainly: the nature of the dye; the application of the dye (mordant, direct or vat dye), the sample size available, the level of degradation seen and the research question. Many different protocols have been

developed,^{4,6,19–21} which broadly fall under three categories: hydrolysis, use of a complexation agent and extraction with organic solvents.^{2,11}

The hydrolytic extraction commonly used was first published by Wouters in 1985.²² In it, the sample is heated at 100 °C for 10 minutes after an extraction solvent of 37 % HCl:H₂O:MeOH 2:1:1 v/v/v is added. This protocol is regarded as a “strong” extraction method in comparison to the use of complexation agents and organic solvents. Most common complexation agents are C₂H₂O₄ (oxalic acid, OA),^{5,23} CH₂O₂ (formic acid, FA) and C₂HF₃O₂ (trifluoroacetic acid, EDTA) and the predominant organic solvents used are (CH₃)₂SO (dimethylsulfoxide, DMSO), C₃H₇NO (dimethylformamide, DMF) and C₅H₅N (pyridine).²

The advantage of a strong extraction method is the high yield obtained, making it the preferred choice if the concentration of the dyestuff is low. However, it has a marked effect on the chemistry of the sample.^{5,24} It has been shown to break glycosidic bonds and increase the esterification of phenolcarboxylic compounds as well as the decarboxylation or dehydration of molecular markers.⁵ It also has the disadvantage of often completely consuming the fibrous structure of the textile, making replicate analyses of the same sample impossible.²⁵

The main advantage of mild extraction methods is thus the preservation of more labile compounds, particularly the glycosidic conjugates of the main chromophores. In recent years, the presence of glycosidic compounds and the glycoside : aglycone ratio have been shown to be important for species identification and the elucidation of historic dye bath conditions.^{4,7} Such studies focussed on going beyond pure dyestuff identification require larger datasets and replicate analysis to support any conclusions.^{8,26} It would therefore be of advantage for the high-throughput workflow developed to preserve the labile compounds present, so a mild extraction method was chosen. Furthermore, the silicone cover for the well plate used tended to release under the high temperatures used for the HCl extraction, which was another important reason that an efficient mild extraction method was chosen.

The extraction method using MeOH:CH₃COCH₃:H₂O:OA (0.21 M aq) (30:30:40:1 v/v/v/v) solution is popular due to its high yield relative to other mild extraction solvents, its preservation of the glycosidic components of both weld and madder species and its low toxicity.⁵ This extraction method is well-established in dye analysis, which also makes comparisons between studies possible. These reasons made the OA protocol the starting point for the optimisation.

3.3.1 Extraction step optimisation

First, the effect of heating the acidic extraction solvent in the 96 well plates and covering it with the silicone cover was investigated. 50 μL of MeOH:CH₃COCH₃:H₂O:OA (1 M aq) (30:30:40:1 v/v/v/v) was added to a well on a clean well plate and was analysed immediately after addition using the UHPLC-PDA. The same volume of extraction solvent was added to a different well on the same well plate, covered with a silicone cover and heated at 60 °C for 30 minutes before it was let to cool and then injected into the UHPLC-PDA. These experiments were repeated three times and the results compared (Fig 3.3).

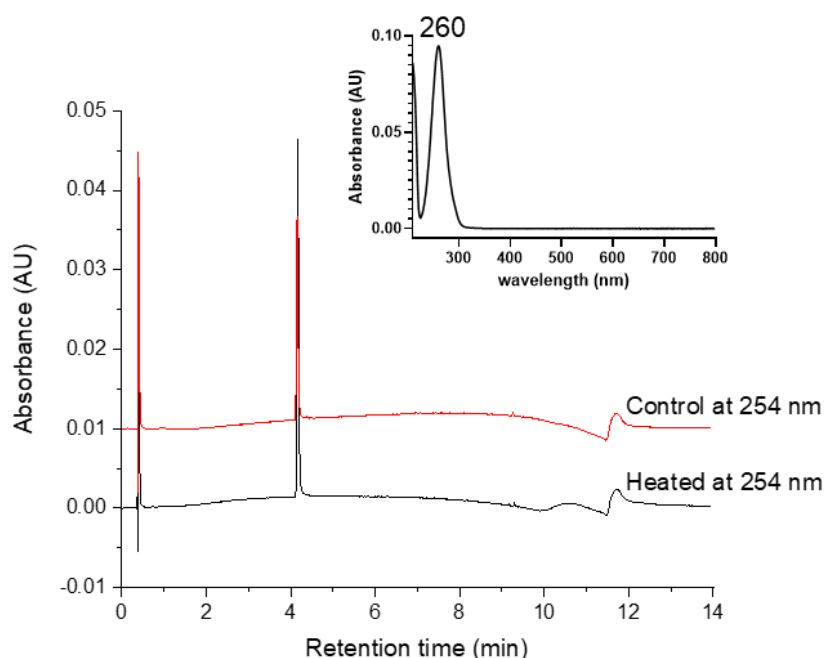


Figure 3.3: Overlaid UHPLC-PDA chromatograms monitored at 254 nm of MeOH:CH₃COCH₃:H₂O:OA (1 M aq) (30:30:40:1 v/v/v/v) solution

The resulting chromatograms both showed clean spectra except for the presence of a yet unknown contaminant peak at 4.2 min with $\lambda_{\text{max}} = 260 \text{ nm}$ (Fig 3.3). The contaminant peak showed a stronger intensity for the sample in the heated well, but from the available data it is not possible to determine the source of this increase. Potentially, the difference could be from the heating, the extended time acid was present in the heated well in comparison to the control well or from a difference in solvent preparation. Regardless, the presence of the contaminant in both the spectra of the controls and heated samples suggest that the well plates and silicone covers are resilient to the addition of acid and heating. Thus, the well plates and silicone

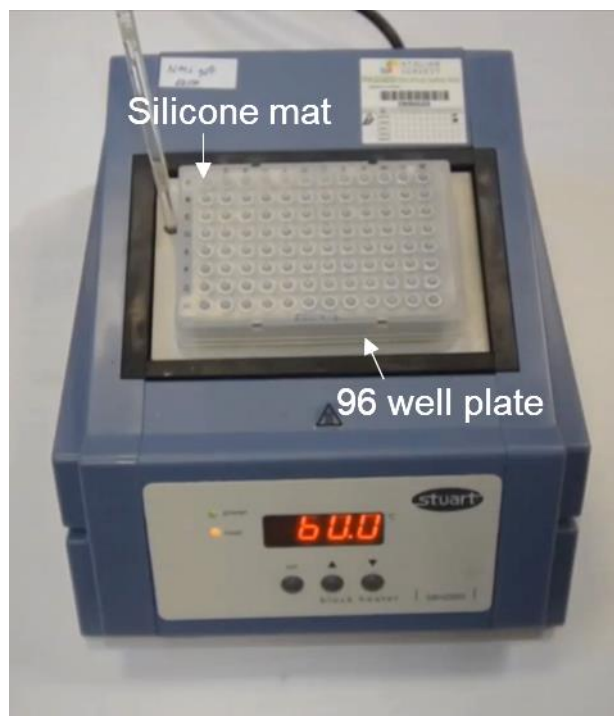


Figure 3.4: Extraction set-up on a Stuart Block heater (SBH2000D) with a 96 well plate aluminium insert. The 96 well plate is covered with a silicone sealing mat (Starlab).

covers can be used in the sample preparation keeping in mind the presence of the contaminant.

To determine if the level of dyestuff obtained could be improved compared to the levels from HCl extraction and literature methods for OA extraction, studies varying the concentrations of OA and conducting pre-treatment of the fibres before OA extraction were done. Evaluating whether the HCl extraction at lower concentrations, or temperature could preserve the glycosides whilst keeping the high yield of the HCl protocol was also investigated. Silk samples dyed with weld from the MODHT project (Y/S1a) was used as the reference cloth for all extraction experiments.²⁷ Weld was a common yellow in Europe and the chromophores of interests are luteolin (**3**), apigenin (**5**) and chrysoeriol (**6**) together with luteolin-7-O-glycoside (**3-7-O**) (Section 1.4.2.1) which was used as the measure of how well the extraction preserved glycosides.

The first investigation focussed on variation of the concentration of OA in the MeOH:CH₃COCH₃:H₂O:OA (0.21 M aq) (30:30:40:1 v/v/v/v) solution. The three concentrations of OA tested were 0.25 M, 1 M and 1 M in 3:3:4:1 v/v/v/v ratio. All weld samples were extracted in triplicate using the sample preparation developed by Dr L. Troalen.²⁵ The peak area was integrated using ApexTrack™ in Empower 3®.

For reliable peak integration of a chromatogram, two operations need to be conducted: peak detection and baseline determination. When the peaks and baseline in the chromatogram have been defined, the retention time, peak area and peak height for each peak can be calculated. In Waters instruments, traditional chromatographic integration theory bunches the single point data into discrete groups. Peaks are detected by calculating the slope between adjacent data groups and comparing it to minimum threshold values either automatically or manually set. The baseline is then constructed based on the detected peaks.

ApexTrack uses the second derivative of the chromatogram for peak detection and baseline determination instead of changes in slope. In the second derivative chromatogram, the apex is the maxima, the inflection points are where $y = 0$ and the start and end of the peak is the curvature minima (Fig 3.5).

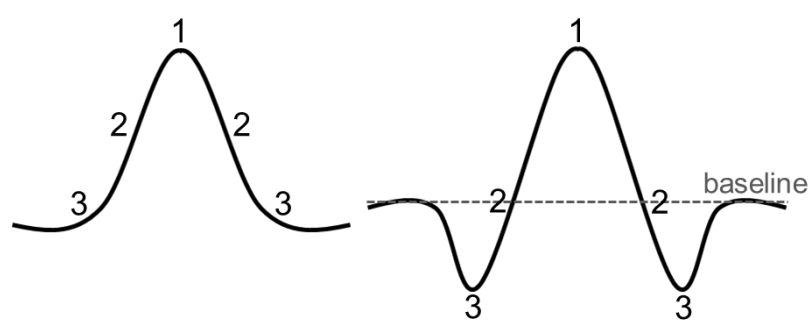


Figure 3.5: **Left:** Sketch of an ideal Gaussian peak. **Right:** The second derivative plot of the ideal Gaussian peak. 1 = peak apex, 2 = inflection points, 3 = liftoff and touchdown points of the peak. The second derivative plot was multiplied by -1 so the apex of a positive peak appears as a positive second derivative.

The main advantage of the second derivative approach is increased resolution for peak detection and integration of peak shoulders. It also is of advantage for chromatograms where the baseline drifts. The ApexTrack approach was used throughout this project with the default parameters of liftoff: 0.5 %, touchdown: 0.5 %, start: 0.3 min and end: 9.0 min. Liftoff and touchdown determine the peak boundaries by setting the required change of angle for peak detection as a percentage of the slope at the inflection points.²⁸

When the chromophores of interest were known, the minimum area and height for the integration was manually set for each run as the area of the smallest peak of interest to not overwhelm the number of peaks integrated. If they were not known, the minimum area and height was left to be automatically determined by the algorithm.

For weld the chromophores of interests are known and the smallest peak is chrysoeriol (**6**) (Section 4.8.1). To enable comparison between OA concentrations, the peak area obtained was divided by the sample mass used and the peak area μg^{-1} plotted. This was the integration method used throughout the investigations unless otherwise stated.

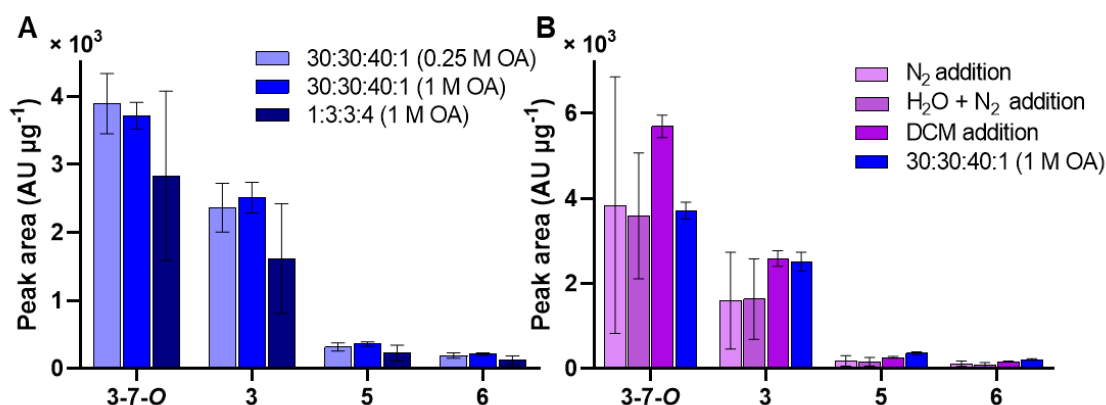


Figure 3.6: **A:** peak area μg^{-1} of chromophores in weld upon variation of OA concentration in the extraction solvent. ($n = 3$, mean \pm S.D). **B:** Peak area μg^{-1} of chromophores in weld upon pre-processing of the fibre by addition of liquid N₂, H₂O followed by liquid N₂ or DCM. 1 M OA extraction result shown as the control. (For N₂ and H₂O + N₂: $n = 4$, mean \pm S.D). (For DCM and 1 M OA: $n = 3$, mean \pm S.D). All chromatograms extracted at 254 nm. **3-7-O** = luteolin-7-O-glycoside, **3** = luteolin, **5** = apigenin, **6** = chrysoeriol.

The impact of changes in concentration of OA in the MeOH:CH₃COCH₃:H₂O:OA (0.21 M aq) (30:30:40:1 v/v/v/v) solution is shown in Figure 3.6A. The concentrations 0.25 M and 1 M OA gave a similar peak area μg^{-1} with 0.25 M OA showing slightly larger standard deviations for all chromophores studied. Despite the concentration of 1 M OA in the 1:3:3:4 v/v/v/v solution being increased by a factor of 10 in comparison to the 1 M OA in 1:30:30:40 v/v/v/v solution, the yield for any of the weld chromophores did not increase. Instead, larger standard deviations for (**3-7-O**) and (**3**) were found, probably due to fluctuating extent of deglycosylation. Because of the slightly better standard deviations, 1 M OA was decided as the control for the following investigations.

One idea to increase the extraction efficiency of OA extraction was to increase the surface area of the sample before addition of the extraction solvent. This was attempted in two main ways; flash freeze of the sample in the well using liquid N₂ before pestling, and addition of dichloromethane (DCM) to the sample in the well before addition of the extraction solvent, seen to enhance yield.^{29,30} The flash freezing

was done with both dry and wet samples to note any difference the addition of H₂O had on the yield with the working hypothesis that mechanically breaking the fibre would increase the surface area and consequently how many dye molecules would be in contact with the extraction solvent. The investigations were carried out in triplicate or quadruplicate and the peak areas were integrated and processed using the ApexTrack™ method described for the OA concentration variations.

Both pre-processing attempts were difficult to control practically. The addition of liquid N₂ even on the wet samples led to the samples often jumping out of their wells with the evaporation of the gas. This increased the risk of cross-contamination immensely even without adding the cross-contamination from re-using the pestle for each well. The rapid evaporation of the gas also meant that the samples were only frozen a short time, making the pestling difficult to perform practically. The effect of the cross-contamination and practical difficulties can be seen in the large standard deviations for both the dry and wet samples (Fig 3.6B).

The addition of DCM was easier in practice and resulted in less cross-contamination shown in the lower standard deviation seen (Fig 3.6B). In comparison to 1 M OA extraction solution, adding a DCM step also increased the peak area of **3-7-O** by 65 % while yielding an equivalent peak area ug⁻¹ of **3**. However, the increase in yield was not consistent as an average of 26 % lower peak area ug⁻¹ was seen for the minor flavonoids (**5**, **6**). An addition of another step to the workflow would inevitably introduce more random error and increase the risk of cross-contamination. Thus, the increase in yield of **3-7-O** obtained was not seen as advantageous enough to rationalise the addition of another step to the workflow especially as it did not consistently increase the yield of all chromophores investigated.

A third attempt to increase the yield while still preserving glycosidic compounds was carried out using HCl at lower temperature and concentration (Fig 3.7). The common HCl extraction protocol uses 37 % HCl: H₂O:MeOH 2:1:1 v/v/v at 100 °C for 10 min.²² The effect of reducing the temperature to 60 °C and the use of HCl-based extraction solvents at 1:1:1 v/v/v, 2:1:1 v/v/v and 3:1:1 v/v/v ratios on the yield of the chromophores in weld was investigated. The peak areas were integrated and processed using the ApexTrack™ method described for the OA concentration variations.

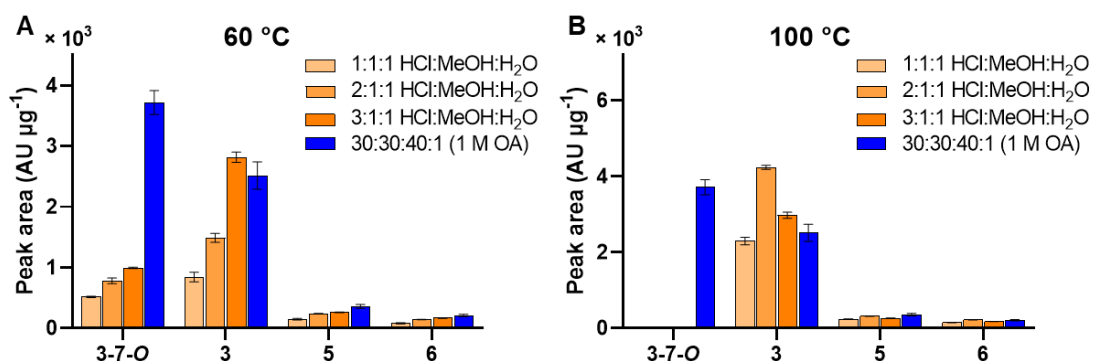


Figure 3.7: **A:** peak area μg^{-1} of chromophores in weld upon variation of HCl concentration in the extraction solvent and extraction temperature of 60 °C. **B:** peak area μg^{-1} of chromophores in weld upon variation of HCl concentration in the extraction solvent and extraction temperature of 100 °C. 1 M OA extraction result shown as the control. ($n = 3$, mean \pm S.D). All chromatograms extracted at 254 nm. 3-7-O = luteolin-7-O-glycoside, 3 = luteolin, 5 = apigenin, 6 = chrysoeriol.

The use of HCl at 60 °C and lower concentrations showed a decrease in glycoside preservation without any major increase in aglycone concentration (Fig 3.7A), so a HCl extraction method was discarded. To see if the temperature or the concentration of HCl has a larger impact on glycoside preservation, the same series of experiments were conducted but at 100 °C which showed no glycoside preservation even for the lowest concentration (Fig 3.7B). This suggest that temperature has a larger impact on the consumption of glycosidic compounds than the acid concentration.

Overall, none of the additional sample preparation protocols increased the yield of dye markers without decreasing the glycosidic yield enough to rationalise adding another step to the workflow. Hence, the MeOH:CH₃COCH₃:H₂O:OA (1 M aq) (30:30:40:1 v/v/v/v) solution was decided to be the most appropriate extraction protocol.

The OA extraction was followed by a DMSO extraction for any dyestuff that cannot be extracted using complexation agents. The DMSO extraction used followed a process reported by Mantzouris *et al.*³¹ 25 μL DMSO was added to each sample well; the well plate was covered with the same silicone cover and heated at 80 °C for 15 min.

To investigate if the order the OA and DMSO extractions had an impact on the analytes obtained, MODHT silk and wool weld samples overdyed with woad were

used. The samples were extracted in triplicate using OA then DMSO extraction and DMSO then OA extraction and the peak area μg^{-1} compared (Fig 3.8).

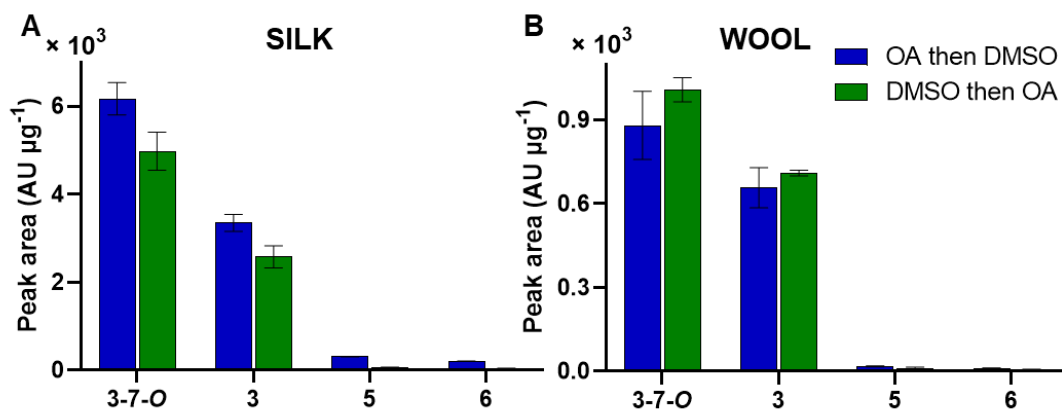


Figure 3.8: **A:** Peak area μg^{-1} of chromophores in silk samples dyed using weld overdye with woad following OA then DMSO extraction and DMSO then OA extraction. **B:** Peak area μg^{-1} of chromophores in wool samples dyed using weld overdye with woad following OA then DMSO extraction and DMSO then OA extraction. ($n = 3$, mean \pm S.D). All chromatograms extracted at 254 nm. **3-7-O** = luteolin-7-*O*-glycoside, **3** = luteolin, **5** = apigenin, **6** = chrysoeriol.

OA then DMSO extraction method gave a 24 % and 30 % increase in **3-7-O** and **3** yield respectively in comparison to the DMSO then OA method (Fig 3.8A). The opposite effect can be seen for wool (Fig 3.8B) although the greater standard deviation of OA then DMSO does not make it possible to draw any statistical conclusions.

Despite some uncertainty due to the results observed in the wool samples, the OA then DMSO extraction method was chosen. The increase in yield of the flavonoids in silk samples when using the OA then DMSO extraction was used to rationalise this decision. Another major advantage of using the OA then DMSO extraction method would make direct comparison of the OA result between samples not requiring DMSO extraction (e.g. yellow) and samples needing DMSO extraction (e.g. green) possible. Another benefit influencing the decision was that it was not possible to completely dry OA extracts following DMSO extraction. This was not an issue for DMSO extracts following OA extraction as the DMSO extracts were not dried. The extracts were not combined in the drying step to reduce the number of transfers and make it possible to use the same method preparation for LC analyses as well as more DMSO-sensitive techniques such as MS.

3.4 Filtration step

Since dirt and other solid contaminants often are present on historical samples, the filtration step was seen as an essential step to remove any particulates that could block instrumentation. Filtration inherently involves a loss of volume so to reach the aim of a more reproducible analysis, the percentage recovery needs to be consistent across concentrations and volumes.

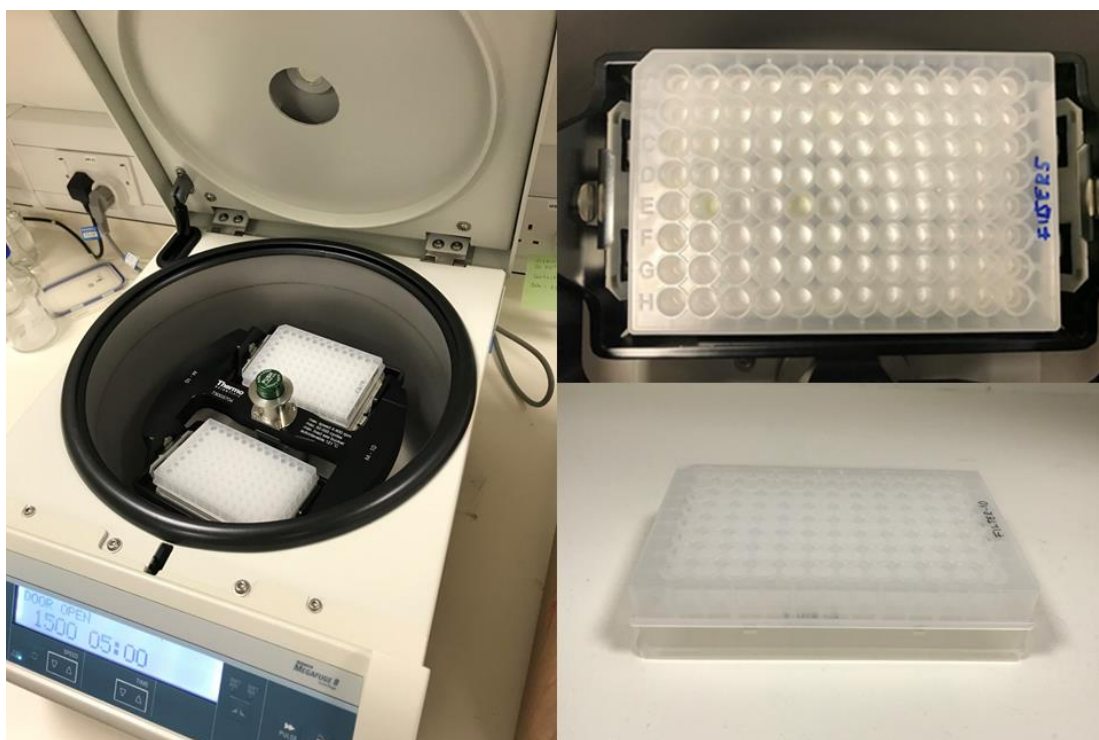


Figure 3.9: Filtration set-up with a 96 well filter plate over a receiving plate shown in a Thermo Scientific Megafuge 8 centrifuge with a M10 Microplate swinging bucket rotor. Detail of well plate set-up on the right.

The filtration set-up was a 96 well filter plate on top of a 96 well receiving plate, which was placed in the centrifuge (Fig 3.9). Polytetrafluoroethylene (PTFE) filters have been used with success for most natural dye extracts. The filter well plate chosen had 0.2 μm PTFE membranes with a hold-up volume of 2 μL (Section 2.2.1). The parameters to optimise were 1: the need for washes, 2: the centrifugation speed and 3: centrifugation time, before evaluation of the percentage recovery and linearity could be conducted.

3.4.1 Filtration step optimisation

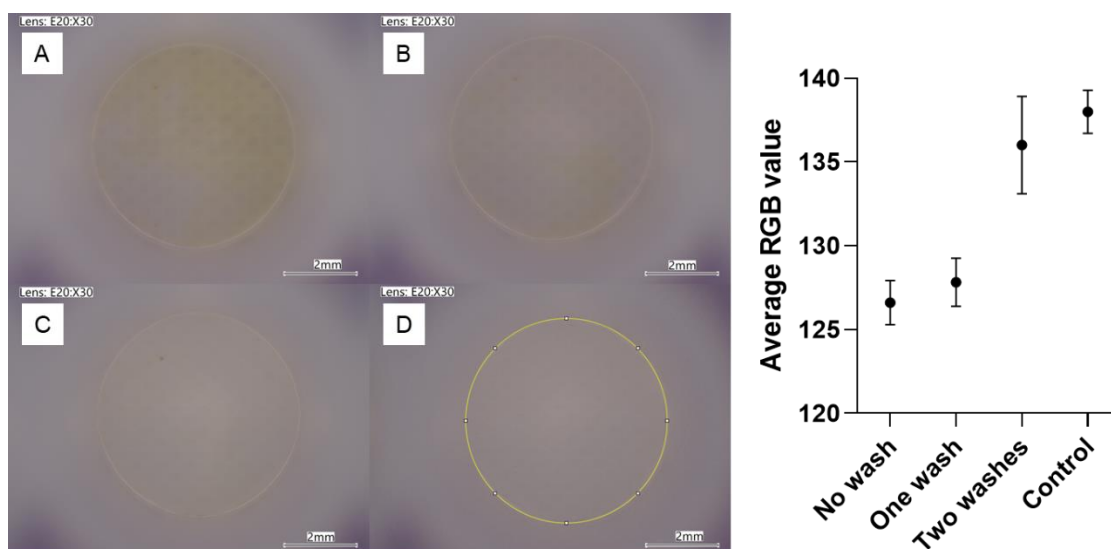


Figure 3.10: Left: **A:** Microscope image of filter plate well of 50 μL standard mixture 1 ($20 \mu\text{g mL}^{-1}$) after filtration by centrifugation (5 min \times 1500 rpm) and no wash. **B:** Microscope image of filter plate well of 50 μL standard mixture 1 ($20 \mu\text{g mL}^{-1}$) after filtration by centrifugation (5 min \times 1500 rpm) and one wash (25 μL 1:1 MeOH:H₂O v/v). **C:** Microscope image of filter plate well of 50 μL standard mixture 1 ($20 \mu\text{g mL}^{-1}$) after filtration by centrifugation (5 min \times 1500 rpm) and two washes (2 \times 25 μL 1:1 MeOH:H₂O v/v). **D:** Microscope image of clean filter plate well (control) showing the selection area used for all RGB measurements. Right: The average RGB value obtained for each of the wells showing the overlap of two washes and the control.

The need for washing the filter plate wells was made obvious when a faint taint of yellow could still be seen on the filter after filtration of the standard mixture 1 (Fig 3.10A). The number of required washes was determined by filtering 50 μL standard mixture 1 ($20 \mu\text{g mL}^{-1}$) at 1500 rpm for 5 min and captured a microscopy image of the well. The wells were then washed with 25 μL 1:1 MeOH:H₂O v/v, the well plate filtered and photographed. A second wash was conducted, and the procedure repeated.

The bottom of the wells was selected (3.10D) and the average RGB value of the selected area was found by ImageJ and compared to the average RGB value of controls (Fig 3.10, Right). The RGB colour model assigns a red, green and blue colour value to all colour hues, which can either be used individually or as an average. The scale goes from black (average RGB = 0) to white (average RGB = 255).³² The results show the expected increase in average RGB value with the number of washes as colour is removed from the wells. Two washes were found to be enough to match the

average RGB value of the controls (Fig 3.10, Right) and was the number of washes employed in the workflow.

Secondly, the optimised filtration speed was recommended to 1500 rpm by suppliers³³ so 1500 rpm was used as the starting point for the centrifugation speed investigation. Fixed volumes (50 μL) of standard mixture 1 (20 $\mu\text{g mL}^{-1}$) (Section 2.2.2) were filtered in triplicate at 1000, 1500 and 2000 rpm for 5 minutes before immediate injection into the UHPLC. It was found that the product recommendations of 1500 rpm was indeed the optimised speed as all peaks in the chromatograms using 1500 rpm were taller than the peaks of the other speeds (Fig 3.11A).

The third variable, the centrifugation time, was decided the same way as the filtration speed. The supplier recommendation was 5 minutes, 50 μL standard mixture 1 (Section 2.2.2) at concentration 20 $\mu\text{g mL}^{-1}$ was filtered at 1500 rpm for 2.5, 5 and 10 minutes and the results compared (Fig 3.11B). The difference between the 5 and 10 min run was negligible and as one of the overall aims of the workflow developed was increased time efficiency, 5 minutes was decided to be the centrifugation time.

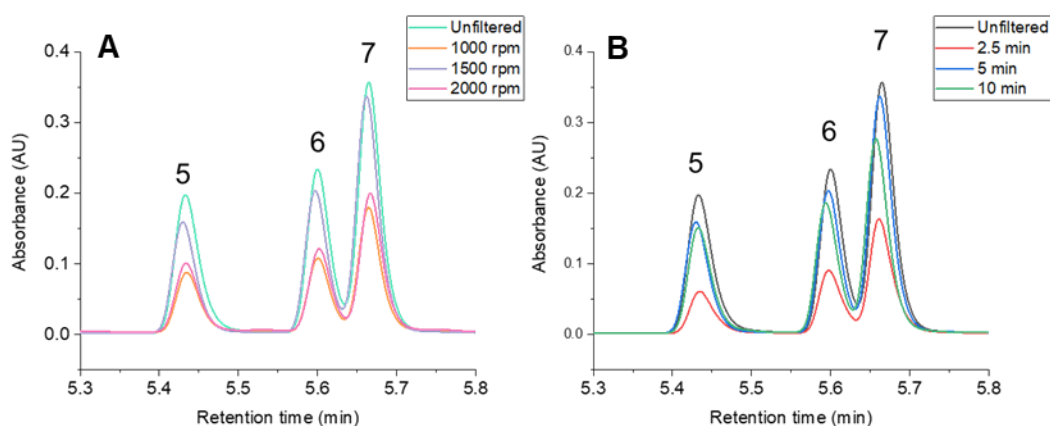


Figure 3.11: **A:** Zoomed-in overlaid chromatograms comparing the peak heights of apigenin (5), chrysoeriol (6) and diosmetin (7) in standard mixture 1 (20 $\mu\text{g mL}^{-1}$) after filtration with different centrifugation speeds (1000, 1500, 2000 rpm) compared to a control of unfiltered standard solution (20 $\mu\text{g mL}^{-1}$). **B:** Zoomed-in overlaid chromatograms comparing the peak heights of apigenin (5), chrysoeriol (6) and diosmetin (7) in standard mixture 1 (20 $\mu\text{g mL}^{-1}$) after filtration with different centrifugation times (2.5, 5, 10 min) compared to a control of unfiltered standard solution (20 $\mu\text{g mL}^{-1}$). Chromatograms extracted at 254 nm.

3.4.2 Filtration step evaluation

The filtration step must show a good and consistent percentage recovery to minimise the sample mass required as filtration inherently involves a loss of volume. The percentage recovery was tested at seven concentrations ($0.1 - 20 \mu\text{g mL}^{-1}$) using five repeats of $50 \mu\text{L}$ standard mixture 1 (Section 2.2.2) (Fig 3.12). The percentage recoveries of the standards were calculated by dividing each filtered peak area by each unfiltered peak area and finding the average and standard deviation. Figure 3.12 shows the calculated percentage recovery of all standard mix chromophores at a low and high concentration ($0.5 \mu\text{g mL}^{-1}$ and $20 \mu\text{g mL}^{-1}$). The other five concentrations are reported in Appendix A1.

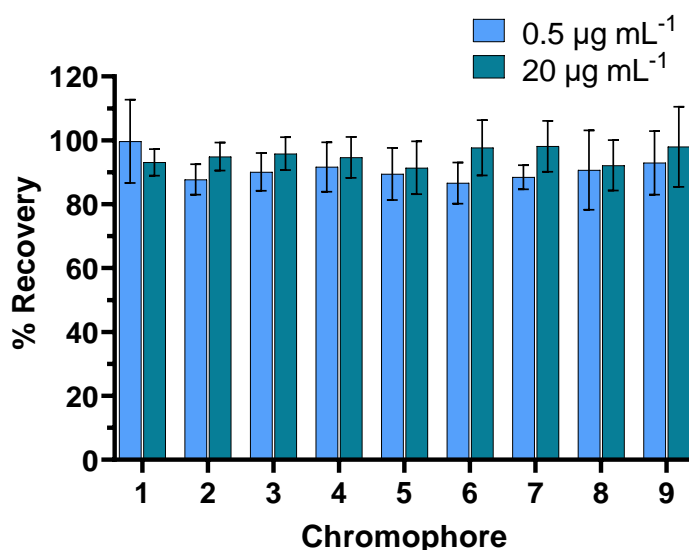


Figure 3.12: Left: Average percentage recovery and standard deviation ($n = 5$, mean \pm S.D) of the chromophores in standard mixture 1 (Section 2.2.2) at low ($0.5 \mu\text{g mL}^{-1}$) and high ($20 \mu\text{g mL}^{-1}$) concentration. All chromatograms extracted at 254 nm .

Across all standards and concentrations ($0.1 \mu\text{g mL}^{-1} - 20 \mu\text{g mL}^{-1}$), the percentage recovery was $> 85 \%$ making the volume loss acceptable even for low concentrations. The standard deviations for the high and low concentrations are all $< 10 \%$ except for **9** (high concentration) and **1, 8** (low concentration), which have standard deviations $< 13 \%$. These larger variations are still within the limit recommended by the FDA for bioanalytical method validations³⁴ ($\pm 15 \%$), so the reproducibility shown will allow quantitative analysis if necessary. The larger variation of **8** might be due to partial protonation of anthraquinones in the UHPLC method developed³⁵ impacting the analysis at low concentration, while the larger variability of **9** at high concentration

might be due to reduced solubility³⁶ in the solvent used (MeOH:H₂O 1:1 v/v), as the greater variability is observed in the unfiltered samples.

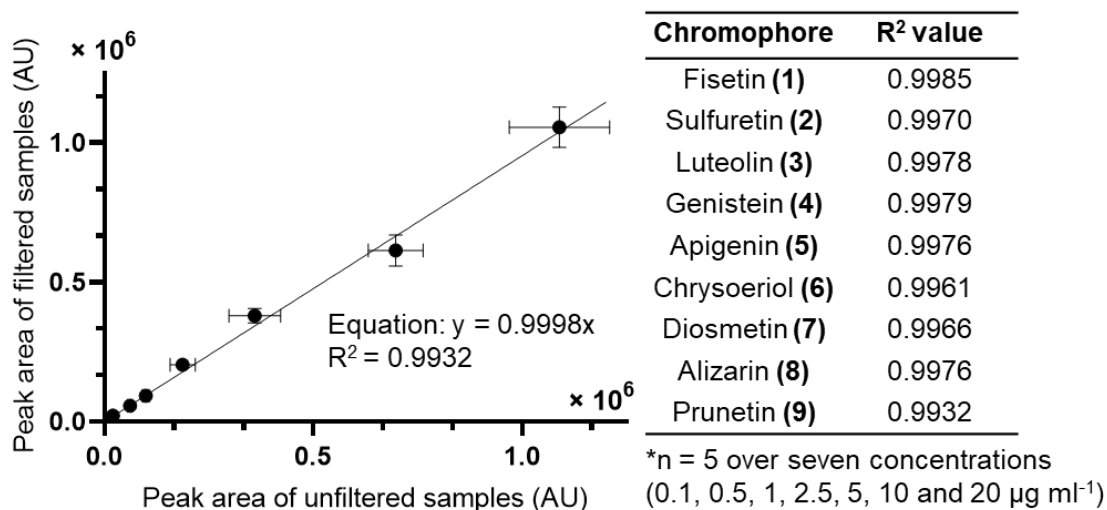


Figure 3.13: Filtered vs unfiltered peak areas graph of prunetin (9) in standard mixture 1 at seven concentrations ranging from 0.1 – 20 µg mL⁻¹ shown as an example. All graphs shown in Appendix A1. The resulting adjusted R² values from the filtered vs unfiltered graphs for all chromophores in standard mixture 1 shown in the table. Peak areas found from chromatograms extracted at 254 nm, n = 5.

The other factor evaluated for the filtration step was the linearity of the volume loss across the concentrations. Many dye analysis studies use relative peak areas, and the mentioned increased use of ratio of aglycone : glycoside for individual dye compounds (Section 3.3) means that it is important that the sample preparation method does not affect the relative ratio of the chromophores in the sample at any concentration at the chosen wavelength of the analysis. To test the linearity of the volume loss, the peak area of the unfiltered vs the peak area of the filtered was plotted and the intercept fixed at 0 (Fig 3.13). All chromophores show linearity of volume loss (R² = 0.9932 – 0.9985), meaning that the volume loss is consistent across all concentrations.

This level of linearity demonstrates that the sample preparation method is unlikely to impact the relative aglycone:glycoside ratio of the tested dyestuffs at any concentration, meaning that this ratio can be used in further research. This impact of on glycone : aglycone ratio was further investigated using a 1:1 v/v solution of standard mixture 1 (20 µg mL⁻¹) and luteolin-7-O-glycoside (3-7-O) (36 µg mL⁻¹). Triplicates of filtered and unfiltered samples of this solution were run on the UHPLC-

PDA and the glycone : aglycone ratio of each sample calculated using the peak area of **3-7-O** and **3**.

The average **3-7-O** : **3** ratio of the filtered samples was found to be 3.23 ± 0.07 ($n = 3$) and for the unfiltered, the ratio was calculated as 3.19 ± 0.01 ($n = 3$) (Appendix A1). The ratio values for the filtered and unfiltered samples overlap, which supports that the filtration step has a negligible effect on the glycone : aglycone ratio of **3**.

Overall, the percentage recoveries of compounds **1-9** in standard mixture 1 at 20 and $0.5 \mu\text{g ml}^{-1}$ show an average of 93 % (range 87 – 100 %) with an average relative standard deviation of 7.7 % (range 3.8 – 13 %) and all compounds show a linear volume loss (> 0.9932). This means that the filtration step can be used in dye analysis studies with confidence.

3.5 Drying and reconstitution step

The last factor that will influence the efficiency of the sample preparation method is the reconstitution solvent. High solubility of all dyestuffs in the reconstitution solvent is necessary to increase the concentration of the analyte and thus minimise the sample size required. The reconstitution solvent must thus be chosen with care and ideally be MS compatible and show low toxicity. The last point is the reason DMSO but not DMF was tested. The main limitation of the reconstitution step was the reliance on pipetting skill, increasing the risk for spilling.



Figure 3.14: Left: Placing the 96 well plate with the samples in the desiccator. Right: Reconstituting the samples in the wells.

The solubility power of four different solvents: DMSO, 10 % DMSO in MeOH:H₂O 1:1 v/v, MeOH:H₂O 1:1 v/v and 0.1 % FA in MeOH:H₂O 1:1 v/v were tested by drying 50 μl unfiltered solution of compounds **1-9** ($20 \mu\text{g mL}^{-1}$) in a desiccator and reconstitution

at three different volumes (10 μL , 25 μL , 50 μL) for all four solvents. The experiment was performed in triplicate and the peak areas compared to each other and a control of 50 μL of the initial, unfiltered solution of compounds **1-9** (Fig 3.15).

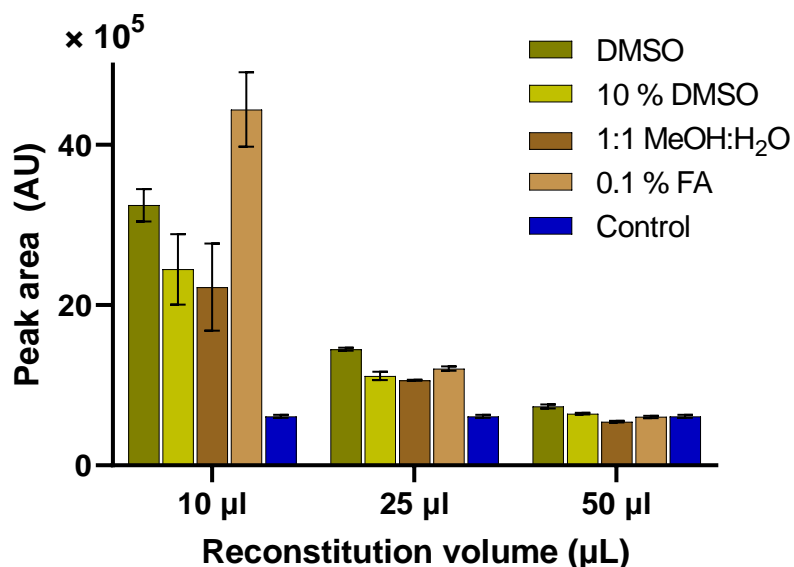


Figure 3.15: Comparison of four reconstitution solvents at three different volumes. Prunetin (**9**) shown as an example of the general trend seen across the chromophores (Appendix A1). ($n = 3$, mean \pm S.D). All chromatograms extracted at 254 nm.

An expected doubling in concentration of all chromophores in standard mixture 1 was seen for all solvents in the 25 μL run compared to the control sample, highlighting the impact of the reconstitution step. The lower reconstitution volume of 10 μL show at minimum a quadrupling of chromophores. However, as the reconstitution was conducted manually, the practical difficulty of pipetting 10 μL can be seen in the large standard deviations obtained, decreasing the reproducibility of the method. 25 μL was thus chosen as the reconstitution volume.

The error of all solvents for all standards were $< 5\%$, so 0.1 % FA in MeOH:H₂O 1:1 v/v was chosen as the reconstitution solvent based solely on the better recovery of chromophores **1 – 9** from this solvent. Experimentally, it was observed that the peaks obtained for the flavonoid glycosides luteolin-7-*O*-glycoside (**3-7-O**) and apigenin-8-*C*-glycoside (**5-8-C**) were not symmetrical with any of the solvents tested. Instead, MeOH:H₂O 1:3 v/v was found to be the reconstitution solvent that gave the most symmetrical peaks for these compounds (Fig 3.16).

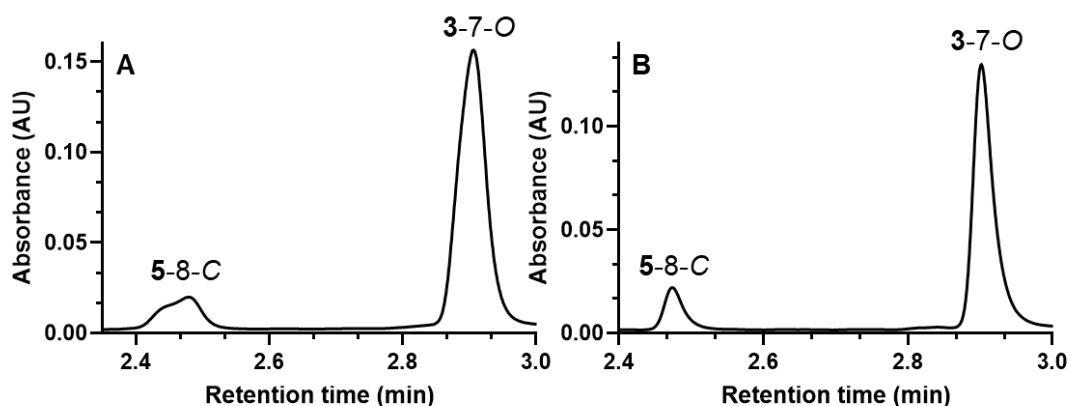


Figure 3.16: **A:** Zoomed-in chromatograms of luteolin-7-*O*-glycoside (**3-7-O**) and apigenin-8-*C*-glycoside (**5-8-C**) in weld samples reconstituted using 0.1 % FA in MeOH:H₂O 1:1 v/v. **B:** Zoomed-in chromatograms of luteolin-7-*O*-glycoside (**3-7-O**) and apigenin-8-*C*-glycoside (**5-8-C**) in weld samples reconstituted using MeOH:H₂O 3:1 v/v. Chromatograms extracted at 254 nm.

3.6 Liquid chromatography

Reverse-phased LC, which has a polar mobile phase (MP) and a non-polar solid phase (SP), is usually used in natural dye analysis resulting in the more polar compounds in the sample partitioning less and eluting earlier. The separation of two peaks is described by the resolution factor (R_s) (Equation 3.1 and 3.2) which is the factor to optimise during the method development stage. Typically, R_s values > 1.5 are seen as the limit for complete separation of two components.^{37,38}

$$R_s = \frac{(t_2 - t_1)}{0.5(W_1 + W_2)} \quad \text{Equation 3.1}$$

t_2 and t_1 = retention time of the peaks investigated, W_1 and W_2 = width of the peaks investigated.

Resolution of a method can also be described by Equation 3.2 which highlights the three factors affecting the resolution: efficiency (N), selectivity (α) and retention (k) (Fig 3.17).³⁸

$$R_s = \frac{k}{k-1} \times \frac{\alpha-1}{\alpha} \times \frac{1}{4} \sqrt{N} \quad \text{Equation 3.2}$$

N = plate number, α = selectivity factor and k = retention factor.

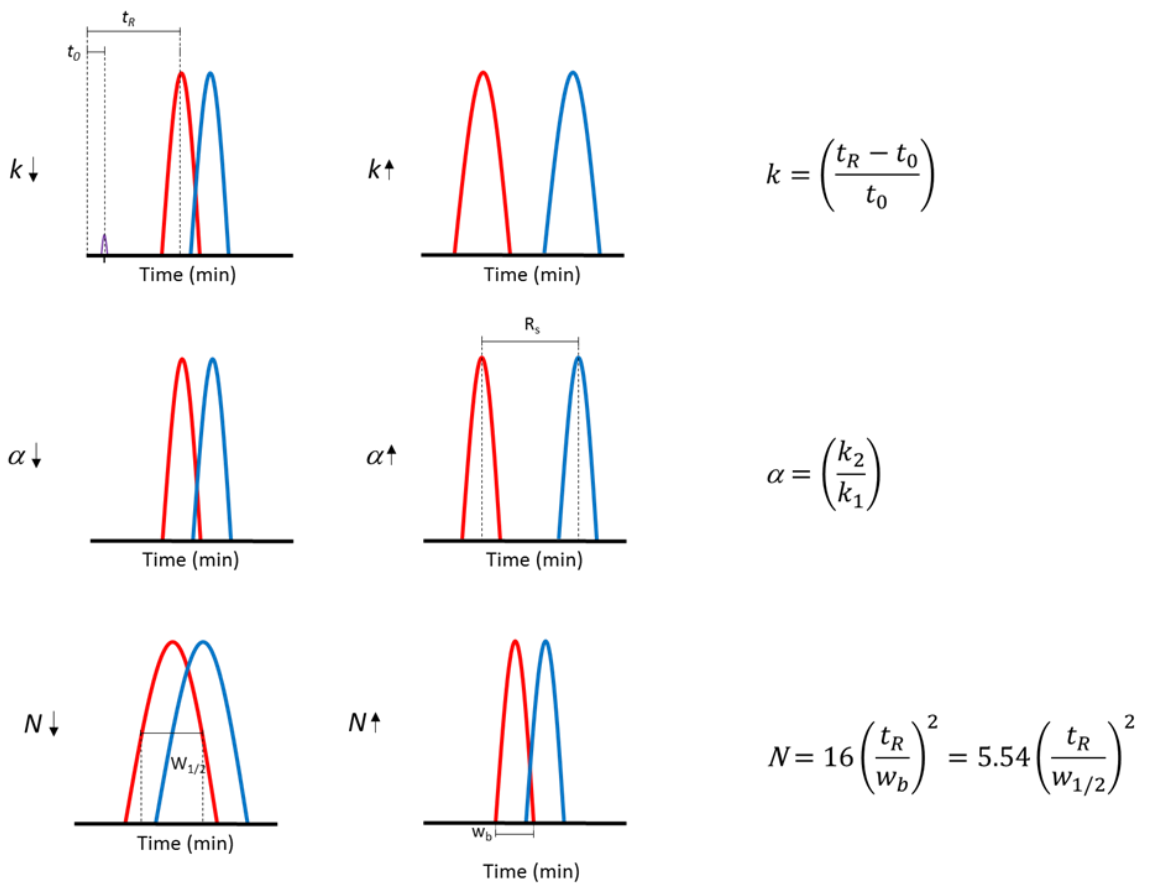


Figure 3.17: **Top row:** shows how k influences peak separation. **Left:** schematic of chromatogram when k is small. **Right:** schematic of chromatogram when k is large. Graphical definitions of variables t_R and t_0 also shown. **Middle row:** shows how α influences peak separation. **Left:** schematic of chromatogram when α is small. **Right:** schematic of chromatogram when α is large. Graphical definition of variable R_s also shown. **Bottom row:** shows how N influences peak separation. **Left:** schematic of chromatogram when N is small. **Right:** schematic of chromatogram when N is large. Graphical definitions of variables $W_{1/2}$ and W_b also shown.

3.6.1 Retention

The time each component interacts with the SP is described by the retention factor, k , (Equation 3.3) which is a relative measure of the rate of elution of each component.

$$k = \frac{(t_R - t_0)}{t_0} \quad \text{Equation 3.3}$$

k = retention factor, t_R = retention time of the peak investigated, t_0 = unretained time, also known as the solvent peak.

Ideally, k should be 1 – 5, because if $k < 1$, the elution will occur so quickly it will be difficult to measure accurately and > 5 , the analytical time will be too long to be efficient. The retention factor can be changed by tuning the nature of the MP and SP, as well increasing the number of particles in the column, giving more opportunity for partition.³⁸

3.6.2 Selectivity

Selectivity is a measure of how the different chemistries of the compounds present in the sample interact with the SP. α is a measure of the relative selectivity between two compounds and is determined as the ratio of k of the two peaks in question (Equation 3.4). Selectivity can be difficult to predict and can be affected by changes in pH or temperature, but also by changing the nature of either the stationary or mobile phase.³⁷

$$\alpha = \frac{k_2}{k_1} \quad \text{Equation 3.4}$$

α = selectivity factor, k_1 and k_2 = retention factor of the peaks investigated.

3.6.3 Efficiency

Efficiency is the last factor that influences resolution, and it is a measure of how broad the peaks are. Sharper peaks lead to fewer peaks overlapping and thus better resolution, so maximising the efficiency is important during method development. The theory of efficiency has its roots in distillation theory, where separations are increased by amplifying the number of plates on which the components could re-condense in the distillatory tube. Plates are non-existent in LC, but plate number is still a term used to describe the efficiency of a LC method (Equation 3.5) and a large plate number means a better separation.³⁸

$$N = 16 \left(\frac{t_R}{w_b} \right)^2 = 5.54 \left(\frac{t_R}{w_{1/2}} \right)^2 \quad \text{Equation 3.5}$$

N = plate number, t_R = retention time of peak, w_b = baseline width of peak and $w_{1/2}$ = width at half the height of peak.

A more common term used when discussing efficiency is height equivalent to a theoretical plate (HETP) term, which describes the length of one plate in the column (Equation 3.6). As can be seen, a smaller HETP means a bigger N and a more efficient method.

$$HETP = \frac{L}{N} \quad \text{Equation 3.6}$$

HETP = height equivalent to a theoretical plate, N = plate number and L = length of the column.

The plate height and by extension, the efficiency is also related to the flow rate following the van Deemter equation (Equation 3.7)

$$HETP = A + \frac{B}{v} + Cv \quad \text{Equation 3.7}$$

HETP = height equivalent to a theoretical plate, A = eddy diffusion parameter, B = longitudinal diffusion coefficient, C = mass transfer coefficient, v = flow rate, also known as linear velocity.

The eddy diffusion parameter, A , describes the possible paths of an analyte through the column and decreases with particle size and even packing of the column. Longitudinal diffusion coefficient, B , is inversely related to v while C is directly related to the flow rate, and it has been shown that B is the more important term at low flow rates, and C is the more important term at high flow rates. These terms, as well as the maximum back pressure possible of the instrument all need to be taken into consideration when developing a new method.

3.6.4 HPLC vs U(H)PLC

High-performance liquid chromatography (HPLC) and Ultra-performance liquid chromatography (UHPLC™) utilise this theory and the technological improvements of pumps and columns.³⁹ HPLC instruments can handle pressures < 4,000 psi, while UHPLC instruments can work with pressures < 18,000 psi, meaning that smaller particles for the SP and a higher flow rate can be exploited in a UHPLC experiment in comparison to HPLC. This means a shorter analytical time is possible for the same separation and a reduction in volume of MP going to waste.

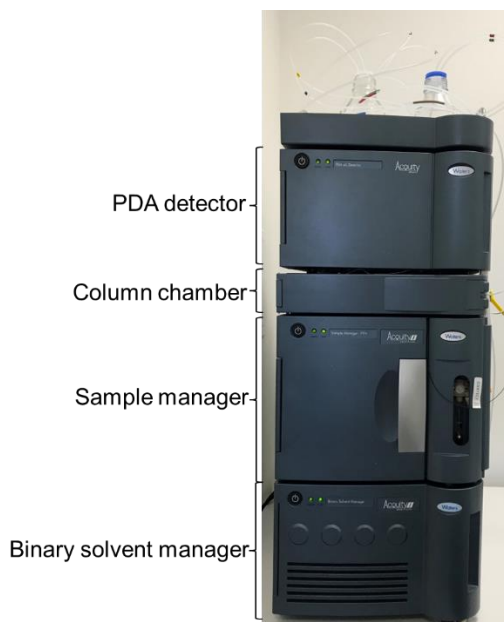


Figure 3.18: The Waters Acquity UHPLC-PDA instrument in NMS science laboratory. The PDA detector, column chamber, sample manager and binary solvent manager are labelled.

The science laboratory at NMS houses a Waters Acquity UHPLC-PDA instrument (Fig 3.18) which was used throughout this project. This instrument was used for optimisation of the method and all UHPLC-PDA analyses. To reduce the analytical time, a shorter column can be used, which also means all components have a shorter time partitioning through the column, reducing k . Additionally, Equation 3.6 shows that a shorter column means a larger HETP and a worse efficiency. To counter the loss in resolution from k and N , SP with smaller size particles and optimisation of the gradient and flow rate can be done. For this purpose, a Cortecs BEH C18 75 × 2.1 mm (length × i.d.), 90 Å (pore size), 1.6 μm (particle size) column, was purchased.

3.7 UHPLC method development

The developed method (Method 1) was based on and compared to the UHPLC method developed by Dr Lore Troalen²⁵ for the analysis of natural dyes in the laboratory in National Museums Scotland (NMS) (Method 2), which uses a PST BEH C18, 150 × 2.1 mm, 300 Å (pore size), 1.7 μm (particle size) column.

To prolong the lifetime of the column, a maximum back pressure of 13,000 psi and operating temperature of 45 °C were set as the upper limits for these parameters based on supplier recommendations. These limitations determined the flow rate to maximum 400 μL min⁻¹.

Since Method 1 will be used on the same compounds as Method 2, the gradient was translated to the new conditions using the Acquity column calculator transfer programme. This programme calculates the equivalent column volumes i.e. the volume of solvent present in the column when saturated, flow rates and gradient profiles between two methods using equations 3.8, 3.9 and 3.10, giving the gradients in Table 3.1.

$$V = L \times \pi \times r^2 \quad \text{Equation 3.8}$$

V = equivalent column volumes, L = length (cm) of the column and r = diameter (cm) of the column.

$$F_2 = F_1 \times \left(\frac{d_{c2}^2}{d_{c1}^2}\right) \times \left(\frac{d_p^2}{d_p^2}\right) \quad \text{Equation 3.9}$$

F_2 = new flow rate, F_1 = initial flow rate, d_c = internal diameter (mm) of each column and d_p = particle diameter (μm) of each column.

$$t_{g2} = t_{g1} \times \left(\frac{V_{02}}{V_{01}}\right) \times \left(\frac{F_2}{F_1}\right) \quad \text{Equation 3.10}$$

t_{g2} = new gradient profile, t_{g1} = initial gradient profile (min), V_0 = column void of each column, F_2 = flow rate of new method, F_1 = flow rate of initial method.

Table 3.1: Gradient profile of Method 1 and Method 2.

Method 1			Method 2		
Time (min)	A (%)	B (%)	Time (min)	A (%)	B (%)
0	77	23	0	77	23
1.17	77	23	3.33	77	23
10.92	10	90	29.00	10	90
11.29	77	23	30.00	77	23
13.92	77	23	37.33	77	23

The analytical time for a complete run of the method developed was just below 14 min and the total volume of solvent used per run is < 6 mL. The highest pressure reached is < 12,000 psi and typically 5 μL injection volume was used for each sample if the concentration was sufficient.

3.8 UHPLC method evaluation

Method 1 was evaluated by its performance characteristics chosen in accordance with IUPAC recommendations⁴⁰ on the standard mixture 1 (Section 2.2.2). Evaluation tests of resolution factors, repeatability, linearity, limit of detection (LoD) and limit of quantification (LoQ) were performed and compared to Method 2. Standard mixture 1 at seven concentrations ranging between $0.1 \mu\text{g mL}^{-1}$ – $20 \mu\text{g mL}^{-1}$ was used for the evaluation. For Method 2, standard mixture 2,²⁵ which includes 8 of the 9 compounds of standard mixture 1, at $0.2 \mu\text{g mL}^{-1}$ – $40 \mu\text{g mL}^{-1}$ was used.

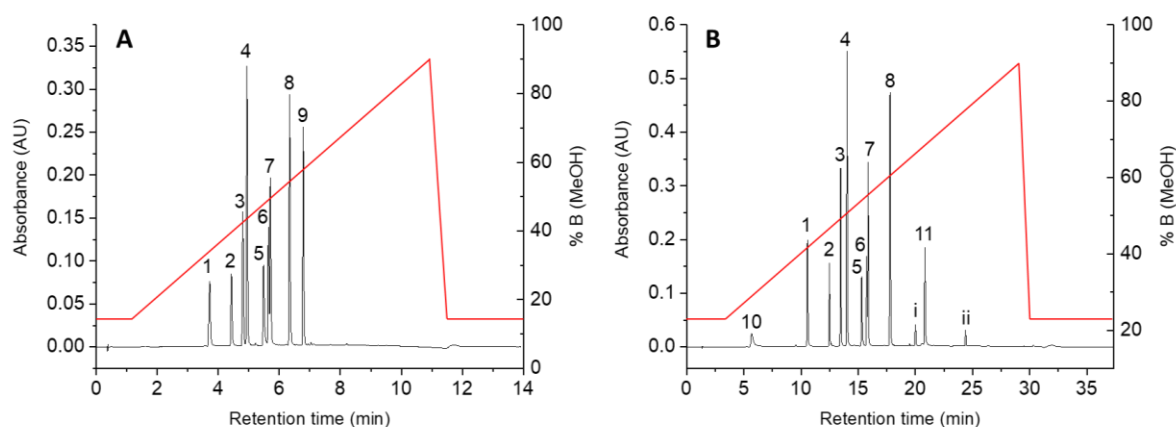


Figure 3.19: Chromatograms at 254 nm overlaid with the gradient profile for **A:** Method 1 using standard mixture 1 and **B:** Method 2 using standard mixture 2.

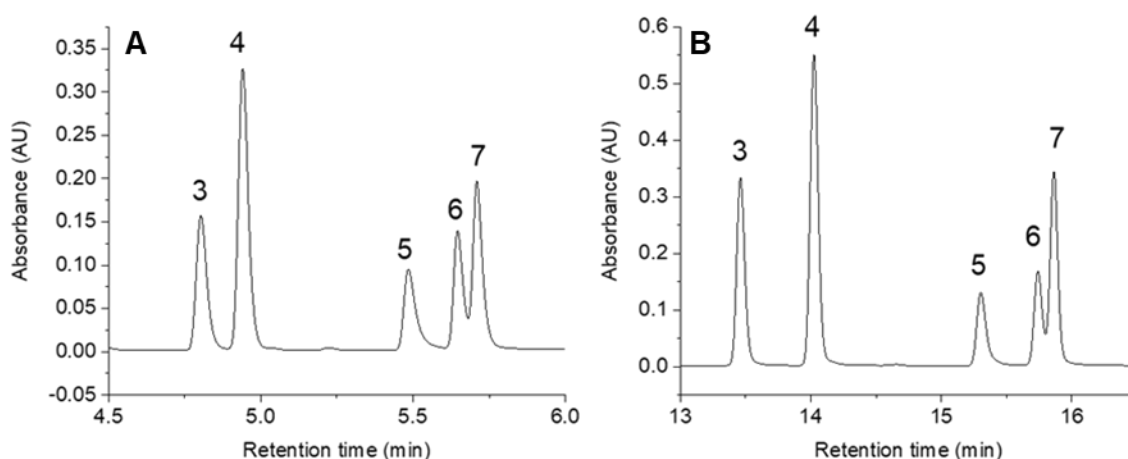
3.8.1 Repeatability and resolution factors

The need for good repeatability is highlighted by all chromophores in standard mixture 1 eluting within a 3 min range under Method 1, with compounds **3** – **7** eluting in a 1 min interval. The elution trials of **1** – **9** shows good overall repeatability, with a standard deviation range of 0.009 – 0.013 min ($n = 6$) (Table 3.2). Even the peak for compound **3**, which shows the greatest standard deviation (0.013 min), does not overlap with the range of its adjacent compounds. The retention times can thus be used for identification of the compounds in standard mixture 1 using Method 1. Method 2 shows similar repeatability for the compounds in standard mixture 2 with a range 0.004 – 0.012 min ($n = 12$).²⁵

Table 3.2: Retention time (n = 6) for compounds 1 – 9.

Chromophore	Retention time (min)	s.d. (min)
1	3.714	0.012
2	4.420	0.012
3	4.787	0.013
4	4.919	0.011
5	5.462	0.012
6	5.622	0.011
7	5.685	0.010
8	6.287	0.010
9	6.738	0.009

To establish the extent of co-elution, the resolution factors R_s (Equation 3.1) of adjacent compounds in standard mixture 1 were calculated. The average width of the peaks was determined by extrapolating the slope of the peaks and noting the retention time at $y = 0$. The R_s values for all adjacent peaks were > 1.5 , except for **6** and **7** which had a R_s value of 1.15 (Fig 3.20). In contrast, the R_s values of Method 2 were 1.32 for **6** and **7**, predictably giving a more efficient, although not a complete, separation overall. Compounds **6** and **7** are regioisomeric methylated flavones so are difficult to fully separate even on longer chromatographic methods. Both Method 1 and 2 show two clear peak maxima of **6** and **7** despite the co-elution and since most dye analysis investigations are semi-quantitative, the level of separation obtained was considered acceptable.

**Figure 3.20:** Zoomed-in chromatograms at 254 nm showing the extent of co-elution seen for compounds 3 – 7 of **A:** Method 1 using standard mixture 1 and **B:** Method 2 using standard mixture 2

3.8.2 Linearity and calibration curves

Peak height was plotted against change in concentration in the calibration curves constructed for all chromophores in standard mixture 1. Peak area can also be used and is often preferred for calibration curves of HPLC methods as the peaks in HPLC chromatograms often are asymmetric. Thus, the peak height is also influenced by other factors than change in concentration. However, the disadvantage with peak area is that very diluted samples must be used as estimates for blank samples. In UHPLC, the peaks are generally symmetrical so peak height and blanks can be used.³⁴

Linearity of the chromatographic response with the change in concentration was determined by constructing calibration curves (concentration ($\mu\text{g mL}^{-1}$) vs peak height (AU)) of the reference compounds in standard mixture 1 using an injection volume of 5 μL . Seven concentrations ($0.1 \mu\text{g mL}^{-1}$ – $20 \mu\text{g mL}^{-1}$) were used and each concentration was repeated five times. The lines-of-best-fit and correlation coefficients (R^2) of the calibration curves were evaluated to determine the linearity.

Table 3.3: Equation, calculated slope error and R^2 values of the calibration curves (Peak Height (AU) vs Concentration ($\mu\text{g mL}^{-1}$), (7 concentrations ($0.1 \mu\text{g mL}^{-1}$ – $20 \mu\text{g mL}^{-1}$), $n = 5$))

Chromophore	R^2 value
1	0.9958
2	0.9997
3	0.9995
4	0.9999
5	0.9729
6	0.9653
7	0.9999
8	0.9935
9	0.9842

The largest diversion from a linear response ($R^2 = 1$) was found to be chrysoeriol (**6**) with a $R^2 = 0.9653$ (Table 3.3). This is likely due to the co-elution of **6** and **7** as shown by their $R_s = 1.17$. Apigenin (**5**) and prunetin (**9**) are the only other two that have a $R^2 < 0.99$, which probably has to do with imperfect peak shape (Fig 3.20) and solubility³⁶ respectively. The linearities obtained are comparable to the linearities of Method 2, which are in the range of $0.9675 - 0.9999$,²⁵ making the values acceptable for the dye analysis field.

3.8.3 Limit of detection (LoD) and limit of quantification (LoQ)

The limit of detection (LoD) and limit of quantification (LoQ) was calculated by the signal-to-noise-method and are measures of the lowest amount of each chromophore in standard mixture 1 that can be confidently detected and quantified. The limits for LoD and LoQ used were: $LoD \geq 3.3 |N|$ and $LoQ \geq 10 |N|$.^{21,41} The noise N was defined as the average signal obtained in blank samples ($n = 3$) (Appendix A1) around the retention time (± 0.25 min) of each analytical peak.

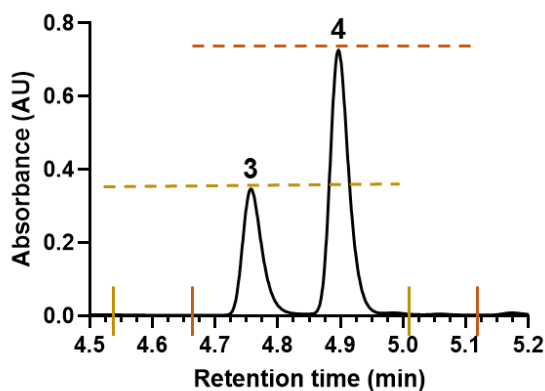


Figure 3.21: Zoomed in chromatogram of standard mixture 1 ($20 \mu\text{g mL}^{-1}$) showing luteolin (3) and genistein (4). The range of values used for the noise determination (retention time ± 0.25 min) is shown in yellow (3) and in orange (4).

Table 3.4: Limit of detection (LoD) and limit of quantification (LoQ) for chromophores in standard mixture 1 calculated using the signal-to-noise method ($n = 5$ for all concentrations, $n = 3$ for blanks).

Chromophore	LoD ($\mu\text{g ml}^{-1}$)	s.d.	LoQ ($\mu\text{g ml}^{-1}$)	s.d.
1	0.29	0.03	0.88	0.03
2	0.40	0.03	1.21	0.03
3	0.21	0.03	0.65	0.03
4	0.11	0.03	0.32	0.03
5	0.44	0.07	1.33	0.07
6	0.37	0.07	1.13	0.07
7	0.27	0.02	0.83	0.02
8	0.19	0.06	0.59	0.06
9	0.27	0.06	0.83	0.06

The LoD and LoQ ranges obtained (Table 3.4) show the the highest LoD and LoQ at 0.44 and 1.33 $\mu\text{g mL}^{-1}$ relate to apigenin (**5**) which may again be explained by its imperfect peak shape (Fig 3.20). The ranges of Method 1 are comparable to the LoD and LoQ of Method 2 using the same injection volume of 5 μL (LoD: 1.01 – 0.10 $\mu\text{g mL}^{-1}$, LoQ: 3.06 – 0.32 $\mu\text{g mL}^{-1}$)²⁵ as well as similar natural dye studies using UHPLC-PDA.^{39,42,43}

Overall, the evaluation showed that the UHPLC method developed can be used for dye analysis with confidence. This shorter method in combination with the developed sample preparation workflow thus reduces the analytical time and resources needed whilst the overall reproducibility is increased.

3.9 Application of workflow

The developed sample preparation protocol and chromatographic method were applied to silk and wool samples dyed with natural dyestuffs (Section 2.2.3) and samples from Flora MacDonald's wedding tartan (Section 2.2.3). The protocol and chromatographic method were also applied to the samples collected from the embroidery collection at NMS (Chapter 4).

3.9.1 Application to natural dye references

To test the method's efficiency on a variety of natural dyestuffs as well as the bulk capacity of the method, a total number of 85 samples dyed with 12 dyestuffs were simultaneously prepared and analysed by the sample preparation protocol and UHPLC-PDA method developed. To see if the fibre had any impact on the analysis, 5 of the dyestuffs were investigated on both wool and silk (Table in Fig 3.23).

The reproducibility of the method was evaluated using the relative percentage peak areas of characteristic markers for each dyestuff ($n = 5$). The key markers for each dye were determined by literature (Section 1.4) and the relative peak area of the key compounds were integrated using the ApexTrack approach (Section 3.3.1). The chromatograms were monitored at the various wavelengths that are commonly used for dyestuff identification.² The chromatogram and subsequent relative percentage peak area calculated for madder (*Rubia tinctorum* L.) on silk is shown as an example of how the relative percentage peak areas were calculated (Figure 3.22).

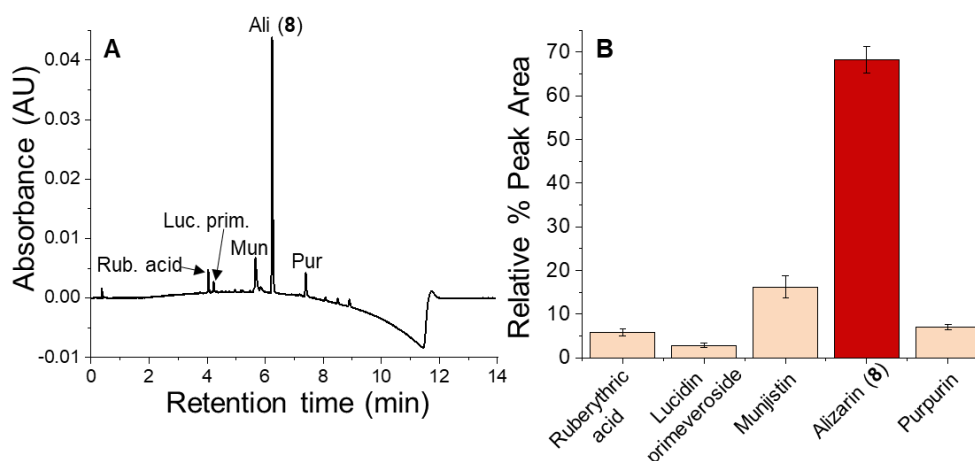
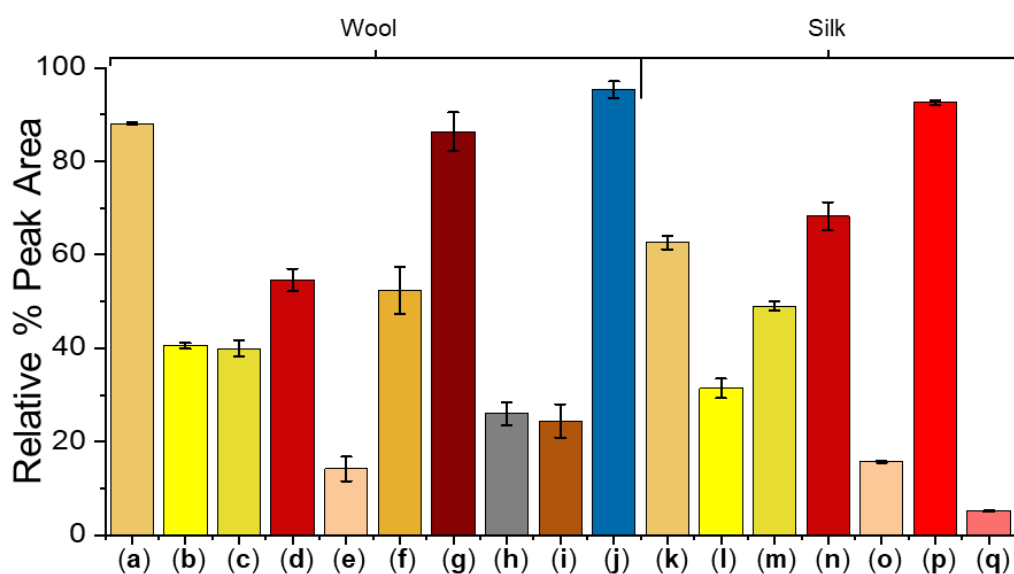


Figure 3.22: **A:** chromatogram monitored at 430 nm of madder (*Rubia tinctoria* L.) on silk. The key markers of madder are labelled. **B:** the integrated peak area of all the key markers normalised to 100 % ($n = 5$, mean \pm s.d.). Figure reproduced from E. Sandström *et al.*¹² with permission from the Royal Society of Chemistry.

The key markers for *Rubia tinctoria* madder are alizarin (**8**), purpurin and munjistin with their glycosidic conjugates. Ruberythric acid is an alizarin glycoside and lucidin primeveroside a lucidin glycoside. The integrated peak areas of the key markers were calculated and normalised to 100 % (Fig 3.22B). The variability ($n = 5$) of the main chromophore for each dyestuff was then calculated (Fig 3.23). The principal characteristic chromophore is not always the most abundant, explaining the variety in percentage areas shown for each dyestuff.

The OA extracts for all samples were used with the exception of the investigation of indigotin in woad on weld, which used the DMSO extract. Woad on weld was used instead of woad alone so that the chromophores present in weld could be seen for comparison. For these samples, the peak areas of the yellow compounds were extracted at 350 nm and the peak area of indigotin was extracted at 630 nm and these were used to calculate the relative percentage and variability of indigotin in the samples.



Dyestuff	Fibre	Key chromophore	Relative % Area	s.d.	Monitored at λ (nm)
(a) Young fustic	Wool	Sulfuretin (2)	88.08	0.26	350
(b) Weld	Wool	Luteolin (3)	40.60	0.60	350
(c) DGW	Wool	Genistein (4)	39.93	1.70	350
(d) Madder	Wool	Alizarin (8)	54.63	2.39	430
(e) Brazilwood	Wool	Brazilin	14.22	2.63	254
(f) Turmeric	Wool	Curcumin	52.45	5.09	430
(g) Kermes	Wool	Kermesic acid	86.32	4.19	475
(h) Logwood	Wool	Hematein	26.05	2.44	254
(i) Oakgalls	Wool	Ellagic acid	24.48	3.58	254
(j) Woad (on weld)	Wool	Indigotin	95.32	1.80	350/630
(k) Young fustic	Silk	Sulfuretin (2)	62.64	1.40	350
(l) Weld	Silk	Luteolin (3)	31.47	2.08	350
(m) DGW	Silk	Genistein (4)	49.07	1.03	350
(n) Madder	Silk	Alizarin (8)	68.24	3.05	430
(o) Brazilwood	Silk	Brazilin	15.75	0.18	254
(p) Cochineal	Silk	Carminic acid	92.64	0.45	475
(q) Safflower	Silk	Carthamin	5.23	0.14	300

Figure 3.23: The average relative % area of the key chromophore of each reference dyestuff used ($n = 5$, mean \pm s.d.). The dyestuff, fibre, key chromophore, relative % area, standard deviation and what wavelength was used can be seen in the table. Figure reproduced from E. Sandström *et al.*¹² with permission from the Royal Society of Chemistry.

The repeatability of the method was shown by the low standard deviation seen across all reference samples, with the highest standard deviation being 4.2 %. One exception, turmeric (5.1 %) can be explained by the partial co-elution of curcumin with bisdemethoxycurcumin and demethoxycurcumin, which are all abundant in turmeric extracts.²⁰

No major difference in repeatability between the wool (Fig 3.23a – j) and silk (Fig 3.23k – q) can be seen, meaning that the method is efficient on both fibre types. The low standard deviations also suggest that the method can be used on all dye classes: vat dyes (woad on weld), direct dyes (safflower and turmeric) and mordant dyes (all others). The complete analysis of the 85 samples took < 24 h including all the UHPLC analyses which were run overnight. This highlights the advantage of the method when a large number of samples is available. The low standard deviations also show the benefit of a more automated approach, meaning that less error is introduced overall.

3.9.2 Flora MacDonald wedding tartan

The sample preparation workflow and chromatographic method was also applied to historical samples from the wedding tartan of Flora MacDonald (WHM.1961.02) housed in the West Highland Museum, Fort William. The tartan is the focus of a Spirit of the Highlands project (Highlife Highland) led by dress historian Jo Watson.⁴⁴



Figure 3.24: **Left:** Portrait of Flora MacDonald by Allan Ramsay c. 1749 – 1750 ©Ashmolean Museum, University of Oxford, potentially wearing the tartan found in the West Highland Museum 2021. **Right:** the tartan piece sampled (WHM.1961.02) ©Jo Watson.

Flora MacDonald was instrumental in the escape of Bonnie Prince Charlie back to France after the devastating defeat of the Jacobites at the Battle of Culloden in 1745. She famously was said to have secured passage for the Prince to the Isle of Skye by dressing him as an Irish spinning maid to avoid British capture.⁴⁵ She was imprisoned in the Tower of London for her troubles but was released in 1747 and returned to Scotland. It was in 1750 she wore the tartan analysed during her wedding to Allan MacDonald. The couple emigrated to America in 1774 but were forced to return to

Scotland in 1779 after her husband, who had joined the British side in the American Revolution, was captured by American rebels and their plantation destroyed. She was buried on the Isle of Skye in 1790.

Her actions helping Bonnie Prince Charlie made her a celebrated Jacobite legend and Scottish national hero, despite no evidence that she was particularly sympathetic to the Jacobite cause. Instead, she has been recorded stating that the reason for her actions was borne out of sympathy for a desperate man more than any political agenda.⁴⁵ Regardless of where her loyalty laid, her wedding tartan signifies a tumultuous time in Scottish history. Characterising the dyes used in it will help with display and conservation of the tartan piece as well as help put it in a global context.

The tartan shows a red ground with blue, green, and brown patterns and all four colours were sampled by Jo Watson (Fig 3.25).



Figure 3.25: Investigated samples from the wedding tartan of Flora MacDonald. Samples collected by Jo Watson.

The blue sample was identified to have been dyed with indigo dye by the presence of indigotin (Section 1.4.3) (Fig 3.26A). Fisetin (1), sulfuretin (2) and luteolin (3) were also characterised, indicating the use of young fustic (Section 1.4.2.1). Additionally, alizarin (8), the main component in dyer's madder (Section 1.4.2.2) were also found. The addition of young fustic and madder were likely done to brighten and deeper the blue colour to reach the desired shade.

The red sample was dyed with cochineal by the identification of carminic acid, dcII, dcIV, dcVII and flavokermesic acid (Section 1.4.2.2) (Fig 3.26B). Statistical models

using the minor components present in cochineal samples have been constructed to differentiate between species of cochineal.^{8,26} Unfortunately, these require large datasets of reference materials not available to this study, so species identification could not be established. However, Mexican cochineal has been identified in tartans contemporary to Flora's,⁴⁶ so it is likely that Mexican cochineal was used.

The green sample was dyed with a mixture of old fustic and Saxon blue indicated by the presence of the flavonoids morin, maclurin and kaempferol (Section 1.4.2.1) and indigo carmine and indigotin (Section 1.4.3) (Fig 3.26C). Saxon blue was invented in Germany in 1743 so it would be available to the makers of the wedding tartan in 1750.⁴⁷ The increased water solubility of the sulfonated indigotin meant that a vat dyeing process was not needed but it also resulted in a poorer washfastness of the dye.

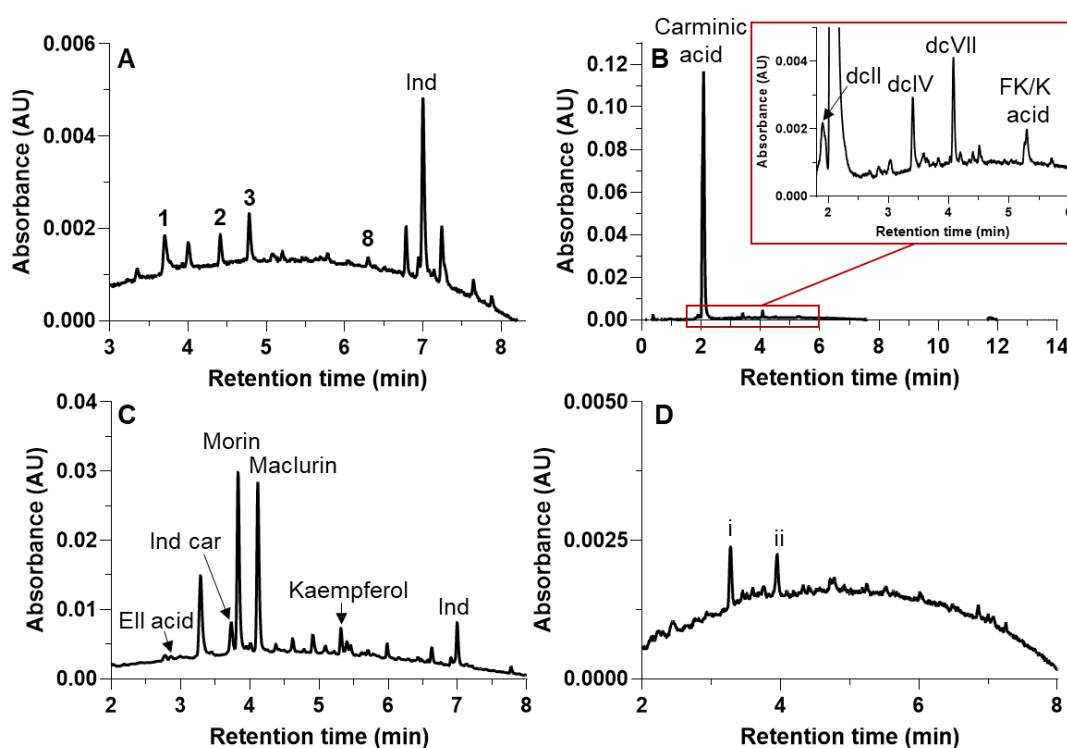


Figure 3.26: **A:** UHPLC-PDA chromatogram of oxalic acid extract monitored at 350 nm of the blue sample. **B:** UHPLC-PDA chromatogram of oxalic acid extract monitored at 475 nm of the red sample. **C:** UHPLC-PDA chromatogram of oxalic acid extract monitored at 350 nm of the green sample. **D:** UHPLC-PDA chromatogram of oxalic acid extract monitored at 254 nm of the brown sample. **1** = fisetin, **2** = sulfuretin, **3** = luteolin, **8** = alizarin, Ind = indigotin, K/FK acid = kermesic/flavokermesic acid, Ell acid = ellagic acid, Ind car = indigo carmine, i = unknown 1, ii = unknown 2.

The brown sample (Fig 3.26D) could not be identified by the references available in the NMS science laboratory. The working hypothesis based on the PDA spectra obtained (Fig 3.27) is that a lichen source was used for the brown based on the similarities to reference samples dyed with unidentified lichens found locally. Using lichen for brown and yellow colours were a known dye practise in Scotland at the time, particularly on the west coast.⁴⁸

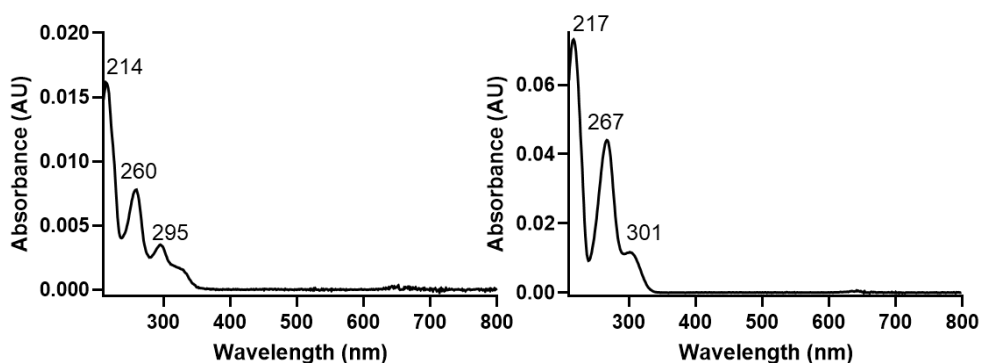


Figure 3.27: PDA spectra of unknown 1 and unknown 2 in the brown sample.

In summary, the wedding tartan of Flora MacDonald was dyed using many dye sources, indicating the contemporary dyeing knowledge to reach the desired shade of colour. It also suggests that extra care and cost was put to deciding on the colour of the tartan. Cochineal was a popular red dye source for 18th century tartans^{Eva, Anita} despite its cost in comparison to other red dyes, so its presence is not surprising, but it suggests that the tartan was made to be valued. However, the use of both indigo and Saxon blue for two different colours highlights the availability of multiple dyestuffs, even recently invented ones. Young and old fustic are common yellow dye sources and were often used when a true yellow was not required. The brown sample has not yet been identified but it could potentially be a lichen dye, reflecting a local dyeing tradition; but additional references are required for confident assignment.

3.10 Conclusion

An optimised sample preparation workflow and a UHPLC-PDA method for natural dye analysis have been developed. The method was shown to have a good percentage recovery and allows rapid acquisition of high-quality results from a smaller mass. The sample preparation workflow and UHPLC-PDA method were used with success on reference silk and wool samples dyed with 12 different dye sources as well as historical samples from the wedding tartan of Flora MacDonald.

The extraction step was optimised by investigations into the effect of complexation agent concentration, pre-processing step and milder HCl extraction methods on the obtained yield, although without success. Thus, the extraction method used was MeOH:CH₃COCH₃:H₂O:OA (1 M aq) (30:30:40:1 v/v/v/v).

The filtration step was optimised to use 2 washes of 25 µL MeOH:H₂O 1:1 v/v and a centrifugation speed and time of 1500 rpm and 5 min. It was found to give percentage recoveries of > 85 % for all compounds in standard mixture 1. The standard deviations for the high and low concentrations are all < 13 %, which are below the FDA limit for bioanalytical method validations.

The drying and reconstitution step was investigated by the solubility of compounds in four solvents. Of all solvents tested, MeOH:H₂O 1:1 v/v + 0.5 % FA gave the response with the smallest standard deviation for the compounds in standard mixture 1 and was chosen except for samples with flavonoid glycosides for which MeOH:H₂O 3:1 was used.

The UHPLC-PDA method developed reduced the analytical time to 14 min from the 37.33 min used for Method 2. The repeatability of the compounds in standard mixture 1 showed standard deviation < 0.013 min, making it possible to differentiate compounds **1** – **9**, despite compound **6** and **7** having a separation factor of 1.17. The linearity between chromatographic response and change in concentration was acceptable with the lowest R² = 0.9653 (**6**) probably being a result of co-elution and not method parameters. The LoD and LoQ for the chromophores in standard mixture 1 were all below 0.44 and 1.33 µg ml⁻¹ respectively, making it possible to confidently identify traces of relevant chromophores.

The analysis of 85 samples of references of natural dyes as well as historical samples showcased the applicability of the sample preparation workflow to both a wide variety of dyestuffs and samples from heritage objects.

The increased reproducibility of the results and increased time efficiency of the dye analysis from start to finish using the sample preparation workflow and UHPLC-PDA method developed will hopefully contribute to helping the dye analysis field in being able to produce more reliable data and use more statistical methods to address questions beyond merely dyestuff identification.

3.11 References

- 1 W. Nowik, in *Elsevier Reference Module in Chemistry, Molecular Sciences and Chemical Engineering*, ed. J. Reedijk, Elsevier Inc., Waltham, 2013.
- 2 I. Degano and J. La Nasa, *Top. Curr. Chem.*, 2016, **374**, 263–290.
- 3 J. Wouters, *Stud. Conserv.*, 1985, **30**, 119–128.
- 4 X. Zhang and R. A. Laursen, *Anal. Chem.*, 2005, **77**, 2022–2025.
- 5 J. Wouters, C. M. Grzywacz and A. Claro, *Stud. Conserv.*, 2011, **56**, 231–249.
- 6 A. Manhita, T. Ferreira, A. Candeias and C. B. Dias, *Anal Bioanal Chem*, 2011, **400**, 1501–1514.
- 7 L. G. Troalen, A. S. Phillips, D. A. Peggie, P. E. Barran and A. N. Hulme, *Anal. Methods*, 2014, **6**, 8915–8923.
- 8 A. Serrano, M. M. Sousa, J. Hallett, J. A. Lopes and M. C. Oliveira, *Anal. Bioanal. Chem.*, 2011, **401**, 735–743.
- 9 C. Miguel, W. Jacobs, C. B. Dias, A. Manhita, T. Ferreira, A. F. Conde and A. Candeias, *Eur. J. Sci. Theol.*, 2020, **16**, 151–164.
- 10 P. Nabais, M. J. Melo, J. A. Lopes, M. Vieira, R. Castro and A. Romani, *Herit. Sci.*, 2021, **9**, 32.
- 11 V. Pauk, P. Barták and K. Lemr, *J. Sep. Sci.*, 2014, **37**, 3393–3410.
- 12 E. Sandström, H. Wyld, C. L. Mackay, L. G. Troalen and A. N. Hulme, *Anal. Methods*, 2021, **13**, 4220–4227.
- 13 J. R. Wiśniewski, A. Zougman, N. Nagaraj and M. Mann, *Nat. Methods*, 2009, **6**, 359–362.
- 14 L. Switzar, J. van Angeren, M. Pinkse, J. Kool and W. M. A. Niessen, *Proteomics*, 2013, **13**, 2980–2983.
- 15 J. Potriquet, M. Laohaviroj, J. M. Bethony and J. Mulvenna, *PLoS One*, 2017, **12**, e0175967.
- 16 M. R. Wilson, J. A. DiZinno, D. Polanskey, J. Replogle and B. Budowle, *Int. J. Legal Med.*, 1995, **108**, 68–74.
- 17 L. Norén, R. Hedell, R. Ansell and J. Hedman, *Investig. Genet.*, 2013, **4**, 8.
- 18 M. Shahid, J. Wertz, I. Degano, M. Aceto, M. I. Khan and A. Quye, *Anal. Chim. Acta*,

- 2019, **1083**, 58–87.
- 19 L. Ford, R. L. Henderson, C. M. Rayner and R. S. Blackburn, *J. Chromatogr. A*, 2017, **1487**, 36–46.
- 20 J. Han, J. Wanrooij, M. van Bommel and A. Quye, *J. Chromatogr. A*, 2017, **1479**, 87–96.
- 21 A. Villela, E. J. C. van der Klift, E. S. G. M. Mattheussens, G. C. H. Derksen, H. Zuilhof and T. A. van Beek, *J. Chromatogr. A*, 2011, **1218**, 8544–8550.
- 22 J. Wouters, *Stud. Conserv.*, 1985, **30**, 119–128.
- 23 P. Guinot, PhD Thesis, Universite de Lille 2, 2006.
- 24 C. Mouri and R. Laursen, *Microchim. Acta*, 2012, **179**, 105–113.
- 25 L. G. Troalen, PhD Thesis, the University of Edinburgh, 2013.
- 26 R. Santos, J. Hallett, M. C. Oliveira, M. M. Sousa, J. Sarraguça, M. S. J. Simmonds and M. Nesbitt, *Dye. Pigment.*, 2015, **118**, 129–136.
- 27 A. Quye, K. Hallett and C. Herrero Carretero, *Wrought in Gold and Silk: Preserving the Art of Historic Tapestries*, NMS Enterprises Limited, Edinburgh, 2009.
- 28 Waters corporation, *Empower Software Data Acquisition and Processing guide*, 2002.
- 29 S. Schwaiger, C. Seger, B. Wiesbauer, P. Schneider, E. P. Ellmerer, S. Sturm and H. Stuppner, *Phytochem. Anal.*, 2006, **17**, 291–298.
- 30 A. M. Juszczak, M. Zovko-Koncic and M. Tomczyk, *Biomolecules*, 2019, **9**, 731.
- 31 D. Mantzouris, I. Karapanagiotis and C. Panayiotou, *Microchem. J.*, 2014, **115**, 78–85.
- 32 P. Menesatti, C. Angelini, F. Pallottino, F. Antonucci, J. Aguzzi and C. Costa, *Sensors*, 2012, **12**, 7063–7079.
- 33 Pall Corporation, AcroPrep Filter Plates Brochure, 2021, Print GN21.0601.2.
- 34 O. González, M. E. Blanco, G. Iriarte, L. Bartolomé, M. I. Maguregui and R. M. Alonso, *J. Chromatogr. A*, 2014, **1353**, 10–27.
- 35 W. Nowik, M. Bonose-Crosnier de Bellaistre, A. Tchapla and S. Héron, *J. Chromatogr. A*, 2011, **1218**, 3636–3647.
- 36 S. T. Talcott, J. E. Peele and C. H. Brenes, *Food Res. Int.*, 2005, **38**, 1205–1212.

- 37 A. Kruve, R. Rebane, K. Kipper, M. L. Oldekop, H. Evard, K. Herodes, P. Ravio and I. Leito, *Anal. Chim. Acta*, 2015, **870**, 29–44.
- 38 S. Fanali, *Liquid chromatography : fundamentals and instrumentation*, Elsevier, Amsterdam, 2013.
- 39 A. Serrano, M. Van Bommel and J. Hallett, *J. Chromatogr. A*, 2013, **1318**, 102–111.
- 40 L. A. Currie, *Pure Appl. Chem.*, 1995, **67**, 1699–1723.
- 41 FDA, *Bioanalytical Method Validation Guidance for Industry*, 2018.
- 42 I. Degano, M. Biesaga, M. P. Colombini and M. Trojanowicz, *J. Chromatogr. A*, 2011, **1218**, 5837–5847.
- 43 D. Zasada-Kłodzińska, E. Basiul, B. Buszewski and M. Szumski, *Crit. Rev. Anal. Chem.*, 2021, **51**, 411–444.
- 44 J. Watson, Flora MacDonald, <https://joannafwatson.co.uk/flora-macdonald/>, accessed: December 2022.
- 45 H. Douglas, *Flora MacDonald: The Most Loyal Rebel*, The History Press, Cheltenham, 2003.
- 46 A. Quye and H. Cheape, *Costume*, 2008, **42**, 1–20.
- 47 M. De Keijzer, M. R. Van Bommel, R. Hofmann-De Keijzer, R. Knaller and E. Oberhumer, *Stud. Conserv.*, 2012, **57:sup1**, S87–S95.
- 48 S. Grierson, *The colour cauldron*, Mrs. S. Grierson, Perth, 1986.

Chapter 4 Dye analysis of a 16th and 17th centuries embroidery collection at National Museums Scotland

4.1 Aims

The aim of this investigation was to analyse the dyes in a collection of 16th and 17th centuries housed at the National Museums Scotland (NMS) using the developed analytical protocol (Chapter 3) to showcase the applicability of the method and gain a better understanding of the socioeconomic context of the objects' production. The result of this study will help increase our knowledge of by and for whom the textiles were made; what they meant to their original owners; and how their raw materials affect how they were viewed and perceived. It will also aid our understanding of European and global trade in the 16th and 17th centuries as well as to try to put these perceived 'English' objects into a global context.

4.2 Introduction

The evolution of embroidery from the rudimentary need for strengthening seams and mending holes in clothes to the purely decorative art of later centuries is easy to imagine despite no written record of its origin. It is an often overlooked art form, likely due to the low survival rate of textile objects to the modern day and its close connection to women and the domestic sphere. In its essence, embroidery is the application of material to a ground, often cloth, for the creation of designs. The expensive materials used, such as silk, metal thread, sequins and semi-precious stones, in most surviving examples, reflect the use of many embroideries to assert positions of power and social standing.^{1,2}

Embroidery saw rapid growth in popularity as an amateur pastime in Scotland and England in the 16th and 17th centuries, spurred by technological advancements and economic growth.³ Embroidery was an entire industry in itself with print sellers, pattern drawers and haberdashers being involved before the embroiderer could even start their work. Embroidery patterns could either be traced from pattern books by the embroiderer themselves, by a pattern drawer hired by the household or the patterns could be bought already traced onto cloth.⁴ Thus, the European invention of mechanical printing led to a wider dissemination of printed pattern books specifically for embroidery and lace making. Simultaneously, European colonial expansion

resulted in an influx of wealth and the availability of new materials and designs available to Scottish and English embroiderers.

Parallel to the domestic embroiderers, professional embroidery workshops also existed, evidenced by the Broderers' Company being granted its Royal Charter in 1561.² These professional embroiderers were men that likely enjoyed wealth and a high standing in society, with a famous example being Edmund Harrison, King's embroiderer at the courts of James I, Charles I and Charles II.⁵ However, the great skill of many domestic embroiderers and their access to similar materials as professional workshops in combination with many designs being based on similar sources means that it is difficult to distinguish between professional and domestic works in museum collections.

The Spanish conquest of Central and South America in 16th century led to the introduction of many new dyestuffs. The expansion of European countries and the use of enslaved indigenous people also dramatically increased the supply of already known dyestuffs. Additionally, the colonisation eastward and the founding of national trade companies during the 17th century expanded trade with Southeast Asia and India. In some instances, the imported dyestuff was of higher quality in comparison with domestic European sources and rapidly almost completely outcompeted the European alternative.⁶ This increased supply of raw material to Europe made decorative embroidery more accessible to a larger group of social classes.⁷

Embroidery was an art largely exclusive to upper middle and noble women that had both the time and resources to create decorative pieces. The growing global power of Scotland and England that came with colonial expansion increased the number of Scots and Englishmen wealthy enough to supply their wives and daughters with enough time and resources to not have to work for wages. Instead, the women could dedicate their time to become virtuous and industrious women. Embroidery was regarded as an industrious but ultimately non-threatening pastime and came to be seen as an important part of demonstrating the moral standing of women. The close connection between embroidery and female virtue has stayed relevant in Western culture for centuries and embroidery was seen as an essential part of elite female education up until the modern age.⁸

The embroideries present in museum collections not only reflect the production of the 16th and 17th centuries but also the preferences and attitudes of the time of collection. During the late 19th and early 20th centuries, Scottish and English embroideries from

the 16th and 17th centuries started to rise in popularity as collection items in Britain and the United States. In this post-industrial society of the Victorian age, the naivety of the designs in Tudor and Stuart embroideries came to be seen as 'quintessentially English,' reflecting an idyllic period in English history.^{4,8} Worthy of note is that some textiles collected as English could also be of Scottish production. Despite Scotland and England being two separate countries for part of the studied time period, they are treated as one unit in this study as it is difficult to attribute objects to either country purely stylistically and without archival evidence.

Many of the embroideries found in museum collections today were donated by private collectors active during this period. Important collectors include Viscount Leverhulme, Sir William Burrell, and Irwin Untermyer.^{8,9} Consequently, the objects present in museums are not only reliant on what objects managed to survive to modern time, but also on the selection strategy and taste of private collectors. The choice of objects to be studied in this project were therefore dependent on two constraints; what has been collected and what could be sampled.

4.3 The collection at National Museums Scotland (NMS)

National Museums Scotland (NMS) has the third largest collection of European textiles in the UK following the V&A and Bath Fashion Museum. It includes embroideries stretching from two examples of *Opus Anglicanum* (early 14th century) to the modern day. The collection of early modern embroideries includes both clothing items and furnishings from the late 15th and early 16th centuries, professionally embroidered liturgical textiles and 18th century domestic cross-stitched seat covers and samplers. An array of techniques is present in the collection, including blackwork, appliqué, raised work, and canvas work. It also includes works in silk, wool, and metal threads.

The constraints mentioned dictated the date parameters of the studied objects as many of the embroideries pre-1550 present in the collection were either too fragile or sewn to a support, making it impossible to sample them ethically. Conservation treatments of other important works, e.g. one known embroidery from the workshop of Edmund Harrison, also made sampling impossible. These constraints resulted in the sampled objects mainly being smaller, domestic works made predominantly with silk thread within the time period 1550 – 1720.

26 objects were sampled including two blackworks, two stomachers, two coifs, seven bed valances, three crewelworks, one altar frontal, seven panels, and two book covers (Table 4.1). Of the 26 objects investigated, six were embroidered with wool and the rest with silk thread.

4.4 Embroidered clothing

Much of the embroidery produced in the 16th century was made to decorate garments. The absence of banks for personal capital deposits resulted in the wealthy using expensive clothing like currency. This combined with the importance of being fashionable at court made embroidered clothing an important part of the wardrobes of the nobility.⁸ The male Elizabethan formal dress included doublet (jacket), hose (or breeches), and cloak while female dress included gown, kirtle, sleeves, stomacher, petticoats as well as a headdress such as French or English hoods, coif or cap.¹⁰ Most parts of both male and female dress could be embroidered but the extent varied with social class and occasion. Additionally, accessories such as gloves, bags, and shoes could be heavily decorated.⁸ Of the 26 embroideries studied, five objects were made to be worn: one unfinished sleeve (A.1929.152), two stomachers (A.1894.125, A.1962.1067) and two coifs (A.1956.1198, A.1965.722).

4.4.1 Blackwork

A.1929.152 is one of two blackwork objects sampled and with its repeated scroll pattern, known as *rinceaux*, interspersed with floral designs in black silk and gold metal thread, it is a good example of blackwork produced in the 16th century. Blackwork is a counted-thread embroidery technique commonly worked in black and metal threads on a white ground, highly popular during the Elizabethan era.¹ The large sleeves and stomachers of Tudor fashion lend an appreciative canvas for the blackwork technique and intricate designs. The object was likely made to be a part of a pair of balloon sleeves such as seen in Figure 4.1 but was never finished. The complexity of the work makes it likely that it was executed by a professional embroiderer. This, combined with the expensive materials of black silk and metal thread, showcases how blackwork was often used to signal personal wealth and power.



Figure 4.1: **Left:** Queen Elizabeth I, unknown artist, 1590 © Jesus College, The University of Oxford. **Centre:** A.1929.152 © NMS with similar *rinceaux* motif as sleeves in the portrait. **Right:** A.1938.580 © NMS with a geometrical design and embroidered border making it likely to be of original dimensions and a probable chalice veil.

Other designs which were popular designs were geometrical motifs. These are reflected in the second blackwork object investigated. A.1938.580 was probably not made to be worn, but was instead possibly made as a chalice veil. It includes floral designs in a more structured composition than the previous object. It has a carnation, a pomegranate, and two bird designs centred in four squares made with a thick border and corner flowers. The embroidered border around the edges of the linen ground makes this likely to be the original dimension and appearance of this object, suggesting its use as a chalice veil.

Blackwork fell out of fashion over the course of the 17th century, making it an iconic example of Elizabethan skill, fashion and taste. The reminiscence of the popular designs of blackwork, particularly *rinceaux*, can however be seen long after blackwork fell out of fashion.⁸

4.4.2 Stomachers

The stomacher was an essential part of Western European female gowns from the late 16th to the late 18th centuries.¹⁰ It is a triangular, detached piece of cloth pinned in place on the central front of the wearer.¹¹ Because of its central position and the possibility to be exchanged for different effects, many stomachers were heavily decorated and embroidered. The two stomachers sampled, A.1894.125 and A.1962.1067 both show floral motifs worked in silk and metal thread. The regular



Figure 4.2: Left: A.1894.125 © NMS stomacher with a couched metal thread background and floral motifs. Right: A.1962.1067 © NMS Stomacher with nature motifs. The 3-D nature of the pea pods is shown in the inserted image.

design, heavy featuring of metal thread and sequins and the obvious technical skill displayed make these likely to be professional works.

A.1894.125 has been dated to the second half of the 17th century stylistically. Its linen ground is covered in metal thread with the couching thread forming a chequered pattern, giving a textured finish to the piece. Carnations are embroidered surrounded by leaves and small, blue flowers, possibly forget-me-nots. Carnations feature in the second stomacher (A.1962.1067) as well however, where A.1894.125 show a central floral design, A.1962.1067 shows a more regular floral pattern. Carnations, roses, and pea pods are surrounded by stems worked in metal thread in scroll formation on the linen ground. This pattern is reminiscent of the *rinceaux* pattern heavily favoured in Elizabethan blackwork (Section 4.4.1). Worthy of note are the pea pods worked in detached buttonhole stitch, giving a three-dimensional effect (Fig 4.2).

The embroidery of A.1962.1067 is likely to have been finished around 1600 but not worked into a stomacher until late 17th century. Its original function could potentially have been a jacket. Such a repurposing of the second stomacher shows how the embroidery was appreciated as something separate from its function. It shows an artistic interest in the object and how it has been a treasured possession throughout its history. The expensive materials and the obvious skill involved in the production of both these stomachers again highlight the use of embroidery in dress to signal status.

4.4.3 Coifs

A coif was a close-fitting cap worn by both men and women either by itself or as an undercap.¹⁰ They were often made of linen, which is the case for both coifs sampled (Fig 4.3). Object A.1956.1198, dated 1600 – 1630 shows a similar *rinceaux*-inspired design as the blackwork with its scrolling stems worked in metal thread with central flower, berry, and pod motifs. The second coif (A.1965.722) is one of two objects sampled that are known to be continental in origin. A.1965.722 is contemporary to the first coif and likely Italian or French in provenance. It has three floral designs framed with metal and colourful silk threads. The rest of the linen ground is filled with ornamental scrolls worked in the same style as the frames. It is however unfinished with ink patterns showing where the rest of the embroidery should be worked. The clearly repeated designs, high skill and costly materials likely make both coifs professional works.



Figure 4.3: Top: A.1956.1198 © NMS, linen coif with *rinceaux* influenced design. **Bottom:** A.1965.722 © NMS, linen coif of French or Italian design, insertion shows examples of ink pattern (circled in blue) highlighting the unfinished state of the object.

4.4.4 Inspired by Nature

All objects discussed include designs based in nature. The improvement of printing and etching combined with the heightened interest in naturalism increased the popularity of flora and fauna encyclopaedias and many patterns were based on these prints.^{4,12,13} Natural motifs are not only beautiful but also have a connected symbolism which often was utilised in embroideries.

With the religious and political scenes being highly volatile in Scotland and England during the 17th century, the embroidered designs could have religious, secular or political symbolism. Of course, much of the symbolism is subjective and dependent on the context of production. However, the Reformation and establishment of the Anglican church in the 1530s, the English Civil Wars in the 1640s, the establishment of the Commonwealth 1649-1660 and subsequent Restoration of Charles II in 1660 lent many embroiderers a way to show loyalty in a way that could easily be dismissed as a woman's notion.

It can therefore be argued that the sunflower and the oak tree were used by royalists to show their support for the Stuart King during the Civil Wars. Also, Mary Queen of Scots often relied on political symbolism, embroidering caged thistles and the Tudor rose shading a thistle as commentary on her imprisonment by Elizabeth I.¹⁴ Although without any accompanying written explanations, how the symbolism was meant to be understood remains speculation.

4.5 Embroidered furnishings

With the emerging preference for lace decorated clothing across the 17th century, much embroidery moved from decorating clothing to be applied to furnishings for display in the home. The embroidered furnishings sampled in this study included seven bed valances, three crewelworks, one altar frontal, seven panels, and two book covers.

4.5.1 Larger furnishings

The four-poster bed was one of the most important furnishings in Scotland and England during the 17th century. Due to the cold climate, especially in Scotland, the bed was furnished with large textiles including curtains, canopy and bed valances. The bed valances are located along the roof of the bed and could be richly decorated.¹³ (H.RHB.25.1 – H.RHB.25.11) are all part of a set embroidered with the date 1632 and an inscription of “Sir Coline Campbell of GK” (top) “Dame Ieliane Campbell 1632” (bottom) (Fig 4.4). They were likely domestically made for Sir Colin Campbell of Glenorchy and his wife Juliana who were married in 1594. Between the letters, flowers, berries, and insects worked in fine stitches can be seen. Whether these were made with the intention of being bed valances is debated, as bed valances usually are worked horizontally while these are all needed to be displayed vertically.



Figure 4.4: Set of bed valances with the inscription “Sir Coline Campbell of GK” along the top of the objects and “Dame Ieliane Campbell 1632” on the bottom. Sir Colin Campbell of Glenorchy and his wife Juliana were married in 1594 and this set of embroideries were likely embroidered domestically by or for them. Top, left to right: H.RHB.25.1 – H.RHB.25.6 and bottom, left to right: H.RHB.25.7 – H.RHB.25.11 © NMS.

They are also unusually small in comparison to other surviving examples of bed valances as these were usually wrought to cover the full sides of the bed. Potentially, they could have been stitched together vertically or stitched to a ground for the use as a bed valance. Only seven of the eleven bed valances were sampled (Table 4.1).



Figure 4.5: The three crewelworks sampled. **Left:** A.1949.224, **centre:** A.1955.120, **Right:** 1938.584 A © NMS.

The three crewelworks sampled (Fig 4.5) were all intended as larger furnishings; A.1955.120 being made as curtain and A.1949.224 likely a cover based on its dimensions. A.1938.584 A is part of a larger furnishing set. All are worked on a fustian ground, which is a mix of linen and cotton and was often use for crewelworks.¹⁵ Crewelwork is defined as embroidery done in wool and the common designs were large fleshy leaves and the 'Tree of Life' motif inspired by Indian textiles (see A.1955.120).¹⁵ They are all attributed to the late 17th or early 18th centuries. Wool was cheaper than silk and thus more cost-effective for the larger furnishings that gained in popularity towards the end of the 17th century.

A.1955.120 has the 'Tree of Life' motif, showing trees with large leaves growing from a small, hilly landscape. A stag can be seen prancing across the hills and among the trees, squirrels, birds and flowers can be seen. The colour palette is limited to greens, browns, yellows and reds. Another design that was popular across embroidery techniques can be seen in A.1949.224 with the central design of a shepherd and shepherdess in contemporary dress. To complete the picture, a dog and sheep are included together with the man and woman in the centre. The entire design is surrounded by borders of flowers. In each corner there are four animals – a stag,

leopard, lion and peacock, a combination of animals that was a common design in the mid-17th century.²

The altar frontal K.2001.637 (Fig 4.6) is unique among the sampled objects. Not only because it was clearly made for an ecclesiastical setting, but it is the only one containing appliqué embroidery and worked on a ground of red damask. Appliqué embroidery refers to the technique of working the embroidery on a smaller piece of cloth that is later stitched onto the ground.² The design includes flowers, stars, and scrolls in a repeated pattern divided by richly decorated borders made in metal thread and it is likely from the late 16th – early 17th century. Stylistically, it is difficult to determine its provenance, but it is likely continental, possibly French or Italian in origin. Due to its liturgical use and repeated pattern, it is likely to be a professional work.



Figure 4.6: K.2001.637 © NMS, altar frontal with appliqué embroidery on a damask ground.

4.5.2 Biblical imagery

Much of the embroidery produced by professional embroiderers before the reformation was, like the sampled altar frontal, ecclesiastical in nature. England, in particular, earned a high reputation throughout Europe with its *Opus Anglicanum*, which production decreased significantly with the outbreak of the Black Death in mid-14th century and later ended.¹⁶ The iconoclasm during the reformation in England and Scotland meant that not much of this rich heritage has survived. However, despite this harsh iconoclasm, biblical scenes were popular designs throughout the 17th century as they were not seen as religious icons but rather as important moral lessons for the embroiderer.

Biblical heroines, such as Esther, Susanna, Judith and Jael were incredibly popular with the domestic embroiderer. Esther was particularly popular as she could be seen as the biblical model for the modest wife who knows when to speak and what to say to help her husband.¹⁷ Embroidering these scenes would thus give the embroiderer time to contemplate the virtues of these biblical heroines while honing her craft. It can be argued that these stories were not only used as reference for ideal womanhood but also as a risk-free way of experiencing the wider world from the often-restricted domestic sphere available to women.⁸ Because of the religious tension in 17th century Scotland and England, particularly for the many Catholics that were forced to follow Protestantism in public, the Biblical motifs can also include a devotional aspect and not purely a moral lesson.¹⁷

Two of the sampled objects have clear biblical origins: A.1958.85 (Fig 4.7) and A.1958.291 (Fig 4.8). Both are likely to have been produced mid – late 17th century and their original function is unknown. Although, based on size, A.1958.85 was likely meant to be a cushion cover and A.1958.291 could have been made as a panel for a casket, a popular use of embroidery in the 17th century.⁴ Both depict pivotal scenes from the story of Abraham.

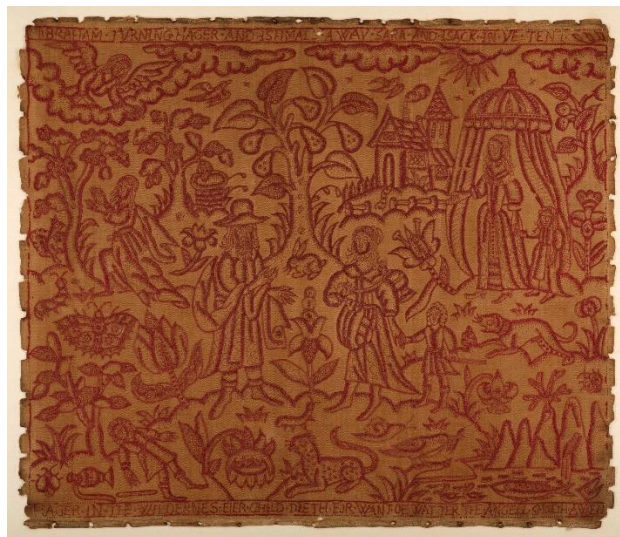


Figure 4.7: A.1958.85 © NMS, monochrome depiction of Abraham banishing Hagar and Ishmael.

A.1958.85 is embroidered in a monochrome design in red wool thread with a central image of Abraham sending Hagar and Ishmael away with Sarah and Isaac present in the tent top right. In the left foreground Ishmael is shown dying from thirst and above his mother is shown praying to God and being shown a well. The scenes are

surrounded by flowers, trees, animals and a house. Inscriptions in English explaining the scenes depicted are embroidered along the top and bottom edges. The inclusion of English words makes this an embroidery of known English or Scottish origin.

The second object (A.1958.291) shows the sacrifice of Isaac at the moment where the angel commands Abraham to stop (Fig 4.8). Similarly to the previous object, a house and designs from nature including insects, birds and animals surround the biblical scene. The panel is embroidered in silk thread and the grass beneath Abraham is silk purl. Silk purl is metal thread wound together with silk thread and then coiled. The commercial aspect of embroidery patterns, where they could either be traced from pattern books by the embroiderer themselves, a pattern drawer hired by the household or bought already traced onto cloth is shown by the close resemblance between the sampled object and another NMS embroidery with a similar design (Fig 4.8).



Figure 4.8: Objects with likely similar source of embroidery pattern depicting the sacrifice of Isaac. **Left:** A.1958.291, **Right:** H.RHB.2 © NMS.

4.5.3 Pictures and book covers

The objects in Section 4.5.2 are referred to as pictures or panels in the museum collection. The original function of these is not always known but many could have been made to be glued to caskets, a decoration strategy popular in the 17th century.⁴ No archival evidence supports the idea that embroideries were displayed framed vertically on walls during the 17th century. The vertical presentation of embroideries on walls instead became popular in the 19th and 20th centuries, highlighting a changed

attitude toward embroideries.⁸ With the loss of knowledge of their original function, the embroidery in itself became the object that was collected. The end to the use of embroideries as functional objects thus makes it impossible to know for certain what they were originally produced for, although educated guesses can be made.



Figure 4.9: Remaining objects sampled described as pictures or panels, all of probable domestic production. **Top left:** A.1894.234, **Top centre:** A.1956.1484, **Top right:** A.1925.418, **Bottom left:** A.1989.202 **Bottom right:** 1960.231, © NMS.

Five other objects in the NMS collection (Fig 4.9) are described as pictures, including the objects that set the upper limit of the date parameter for sampling: A.1894.234 and A.1956.1484. Both are attributed to the first half of the 18th century, with A.1894.234 having a more specific date of 1710 – 1720. Both embroideries show a central rose motif surrounded by a floral design and both are made in wool thread. A.1894.234 is a canvas work with the ground covered in red tent stitch and it was likely made as a seat cover. The original function of A.1956.1484 is not known. Interestingly, despite the small sample size of 26 objects, a tonal change from the more acidic greens and yellow of the 17th century to the more vibrant reds and pinks popular in the 18th century can be seen when comparing these embroideries with earlier examples such as A.1989.202 and A.1960.231.

A.1989.202 is the only one of these objects of known continental European provenance, likely Portugal around 1620. The design is created by the absence of the green silk thread otherwise covering the entire ground. Three women and a mansion are shown surrounded by floral motifs is shown and along the top, the words 'Toreo das Damas Adonas' can be read.

A.1960.231 heavily features silk purl, which can also be seen in A.1925.418. A.1925.418 shows a central flower surrounded by leaves and flowers, creatively made by manipulating the silk purl thread to give different effects. The grass underneath the vase is created by winding up the silk purl, producing a tight curl reminiscent of actual grass. In another instance, smaller sections of silk purl have been placed within the leaves to give a sense of direction. In contrast, A.1960.231 uses both silk purl and silk thread. It shows a woman holding a flaming heart next to a resting stag embroidered onto a satin ground and is thought to be from mid-17th century. Silk purl designs give a textured feel to the grass area of the picture which stands in great contrast with the embroidered woman and the ink painted sky. It could possibly have been made as a casket cover similar to A.1958.291.



Figure 4.10: Embroidered book covers. **Left:** A.1926.168. **Right:** A.1949.220 © NMS.

In contrast, the original function of the last two objects, A.1926.168 and A.1949.220, as book covers is known due to the shape of the embroideries (Fig 4.10). Both are likely domestic works with A.1929.168 even showing small patches along the top edge where the embroiderer tested the stitches to be used. This edge would have been folded down and not seen when the embroidery was used in its original function and glued onto a book. It is likely to date from the first half of the 17th century and is a tent stitch canvas work with green and yellow silk thread covering the linen ground. Central on each side is a carnation and an iris, respectively, and these are surrounded by insects such as butterflies, dragonflies, and centipedes. Twilled threads, i.e. threads made from two different coloured fibres plied together were used for the details on the flowers (Samples A.1929.168-14 and A.1929.168-19, Appendix A3). This technique gives a depth to the colours seen, giving a slight three-dimensional feel to the two-dimensional design. The other book cover, A.1949.220, stands in stark contrast to this. It showcases a central medallion on each side with a gentleman and lady in

contemporary dress surrounded by scrolls and flowers made in silk purl. It is dated 1634 – 1667 and is likely to be English in origin.

Table 4.1: Objects sampled ordered by accession number showing the type, probable date, providence and producer of each object.

Accession number	Type	Production date	Probable providence	Probable producer
A.1894.125	Stomacher	1650-1700	Scottish or English	Professional
A.1894.234	Seat cover	1710-1720	Scottish or English	Domestic
A.1925.418	Silk purl picture	unknown	Scottish or English	unknown
A.1926.168	Book cover	1600-1650	Scottish or English	Domestic
A.1929.152	Blackwork	c. 1580	Scottish or English	Professional
A.1938.580	Blackwork	1550-1600	Scottish or English	Domestic
A.1938.584 A	Crewel work	c. 1700	Scottish	Domestic
A.1949.220	Book cover	1634–1667	Scottish or English	Domestic
A.1949.224	Crewel work (cover)	c. 1700	Scottish	Domestic
A.1955.120	Crewel work (curtain)	1650-1700	Scottish	Domestic
A.1956.1198	Woman's coif	Late 1600	Scottish or English	Professional
A.1956.1484	Panel	Early 1700	Scottish or English	Domestic
A.1958.291	Picture	1650-1700	Scottish or English	Domestic
A.1958.85	Picture	c. 1650	Scottish or English	Domestic
A.1960.231	Picture	c. 1650	Scottish or English	Domestic
A.1962.1067	Stomacher	embroidery c. 1600, stomacher late 1600	Scottish or English	Professional
A.1965.722	Woman's coif	1568-1600	Italian or French	Professional
A.1989.202	Panel	c. 1620	Portuguese	Domestic
K.2001.637	Altar frontal	late 1500-early 1600	Italian, French or English	Professional
H.RHB.25.1	Bed valance	1632	Scottish	Domestic
H.RHB.25.4	Bed valance	1632	Scottish	Domestic
H.RHB.25.5	Bed valance	1632	Scottish	Domestic
H.RHB.25.6	Bed valance	1632	Scottish	Domestic
H.RHB.25.7	Bed valance	1632	Scottish	Domestic
H.RHB.25.9	Bed valance	1632	Scottish	Domestic
H.RHB.25.10	Bed valance	1632	Scottish	Domestic

4.6 Sampling strategy

Embroideries, in comparison to tapestries and other decorative textiles, are difficult to sample due to the minimal access to loose threads. The back of tapestries often contain long ends of thread ideal for sampling. The back of embroideries do not often display the presence of similar long ends and depending on the meticulousness of the embroiderer, the access to any ends of threads might be limited. However, to minimise the impact on the structural integrity of the objects, sampling was done on the available loose ends on the back of the embroideries (Fig 4.11). Already frayed ends and threads after knots were targeted to the extent possible. The reverse of the embroideries is also often cleaner and less degraded due to the lower light exposure, thus increasing the chromophore concentration and simplifying the interpretation of the chemical analysis. The sample size needed for UHPLC analysis is small; < 1 mg is enough, which translates to a few millimetres of thread. The developed sample preparation protocol (Chapter 3) can give results from sample masses $> 0.02 \pm 0.005$ mg, making it ideal for the small sample sizes available from embroideries.



Figure 4.11: Detail of A.1926.168 showing the difference in colour intensity between the front (left) and the back (right) and the presence of loose threads on the back.

The sampling approach used in this project started with a visual assessment of the number of colours and different hues as well as potential sampling areas for each object (Fig 4.12). It also included an assessment of any areas of potential restoration and/or conservation. The hues were then ordered from palest to darkest, and each hue given a letter (with *a* being the palest hue). These lists of hues were based purely on visual investigation and mainly constructed to be used as reference during analysis, so they were not standardised between objects or colours.



Figure 4.12: The visual investigation of A.1955.120. The transition from green to more blue green hues going from left to right across the object is an example of visual observation that would be noted.

The areas from which the samples were taken were recorded on a printed photo of the object (Fig 4.13, Appendix A2) and each sample was also recorded in a spreadsheet. The spreadsheet included the colour and letter assigned to the sample, a short description of the sampling location and any potential concerns.

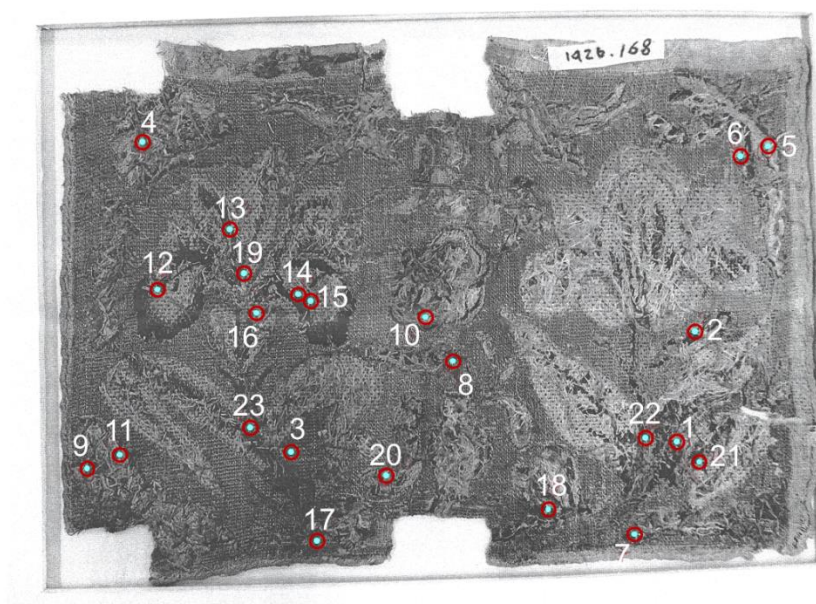


Figure 4.13: Example of a marked photograph showing all sampling sites of object A.1926.168. The sampling sites were noted in pen on the picture and are shown here electronically for visibility purposes. All sampling photos in Appendix A2.

Important visual observations recorded include the degradation of the black and dark brown threads in the blackwork objects, making the presence of iron gall dyed threads

likely. The changing shade of green in A.1955.120 was also an interesting observation (Fig 4.5) as well as the ink underdrawing in A.1967.722 (Fig 4.3), showing that it is an unfinished work.

270 samples were collected from the 26 objects described in Section 4.4 and 4.5 (Table 4.1). The samples included 12 metal thread samples and 5 samples not related to the embroidery, such as paper solids from the surface and undyed threads from the ground cloth (Appendix A3), resulting in 253 samples available for dye analysis. The colour palette collected leans towards earthy tones of acidic greens, yellows and browns with the second largest group being pink samples (Table 4.2).

Table 4.2: Number of samples assigned to each colour of the 253 samples analysed.

Colour of sample	Number of samples
Yellow	22
Green	78
Black	4
Brown	39
Blue	24
Purple	9
Grey	4
Red	18
Orange	11
Pink	44

4.7 UHPLC-PDA analysis of the NMS embroidery collection

The samples were prepared and analysed following methods outlined in Section 2.3.1 – 2.3.4 and discussed in Chapter 3. The analysis identified 11 dye sources (Figure 4.14) used in the embroidery samples collected: 10 natural sources and one semi-synthetic (Saxon blue, Section 4.10.2). 167 of the 253 analysed samples were dyed with more than one dye source. The main dyes characterised were weld (Section 4.8.1) and indigo (Section 4.10.1) which were present in 85 % of the analysed samples (Fig 4.14), indicating a preference for these dyestuffs in Scottish and English Renaissance embroidery.

Additionally, 20 samples were either too small, potentially undyed or contained too little dye marker to have their dye source confidently identified. These included all four

grey samples, five green, four brown, one blue, three pink and three metal core thread samples (Appendix A3).

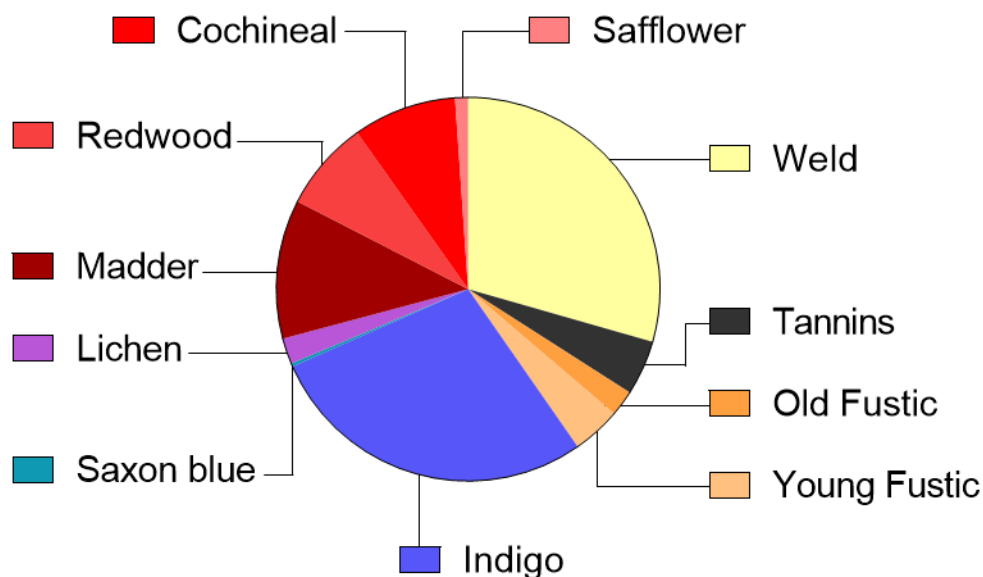


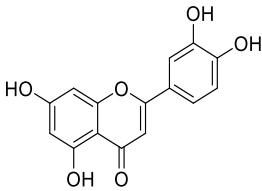
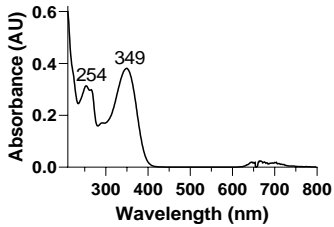
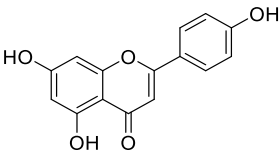
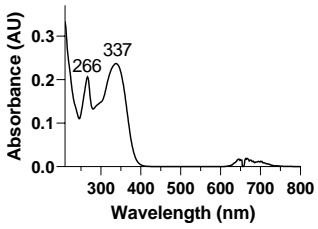
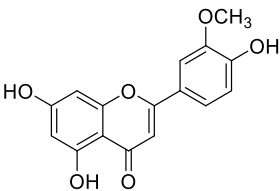
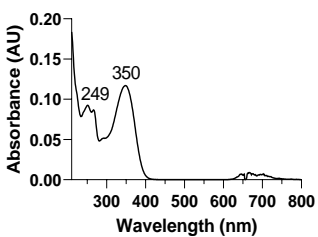
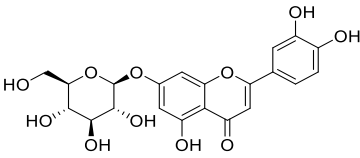
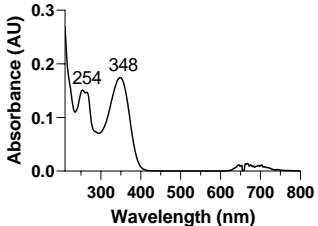
Figure 4.14: Number of samples identified to contain each of the eleven characterised dye sources (117 weld, 19 tannins, 9 old fustic, 16 young fustic, 106 indigo, 1 saxon blue, 10 lichen, 42 madder, 28 soluble redwood, 32 cochineal and 4 safflower.) Most samples contained more than one dyestuff and were thus recorded in more than one pie slice.

4.8 Yellow and green

4.8.1 Weld (*Reseda luteola* L.)

Weld is identified by the presence of the flavones luteolin (**1**), apigenin (**2**) and *O*-methylated flavone chrysoeriol (**6**). Glycosidic versions of these compounds can also be present, in particular luteolin-7-*O*-glycoside (**1-7-O**) (Table 4.3). Luteolin (**1**), either as an aglycone or as its glucoside, is the main chromophore in weld. All of these compounds are flavones, which has been shown to have the greatest lightfastness of all flavonoid sub-groups (Section 1.4.2.1).

Table 4.3 Identification of components of weld (*Reseda luteola* L.) dye.

Compound	Structure	Retention time ^a (min)	UV-Vis spectrum
Luteolin (1)		4.79	
Apigenin (2)		5.46	
Chrysoeriol (3)		5.62	
Luteolin-7-O-glucoside, (1-7-O)		2.95	

^aUHPLC-PDA method in Section 2.3.4.

Weld was found in 117 of the collected samples, including all but four of the 100 yellow and green samples. In the green samples, weld was combined with indigo in varying ratios to give the desired hue. Beyond the yellow and green samples, weld was found in blue, brown, red, orange and pink samples (Fig 4.15) indicating the versatility and availability of this dyestuff in Scotland and England.

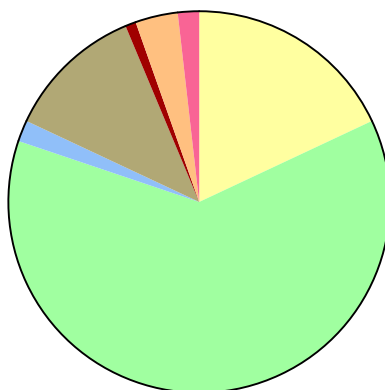


Figure 4.15: Distribution of colours of samples identified to contain weld (22 yellow, 70 green, 2 blue, 15 brown, 1 red, 4 orange, 3 pink, total: 117 samples).

Weld was the most popular yellow dye source but other flavonoid-containing plants such as dyer's greenweed (*Genista tinctoria* L.) and young and old fustic (*Rhus cotinus* L. and *Maclura tinctoria* L.) were also in use. Previous studies on contemporary tapestries from both England and the European continent showed the use of multiple sources for yellow, particularly dyer's greenweed.^{18,19} The exclusive use of weld in the embroideries is therefore somewhat surprising and may suggest a difference in manufacturing approach of the material intended for embroidery and tapestry. Of course, a larger sample set is required to draw any major conclusions.

The use of the sample preparation workflow developed (Chapter 3) and a mild extraction method (Section 3.3) preserved the glycosidic components and the glycone : aglycone ratio of the weld samples. Interestingly, the number of glycosides present as well as the luteolin-7-O-glycoside (**3-7-O**) : luteolin (**3**) ratio differed greatly both across samples and within objects (Fig 4.16).

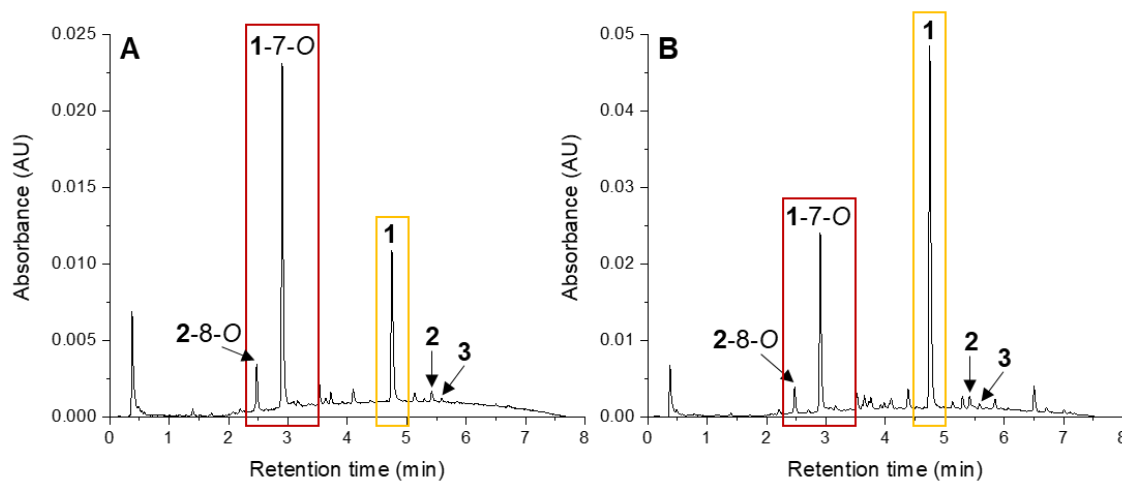


Figure 4.16: A: UHPLC-PDA chromatogram of oxalic acid extract monitored at 350 nm of sample A.1956.1484-1 showing a large luteolin-7-O-glycoside (1-7-O) peak (red box) in comparison to aglycone luteolin (1) (yellow box). **B:** UHPLC-PDA chromatogram of oxalic acid extract monitored at 350 nm of sample A.1956.1484-3 showing a small luteolin-7-O-glycoside (1-7-O) peak (red box) in comparison to aglycone luteolin (1) (yellow box). 1-7-O = luteolin-7-O-glycoside, 2-8-C = apigenin-8-C-glycoside, 1 = luteolin, 2 = apigenin, 3 = chrysoeriol.

The glycone : aglycone ratio was found by adding the peak areas of the 3-7-O and the 3 peaks and dividing each peak area with this sum then multiply by 100 to get the relative percentage. The yellow samples have 3-7-O : 3 ratios in the range of 11 : 89 – 89 : 11 and the green show ratios between 37 : 63 and 96 : 4 so no clear trend in glycone : aglycone ratio can be seen across the yellow and green samples dyed with weld.

One likely explanation for the lack of a trend in the ratios seen could be that the ratios are a result of degradation processes.²⁰ Deglycosylation into the flavonoid aglycones is a known degradation pathway, so the diversity of storage and display conditions for the sampled objects could explain the variety seen.²¹ However, degradation cannot explain the differences in ratios seen even within an object (Fig 4.16).

Instead, potentially the difference in ratio seen is an effect of dye bath conditions. It can be theorised that higher temperature dye bath conditions break the glycosidic bond to a higher degree than lower temperatures for flavonoids.²² Thus, the variety in ratios seen could be because of varying dye house practices. Additionally, the natural variation of glycosides and aglycones in weld plants depending on soil and growing conditions also most likely have an impact on the ratios obtained. The correlation between dye bath conditions, plant variety and the ratios seen in the textile samples

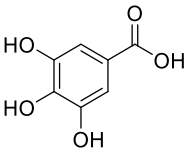
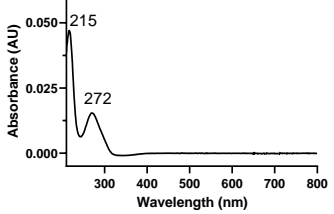
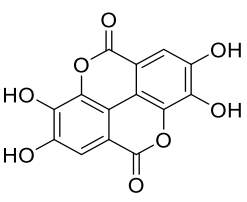
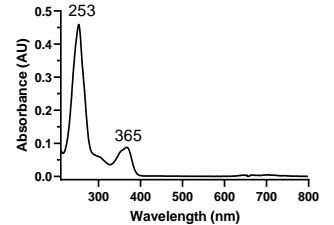
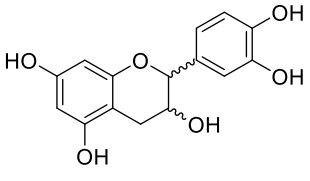
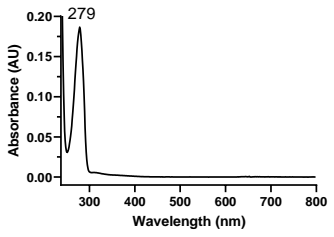
is difficult to prove or disprove without further studies. Potentially stable isotope mass spectrometry studies as used for ancient diet studies could be employed.²³ However, important information about provenance could be deduced if a correlation between the glycosidic ratio and cultivation region of the plant could be established.

4.9 Black and brown

4.9.1 Tannins (mainly *Quercus infectoria* L. and *Rhus* spp.)

Tannins are polymeric polyphenolic compounds widely distributed in the plant kingdom, commonly classified as hydrolysable (gallotannins and ellagitannins) or condensed (proanthocyanidins) tannins, also known as proanthocyanidins (flavan-3-ol or catechin, epicatechin oligomers and polymers). Oak galls commonly from *Quercus infectoria* L. and sumac (*Rhus* spp.) were historically important sources for vegetable tannins (Section 1.4.2.4).^{24–26}

Table 4.4 Identification of common monomers of hydrolysable tannins.

Compound	Structure	Retention time ^a (min)	UV-Vis spectrum
Gallic acid (monomer) (4)		0.42	
Ellagic acid (monomer) (5)		2.97	
Catechin (monomer) (6)		0.60	

^aUHPLC-PDA method in Section 2.3.4.

Ellagic acid was identified in 19 samples, including all the black and seven brown samples (Fig 4.17). Three of the four black samples were from A.1929.152, a blackwork piece, and the fourth one was from the bed valance collection (H.RHB.25.9). The additional 14 samples included one blue, seven brown, one red, one orange and four pink samples from eight objects worked in both wool and silk (Appendix A3). The presence of tannins in the four silk objects could be from the weighting process of the degummed silk²⁷ or from use as an additive to obtain the desired shade.

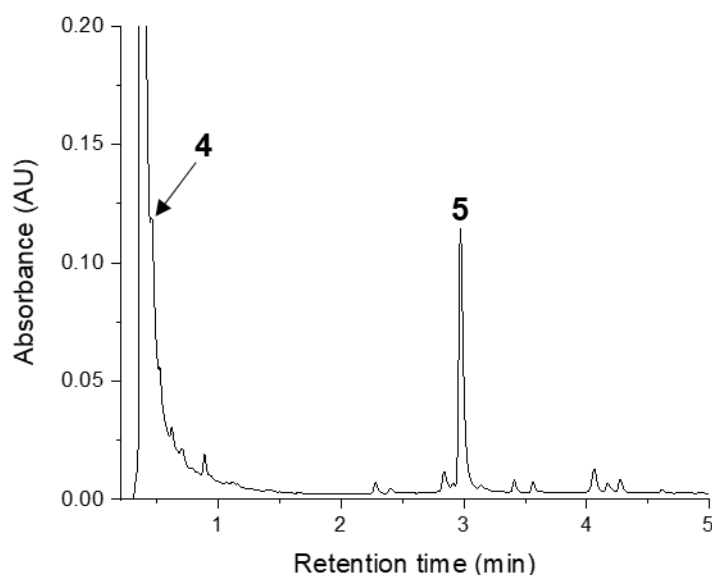


Figure 4.17: UHPLC-PDA chromatogram of oxalic acid extract monitored at 254 nm of sample H.RHB.25.9-3 showing the small shoulder of gallic acid (**4**) and the main peak of ellagic acid (**5**) monomer.

All black samples collected showed visual disintegration of the threads (Figure 4.18), making it likely that an iron mordant was used to dye the thread.^{26,28,29} Confirmation of iron-tannate complexes can be obtained by elemental analysis such as X-ray fluorescence (XRF).²⁶ The likely identification of iron-tannate complexes in these objects make them a priority for conservation before complete disintegration. Development of stabilisation treatments of iron-tannate dyed textiles is in progress but there are currently no general procedures available.^{30,31}

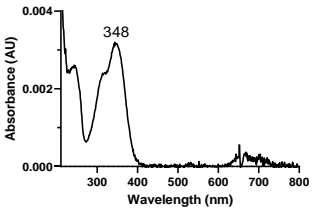
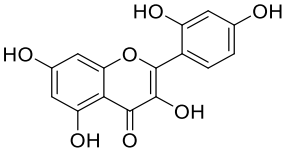
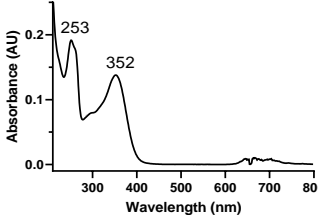
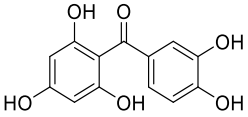
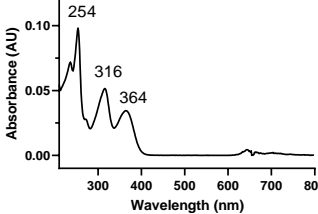
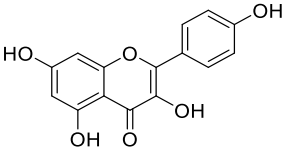
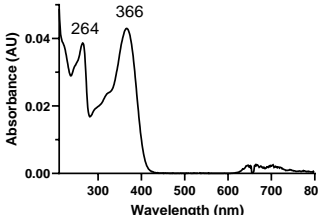


Figure 4.18: Detail of A.1929.152 (left) and H.RHB.25.9 (right) © NMS with red arrows indicating regions of disintegration of tannin dyed thread.

4.9.2 Young fustic (*Cotinus coggygria* Scop.) and old fustic (*Maclura tinctoria* L.)

Table 4.5 Identification of components of young fustic (*Cotinus coggygria* Scop.) dye (fisetin and sulfuretin) and old fustic (*Maclura tinctoria* L.) dye (morin, maclurin and kaempferol). The retention times and UV-vis spectra of unknown components found in old fustic samples also included

Compound	Structure	Retention time ^a (min)	UV-Vis spectrum
Fisetin (7)		3.71	
Sulfuretin (8)		4.42	
Unidentified compound I (9)		3.76	

Unidentified compound II (10)		3.98	
Morin (11)		3.81	
Maclurin (12)		4.09	
Kaempferol (13)		5.28	

^aUHPLC-PDA method in Section 2.3.4.

Young fustic was identified by the presence of (7) and (8) in 16 samples from ten objects. Eight of the samples contained additional dye sources such as weld (Section 4.8.1), madder (Section 4.11.1) or soluble redwood (Section 4.11.2). Myricetin, quercetin or known degradation product 3,4-dihydroxybenzoic acid and its methyl ester were not seen in the embroidery samples.¹⁹ Twelve of the samples did contain an unidentified fisetin-related compound (9) [$R_t = 3.76$ min, $\lambda_{max} = 310$ (sh), 345 nm] and eight of these contained (9) and an additional fisetin-related component (10) eluting at 3.98 min [$\lambda_{max} = 305$ (sh), 348 nm] (Fig 4.19).

Young fustic was well known to have poor lightfastness and it was often a forbidden dye to be used in high-quality textiles due to this.²⁵ Regardless, it has been identified in continental¹⁹ and English¹⁸ tapestries from the same period as the embroideries studied. Although the use of young fustic in the continental tapestries might be due to later restoration work.¹⁹ A mixture of young fustic and weld or dyer's greenweed was found in the English tapestries, either reflecting cross-contamination during the dyeing

process or a deliberate dye house practice.¹⁸ Two of the embroidery samples studied (A.1956.1198-11, H.RHB.25.5-3) were found to contain fisetin (**7**) and luteolin (**1**), pointing toward similar use of young fustic and weld as in the English tapestries. Additionally, young fustic was known to be used as the core in gilded metal thread during the Renaissance²⁴ and it has been identified in Renaissance Italian silk³² and liturgical vestments from the 15th – 17th centuries.³³

The use of young fustic in the embroideries investigated despite its fugitive nature is therefore not surprising when it can be found in contemporary more expensive or high-quality textiles such as tapestries. However, interesting to note, is the use of young fustic, with either a soluble redwood or a tannin source, in the majority of pink samples collected from the Scottish bed valances (H.RHB.25.5-3, H.RHB.25.6-3, H.RHB.25.10-3, H.RHB.25.10-4). Using young fustic dyed silk thread in these objects could be an aesthetic decision, but the extensive use of less expensive dyestuffs can also reflect the smaller economy of Scotland compared to England and continental textile centres.

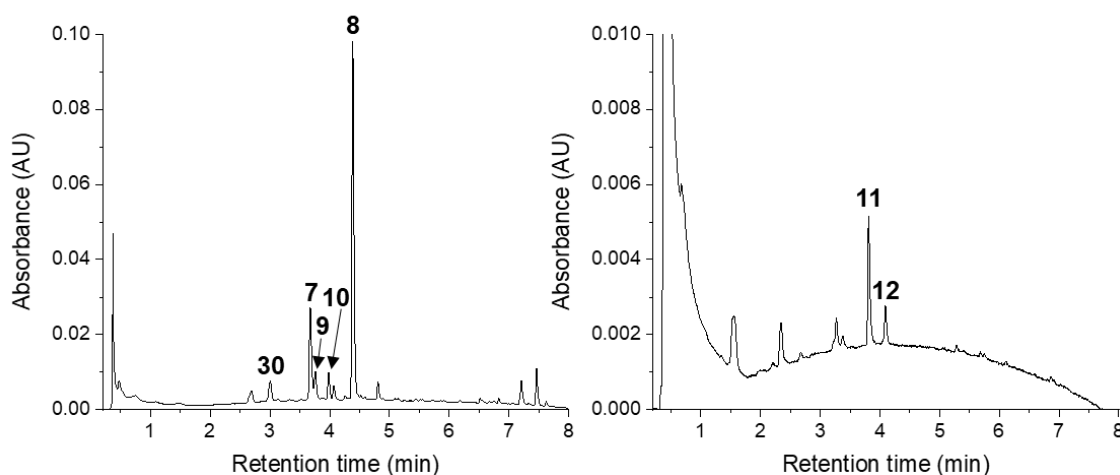


Figure 4.19: **A:** UHPLC-PDA chromatogram of oxalic acid extract monitored at 350 nm of sample H.RHB.25.10-3 in which young fustic (**7**, **8**) in combination with a soluble redwood dye marker (**30**) (Section 4.11.2) was identified. Unidentified compounds related to fisetin labelled **9** and **10**. **B:** UHPLC-PDA chromatogram of oxalic acid extract monitored at 350 nm of sample A.1938.580-3 in which old fustic (**11**, **12**) was identified.

Related to young fustic is old fustic, which is a dye from the heartwood of *Maclura tinctoria* L. Old fustic is native to the Americas, particularly central America and it was brought over to Europe during the Spanish colonial expansion during the 16th century (Section 1.4.2.1).^{24,34} It is identified in samples by the presence of flavonol morin (**11**)

and benzophenone maclurin (**12**) as well as flavonol kaempferol (**13**). Nine samples from four objects were found to contain old fustic due to the presence of morin (**11**). Five of the samples contained maclurin (**12**) as well as (**11**) but only two of the samples (A.1956.1484-7, A.1956.1484-8) also contained kaempferol (**13**).

The absence of (**12**) and (**13**) in a majority of the old fustic samples could be due to using too small sample resulting in the concentration of (**12**) and (**13**) being below the detection limit of the analysis. It could also be due to photodegradation of the chromophores. However, the known degradation products of morin (**11**): 2,4-dihydroxybenzoic acid and its methyl ether,³⁵ could not be found in any of the samples. This absence of degradation products does not rule out severe photodegradation in the samples however as it has been shown that the rate of degradation of (**11**) does not match the rate of formation of 2,4-dihydroxybenzoic acid and its methyl ether.³⁵ Currently, it is unknown what other degradation processes are occurring.

It is not known exactly when old fustic started to be imported to Europe from South America, but it was likely brought over in the beginning of the 16th century.²⁵ Municipal regulations against its use in the 16th and 17th centuries show that it was at least in use during the Renaissance despite it rarely being mentioned in dye manuscripts before the 18th century.^{24,25} Two of the samples collected from blackwork (A.1938.580) show the presence of (**11**), while the third sample contains both (**11**) and (**12**). The object is stylistically dated to c. 1550 – 1580, and if this date was to be confirmed, it would be one of the oldest European objects known to contain old fustic, adding to the understanding of the start of the Spanish South American dye trade.

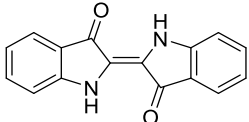
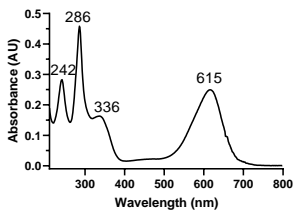
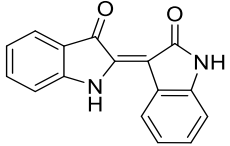
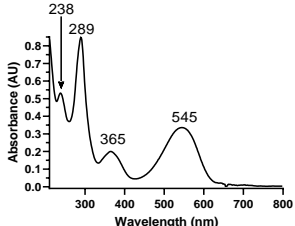
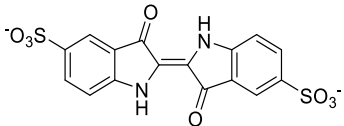
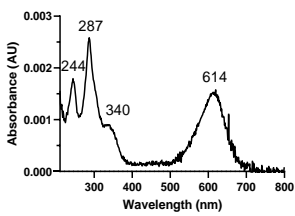
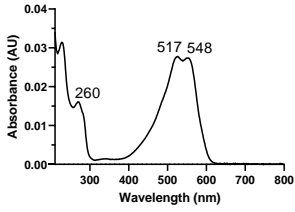
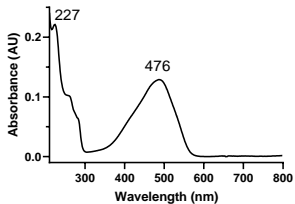
A soluble redwood (Section 4.11.2) dye source in combination with madder was characterised in three samples as the red source (Fig 4.19A). However, the most common red and yellow dye source combination used was madder (Section 4.11.1) with weld, young fustic, or old fustic (Fig 4.19B). The use of old and young fustic for colours other than yellow despite their appearance, reinforces the attitude of the dyestuffs as of poorer quality compared to other yellow sources such as weld.

4.10 Blue, grey, and purple

None of the grey samples were found to be dyed. Three of the four grey samples were worked in wool thread from object A.1894.234, so it is a possibility that the grey shade seen was either the natural wool of the sheep or the dye too degraded for analysis.

The use of undyed wool thread was common for lower status wool textiles, so the presence of such threads in a luxury textile such as embroidery would be unusual and indicate a likely domestic origin. The fourth grey sample (A.1962.1067-20) could possibly be undyed and just very dirty (Appendix A3).

Table 4.6 Identification of components of indigo dye (indigotin (**14**) and indirubin (**15**)), Saxon blue (**16**) and lichen purple dye (orchil marker I (**17**) and II (**18**)).

Compound	Structure	Retention time ^a (min)	UV-Vis spectrum
Indigotin (14)		6.93	
Indirubin (15)		7.83	
Indigo carmine (Saxon blue) (16)		3.73	
Orchil marker (17)		5.81	
Orchil marker (18)		7.05	

^aUHPLC-PDA method in Section 2.3.4.

4.10.1 Indigo (*Indigofera* spp.) and woad (*Isatis tinctoria* L.)

As expected, all of the blue samples were found to be dyed with indigo, identified by the presence of indigotin (**14**). Indirubin (**15**) could only be found in trace amounts in few (eight blue and purple) samples. Indigo can be sourced from multiple plant species, in particular the *Indigofera* family.²⁴ Historically, the two main sources used in Europe were *Indigofera tinctoria* L., known as indigo and grown mainly in India and *Isatis tinctoria* L. also called woad and grown across Europe.³⁶ (Section 1.4.3).

Unfortunately, both species have identical chemical fingerprints, so it is difficult to determine the plant source of the indigo used. Methods using the ratio between indigotin and minor components such as indirubin have been suggested,³⁷ but it has been shown that these ratios are highly dependent on multiple variables beyond plant species.³⁸ Recently, statistical techniques based on mass spectrometry data has shown promising results in reliable differentiation,³⁹ but it requires access to large databases and sophisticated computations.

All except two of the purple samples also contained indigo, identified by the presence of indigotin (**14**). The indigo was either combined with a red dye source to create purple (Section 4.11) or used to deepen the purple colour obtained from orchil lichens (Section 4.10.3). Indigo was probably not added to the two remaining purple samples (A.1894.234-24, A.1956.1484-10) due to the light or reddish shade desired (Appendix A3).

4.10.2 Saxon blue

Known as a semi-synthetic dye, indigo carmine (**16**) or Saxon blue, is a sulfonated version of the indigo molecule (Table 4.6). It was invented in 1743 by Johann Christian Barth and was patented in England 1748.⁴⁰ The presence of Saxon blue in one sample of A.1894.234 (Fig 4.20, chromatogram Fig 4.21), thought to be made 1710 – 1720 therefore suggests that it either was produced later than estimated, or that it was repaired using Saxon blue dyed thread sometime after 1743. The presence of natural indigo in the other blue samples from the object suggests that restoration at a later date is more likely the case.



Figure 4.20: A.1894.234 with sampling position of sample 34 containing Saxon blue. During sampling, the sample was described as olive green.

The added sulfonic groups make the chromophore water soluble which make the laboured process of vat dyeing redundant and instead a direct or mordant dyeing process can be used (Section 1.3). The water solubility and ease of application was its major selling point as the lightfastness is poorer than natural indigo.^{25,40} The use of Saxon blue in one of the later, likely domestic, objects investigated, indicates that a wider range of dye sources, even experimental ones, steadily became available to more social classes across the 18th century.

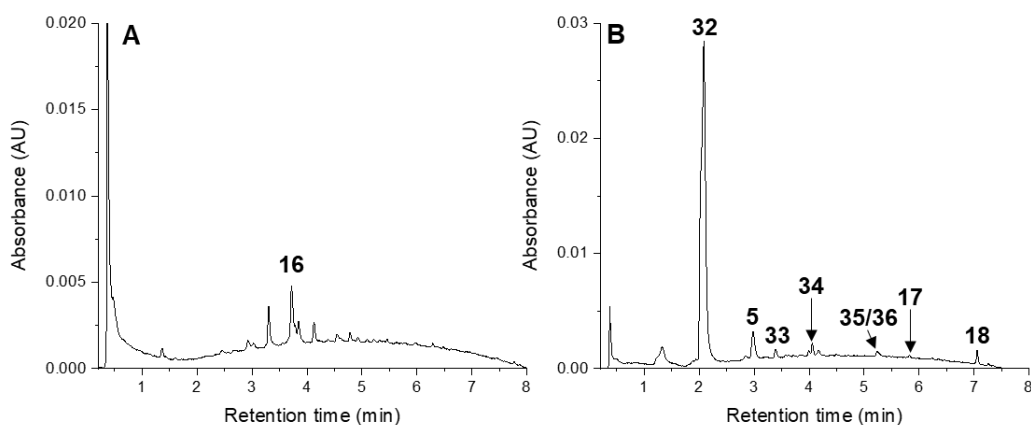


Figure 4.21: **A:** UHPLC-PDA chromatogram of oxalic acid extract monitored at 350 nm of sample A.1894.234-34 containing Saxon blue (**16**) and unidentified peaks. **B:** UHPLC-PDA chromatogram extracted at 430 nm of sample H.RHB.25.5-1 showing the presence of lichen purple (**17**, **18**) together with cochineal (**32** - **36**) and a tannin source (**5**).

4.10.3 Lichen dyes

Lichen purple was identified in 10 samples by the presence of orchil markers (Table 4.6),^{41,42} including five of the nine purple samples. The UV-vis spectra for the orchil markers are unique to the use of orchil but they cannot be assigned to a particular molecular structure of orcein without MS confirmation.^{41,43,44} Hence, the structures are not specified in Table 4.6 but the UV-vis spectra are used to determine the use of orchil purple.

Orchil was a dye obtained from lichens often locally sourced⁴⁵ and was used as a more cost-effective alternative to shellfish purple or purples obtained from expensive cochineal overdyed with indigo (Section 4.11.3).^{24,25} Three of the lichen samples collected from A.1894.234 contained indigo, which was probably added to deepen the colour to the shade desired. Only the orchil markers could be characterised in the two other purple samples (A.1894.234-24 and A.1959.1484-10), explaining their more reddish purple (Fig 4.22).

Orchil was found in three objects of which two were embroidered in wool and dated from the early 18th century: A.1894.234 and A.1956.1484. Both of these objects are likely to be domestic works, so a desire to lowering the cost could explain the use of lichen. For A.1894.234, lichen is used in both purple and pink samples (Fig 4.22) demonstrating the colour variety possible for lichen dyes. Despite lichen purple known poor lightfastness,⁴² it was known to be used in Dutch workshops in the production of low-quality tapestries.²⁵ Its use has been found in liturgical paraments⁴⁶ and Renaissance tapestries.^{19,47,48} The identification of lichen purple in the embroidery samples therefore suggest that the embroiderer had access to similar material as the tapestry maker in Renaissance Scotland and England.



Figure 4.22: Samples containing lichen purple showing the variety in colour achieved. **A:** A.1894.234-24, described as purple a. **B:** A.1894.234-23, described as purple c. **C:** H.RHB.25.5-1, described as red.

The third object containing lichen (RHB.25.5) is of known Scottish origin. The red sample collected was found to contain the unusual combination of lichen purple and cochineal (Fig 4.21B). The involved process and stark red colour of cochineal made it an expensive dyestuff (Section 1.4.2.2). The colour of the sample (Fig 4.22) and the known expense of cochineal dye, probably means that the lichen dye was used as an additive to brighten the cochineal red rather than as the main dye source, similarly to the use of indigo.²⁵ The combination of such an expensive dyestuff with the economical lichen purple is uncommon and may indicate domestic interference in the dyeing process. That this combination is found in a known Scottish object strengthens the link between the use of lichen and Scottish dyeing tradition.⁴⁵

4.11 Red, orange, and pink

The second largest group of samples collected containing the red, orange, and pink samples showed the largest range of dyestuffs combined, with ten dye sources identified in the three colours. The main red dye sources used throughout the collection were madder identified in 42 samples of which 26 were red, orange, or pink; soluble redwood, present in 28 samples overall and 22 red, orange, or pink samples; cochineal was found in 32 red, pink or purple samples; and safflower characterised in four orange or pink samples. All of the other dye sources identified except Saxon blue could be found in combination with these main red dyestuffs in 31 of the 73 red, orange, or pink samples collected.

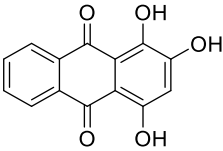
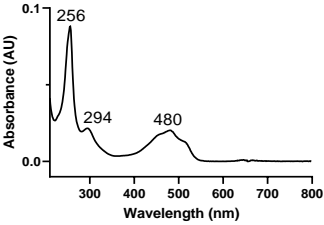
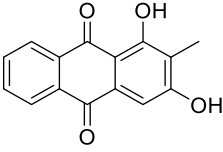
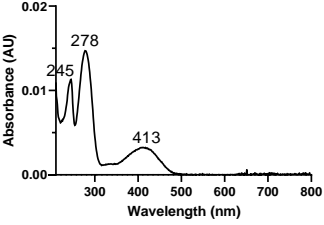
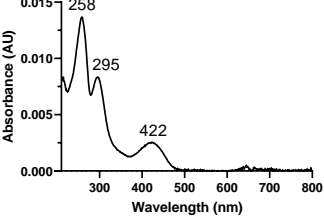
4.11.1 Madder (*Rubiaceae* spp.)

Many anthraquinone-containing *Rubiaceae* plant roots have been used across the world for dyeing red.²⁴ In Europe, cultivated madder (*Rubia tinctorum* L.) and wild madder (*Rubia peregrina* L.) were the main sources of madder dye but many other species were also in use, including woodruff (*Aperula* spp.) and bedstraw (*Galium* spp.) species.^{24,25} In Scotland, the use of lady's bedstraw (*Galium verum* L.) has been historically documented, particularly in the Western Isles.⁴⁵ (Section 1.4.2.2).

The anthraquinone content found in an analysed textile sample is dependent on multiple variables, including the species, age and environment of the plant used as well as the preparation of the roots, dye bath conditions and analytical protocol followed (Section 1.4.2.2).^{24,25,49–55} The effect of these variables is difficult to predict which makes it complicated to determine the species used based on the anthraquinone content.⁴⁹

Table 4.7 Main components of madder dye (*Rubia tinctorum* L.).

Compound	Structure	Retention time ^a (min)	UV-Vis spectrum
Ruberythric acid (19)		4.04	
Lucidin primeveroside (20)		4.23	
Munjistin (21)		5.32	
Xanthopurpurin (22)		5.67	
Pseudopurpurin (23)		5.83	
Alizarin (24)		6.29	

Purpurin (25)		7.45	
Rubiadin (26)		8.55	
(27)		8.96	

^aUHPLC-PDA method in Section 2.3.4.

Madder was found in 42 of the samples analysed by the presence of alizarin (**24**) and purpurin (**25**). Both compounds were found in all samples except three (A.1960.230-5, 1962.1067-3 and A.1894.234-14) which only contained trace amounts of alizarin (**24**). Munjistin (**21**) and xanthopurpurin (**22**) could not be separated by the UHPLC-PDA method used but their combined peak was found in 20 samples. Rubiadin (**26**) was seen in eight samples while pseudopurpurin (**23**) only was present in one sample (A.1894.234-13). Glycosidic precursors (**19**, **20**) were found in 12 samples. No nordamnecanthal or lucidin, that are common madder components,⁵⁰ were found in any of the samples but the unknown anthraquinone (**27**) was characterised in 11 samples.

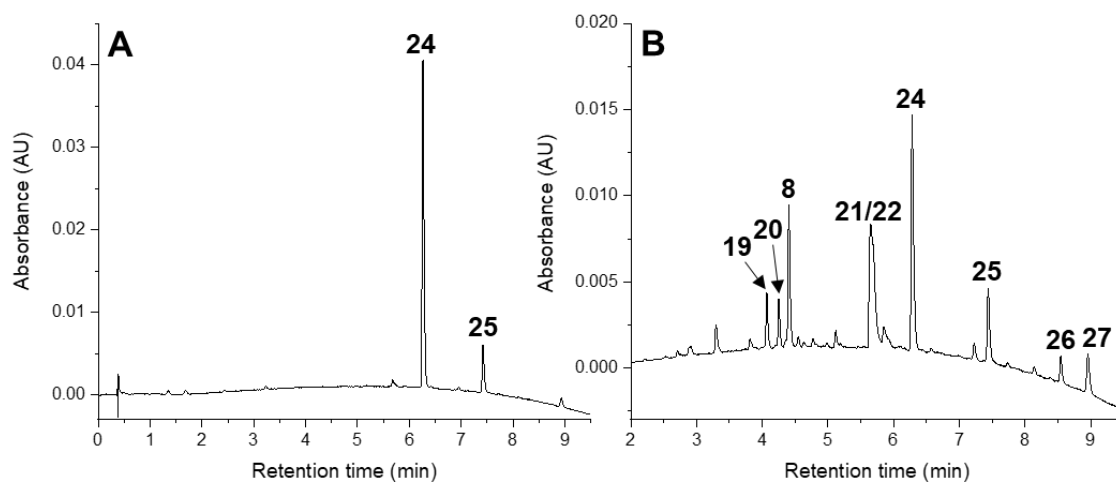


Figure 4.23: A: UHPLC-PDA chromatogram of oxalic acid extract monitored at 430 nm of sample A.1938.584 A-15 showing the presence of only alizarin (**24**) and purpurin (**25**). **B:** UHPLC-PDA chromatogram of oxalic acid extract monitored at 430 nm of sample A.1894.234-46 showing the combination of madder and young fustic (sulfuretin (**8**)) for the orange colour of the sample. Labelled are ruberythric acid (**19**), lucidin primeveroside (**20**), sulfuretin (**8**), munjistin/xanthopurpurin (**21/22**), alizarin (**24**), purpurin (**25**), rubiadin (**26**) and unknown anthraquinone (**27**).

The ratio of alizarin (**24**) and purpurin (**25**) in the samples was investigated by collecting the peak areas of the compounds in chromatograms extracted at 430 nm, normalising the two areas to 100 and finding the ratio. The ratios are reported as the relative percentage of alizarin compared to purpurin (Fig 4.24A).

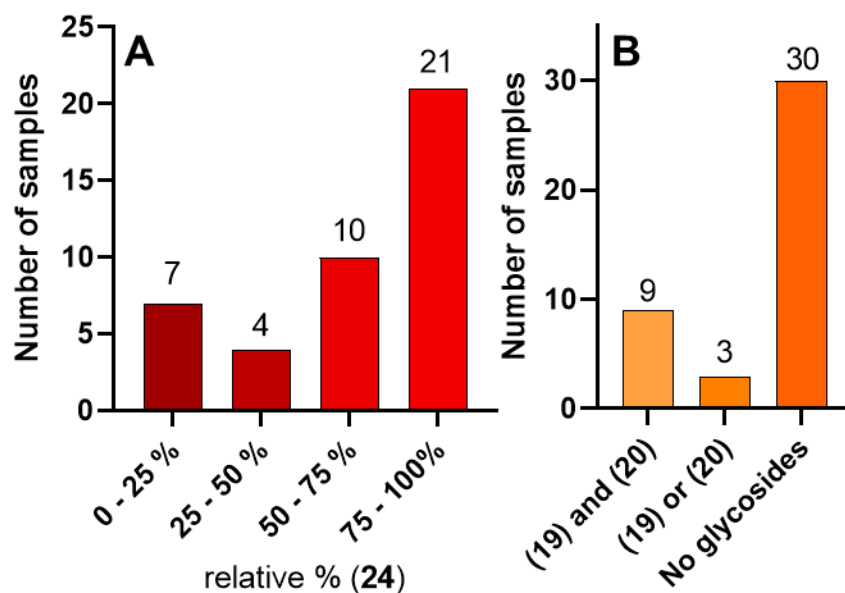


Figure 4.24: **A:** Relative percentage of alizarin when the alizarin and purpurin content of each sample is normalised to 100. **B:** Number of samples containing one, two or no glycosides.

Madder was the red dye source found in the largest number of samples compared to the other red dye sources identified (soluble redwoods (Section 4.11.2), cochineal (Section 4.11.3), safflower (Section 4.11.4)). This observation is unsurprising based on the documented popularity of madder.^{24,25} The versatile use of madder is shown by its presence in 17 brown, 9 red, 4 orange and 12 pink samples and it was found in combination with all other dye sources identified except safflower and Saxon blue (Section 4.10.2). It was found mixed with weld in six samples and mixed with indigo in three samples, both which are combinations reported to be present in English tapestries contemporary to the embroideries studied.¹⁸

The majority of the samples present in the samples dyed with madder contained over 75 % alizarin (**24**) compared to purpurin (**25**). This suggests that cultivated madder *Rubia tinctorum* L. was likely used to dye all samples. However, the large presence of alizarin may also be due to photodegradation as purpurin has been reported to degrade at a faster rate than alizarin,⁴² influencing the ratios found. Studies have also shown that alizarin (**24**) is dyed preferential to purpurin (**25**) at lower temperatures.⁴⁹

The mild sample preparation protocol employed (Chapter 3) retained glycosidic compounds in 17 samples where ten samples contained both ruberythric acid (**19**) and lucidin primeveroside (**20**) and seven samples contained only one of them (Fig 4.24B). The presence of glycosidic compounds suggests that the roots were either

boiled or steamed shortly after they were harvested or left to dry out before dyeing.^{51,54} The majority of the samples showed no glycosides which either suggest that the roots were soaked to encourage enzymatic deglycosylation^{51,56} or photodegradation of the glycosides into their aglycones have occurred.⁵²

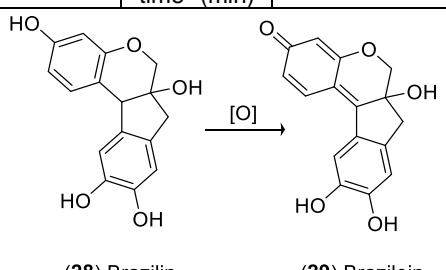
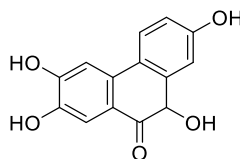
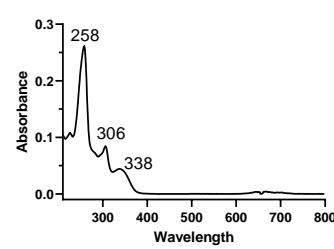
The most common combination of madder observed in the samples analysed was with either soluble redwood or cochineal (11 samples each). Both of these combinations were known to be used historically to produce demi-scarlets and demi-crimsons.^{25,57} The samples found to be dyed with a combination of madder and cochineal were all described as red or dark pink during sampling, while madder and soluble redwood were found in samples categorised as orange (four samples) and brown (two samples) as well as red and pink. The difference in current appearance from the demi-scarlet and -crimson colours obtained from madder and soluble redwoods is most likely due to both the more pink colour obtained from soluble redwood dyes²⁴ as well as the known poor lightfastness of redwood dyes.^{58,59}

Research has shown that madder is more stable on wool in comparison to silk and cotton,⁴² which likely was empirically understood historically as in Europe, madder was mainly used for wool dyeing and less for silk.²⁵ Such a practice is reflected in this study as all six wool objects analysed were found to contain madder samples. Additionally, 33 out of the 42 samples dyed with madder were from wool thread, clearly showing the known preference of wool for madder dyeing even for materials of luxury items such as embroideries.

4.11.2 Soluble redwood (*Caesalpinia* spp.)

Soluble redwood dyes, also known as brazilwood, can be obtained from multiple species, mainly from the *Caesalpinia* genus.^{24,25} The main chromophore of soluble redwoods is brazilein, the oxidised product of brazilin (Table 4.8), which is naturally occurring in soluble redwoods and the colour produced is a fugitive but attractive pink.^{19,34,60} The concentration of brazilein in historical textiles is often too low to be detected and instead the marker urolithin-C can be used to identify a redwood dye source (Section 1.4.2.3).^{19,58}

Table 4.8 Characteristic markers of soluble redwood dye.

Compound	Structure	Retention time ^a (min)	UV-Vis spectrum
Brazilin (28) Brazilein (29)	 <p>(28) Brazilin (29) Brazilein</p>		
Urolithin-C (30)		2.99	

^aUHPLC-PDA method in Section 2.3.4.

Brazilein (29) was not characterised in any sample, but its associated degradation compound urolithin-C (30) was found in 28 samples including one purple, three brown, two red, six orange and 16 pink ones. It was identified in less samples but in a larger range of colours compared to madder and cochineal. This suggests a preference for another red dye source if available, which could be explained by the less intense red obtained from soluble redwood in comparison to madder and cochineal and the lower cost of redwoods in comparison to other pinks.^{24,25}

Soluble redwood dye has been characterised in both English and continental European Renaissance tapestries, most frequently in combination with madder, weld or young fustic.^{18,19} These combinations were also identified in the analysed embroidery samples with a mixture of madder and redwood dye found in the largest number of samples (nine samples). Additionally, redwood dye in combination with lichen (A.1894.234-14, A.1894.234-15) was identified in two samples. Traces of indigo were also found in two samples of twilled pink and blue threads (A.1926.168-14 and A.1926.168-19, Section 4.5.3, Appendix A3). The presence of indigo in these samples was likely from incomplete separation of the dyed threads during the sample preparation step rather than a mixture of redwood and indigo in the pink fibres.

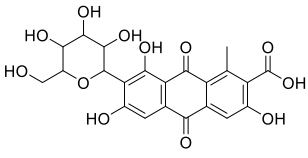
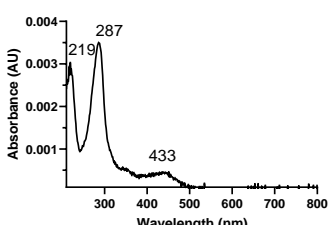
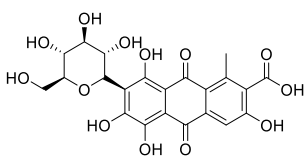
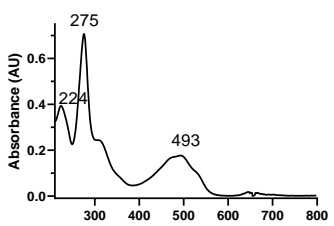
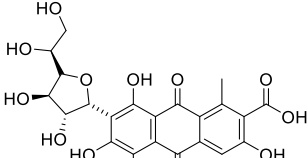
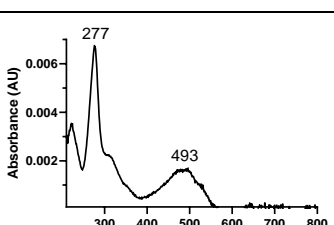
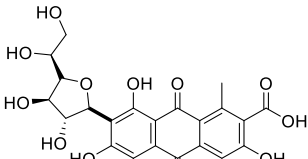
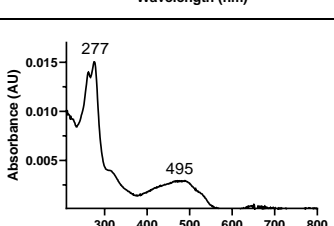
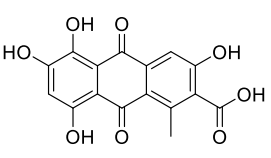
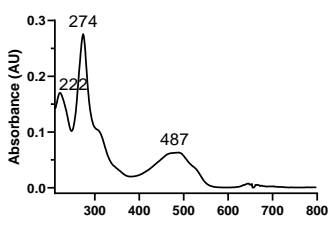
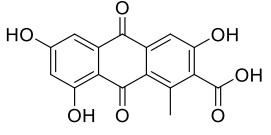
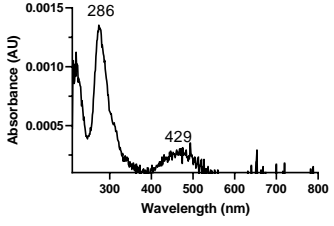
Soluble redwood dyes were imported to Scotland from at least 1597⁴⁵ and could be found in five of the six pink samples collected from the Scottish bed valance set (H.RHB.25.1-11), showcasing the availability of redwood dyed thread in Scotland.

The majority of pink samples from the book cover (A.1926.168) were also characterised to be dyed with soluble redwood dyes. Both these objects are known to be domestic works, so the use of soluble redwood dyes was likely an economical decision.

4.11.3 Cochineal (*Coccoidea* superfamily.)

Cochineal together with kermes and lac are red dyes obtained from insects that were, and still are today, revered for their vibrant scarlet shades and high lightfastness.²⁴ The striking colours obtained required laborious production processes and a large number of insects per grams of dye, making cochineal one of the most expensive natural dyes throughout history and textiles dyed with cochineal were regarded as luxury items and a symbol of wealth.^{6,7,24,25}

Table 4.9 Identification of components of cochineal dye.

Compound	Structure	Retention time ^a (min)	UV-Vis spectrum
dcII (31)		1.93	
Carminic acid (32)		2.06	
dcIV (33)		3.38	
dcVII (34)		4.04	
Kermesic acid (35)		5.23	
Flavokermesic acid (Laccaic acid D) (36)		5.22	

^aUHPLC-PDA method used described in Section 2.3.4.

Cochineal was characterised by the presence of carminic acid (32) in a total of 32 samples: three purple, 13 red and 16 pink ones. In 15 of these samples, cochineal

was combined with another dye source, such as madder (Section 4.11.1), soluble redwood (Section 4.11.2), indigo (Section 4.10.1), and lichen (Section 4.10.3). A source of luteolin (**1**), likely weld (Section 4.8.1), was used in three samples while ellagic acid (Fig 4.25) was found in 14 samples, likely from the degumming process of silk.²⁷

Minor anthraquinone components (**31**, **33** – **36**) were identified in all but seven samples and the average relative percentage area of carminic acid (**32**) across all samples was found to be 97 %. The high percentage of carminic acid (**32**) is indicative of the use of either Mexican or Armenian cochineal as Polish cochineal has been reported to contain higher levels (> 10 %) of kermesic (**35**) and flavokermesic acid (**36**).^{60–64} Further species identification based on these markers was not undertaken due to the reported unreliability of the Wouters and Verhecken model.^{64,65} The variability of this approach would also be increased by the partial co-elution of dcII (**32**) and carminic acid (**31**) seen using the UHPLC-PDA method (Fig 4.25). A multivariate approach^{64,65} was not utilised either as such statistical approaches require access to a large database of reference values which was not available to this project. Species identification can therefore not currently be confidently obtained based on the data available.

However, archival research makes it likely that Mexican rather than Armenian cochineal was used in England and Scotland during the time studied as trade in Mexican cochineal with Spain and textile centres such as Antwerp was documented from at least mid-16th century.^{45,66} Armenian cochineal can be more commonly found in Mediterranean and Middle Eastern objects.^{67,68}

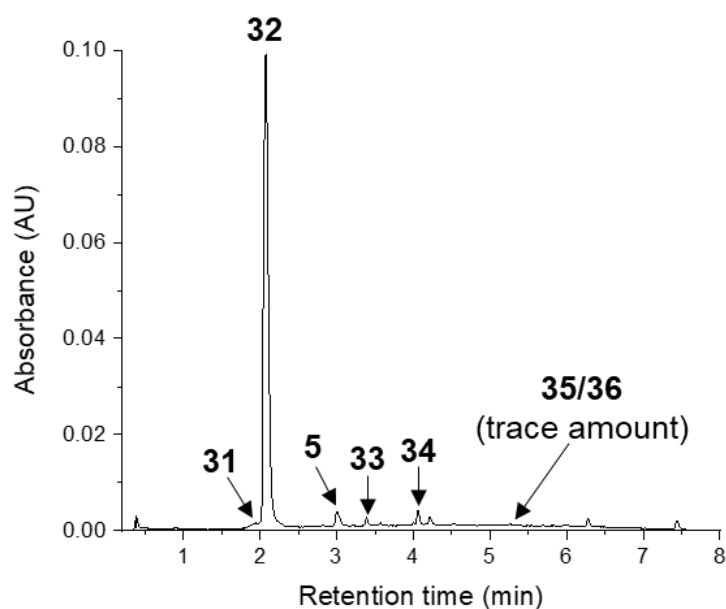


Figure 4.25: UHPLC-PDA chromatogram of oxalic acid extract monitored at 475 nm of sample 1962.1067-14 containing cochineal (**31 - 36**) and a source of tannins (**5**), likely from the weighting of the silk thread used.²⁷

The dye mixtures found in the samples follow known recipes of obtaining a range of colours using cochineal.^{24,25,45} Cochineal combined with indigo was a common practice to obtain purple and dark red shades.²⁵ This combination has been found in English Renaissance tapestries,¹⁸ but was found to only be used for the known continental and professional coif A.1965.722 in this study. The most common combination found was cochineal mixed with madder (13 samples) which has also been reported present in 16th and 17th centuries tapestries from Brussels and Bruges.¹⁹

Cochineal was found to be mixed with lichen purple in one sample of known Scottish origin (H.RHB.25.5-1). This unconventional combination could perhaps be due to a lack of access to other dyestuffs, so lichen had to be substituted in. It could also reflect an unusual Scottish dyeing practice or just a desire for a particular shade of red as the design shows a shading effect of the red petals sampled (Fig 4.26).



Figure 4.26: H.RHB.25.5 © NMS showing the flower design containing cochineal and lichen purple.

The use of cochineal in Scotland has been documented since the 17th century⁴⁵ and it has been found to be the main red dye source in tartans dating from the 18th century onwards.^{69,70} It is a dyestuff known to be used in expensive luxury textiles such as tapestries and fashionable garments.^{24,25} The surprisingly large number of samples from the small, domestic embroideries studied in this project containing cochineal therefore suggests that it was a dyestuff more commonly available than previously thought.

4.11.4 Safflower (*Carthamus tinctorius* L.)

The final dyestuff identified in the embroidery samples was safflower red (*Carthamus tinctorius* L.). The main chromophore in safflower red is carthamin^{24,25} (**41**) but the poor lightfastness of safflower red in comparison to other pink dye sources makes it necessary to use unique markers, Ct1 – Ct4 (**37 – 40**) (Fig 4.27) for identification.⁷¹⁻⁷³ Recently, molecular structures of Ct1 – Ct4 and two related additional markers labelled Ct5 and Ct6 have been proposed⁷⁴ (Table 4.10). Three samples, two orange (K.2001.637-10, K.2001.637-11) and one pink (A.1962.1067-18) were found to contain safflower. Additionally, Ct3 and Ct4 were found in trace amounts in another pink sample (A.1965.722-13) dyed with cochineal.

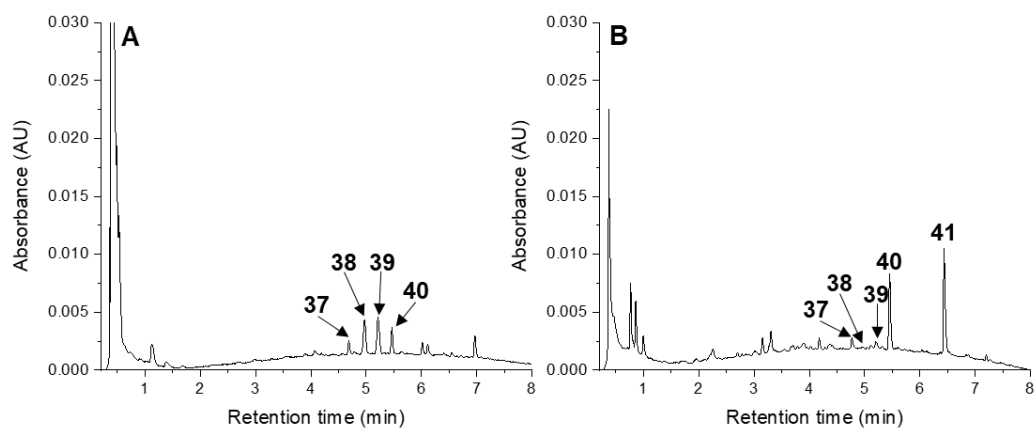
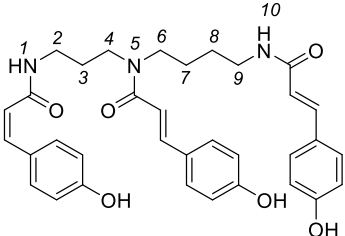
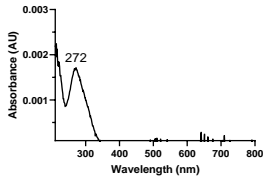
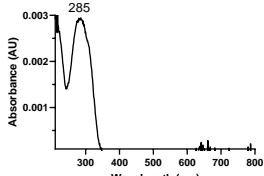
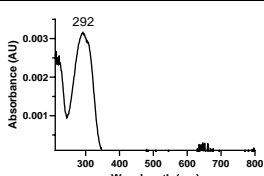
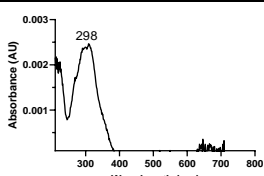
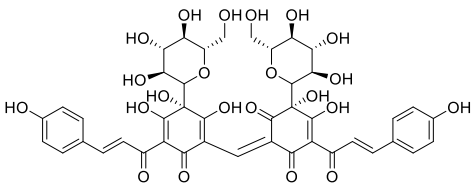
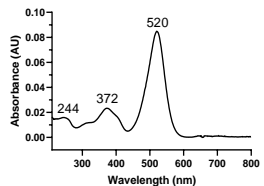


Figure 4.27: A: UHPLC-PDA chromatogram of oxalic acid extract monitored at 300 nm of sample 1962.1067-18 containing safflower red markers Ct1 – Ct4 (**37 - 40**) but no carthamin (**41**). **B:** UHPLC-PDA chromatogram of oxalic acid extract monitored at 350 nm of sample K.2001.637-11 containing safflower red markers Ct1 – Ct4 (**37 - 40**) and carthamin (**41**).

Table 4.10 Identification of components of safflower dye.

Compound	Structure	Retention time ^a (min)	UV-Vis spectrum
Proposed structure for Ct1 - 4 (31) - (34) ³⁷			
			
Ct1 (37)	<p style="text-align: center;">ZZZ isomer N¹ = Z, N⁵ = Z, N¹⁰ = Z</p>	4.66	
Ct2 (38)	Mixture of ZZE, ZEZ, EZZ, ZEE, EZE, EEZ isomers	4.94	
Ct3 (39)	Mixture of ZZE, ZEZ, EZZ, ZEE, EZE, EEZ isomers	5.18	
Ct4 (40)	Mixture of ZZE, ZEZ, EZZ, ZEE, EZE, EEZ isomers	5.43	
Carthamin (41)		6.43	

^aUHPLC-PDA method in Section 2.3.4.

Safflower red was an expensive dyestuff due to the complex dyeing process and low dye content per flower.²⁴ The use of safflower red was more common in Asian⁷⁵⁻⁷⁷ and Coptic⁷⁸ textile production than European, although it has been identified in 16th century Italian silk samples^{71,79} as well as English tapestries from the Renaissance.¹⁸

Safflower was identified in the altar frontal (K.2001.637), one stomacher (A.1962.1067) and possibly in one coif (A.1965.722). All are likely made by professional embroiderers with the altar frontal and coif probably produced in continental Europe. The use of safflower in these suspected continental works reinforces the infrequent use of safflower in Scottish and English dyeing tradition. However, the stomacher A.1962.1067 may be of Scottish or English provenance as it cannot be properly assigned to the continent. Safflower is used as the inner petals of flowers adjacent the deeper reds of the outer petals dyed with cochineal. Such a close connection between safflower and cochineal has been found in English tapestries as well, which may indicate an English workshop practice (Fig 4.28).^{9,18}



Figure 4.28: A.1962.1067 © NMS showing the use of safflower to dye petals surrounded by petals dyed with cochineal. Similar use of these dyestuffs has been seen in contemporary English tapestries possibly indicating an English workshop practice.

4.12 The global dye trade and the NMS collection

The rapid introduction of American dyestuffs on the European market is reflected in the objects analysed by the presence of old fustic and Mexican cochineal. Particularly, the use of old fustic in the blackwork (A.1938.580) from 1550-1600 highlights a rapid adoption of the American dyes by Europeans. Since the blackwork is thought to be a domestic production, the use of old fustic shows that domestic embroiderers did have access to a large global trade network as well as resources to purchase said material.

Of course, the use of lichen in objects that are likely, or known, to be domestic works such as A.1894.234 and RHB.25.5 indicates that local resources were simultaneously still exploited. Many of the samples contained combinations of dyestuffs, which may not only reflect dye practices for the desired shade, but the extent of combinations could also have been an economic decision. For example, combining cochineal with madder, tannins or soluble redwood reduces the amount of cochineal required while still obtaining a vibrant red.

Other material required for embroidery production is the fibre used. As stated, only 6 of the 26 objects studied used wool thread. Scotland and England were large export countries of wool and wool-related products so wool was locally and likely cheaply available to the embroiderer. In contrast, silk had to be imported from either China or Italy as silk cultivation never became successful in England (Section 1.3.1). The employment of silk thread and imported dyes in a majority of the objects studied, even in known domestic works such as the H.RHB.25.1 – H.RHB.11 bed valances, therefore reflect how embroidery was thought of as a luxury item.

Many objects were made to be appreciated and displayed for years as seen in the common use of domestically worked embroideries in the public rooms of noble houses. Thus, the use of expensive material combined with the skill and care seen in most of the objects may indicate that the embroiderer herself might have looked at the produced objects as works of art. At least, it reflects a pride and appreciation in the resulting object. Later alterations, such as the transformation of the embroidery of A.1962.1067 into a stomacher show that embroidery became, or perhaps always was, disconnected from its original function and valued for itself.

4.13 Conclusions

The sample preparation workflow and chromatographic method developed in Chapter 3 were applied to a collection of 16th and 17th centuries Scottish and English embroideries from the collection at National Museums Scotland (NMS). Embroideries are difficult to sample as the loose ends in the back often are secured tightly, reducing the sample sizes available to sample without threatening the structural integrity of the objects. The analysis was successful on 237 of the 253 embroidery samples analysed, showcasing the effectiveness of the developed workflow even on small samples.

The samples were collected from 26 objects dated from mid-16th to early 18th centuries with 20 worked in silk and 6 worked in wool. The main colours sampled were yellow and greens with 100 samples, followed closely by red, pink, and orange which included 73 samples. 37 Blue, grey, and purple samples were collected, while 43 brown and black samples were obtained. The types of objects sampled varied from likely professional clothing pieces to domestic large furnishings and small panels, giving a good overview of the embroidery production in Renaissance Scotland and England.

Ten natural and one semi-synthetic dye sources were identified in the samples, many in combination with each other. Weld (*Reseda luteola* L.) was found in all yellow and green samples as well as a number of oranges and browns, making weld the most used dyestuff in the objects analysed. Indigo (*Indigofera* spp.) or woad (*Isatis tinctorum* L.) was the second most popular dyestuff used in the collection, being present in all blue, seven purple, three brown and two red samples. Madder, soluble redwood and cochineal were used in most of the red, pink, orange and brown samples.

Lichen purple, young and old fustic, tannins, and safflower were the remaining natural dyestuffs identified, used in purple, brown, black, orange and pink samples. Finally, the semi-synthetic dyestuff Saxon blue, the sulfonated version of indigotin, was found in one sample. A synthetic pathway to Saxon blue was not invented until 1743 in Germany, which makes the sample dyed with it a likely restoration from a later date.

The variety of dyestuffs, both locally sourced, such as lichens and weld, and imported, such as old fustic, safflower and cochineal, reflects the wide variety of dyestuffs available to both the domestic and professional embroiderer. Potential regional differences in dye combinations used between Scotland and England could exist, the use of lichen dyes in objects of known Scottish origin is a good example. However, a study of regional differences would require a larger sample size than available to this project but is an interesting area for future research.

The identification of old fustic in a blackwork stylistically dated 1550 – 1580 could be one of the earliest examples of old fustic in an English textile if the date is confirmed. The find suggests that there was no significant delay in introducing the new dyestuffs obtained from the colonisation of the Americas in the beginning of the 16th century. The domestic embroiderer's access to expensive, imported materials, such as cochineal, shows that already in the 16th and 17th century embroidery was dependent

on and a part of global trade. The main use of silk and imported dyestuffs highlights the global aspect of these domestic items giving these perceived English objects a global dimension.

4.14 References

- 1 G. Wingfield Digby, *Elizabethan Embroidery*, Faber and Faber, London, 1963.
- 2 P. Wardle, *Guide to English embroidery*, Victoria and Albert Museum, London, 1970.
- 3 L. Arthur, *Embroidery 1600-1700 at the Burrell Collection*, John Murray in association with Glasgow Museums, London, 1995.
- 4 M. Brooks, *English Embroideries of the Sixteenth and Seventeenth Centuries in the Collection of the Ashmolean Museum*, Ashmolean Museum, Oxford, 2006.
- 5 P. Wardle, *Text. Hist.*, 1994, **25**, 29–59.
- 6 C. M. Salinas, in *Global History and New Polycentric Approaches*, eds. M. Perez Garcia and L. De Sousa, Palgrave Macmillan, Singapore, 2018, pp. 255–273.
- 7 A. Peck, Ed., *Interwoven globe: the worldwide textile trade, 1500-1800*, Metropolitan Museum of Art, New York, NY, 2013.
- 8 J. Reiss, *English Embroidery from the Metropolitan Museum of Art, 1580-1700: 'Twixt Art and Nature*, Metropolitan Museum of Art, New York, NY, 2008, vol. 7.
- 9 E. Cleland, *Tapestries from the Burrell Collection*, Philip Wilson Publishers, London, 2016.
- 10 J. Arnold, *Patterns of fashion. 1-2: Englishwomen's dresses & their construction*, Macmillan, London, reprinted new edition (1977), 1984.
- 11 A. Hart and S. North, *Historical Fashion in detail The 17th and 18th centuries*, V&A Publications, London, 1998.
- 12 M. Swain, *Scottish Embroidery : Medieval to Modern*, B. T. Batsford Ltd, London, 1986.
- 13 M. Swain, *Historical Needlework: A study of Influences in Scotland and Northern England*, Barrie & Jenkins Ltd, London, 1970.
- 14 M. Swain, *The needlework of Mary, Queen of Scots*, Van Nostrand Reinhold Company, Inc., London, 1973.
- 15 N. E. A. Tarrant, *Textile Treasures An Introduction to European Decorative Textiles for Home and Church in the National Museums of Scotland*, National Museums

- Scotland, Edinburgh, 2001.
- 16 C. Browne, G. Davies, M. A. Michael and M. Zoschg, *English Medieval Embroidery: Opus Anglicanum*, Yale University Press in Association with Victoria & Albert Museum, London, 2016.
 - 17 L. M. Poggemoeller, MA Thesis, University of Missouri-Kansas City, 2015.
 - 18 L. G. Troalen, PhD Thesis, University of Edinburgh, 2013.
 - 19 D. A. Peggie, PhD Thesis, University of Edinburgh, 2006.
 - 20 G. J. Smith, S. J. Thomsen, K. R. Markham, C. Andary and D. Cardon, *J. Photochem. Photobiol. A Chem.*, 2000, **136**, 87–91.
 - 21 A. Manhita, T. Ferreira, A. Candeias and C. B. Dias, *Anal. Bioanal. Chem.*, 2011, **400**, 1501–1514.
 - 22 A. Villela, PhD Thesis, Wageningen University, 2020.
 - 23 D. M. Freund and A. D. Hegeman, *Curr. Opin. Biotechnol.*, 2017, **43**, 41–48.
 - 24 D. Cardon, *Natural Dyes: Sources, Traditions, Technology & Science*, Archetype Books, London, 2007.
 - 25 J. H. Hofenk de Graaff, *Colourful Past*, Archetype Books, London, 2007.
 - 26 H. Wilson, C. Carr and M. Hacke, *Chem. Cent. J.*, 2012, **6**, 1–13.
 - 27 M. Hacke, Weighted silk: history, analysis and conservation, *Stud. Conserv.*, 2008, **53**, 3–15.
 - 28 I. Degano, M. Mattonai, F. Sabatini and M. P. Colombini, *Molecules*, 2019, **24**, 2318.
 - 29 J. Kolar, A. Štolfa, M. Strlič, M. Pompe, B. Pihlar, M. Budnar, J. Simčič and B. Reissland, *Anal. Chim. Acta*, 2006, **555**, 167–174.
 - 30 C. A. Smith, B. J. Lowe, J. Swart, P. Fuentes-Cross, M. Mistral and R. Te Kanawa, *Stud. Conserv.*, 2022, **67**, 271–288.
 - 31 M. Škrdlantová, K. Drábková, D. Nagyová, J. Krejčí, H. Paulusová, M. Āurov and Š. Msallamoi, *Restaurator*, 2021, **42**, 87–103.
 - 32 M. van Bommel, I. Joosten, in *Silk Gold Crimson, Secrets and Technology at the Visconti and Sforza Courts*, ed. C. Buss, Silvana Editoriale, Milano, 2009.
 - 33 K. Lech, *J. Cult. Herit.*, 2020, **46**, 108–118.
 - 34 E. S. B. Ferreira, A. N. Hulme, H. McNab and A. Quye, *Chem. Soc. Rev.*, 2004, **33**,

329–336.

- 35 E. Ferreira, PhD Thesis, University of Edinburgh, 2001.
- 36 J. Balfour-Paul, *Indigo*, British Museum Press, London, 1998.
- 37 J. Mocquard, A. C. Le Lamer, P. L. Fabre, C. Mathieu, C. Chastrette, A. Vitrai and V. Vandebossche, *Dye. Pigment.* 2022, **207**, 110675.
- 38 A. Hartl, A. N. Proaño Gaibor, M. R. van Bommel and R. Hofmann-de Keijzer, *J. Archaeol. Sci. Reports*, 2015, **2**, 9–39.
- 39 V. Pauk, J. Michalčáková, K. Jagošová and K. Lemr, *Dye. Pigment.*, 2022, **197**, 109943.
- 40 M. De Keijzer, M. R. Van Bommel, R. Hofmann-De Keijzer, R. Knaller and E. Oberhumer, *Stud. Conserv.*, 2012, **57:sup1**, S87–S95.
- 41 J. Alcántara-García and M. Nix, *Herit. Sci.*, 2018, **6**, 1–15.
- 42 C. Clementi, W. Nowik, A. Romani, F. Cibin and G. Favaro, *Anal. Chim. Acta*, 2007, **596**, 46–54.
- 43 B. Doherty, F. Gabrieli, C. Clementi, D. Cardon, A. Sgamellotti, B. Brunetti and C. Miliani, *J. Raman Spectrosc.*, 2014, **45**, 723–729.
- 44 I. Serafini, L. Lombardi, C. Fasolato, M. Sergi, F. Di Ottavio, F. Sciubba, C. Montesano, M. Guiso, R. Costanza, L. Nucci, R. Curini, P. Postorino, M. Bruno and A. Bianco, *Nat. Prod. Res.*, 2019, **33**, 1040–1051.
- 45 S. Grierson, *The colour cauldron*, Mrs. S. Grierson, Perth, 1986.
- 46 B. Witkowski, M. Ganeczko, H. Hryszko, M. Stachurska, T. Gierczak and M. Biesaga, *Microchem. J.*, 2017, **133**, 370–379.
- 47 H. Wyld, *The Gideon Tapestries at Hardwick Hall, West 86th*, **19**, 231–254.
- 48 L. G. Troalen and A. N. Hulme, in *Tapestries from the Burrell Collection*, eds. E. Cleland, L. Karafel, Philip Wilson Publishers, London, 2017, pp. 46–51.
- 49 V. Daniels, T. Devières, M. Hacke and C. Higgitt, *Technological insights into madder pigment production in antiquity*, *Tech. Res. Bull.*, 2014, **8**, 13–28.
- 50 R. S. Blackburn, *Color. Technol.*, 2017, **133**, 449–462.
- 51 C. Mouri and R. Laursen, *Microchim. Acta*, 2012, **179**, 105–113.
- 52 G. C. H. Derksen, M. Naayer, T. A. van Beek, A. Capelle, I. K. Haaksman, H. A. van

- Doren and Æ. de Groot, *Phytochem. Anal.*, 2003, **14**, 137–144.
- 53 R. Singh, Geetanjali and S. M. S. Chauhan, *Chem. Biodivers.*, 2004, **1**, 1241–1264.
- 54 L. L. Ford, PhD Thesis, University of Leeds, 2017.
- 55 X. Zhang and R. A. Laursen, *Anal. Chem.*, 2005, **77**, 2022–2025.
- 56 L. Ford, R. L. Henderson, C. M. Rayner and R. S. Blackburn, *J. Chromatogr. A*, 2017, **1487**, 36–46.
- 57 J. Haigh, *The Dyer's Assistant in the art of dying wool and woollen goods*, J. Mawman, T. Wilson & R. Spence, London, York, 1800.
- 58 D. A. Peggie, J. Kirby, J. Poulin, W. Genuit, J. Romanuka, D. F. Wills, A. De Simone and A. N. Hulme, *Anal. Methods*, 2018, **10**, 617–623.
- 59 P. Nabais, M. J. Melo, J. A. Lopes, M. Vieira, R. Castro and A. Romani, *Herit. Sci.*, 2021, **9**, 32.
- 60 E. Rosenberg, *Anal. Bioanal. Chem.*, 2008, **391**, 33–57.
- 61 K. Lech and M. Jarosz, *Anal. Bioanal. Chem.*, 2016, **408**, 3349–3358.
- 62 C. J. Cooksey, *Biotech. Histochem.*, 2018, **94**, 100–107.
- 63 J. Wouters and J. Verhecken, *Annls Soc. ent. Fr. (N.S.)*, 1989, **25**, 393–410.
- 64 R. Santos, J. Hallett, M. C. Oliveira, M. M. Sousa, J. Sarraguça, M. S. J. Simmonds and M. Nesbitt, *Dye. Pigment.*, 2015, **118**, 129–136.
- 65 A. Serrano, M. M. Sousa, J. Hallett, J. A. Lopes and M. C. Oliveira, *Anal. Bioanal. Chem.*, 2011, **401**, 735–743.
- 66 R. L. Lee, *J. Mod. Hist.*, 1951, **23**, 248–253.
- 67 D. Mantzouris and I. Karapanagiotis, *Color. Technol.*, 2015, **131**, 370–373.
- 68 D. Mantzouris, I. Karapanagiotis and C. Karydis, *Mediterr. Archaeol. Archaeom.*, 2016, **16**, 159–165.
- 69 A. Quye and H. Cheape, *Costume*, 2008, **42**, 1–20.
- 70 J. Burnett, K. Mercer and A. Quye, *Folk Life*, 2004, **42**, 7–31.
- 71 R. Costantini, I. Vanden Berghe and F. C. Izzo, *J. Cult. Herit.*, 2019, **38**, 37–45.
- 72 J. Wouters, C. M. Grzywacz and A. Claro, *Stud. Conserv.*, 2010, **55**, 186–203.
- 73 D. Mantzouris, I. Karapanagiotis and C. Panayiotou, *Microchem. J.*, 2014, **115**, 75–

- 86.
- 74 K. Lech, J. Nawała and S. Popiel, *J. Am. Soc. Mass Spectrom.*, 2021, **32**, 2552–2566.
- 75 D. Tamburini, *Dye. Pigment.*, 2019, **163**, 454–474.
- 76 D. Tamburini, C. R. Cartwright, M. Pullan and H. Vickers, *Archaeol. Anthropol. Sci.*, 2019, **11**, 1221–1239.
- 77 N. Shibayama, M. Wypyski and E. Gagliardi-Mangilli, *Herit. Sci.*, 2015, **3**, 12.
- 78 D. Tamburini, J. Dyer, P. Davit, M. Aceto, V. Turina, M. Borla, M. Vandenbeusch and M. Gulmini, *Molecules*, 2019, **24**, 1–18.
- 79 I. Degano, J. J. Łucejko and M. P. Colombini, *J. Cult. Herit.*, 2011, **12**, 295–299.

Chapter 5 Construction and application of a desorption electrospray ionisation (DESI) source for historical dye analysis

5.1 Aims

The main aim of this project was to design and build a desorption electrospray ionisation (DESI) source and optimise the source for historical dye analysis. Secondly, the aim was to apply the DESI source for the mass spectrometric analysis of natural and early synthetic dye references as well as late 19th century historical textile samples.

5.2 Introduction

Mass spectrometry (MS) is one of the most used analytical techniques in chemistry and biology and thus also one of the main techniques in the dye analysis field.^{1,2} It is a powerful technique used to determine the mass to charge ratio (m/z) of analytes present in a sample, which makes identification and elucidation of compound structure possible. It is however a micro-invasive and destructive technique which requires sampling of the object investigated.

Despite the limitation of sampling, the comprehensive information obtained as well as the sensitivity and speed of MS analysis in comparison to non-invasive techniques makes it an important technique in dye analysis. The possibility to hyphenate it to separation techniques such as liquid chromatography also makes it highly applicable to the complex sample mixtures often encountered in the field. Thus, analytical strategies utilising the advantages of MS whilst minimising the effect on the object is an important area of research in dye analysis.

One such strategy is the use of ambient MS techniques.³ In recent years, ambient MS has emerged as a field of research which makes MS analysis non-invasive although micro-destructive. Ambient MS analysis requires no sampling or sample preparation as the ionisation step is conducted at room temperature in the open environment, making it possible to analyse samples *in-situ*.^{4,5} Some ambient MS techniques have already been introduced to the field of heritage science such as direct analysis in real time (DART)⁵ and atmospheric solids analysis probe (ASAP[®])-MS.⁶

Other ambient mass spectrometry approaches, such as matrix assisted laser desorption electrospray ionisation (IR-MALDESI)⁷ and laser ablation ionisation⁸ approaches have been used to analyse forensic fibres and pigments in oil paintings, but have yet to be introduced in the dye analysis field. Recently, an *in-situ* micro-extraction method coupled to ESI-MS has also been successfully applied on historical textiles.⁴

Desorption electrospray ionisation (DESI)-MS is an ambient MS technique that relies on the ionisation of analytes directly desorbed from a sample surface.⁹ The non-invasive and rapid analysis provided by DESI-MS would be of great benefit in the heritage science field and its construction and application is thus the aim of this project.

5.3 Ambient mass spectrometry

Mass spectrometry is an important analytical technique due to its versatility and sensitivity. It analyses a sample by first generating gaseous ions in an ion source and separating the ions based on their mass-to-charge-ratio (m/z) via a mass analyser. The separated ions are then measured by a detector and displayed as a mass spectrum, which is a graphical representation of the relative abundance and m/z of the ions in a sample. There are multiple types of each component available depending on the type of sample to be analysed.¹⁰ The components of all mass spectrometers and the common workflow of mass spectrometers are shown in Figure 5.1.

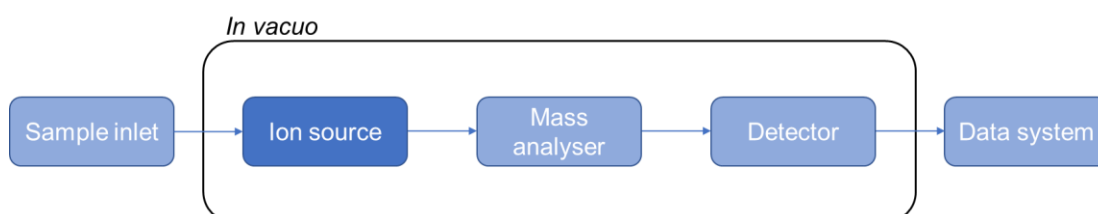


Figure 5.1: Schematic of the components and the workflow of a generic mass spectrometer. The circled sections are performed under vacuum.

The main difference between a generic mass spectrometer workflow and an ambient mass spectrometry approach is that the ion source is moved before the sample inlet and not performed *in vacuo* (fig 5.2). Such a workflow is also used for other mass spectrometers not regarded as an ambient mass spectrometer such as electrospray ionisation (ESI)-MS and atmospheric pressure chemical ionisation (APCI)-MS. However, these techniques are not regarded as ambient techniques as they require

sample preparation.^{3,11} The same mass analyser and detector can be used with both generic and ambient ion sources, demonstrating the versatility of the MS technique.

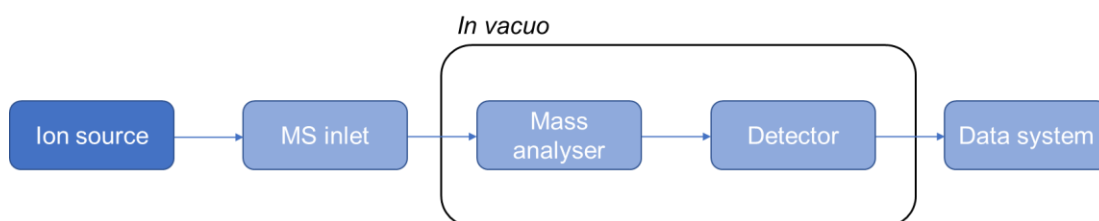


Figure 5.2: Schematic of the workflow of an ambient mass spectrometer. The circled sections are performed under vacuum.

5.3.1 Direct analysis in real time mass spectrometry (DART-MS)

Direct analysis in real time (DART)-MS was developed by Cody, Laramée and Dupont Durst in 2005,¹² and it was one of the first ambient MS techniques introduced alongside DESI-MS.⁹ Ionisation is achieved by directing a flow of heated gas, commonly nitrogen or helium, carrying ionising atoms that have been formed in a plasma discharge. The sample is placed in the gas stream between the DART source and the MS inlet, and analytes are removed from the surface of the sample and ionised via gas-phase ionisation processes such as charge transfer and Penning ionisation.^{3,13}

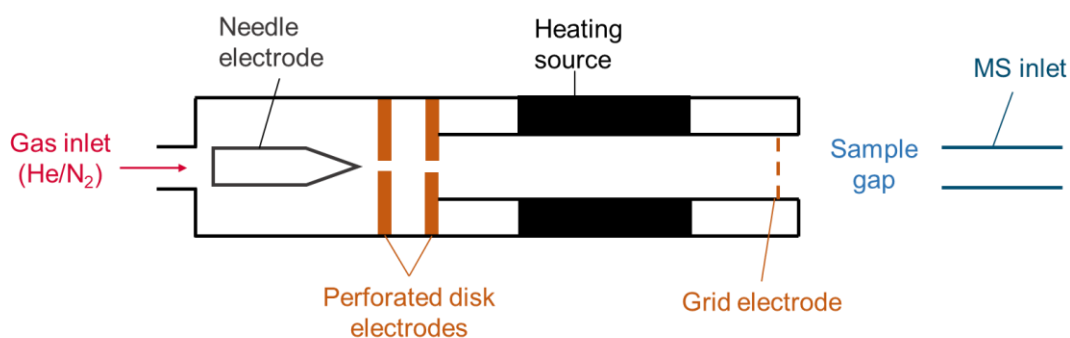


Figure 5.3: Schematic of DART source showing the main components including the discharge chamber where ionised and excited molecules are generated, and the sample gap where the sample is placed and analysed.

DART-MS has been used with success on dyed textile samples, for both natural and synthetic dyes.^{5,14} The main disadvantage of DART-MS is the typically small gap between the source and the MS inlet which limits the size of the samples that can be analysed. Most studies have thus been performed on samples collected for the further use of invasive analytical techniques such as (U)HPLC-PDA/MS or archaeological samples that tend to be fragmented.^{15–17} Modification to the DART set-up by placing

the source and the MS inlet at an angle of each other above the sample surface, similar to a DESI source, circumvents this issue.^{18,19} Such a set-up has been used to study degradation pathways of eosin lake pigments.¹⁴

5.3.2 Atmospheric-pressure solids analysis probe mass spectrometry (ASAP[®]-MS)

Atmospheric-pressure solids analysis probe (ASAP[®])-MS was developed by McEwen, McKay and Larsen in 2005.²⁰ It quickly gained popularity since it is a relatively simple modification to an atmospheric pressure chemical ionisation (APCI) source. APCI-MS was invented by Horning *et al.*²¹ in the 1970s and is based on the ionisation of carrier gas molecules by a corona discharge pin. In APCI-MS, the sample is introduced into the chamber in either liquid or gaseous form and ionised by the charged carrier gas by gas-phase charge transfers.²² The addition of an ASAP[®] device to the APCI source set-up makes it possible to also ionise solid samples, including textile fibres.

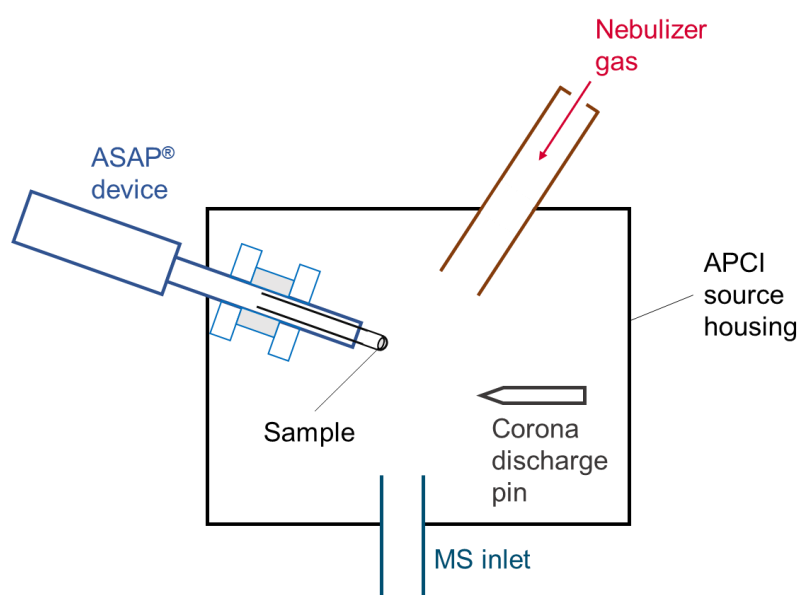


Figure 5.4: Schematic of ASAP[®] source showing the addition of the ASAP[®] device to an APCI source and the sample analysed on the tip of the melting-point tube.

ASAP[®]-MS uses a borosilicate capillary melting-point tube to introduce samples into the APCI source.²⁰ The main limitation of the method is the requirement of the analyte to be relatively volatile as the analytes are thermally desorbed and ionised by the carrier gas.²³ Similarly to DART-MS, the possible size of the sample analysed is limited by the set-up, as it depends on the size of the source housing. Despite these

limitations, it has been successfully used for the analysis of indigo in archaeological samples.⁶

5.4 Desorption electrospray ionisation (DESI)

Desorption electrospray ionisation (DESI)-MS was developed in 2004 by the Cooks research group at Purdue University.⁹ It is an electrospray ionisation (ESI) based technique, popular for its versatility and speed. Ionisation occurs outside of the MS inlet by an electrospray of charged liquid droplets being directed onto the sample. Secondary charged droplets containing dissolved analyte are formed and desorbed from the sample surface and led into the MS inlet by voltages (Fig 5.5).⁹

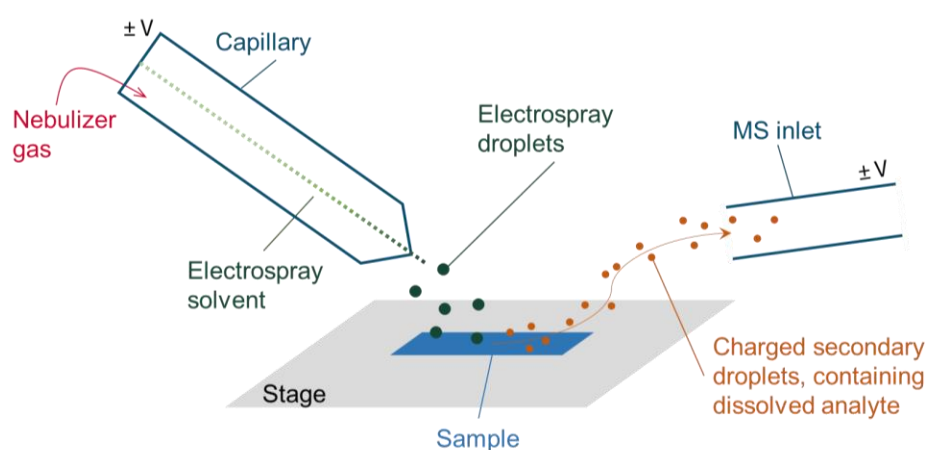


Figure 5.5: Schematic of a DESI source showing the electrospray emitter directing the charge solvent onto the sample surface, forming secondary charged droplets containing analyte which are desorbed and directed into the MS instrument.

DESI-MS was quickly implemented for the analysis of a wide range of analytes, particularly in the biomedical, pharmaceutical, and forensic fields.³ It has been successfully used on samples as diverse as cancerous cells in a clinical setting,²⁴ high-throughput reaction condition screenings²⁵ and lipidomic profiles of fingerprints.²⁶ Recently, it has been introduced into the cultural heritage field by analysis of manuscripts.²⁷ Attempts to apply it in the dye analysis field exist but has not yet been successful.⁴

5.4.1 Desorption and ionisation mechanisms

The desorption and ionisation mechanisms of DESI are not yet fully understood but due to the similarities with ESI-MS in both instrumental set-up and mass spectra appearance, it is likely that ESI-like ionisation mechanisms occur.^{28,29}

ESI is a 'soft' ionisation technique, meaning that it induces little to no fragmentation of the analyte.³⁰ In ESI-MS, the sample is dissolved in a solvent which is passed through a capillary with a high voltage applied. The voltage induces charge separation on the surface of the solution at the tip of the capillary, resulting in a Taylor cone being formed. In sufficiently high electric fields, the Taylor cone becomes unstable, and a fine jet emerges from the cone tip with the help of a nebulising gas. Charged droplets are formed due to the repulsion between the charges present in the jet.^{31,32}

Such electrospray droplets *sans* dissolved sample is used in the DESI source for the desorption of secondary charged droplets containing analyte at the sample surface.²⁸ Simulations have shown that it is likely that the secondary droplets are comprised of a combination of liquid already on the surface and liquid from the incident droplet.^{33,34} This two-step pick-up desorption mechanism proposed is supported by the delay to reach maximum ion abundance after a DESI-MS analysis has begun.³⁵ Thus, wetting the surface of the sample for a time before recording results in mass spectra with more intense ion signals.²⁹ Studies have established that the desorption and consequently the ionisation of analytes are both sample and surface dependent.³⁶⁻³⁹

Ionisation of the analyte in the desorbed secondary droplets likely occurs via standard ESI mechanisms.²⁸ These mechanisms rely on the increase in charge density of the droplets with the evaporation of solvent. This increase in charge density occurs until the coulombic repulsion of the droplet equals the surface tension, known as the Rayleigh limit (Equation 5.1). Droplets at the Rayleigh limit produce smaller, highly charged offspring droplets via jet fission.³²

$$z_R = \frac{8\pi}{e} \sqrt{\epsilon_0 \gamma R^3} \quad \text{Equation 5.1}$$

z_R = Rayleigh limit, e = elementary charges, ϵ_0 = vacuum permittivity, γ = surface tension, R = droplet radius.

There are several theories how the charge transfer from the solvent to the analyte in the droplet occurs (Fig 5.6).³¹ For low molecular weight ions, the most supported model is the ion evaporation model (IEM) and for larger molecular weight ions, the charged residue model (CRM) is viewed as the most applicable.³² Another ionisation model called chain ejection model (CEM) is important for unfolded proteins and is based on the ejection of nonpolar polymer chains.^{40,41} However, the theories are still open to debate.

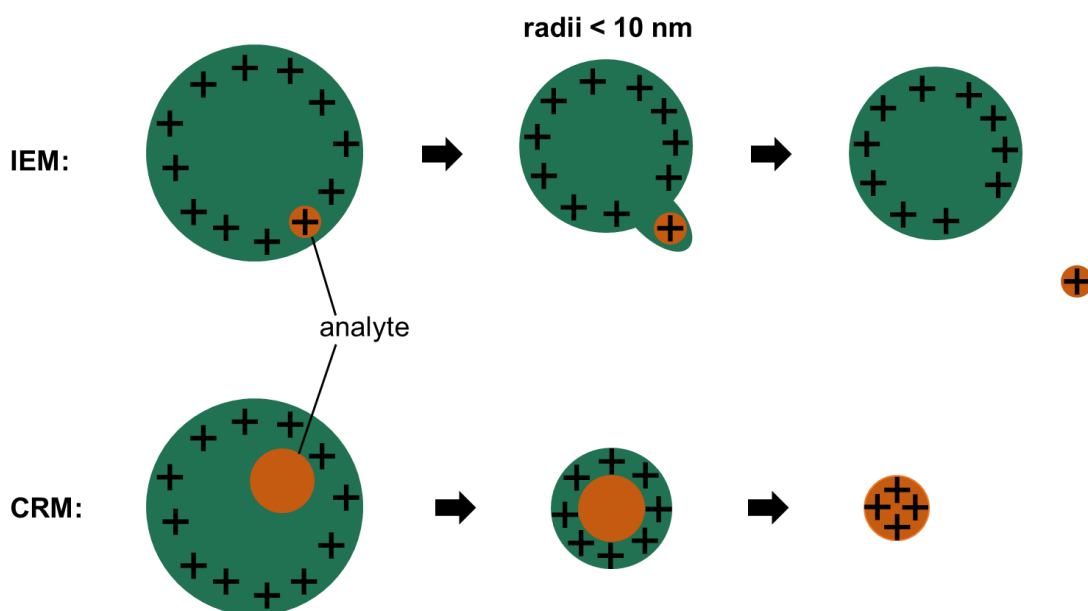


Figure 5.6: Top: Scheme of ion evaporation model (IEM) showing how low molecular weight analytes can be ejected from droplets with radii < 10 nm. **Below:** Scheme of charge residue model in which solvent evaporation to completion of the droplets results in charge transfer to higher molecular weight analytes.

IEM and CRM both occur as a result of continued coulombic fission due to solvent evaporation. The IEM model was introduced by Iribarne and Thomson in 1976⁴² and it has been supported by experimental data and simulations for small molecular ions.^{43–45} In IEM, direct ion emission occurs for droplets with radii < 10 nm. At this limit, the ion evaporation process replaces Coulomb fission by the removal of charge (Fig 5.6). For larger molecular ions, such as proteins, CRM is more plausible.^{31,32}

CRM was first theorised by Dole *et al.* in 1968⁴⁶ and follows the concept of complete solvent evaporation. When all solvent has evaporated in the droplet, the charge present on the solvent molecules is transferred to the analyte present in the droplet. This model is supported by the observation of multiply charged protein monomers, when only one protein is present in the final droplet, as well as protein multimers as a result of more than one protein being present in the final step. Most analytes of interest in dye analysis are small molecules < 500 Da and thus most are expected to follow ionisation by IEM, commonly resulting in singly charged ions being detected.

However, Takats *et al.*²⁸ showed that DESI could also ionise non-polar molecules generally not ionisable by ESI, such as cholesterol, carotene, and TNT.²⁸ They suggested, based on resulting DESI-MS spectra from such analytes, that an APCI-

like ionisation mechanism²⁰ involving gas phase ions occurs for those analytes. There is also evidence that more than the two proposed ionisation mechanisms occur depending on the analyte and substrate.²⁸ The presence of multiple possible mechanisms for the ionisation step of DESI-MS means that different parameters, both instrumental and geometrical, is required need to be optimised depending on the analyte of interest.

5.4.2 DESI source geometry

Optimisation of the source geometry parameters are vital for any DESI-MS measurement as the angle and positions of the sprayer greatly impact the efficiency of the ionisation step.^{28,36–38,47} The source geometry has a direct impact on the droplet size, velocity and dispersion.^{28,33,48,49} The optimised geometry often differs with target molecule and substrate used, making it difficult to standardise optimum geometry for all applications.

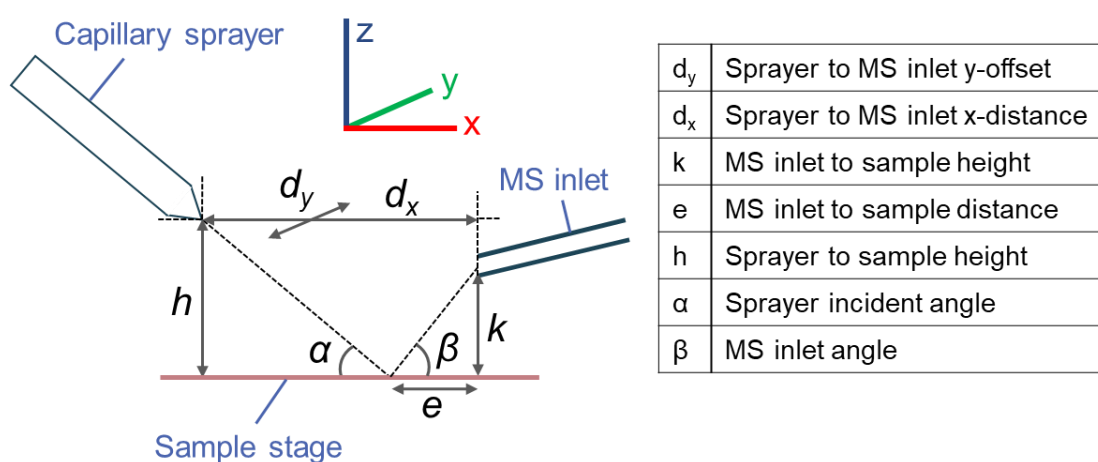


Figure 5.7: Graphic of the relevant geometrical parameters important for DESI-MS analysis. These are summarised in the table on the right.

Many studies have focussed on the optimisation of DESI parameters for biological and forensic samples.^{36,50,51} Although the geometrical parameters are interdependent and a small change in one has an effect on all others, the sprayer angle (α) and sprayer-to-sample height (h) are reported to be key parameters to optimise.^{27,28,38} Common sprayer angles are in the range of 55° - 75° and h should be < 2 mm but large enough not to affect the sample. The MS inlet angle (β) is usually set to 10° but it, together with the MS inlet-to-sample distance (e), have been shown to not have as great an impact on the ion abundance seen.^{38,51}

Of course, source geometry is not the only parameter that influences the analytical quality of DESI-MS and other important parameters such as; capillary protrusion from and position in the DESI sprayer; the pressure of the nebulising gas and solvent flow rate play an important role.³⁶ The solvent system used can also majorly impact the DESI-MS analysis⁵² and the emerging field of reactive DESI-MS utilises this dependency for highly selective studies.^{51,53,54}

5.4.3 Fourier Transform Ion Cyclotron Resonance (FT-ICR)

In this study, a 7T Fourier transform ion cyclotron resonance (FT-ICR) mass analyser was exclusively used. The FT-ICR mass analyser was invented in 1974 by Comisarov and Marshall at University of British Columbia.⁵⁵ It is a high-resolution MS technique (HRMS), which can achieve resolution $> 10^7$ depending on the strength of the magnet used. It requires Fourier transform (FT) as the m/z are measured indirectly by the detection of frequency of rotation of the ions present in the sample.⁵⁶

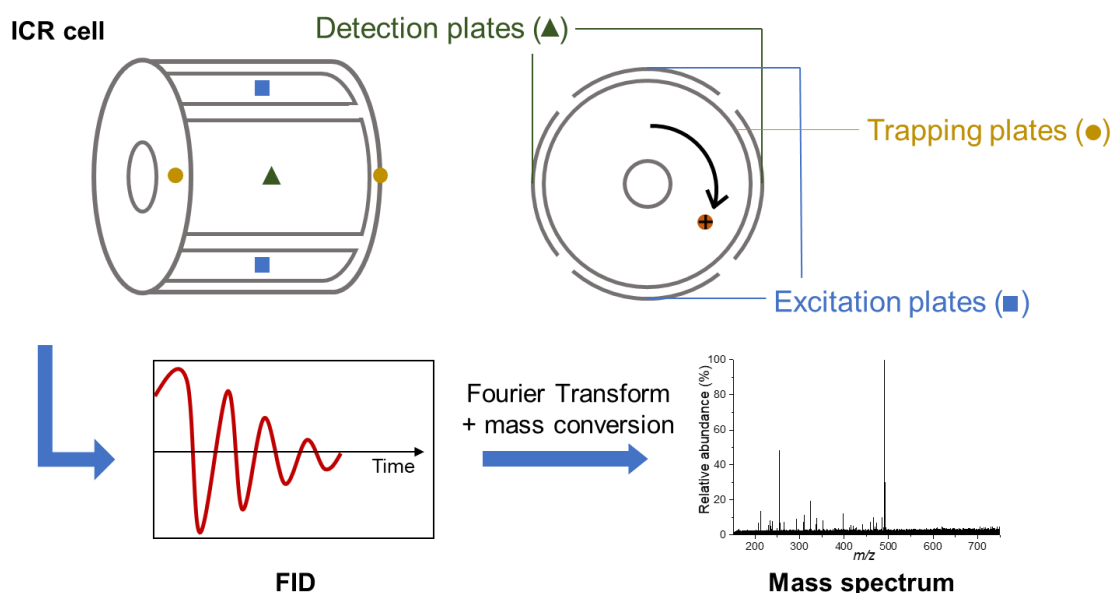


Figure 5.8: Schematic of a FT-ICR mass analyser showing side and front view of the ICR cell.

The ICR cell where ion detection occurs is placed within a strong magnetic field and is composed of six plates: two trapping plates, two excitation plates and two detection plates (Fig 5.8). The entire mass analyser is under high vacuum. The ions entering the magnetic field are bent into a circular motion in the perpendicular plane to the field by the Lorentz force (Equation 5.2) while being trapped axially in the cell by the trapping plates. The Lorentz force observed by the ion in the magnetic field is

dependent on the charge and velocity of the incoming ion as well as the magnetic field.⁵⁷

$$F = zv \times B \quad \text{Equation 5.2}$$

F = Lorentz force, z = charge of the ion, v = incident velocity of the ion, B = magnetic field strength.

The frequency of rotation (ω_c) of the ions is dependent on their m/z ratio and the magnetic field (Equation 5.3).

$$\omega_c = \frac{zB}{2\pi m} \quad \text{Equation 5.3}$$

ω_c = induced cyclotron frequency, z = charge of the ion, B = magnetic field strength, m = mass of the ion.

The excitation plates of the ion cell are used to excite each individual m/z by applying a radio frequency (RF) pulse which will couple to the cyclotron motion of ions of specific m/z and excite them to a higher orbit. The excited ions induce an alternating current between the detector plates which corresponds to the cyclotron frequency of the ions excited by the RF pulse. The amplitude recorded is proportional to the number of charges at each individual m/z . A convoluted frequency vs time spectrum is recorded and deconvoluted to a frequency vs abundance spectrum by FFT mathematical methods. This spectrum is converted to a mass spectrum by Equation 5.4.⁵⁸

$$m/z = \frac{B}{2\pi\omega_c} \quad \text{Equation 5.4}$$

m/z = mass-to-charge ratio, B = magnetic field strength, ω_c = induced cyclotron frequency.

The theoretical background of DESI and mass spectrometry instrumentation was used towards the aim of designing and constructing a DESI source to allow the non-invasive analysis of dyes. The application of DESI-MS to dyed textiles required optimisation of the geometric parameters as well as the flow rate, gas pressure and solvent system.

5.5 Design and construction of the DESI source

Requirements and strategies for constructing a DESI source in-house have previously been reported in the literature.^{28,59,60} This work was particularly inspired by the PhD thesis of University of Glasgow student James Newton as his DESI source was also

applied to cultural heritage material.²⁷ Important design elements to address for the DESI source were the geometrical control of the sprayer and the manipulation of the stage for accommodation of heritage objects. The DESI source was attached to a Bruker 7T Solarix FT-ICR-MS instrument using Compass HyStar 5.1. The commercial electrospray emitter of the instrument was used for all analyses. It has been reported that sprayer design in itself has an impact on the signal abundance and repeatability of DESI-MS analysis;^{36,50,61} an investigation of the sprayer design was outside the scope for this project but is important to consider for future work.

5.5.1 xy stage

Previous work in the Scottish Instrumentation and Resource Centre for Advanced Mass Spectrometry (SIRCAMS) laboratory by Dr C. Logan Mackay involved the building of a metal frame constructed from two rods held above a stainless-steel stage. The stage was placed on two perpendicular stepper motors controlled via an Arduino-compatible board and LaserGRBL (v4.6.0) for movement in the x- and y-directions (Fig 5.9A). In this project the entire stage frame was adhered to a labjack for control of the z-direction and an acrylic plate was added to the stainless-steel stage to electrically insulate it (Fig 5.9B). A metal block designed to thread onto and move along the metal rods was used as the starting point for the sprayer holder set-up (Fig 5.9C).

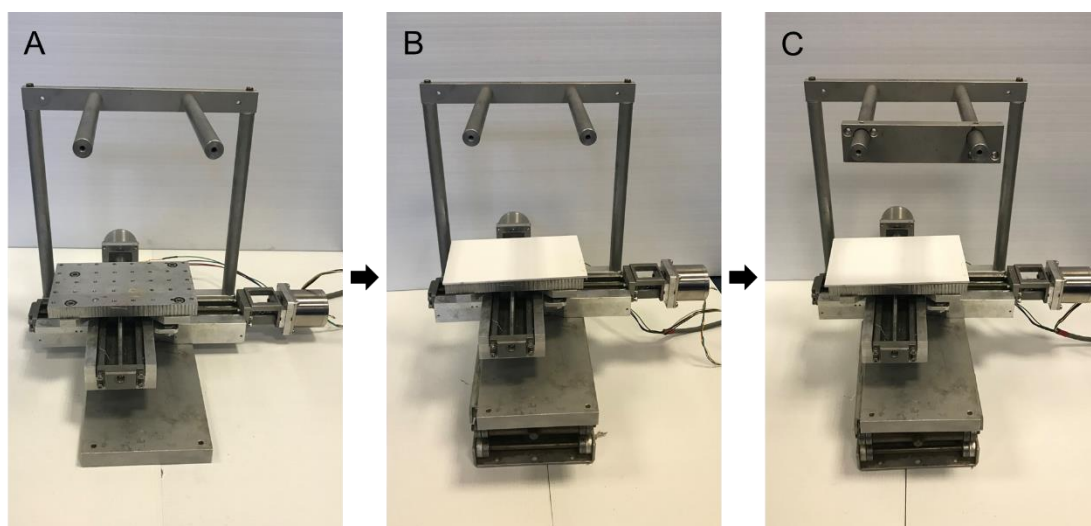


Figure 5.9: **A:** Metal frame from previous work in the SIRCAMS laboratory by Dr C. Logan Mackay. **B:** Metal frame with insulating acrylic stage and labjack. **C:** Addition of the metal block used for the sprayer holder set-up.

5.5.2 Sprayer holder set-up and mass spectrometer inlet

The quality of a DESI-MS measurement is reliant on controlled adjustments of the geometrical parameters of the sprayer as well as fixing the geometry once optimised (Section 5.4.2). It was decided that the use of commercially available x-, y- and z-positioners (Fig 5.10) and an angle rotation mount (Fig 5.10) was the most precise way to control these geometric parameters. To connect the positioners, rotation mount and sprayer, pieces were 3-D printed in polylactic acid.



Fig 5.10: Left: commercial y- and z-positioners used. Centre: commercial x-positioner used. Right: commercial rotation angle mount used.

At least three 3-D printed pieces were required (Fig 5.11); a piece between the positioners (F component D), a piece between the positioners and the angle rotation mount (component E) and one to hold the sprayer (component F).

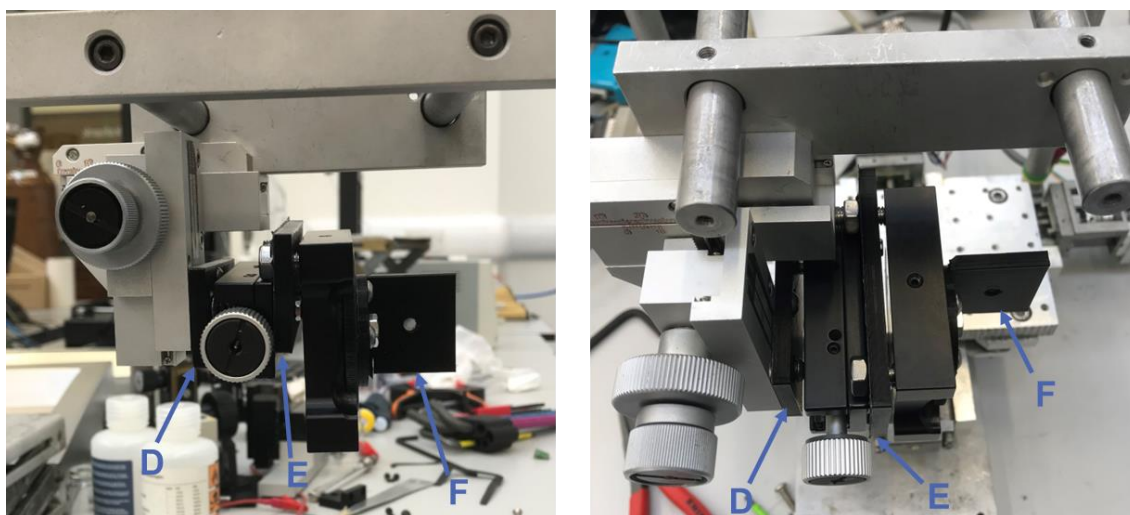


Figure 5.11: Front and top view of the sprayer holder set-up with the first versions of the 3-D printed components. Labelled **D** is the piece connecting the positioners, **E** is the piece between the positioners and angle rotation mount and **F** is the sprayer holder.

The first versions of pieces **D** and **E** were both rectangular with holes for screw attachments (Fig 5.12). This design was not strong enough to support the mass of the rest of the components in the set-up (Fig 5.11). The thickness of **D** was therefore increased and an additional support underneath the x-positioner was included. Piece **E** was extended to cover the entirety of the angle rotation mount so all four screws available on the angle rotation mount could be used for stabilisation of the design (Fig 5.12).

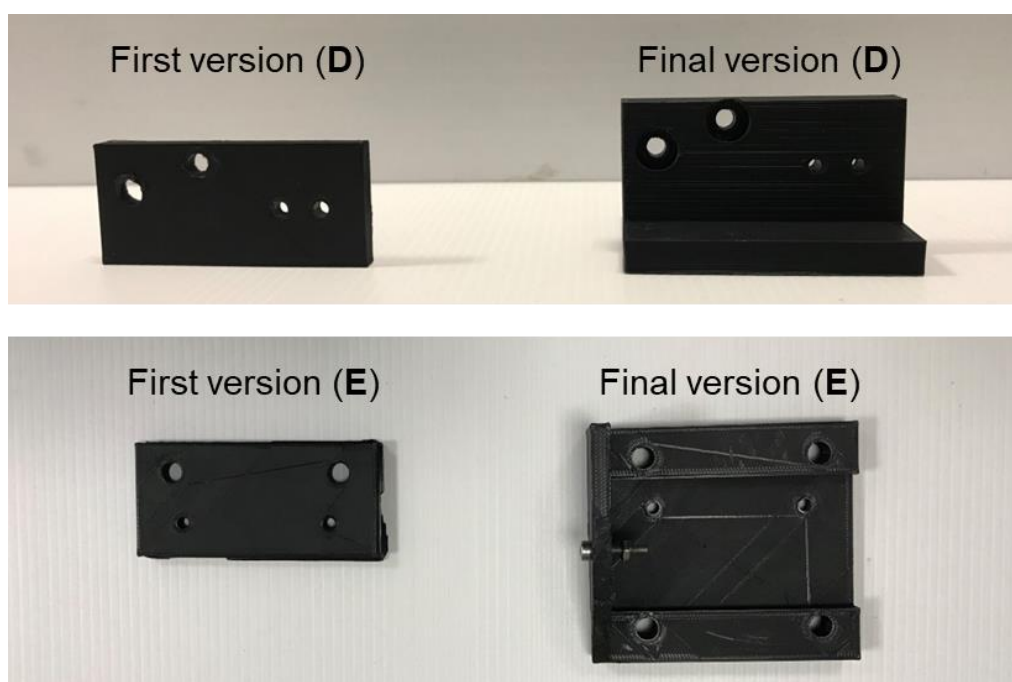


Figure 5.12: First and final versions of 3-D printed pieces **D** and **E**.

The sprayer holder (**F**) also started as a simple design of a square connected to a circular base attached to the centre of the angle rotation mount (Fig 5.13). This design did not allow for full rotation of the sprayer and the angle rotation mount due to collision of the components. The second version with an offset square attached to the circular base (Fig 5.13) made full rotation possible, but it limited the sprayer – sample distance (h) to > 1 cm, which is too far apart for efficient ionisation.

The final design of **F** was based on a rectangle instead of a square as well as adding a space for a remotely controlled camera (Fig 5.13). The elongation of **F** resulted in the angle rotation mount being too weak to fix the angle, so a screw lock was included in the final design of the rotation mount support (**E**) (Fig 5.12) and the side rounded to allow rotation $< 90^\circ$, which is enough for most DESI-MS analysis.

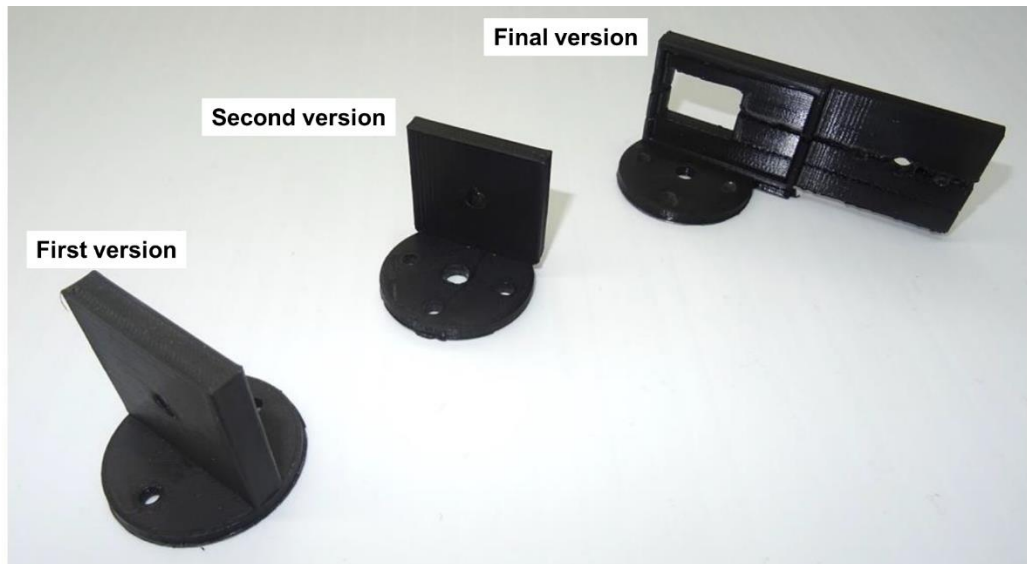


Figure 5.13: First, second and final versions of 3-D printed piece **F**.

A screw lock for the z-axis also became necessary as the entire set-up was found to be too heavy for the z-positioner alone. Attempts to incorporate a z-axis screw lock in component **D** was made but was inefficient due to **D** being anchored to the same piece it tried to hold up. An additional piece (**G**) was instead required as a z-lock (Fig 5.14), attached directly to the z-positioner (Fig 5.15).

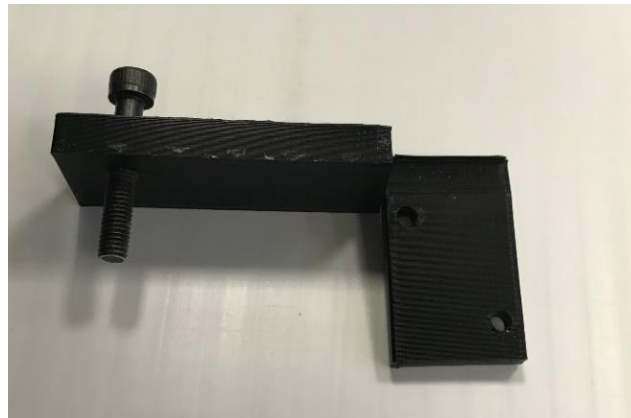


Figure 5.14: Design of 3-D printed z-lock (piece **G**).

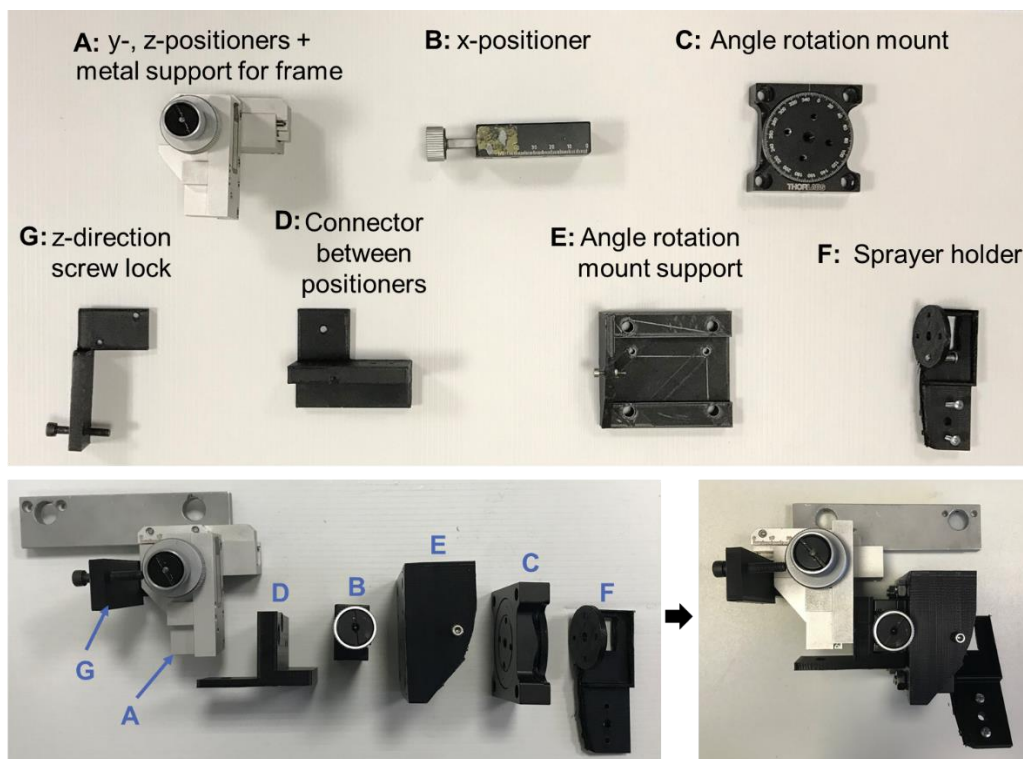


Figure 5.15: Top: Components of the sprayer holder set-up: **A – C:** purchased components of the set-up **D – G:** 3-D printed pieces in polylactic acid. **Bottom left:** order of assembly of components. **Bottom right:** Assembled sprayer holder set-up.

The final component constructed was a mass spectrometer inlet extension made in stainless steel and brass. The stainless-steel tube had an internal diameter of 400 μm and a gold spring was added to the inside of the brass part to make it fit securely around the mass spectrometer inlet. The final set-up of the DESI source can be seen in Figure 5.16.

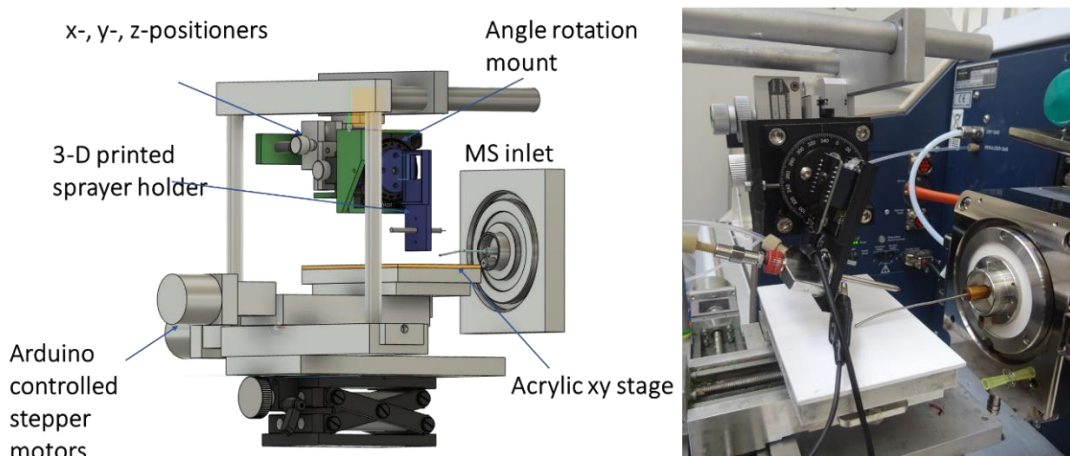


Figure 5.16: Graphic model (Fusion360, Autodesk, San Francisco, CA, USA) and photograph of constructed DESI source.

5.6 Optimisation of the DESI source

5.6.1 Initial qualitative geometry parameter trials on rhodamine B ink on glass

Initial qualitative testing of the geometry parameters (Fig 5.7): MS inlet – sample height (k), sprayer – sample height (h), sprayer – MS inlet y-offset (d_y) and sprayer – MS inlet x-distance (d_x) were conducted using rhodamine B ink on a glass slide and a sprayer angle α of $26^\circ \pm 2^\circ$ and accumulation time of 1.5 s. Rhodamine B was used as a standard due to it being easily ionized, having a characteristic m/z peak and being readily available.^{37,47} It is also representative of the early coal-tar dyes that are the focus of this study, by being a basic dye showing high water-solubility, strong colour and poor lightfastness.⁶²

The effect on the rhodamine B signal abundance when changing the geometry parameters was tested by achieving a stable signal of rhodamine B (m/z 443.23), measuring the physical distances between the MS inlet, sample, and sprayer before starting the mass spectra collection. Focussing on one geometric parameter at a time, the geometrical components were moved, the distanced changed measured and related to the time of the recording.

Using MS inlet – sample height (k) as an example, a stable signal was achieved at $k = 1$ mm which was used as the starting point and the recording started. After 6.5 minutes of assuring that the rhodamine B signal was indeed stable at $k = 1$ mm, the stage was lowered until the signal disappeared at 7.5 minutes and the measured distance of 5 mm. Lifting the sample stage again, the signal returned and increased in signal abundance until the inlet was near touching the sample surface (Fig 5.17), showing that smaller k (< 1 mm) gives higher signal abundance of rhodamine B at a sprayer angle of 26° . The process was repeated for h , d_y , and d_x .

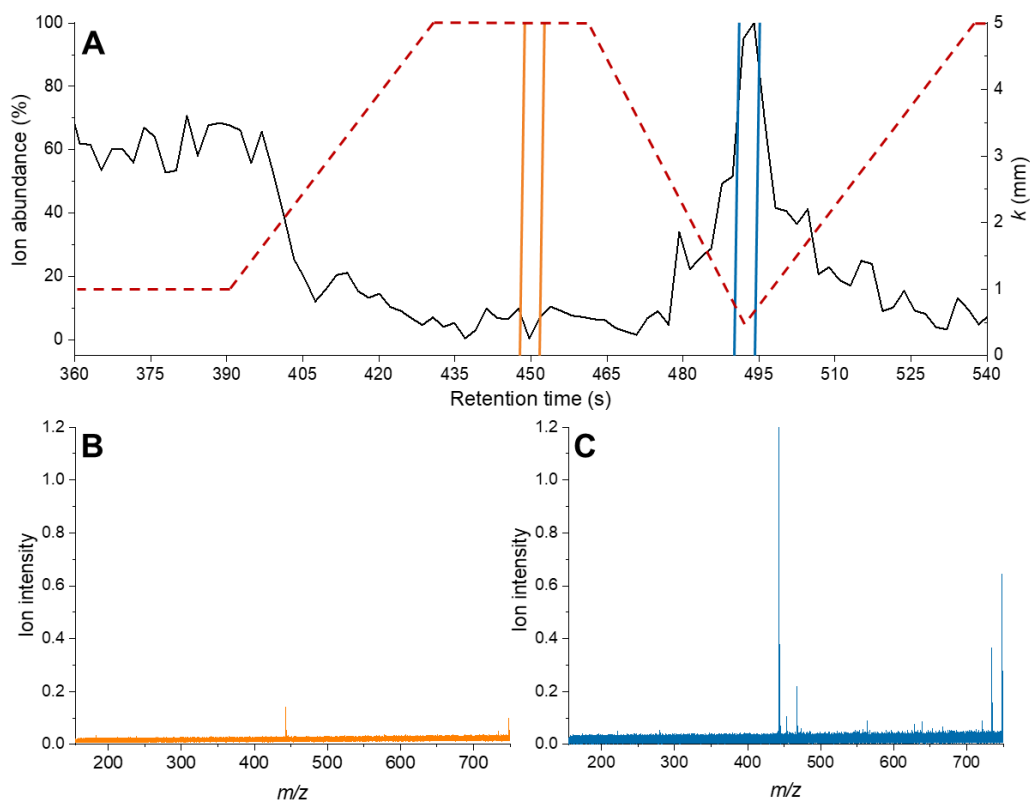


Figure 5.17: A: Region of the extracted ion chromatogram (m/z 443.23) of recording of MS inlet – sample height, k , investigation showing the mass spectra summed for the mass spectra displayed below. **B:** Sum of 2 mass spectra at 7.5 min (450 s) of rhodamine B ink on glass at $k = 5$ mm displaying the ion abundance of rhodamine B $[M-CI]^+$ peak (m/z 443.23). **C:** Sum of 2 mass spectra at 8.25 min (495 s) of rhodamine B ink on glass at $k < 1$ mm displaying the ion abundance of rhodamine B $[M-CI]^+$ peak (m/z 443.23). The MS inlet – sample height, k , used shown in dashed red line.

At angle $26^\circ \pm 2^\circ$, lower heights (h) of < 2 mm gave the largest ion abundance and shorter sprayer – MS inlet x-distances (d_x) (5 – 7 mm) gave better signal-to-noise in comparison to longer d_x distances (13 mm). The most influential geometrical parameter for signal strength was found to be the sprayer and the MS (d_y). Misalignment < 0.5 mm led to complete loss of rhodamine B signal.

The optimised ranges found in this initial study of k (< 1 mm), h (< 2 mm) and d_x (5 – 7 mm) align well with optimised values found in the literature.^{37,38,47} The main difference between reported distances and the distances found was the dependence on d_y . The alignment between the sprayer and the MS inlet has been reported to have little effect in the range of -2 and +2 mm,³⁸ which was not the case found for the DESI

source constructed. This difference can potentially be due to the design of the MS inlet extension which curved shape was manually adjusted

These initial experiments gave an overview of the limits for the geometrical parameters of the constructed DESI source operated when analysing a reference analyte on an ideal surface of glass³⁹ to make sure that the set-up was able to give a reliable signal for rhodamine B. Since signal abundance is reliant on variables that were not controlled during these trials, such as capillary voltage and nebulizer gas pressure, the result on rhodamine B ink obtained was used only to make sure that a stable rhodamine B signal could be achieved as well as indicate what initial geometry set-up was a likely to generate an ion signal of rhodamine B dyed on silk and wool substrates.

5.6.2 Parameter optimisation on silk and wool samples dyed with rhodamine B

Undyed silk (2-ply, 66 Tex, thread count 43 cm⁻²) and wool cloth (3-ply, 158 Tex, thread count 36 cm⁻²) from the MODHT project^{63,64} were dyed with rhodamine B (Section 2.3.13) and used as reference cloth for optimisation. Additional to the geometry parameters, MS parameters including sweep excitation energy, skimmer voltage, source temperature, sprayer capillary voltage, dry gas flow, accumulation and time-of-flight (ToF) have an impact on the ionisation efficiency of the DESI source and thus the ion abundance of the rhodamine B peak on wool.

The effect of each of these MS parameters was investigated using a similar approach to that outlined for rhodamine B ink on glass to estimate the geometry parameter ranges that gave a stable rhodamine B peak on wool cloth. An angle of $26^\circ \pm 2^\circ$ was used. The geometry parameter distances that gave the greatest signal-to-noise ratio for rhodamine B peak on glass ($k < 1$ mm, d_x 5 – 7 mm, $d_y < 0.5$ mm), gave a stable, high abundance rhodamine B peak on wool.

The main difference for the geometrical parameters at $26^\circ \pm 2^\circ$ when analysing cloth compared to glass was the limitation in how small (< 2 mm) the capillary – sample distances (h , Fig 5.7) could be. Upon wetting, silk and wool become slightly conductive^{65,66} which means that lowering the capillary too close to the sample resulted in burning the cloth. A smaller h did however, as with glass, give a higher absolute ion abundance of the rhodamine B peak, so h needed to be minimised as

much as possible without impacting the sample analysed. The optimised height was $h = 2$ mm for most textile samples.

Using the geometrical parameters specified above, the effect of the MS parameters was investigated quantitatively. The experiments were conducted in positive mode and the angle was set at $36^\circ \pm 2^\circ$. The absolute ion abundance of the rhodamine cation $[M-Cl]^+$ peak at m/z 443.23 with the change in parameters was recorded and compared. These initial experiments were repeated at least three times across multiple days to give an idea of the limitations and influence of each parameter on the quality of the analysis at this angle.

The parameters and range of values tested, and the range of optimised values are tabulated in Table 5.1. Optimisation of these parameters is instrument-specific, but it is likely that similar effects will be seen on other MS instruments although the absolute optimised values may vary.

Table 5.1. MS parameters tested for their effect on the absolute ion abundance of Rhodamine B $[M-Cl]^+$ peak (m/z 443.23), the range tested and the optimised ranges.

MS parameter	Range tested	Range for greatest absolute ion abundance (m/z 443.23) ($n = 3$)
Sweep excitation energy	12 – 15 %	15 %
Skimmer voltage	5 – 30 V	15 – 25 V
Source temperature	200 – 300 °C	250 – 300 °C
Sprayer capillary voltage	1 – 5 kV	4 – 4.5 kV
Dry gas flow	1.0 – 5.0 bar	3.5 – 4.0 bar
Accumulation	0.2 – 3.0 s	1.5 – 2.5 s
Time-of-flight (ToF)	0.2 – 0.8 ms	0.5 – 0.7 ms
Flow rate	200 – 2000 $\mu\text{l h}^{-1}$	700 – 800 $\mu\text{l h}^{-1}$

The sweep excitation and skimmer voltage did not seem to have any major effect on the signal abundance obtained, while a higher source temperature saw an increase in absolute ion abundance of m/z 443.23 at higher values within the range tested. The nebulising gas increased ion abundance until 4.0 bar when it saw a decrease again, similar to the sprayer capillary voltage which decreased after 4.5 kV. This is in accordance with the literature which explains the phenomena as resulting from the premature evaporation of the solvent droplets before surface impact due to the small size and high velocity created by the high voltages and gas pressure used.^{28,48}

An increase in accumulation time led to a beneficial increase in ion intensities, however, it also led to an increase in background contaminant ion abundance. A balance between increased target ion abundance and acceptable background ion abundance was found to be around 1.5 s. The optimum time-of-flight was found to be analyte dependent. A ToF time range of 0.5 – 0.7 ms was found to give the greatest signal-to-noise ratio for low mass dye target ions ($m/z < 500$), such as rhodamine B, whilst 0.6 – 0.8 ms was optimum for high mass dye target ions ($m/z > 500$), such as xylidine ponceau (Section 5.8).

The MS parameter ranges found are in good agreement with other studies in the literature.^{36,37} The only parameter that differed significantly when analysing cloth compared to biological and forensic samples was the flow rate required. The greatest signal-to-noise ratio of the rhodamine B $[M-CI]^+$ and background peaks was achieved at $750 \mu\text{l h}^{-1}$, which is significantly higher than standard flow rates for biological and forensic samples ($90 - 300 \mu\text{l h}^{-1}$).^{37,38,47} The high flow rate required for textile samples has been reported previously⁶⁰ and it is likely needed due to the wicking properties of natural fibres.

Simulations have shown that the secondary droplets required for the DESI process are formed from liquid originating from the sample surface combined with liquid originating from the incident droplet.³³ The wicking generated by silk and wool thus reduces the formation of the thin liquid layer on the sample surface required. Too low a flow rate resulted in the need for longer analytical times and gave lower ion abundance, while higher flow rates ($1200 - 2000 \mu\text{L h}^{-1}$) resulted in formation of water droplets on the cloth surface, particularly on wool (Fig 5.18).

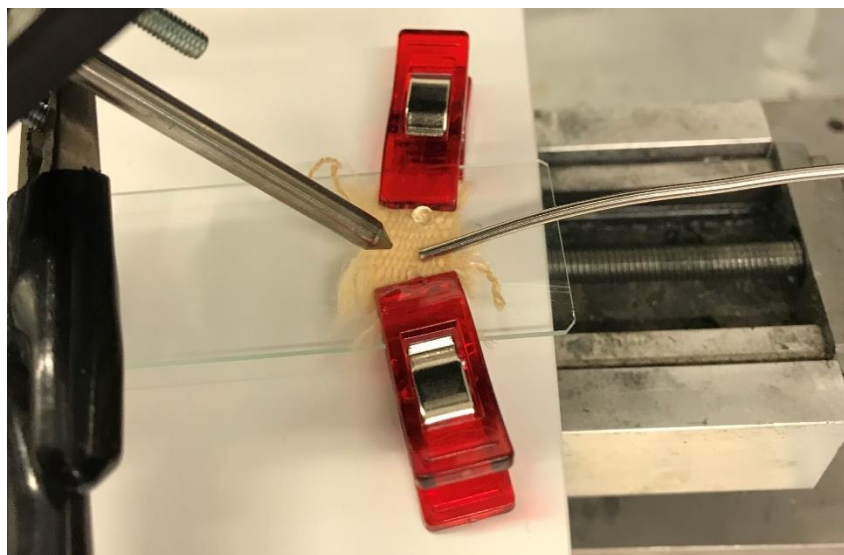


Figure 5.18: Undyed wool cloth being analysed using too high flow rate resulting in droplet formation on the surface.

5.6.3 Sprayer solvent system

Acid or base additives to the solvent system, such as formic acid and ammonium acetate, have been shown to help with ionisation of natural dyestuffs and therefore increase recorded ion abundance.⁶⁷ The effect of solvent additives was tested on early synthetic dye references on silk and wool. Discolouration was observed for some synthetic dye references, in particular the azo dyes aniline yellow, methyl red and disperse orange III Na salt (Fig 5.19). These azo dyes are used as pH indicators, so the discolouration seen was anticipated.⁶⁸ Since it is vital that the object analysed is impacted as little as possible, only additive-free solvent systems were investigated further. Additionally, the solvents used need to be appropriate in a museum setting as well as MS compatible, which limited the choice of solvent to those acceptable in conservation practices.⁶⁹

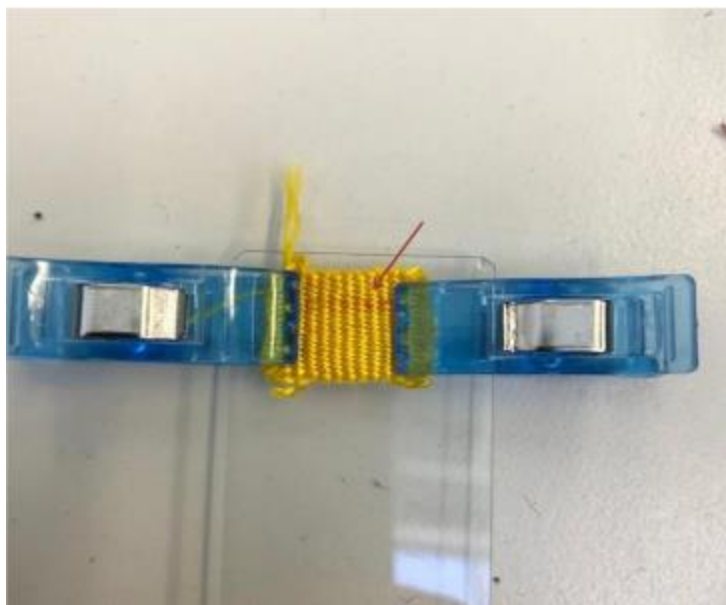


Figure 5.19: Silk sample dyed with azo dye aniline yellow showing discolouration (marked with a red arrow) when using solvent system 1:1 v/v ACN:H₂O + 0.1 % ammonium acetate (1 M).

Four ratios of LC-MS grade CH₃CN (ACN) and MeOH with H₂O were used to investigate the effect of the solvent system on silk and wool substrates. These included 100 % ACN or MeOH as well as 95:5 v/v, 3:1 v/v and 1:1 v/v ACN:H₂O or MeOH:H₂O (Fig 5.20). Repeat measurements ($n = 6$) were performed at different locations on the same reference sample of silk or wool cloth dyed with rhodamine B. Each spot location was wetted for 1 min before recording and a flow rate of 750 $\mu\text{l h}^{-1}$ was used. The values used in Figure 5.20 are the absolute ion abundances from the sum of 10 mass spectra each collected after an ion accumulation time of 1.5 s. The sprayer angle was set at $35^\circ \pm 2^\circ$, h at 2 mm, d_x at 4 mm and k at < 1 mm for all measurements. The y -offset, d_y , was the only geometrical parameter manually monitored at < 0.5 mm due to the complete disappearance of the signal with any misalignment (Section 5.6.1).

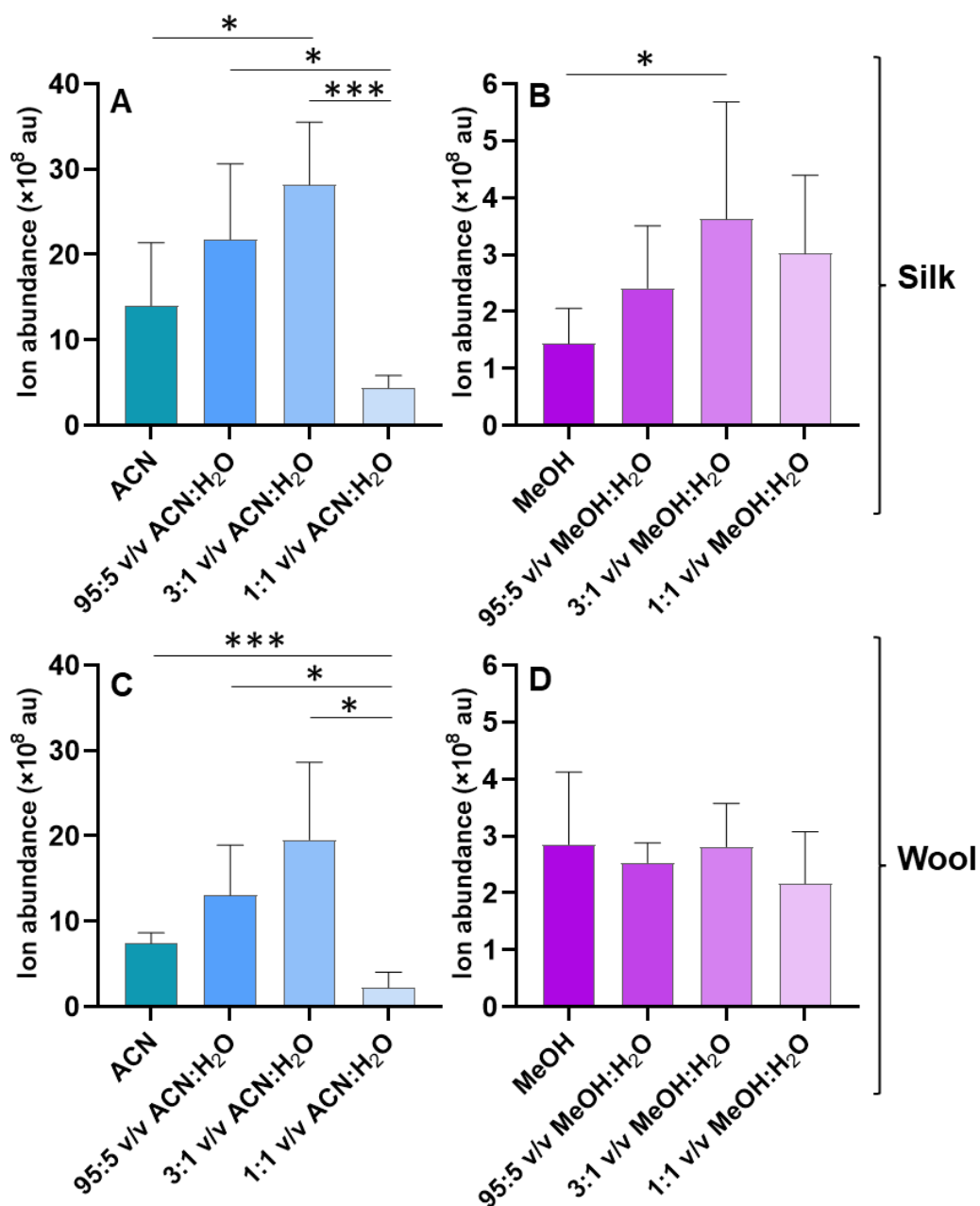


Figure 5.20: **A:** Absolute ion abundance of rhodamine B [M-Cl]⁺ peak (*m/z* 443.23) on silk using four ACN:H₂O solvent systems (*n* = 6, mean ± S.D.). **B:** Absolute ion abundance of rhodamine B [M-Cl]⁺ peak (*m/z* 443.23) on silk using four MeOH:H₂O solvent systems (*n* = 6, mean ± S.D.). **C:** Absolute ion abundance of rhodamine B [M-Cl]⁺ peak (*m/z* 443.23) on wool using four ACN:H₂O solvent systems (*n* = 6, mean ± S.D.). **D:** Absolute ion abundance of rhodamine B [M-Cl]⁺ peak (*m/z* 443.23) on wool using four MeOH:H₂O solvent systems (*n* = 6, mean ± S.D.). * represents *p* values < 0.05 and *** *p* values < 0.001 calculated using Brown-Forsyth and Welch ANOVA test.

Brown-Forsyth and Welch ANOVA test results were performed, highlighting statistical differences between the solvent systems tested (Fig 5.20). Most notable is the ten-fold larger absolute ion abundance observed for solvent ratios based on ACN compared to MeOH for both silk and wool. The overall trend seen for the ACN ratios on both silk and wool and the MeOH ratio on silk (Fig 5.20A, B, C) is an increase in absolute ion abundance with the addition of H₂O to the organic solvent, culminating at ratio 3:1 v/v. Only MeOH on wool (Fig 5.20D) does not follow this trend and suggests instead that all MeOH:H₂O ratios tested on wool have a similar impact on the ion abundance obtained.

The increase in ion abundance with the addition of H₂O suggests that some aqueous component is required on both silk and wool. A likely explanation for this phenomenon could be that the rapid evaporation of pure organic solvents does not allow the natural fibre surface to become properly wetted. However, the decrease in ion abundance seen for 1:1 v/v ACN:H₂O on both silk and wool (Fig 5.20A, C) in comparison to 3:1 v/v ACN:H₂O is statistically significant and shows that there is a limit to how much aqueous solvent should be added. MeOH seems to be more tolerant to the addition of H₂O for both silk and wool (Fig 5.20B, D).

Wool also showed a lower absolute ion abundance in comparison to silk across both ACN and MeOH solvent systems. Both the silk and wool reference cloth were tightly woven with a high thread count with similar yarn diameter, so it is likely that the difference in ion abundance between the fibres is a result of fibre properties rather than the manufacturing process of the cloth. Based on these results, 3:1 v/v ACN:H₂O was determined to be the best solvent system for the analysis of early synthetic dyes on silk and wool cloth.

5.6.4 Sprayer angle

The sprayer angle has been shown to be a crucial parameter and has a direct influence on the spot area.²⁸ The effect of the sprayer on the spot geometry was investigated using solvent-sensitive paper (Fig 5.21). A flow rate of 750 $\mu\text{l h}^{-1}$, a sprayer-to-sample height, h , (Fig 5.7) of 5 mm and an analytical time of 1 min was used for each spot. All solvent systems were tested, and the resulting spot areas were measured in ImageJ (Rasband, W. S., National Institutes of Health, Bethesda, MD, USA).

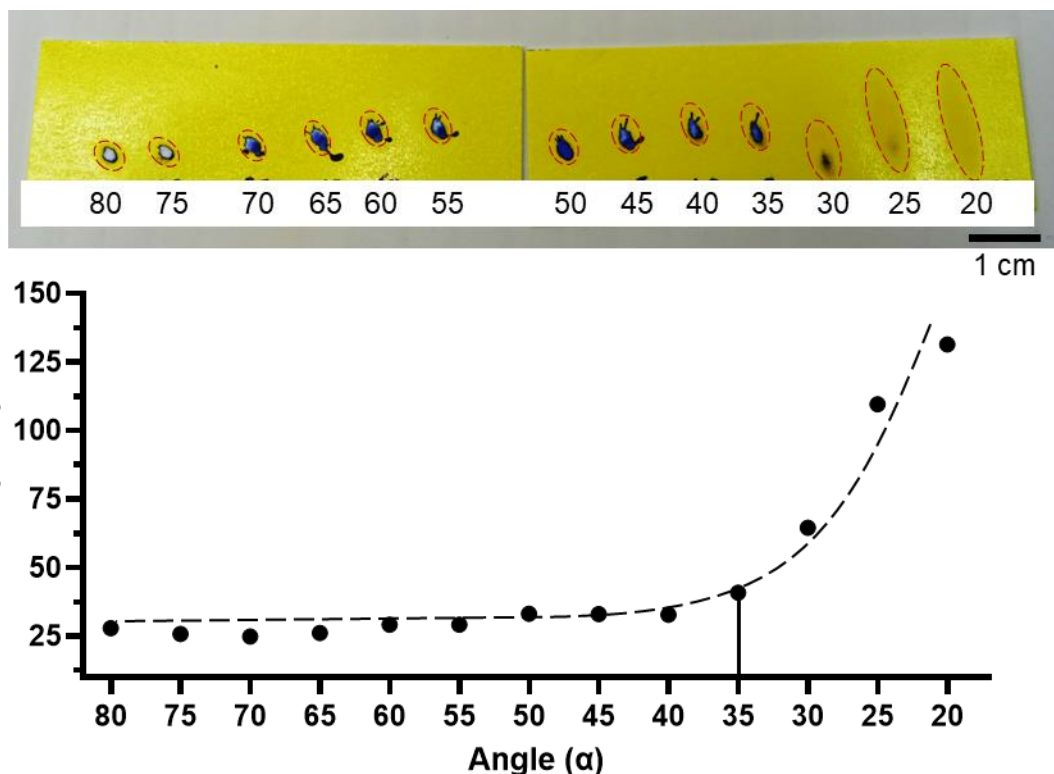


Figure 5.21: Solvent-sensitive paper (Pentair Hypro, Agratech NW Ltd, Rossendale, UK) showing the effect of different sprayer incident angles on the solvent (3:1 v/v ACN:H₂O) spot shape and size. The solvent spots margins are marked by dotted lines. The measured area (mm^2) within the dotted lines graphed below. Fitted curve for data visualisation only. Spot area of 35° highlighted to show position at critical point before rapid increase in spot areas.

The resulting spot of higher angles show a more circular shape with a clear impact of the solvent in the centre and fairly equal spot areas (Fig 5.21). As expected, the spot area increases, and the spot shape becomes more elongated the shallower the angle used. The angles above 35° show similar spot areas across all solvent system tested while an exponential increase in spot area can be seen at angles 35° - 20°. This trend was present for all solvent systems (Appendix A4).

All solvent systems except ACN and MEOH showed splattering of the solvent even at low angles, resulting from the aqueous content and high flow rate used. This is likely not as present when analysing cloth due to wicking properties of the fabric. Splattering and the less precise spots of lower angles are a major disadvantage in imaging and any type of precision work as it increases the risk for cross-contamination. However, lower angles and larger areas result in less damage to the spot investigated (Fig 5.21), as the same volume of solvent is spread over a larger area. This makes shallower angles an advantage when analysing fragile heritage

objects. This can be seen in the softer impact on the water sensitive paper of 20 – 30° sprayer angle.

A larger spot also results in less dependence on the geometrical parameters since d_y becomes marginally more tolerant to misalignment. Such larger, less precise spots were therefore desired in this project where imaging analysis was not the aim. The inclusion of a movable stage makes future application to imaging using the DESI source possible after optimisation of the spot size.

The sprayer angle and consequently the spot shape and area that resulted in the largest ion abundances for the analysis of dyes on textile samples was investigated using rhodamine B on silk and wool cloth. A solvent system of 3:1 v/v ACN:H₂O and the same approach as the solvent experiments was used for the sprayer angle experiment. The resulting graphs (Fig 5.22) show that shallower angles give a larger absolute ion abundance in comparison to steeper angles, in accordance with the results from the spot shape investigation. The asterisks included show the angles that are statistically different from $\alpha = 35^\circ \pm 2^\circ$ for silk (Fig 5.22A) and wool (Fig 5.22B).

It must be noted that silk shows a greater ion abundance than wool overall. This is in accordance with the results from the solvent system trials indicating that silk is better suited for ambient mass spectrometric analysis than wool. Both the silk and wool reference cloth were tightly woven with a high thread count with similar yarn diameter (Section 2.2.4), so it is likely that the difference in ion intensity is a result of fibre properties, such as wicking, rather than textile production.

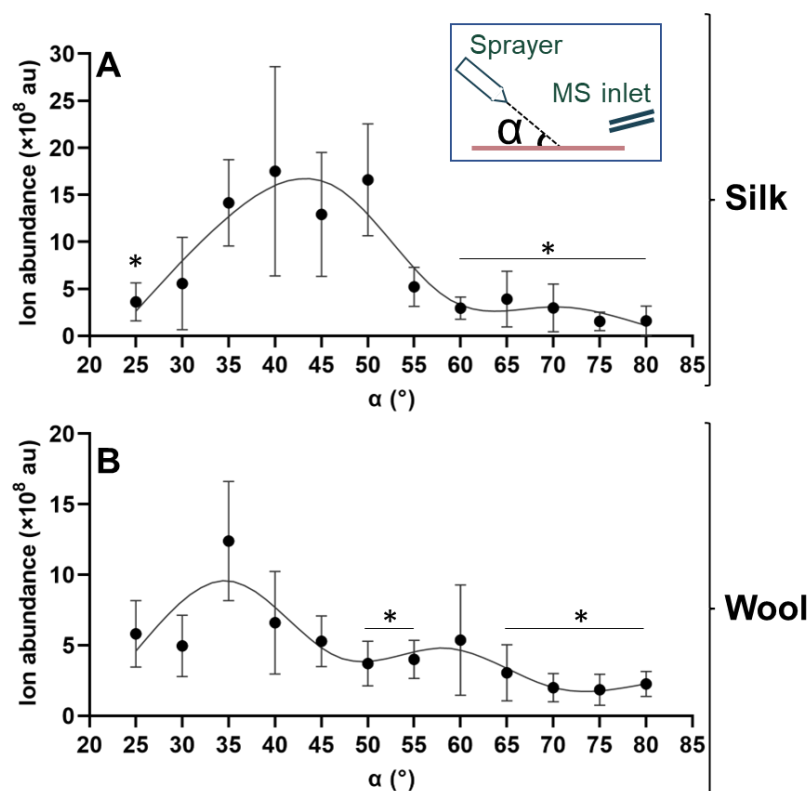


Figure 5.22: A: Absolute ion abundance of rhodamine B $[M-Cl]^+$ peak (m/z 443.23) on silk using different sprayer incident angles, α ($n = 7$, mean \pm S.D.). Insert: A schematic defining incident sprayer angle, α . All other geometrical parameters except d_y fixed. **B:** Absolute ion abundance of rhodamine B $[M-Cl]^+$ peak (m/z 443.23) on silk using different sprayer incident angles, α ($n = 7$, mean \pm S.D.). Fitted curves for data visualisation only, constructed as smoothing spline curves using 5 knots.

For silk, there is a clear divide between the lower and higher angles, with the lower angles showing higher ion abundance but also greater standard deviations. This divide is present but not as clear for wool. The steeper angles ($\alpha = 60^\circ - 80^\circ$) are statistically different to $\alpha = 35^\circ \pm 2^\circ$ for both silk and wool, which suggests that although lower angles for both cloth types give better ion abundances, $\alpha = 35^\circ$ is to be preferred.

The large standard deviations seen for both the solvent and angle measurements could perhaps partly be explained by the necessary manual alignment of the d_y parameter as well as the heterogeneity of the dyed rhodamine B references. Despite effort to dye as evenly as possible, it is probable the dye content varied on a molecular level across the samples analysed.

5.6.5 Background contaminants

One disadvantage with ambient techniques is the difficulty to control contaminants in an open laboratory environment. Consistent contaminants were found repeatedly during DESI-MS analysis and were difficult to remove despite effort. The importance to reduce the number and abundance of background contaminants increases with the decrease in target analyte concentration, making it important to confidently identify background contaminants that can be excluded from the data interpretation. Positive ionisation mode gave a larger number of recurring background peaks that could be likely assigned^{70,71} (Table 5.2). Contamination was not as prominent in negative ionisation mode and no peaks observed could be confidently identified.

Table 5.2: Background peaks repeatedly observed in positive ionisation mode and their possible identification.

Peak <i>m/z</i>	Possible source
231.07	PEG
301.14	Phthalate
309.21	PPG
327.18	PEG
368.43	BTAC-228
413.27	Phthalate
429.24	Phthalate
457.27	Phthalate

The main sources of contaminants during this project were common biochemistry laboratory chemicals (PEG), plastics (phthalates) and most prominent was the presence of BTAC-228, a known additive in hygiene products. However, despite the background contamination, DESI-MS was sensitive enough to successfully analyse historical samples of lower concentration in comparison to reference samples. Future work will need to determine the limit of detection and quantification of DESI-MS analysis of historical dyes.

5.7 DESI-MS analysis of natural dyes

5.7.1 Plant material

Turmeric (*Curcuma longa* L.) was chosen as a standard to determine the applicability of DESI-MS on natural dye chromophores based on it being a direct dye and readily available in both fresh and powder form. Initially, plant material was used to make sure that the DESI-MS set-up could ionise natural dye chromophores without interference from the cloth substrates. Fresh turmeric root purchased from a local grocery store was prepared in cryosections (50 μm), adhered to a glass slide and analysed using the DESI-MS set-up. Additionally, turmeric powder was dissolved in H_2O , added to a glass slide, and left to evaporate overnight. The dried powder slides were then analysed using DESI-MS (Fig 5.23).

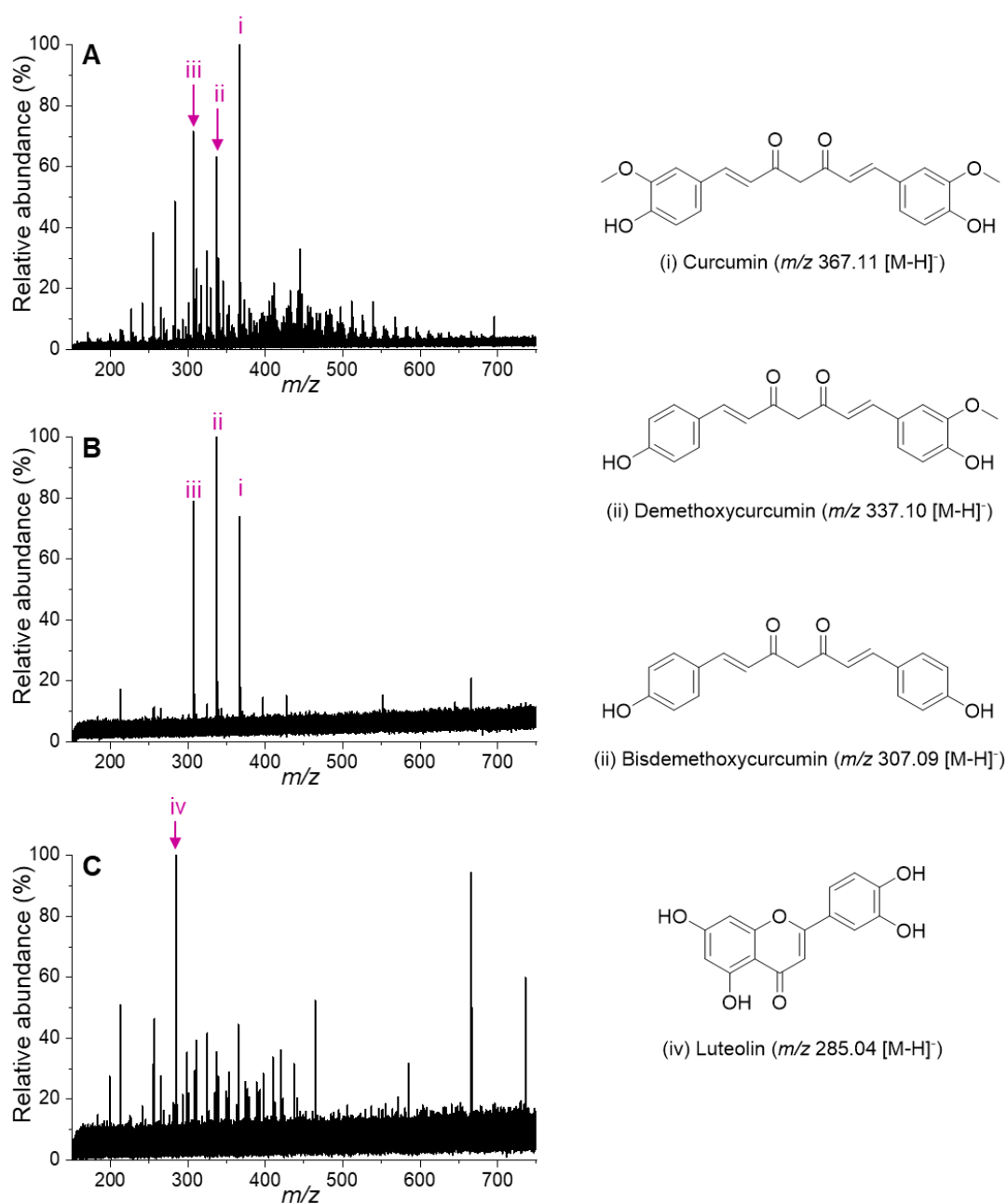


Figure 5.23: **A:** Sum of 20 mass spectra collected over 2 min of a 50 μm cryosections of fresh turmeric. The three components of turmeric are labelled in pink and their *m/z* shown in the legend. **B:** Sum of 20 mass spectra collected over 2 min of turmeric powder dissolved in H_2O and left to evaporate on a glass slide. **C:** Sum of 20 mass spectra collected over 2 min of dried plant material from weld. The main chromophore of weld is labelled in pink and its *m/z* is shown in the legend. All analyses were done in negative mode.

The three components of turmeric: curcumin, demethoxycurcumin, and bisdemethoxycurcumin were all seen in the analysis of both the sectioned fresh and powder sample (Fig 5.23A, B). The mass spectrum obtained from the powder sample

shows a less complex matrix than the fresh sample, likely due to processes during the drying step. Similar phenomenon can be seen in the analysis of fresh and dried madder (*Rubia tinctorum* L.),⁷² which is also a root used for dyeing. The noisier baseline in the turmeric powder spectrum (Fig 5.23B) compared to the fresh turmeric spectrum (Fig 5.23A) suggests that the chromophores are less concentrated in the powder sample. This change in concentration can be rationalised by the thinner sample layer on the glass slide, resulting in faster depletion of the analyte.

Additional to turmeric, dried weld plant (*Reseda luteola* L.) clipped to a glass slide was analysed. The main chromophore luteolin (m/z 285.04) was observed (Fig 5.23C) although no other known components⁷³ of weld were obtained. The luteolin peak was not as intense for dried weld plant as for either of the turmeric samples as can be seen in the noisy baseline. This is likely due to lower concentration of luteolin in the weld plant compared to the three curcumin chromophores in turmeric as much less turmeric than weld is required to dye the same mass of yarn in historical dye recipes.⁷⁴ Overall, the result from the plant materials showed that natural dye chromophores could be ionised and detected using the DESI-MS set-up although not as consistently as for rhodamine B.

5.7.2 Dyed references

Reference samples of weld (*Reseda luteola* L.), madder (*Rubia tinctorum* L.), cochineal (*Dactylopius coccus* Costa) and woad (*Isatis tinctoria* L.) prepared on wool and silk for the MODHT project⁶³ were tested next. Despite multiple attempts and changes in parameters, no clear signal could be obtained from any of the cloth samples analysed. One possible explanation for the lack of signal for natural chromophores on dyed cloth could be the mode of dye application as all of the tested dyes were mordant or vat dyes (Section 1.4).

Silk and wool were thus dyed with turmeric, which is a direct dye, to evaluate the hypothesis that the mordant and vat application of these dyes contributed to the lack of signal seen.

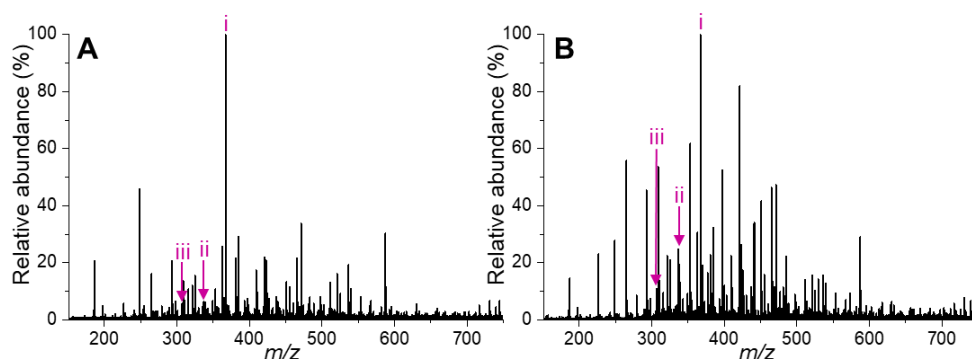


Figure 5.24: **A:** Sum of 10 mass spectra of turmeric dyed on silk cloth. **B:** Sum of 10 mass spectra of turmeric dyed on wool cloth. **(i):** curcumin: m/z 367.11 ($[M-H]^-$), **(ii):** demethoxycurcumin: m/z 337.10 ($[M-H]^-$), **(iii):** bisdemethoxycurcumin: m/z 307.09 ($[M-H]^-$) labelled in pink. For structures see Figure 5.23.

Signal from all three turmeric components could be seen on both silk and wool (Fig 5.24), although the signals were less intense than for the fresh and powder turmeric samples (Fig 23A, B) and many background peaks could be seen. However, the signals were stable across the 12 mass spectra collected and showed a signal-to-noise ratio above 3:1, which is the common limit of detection used in the signal-to-noise method. This makes it likely that the low ion abundance seen for the chromophores can be increased by optimising the DESI parameters for natural direct dyes similarly to the optimisation done for rhodamine B. The presence of the three turmeric peaks in the silk and wool supported the hypothesis that the mordant and vat application of the tested dye sources complicate the DESI-MS analysis.

Unmordanted silk and wool samples were next dyed in dyebaths of standard references of anthraquinones (alizarin, purpurin, carminic acid) to see if any signal of common natural dye chromophores could be obtained from silk and wool upon removal of the mordant. The mass spectra obtained were promising as a high ion abundance of the $[M-H]^-$ peak for each of the tested compounds could be seen (Fig 25). Wool and silk samples dyed with luteolin were prepared but no signal was obtained from either substrate, which suggests that it is not only the mordant that determines the efficiency of DESI-MS analysis of natural dye chromophores but also molecular structure.

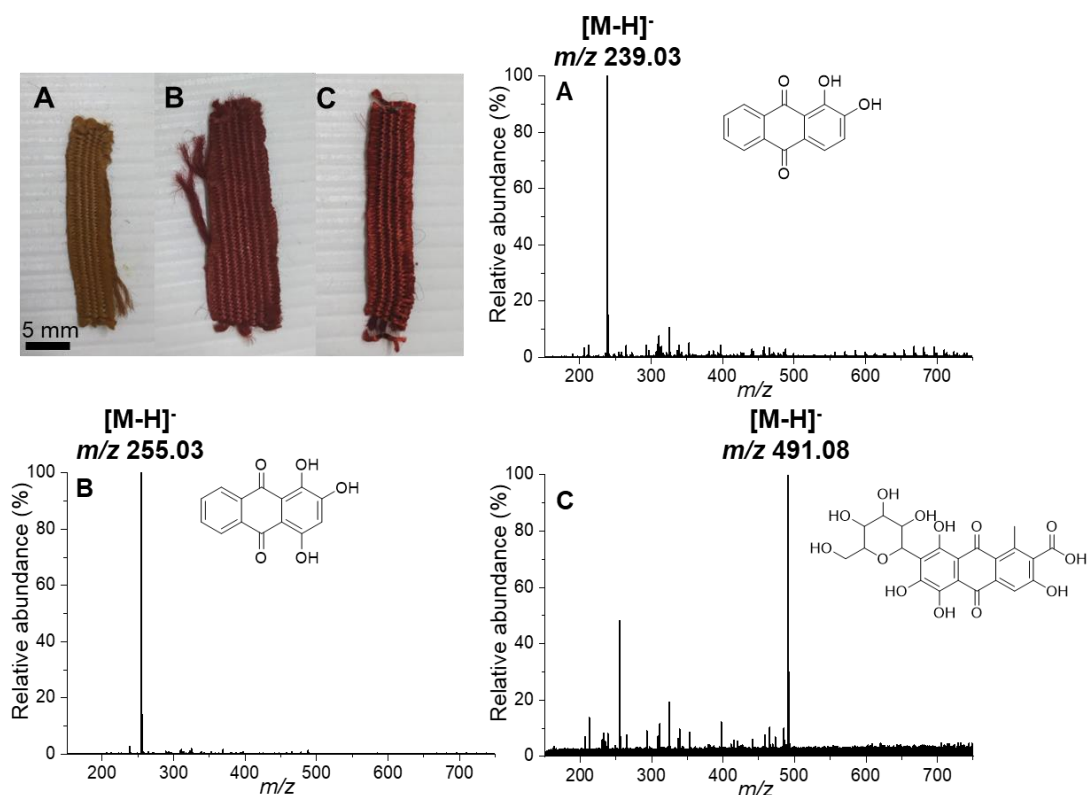


Figure 5.25: **A:** Silk cloth dyed with alazarin, molecular ion labelled in mass spectrum A. **B:** Silk cloth dyed with purpurin, molecular ion labelled in mass spectrum B. **C:** Silk cloth dyed with carminic acid, molecular ion labelled in mass spectrum C.

All natural dye components were analysed with a higher angle (75°) than optimised for rhodamine B to obtain any signal. That the optimised parameters for rhodamine B are not applicable for natural dye components means that a similar optimisation as for rhodamine B on a natural dye standard is required for future work. This was outside the timescale of this project but would be an important next step for DESI-MS analysis of natural dyes.

5.8 DESI-MS analysis of early synthetic dyes

The stability of the DESI-MS signal of rhodamine B suggested a greater applicability of the technique to synthetic dyes in comparison to natural dyes. The lack of need for a mordant when dyeing with synthetic dyes also circumvents the hypothesis that the use of a mordant reduces the success of DESI-MS analysis of dyes.

The discovery of the synthesis of mauveine by the 18-year-old William H. Perkins in 1856 initiated the modern chemical industry, spurred chemical theory and was the start of the exponential introduction of early synthetic dyestuffs. Thus, studying early

synthetic dyes aids our understanding of an important and increasingly industrialised time period. Additionally, the study and identification of early synthetic dyes are important for museum storage and display strategies as many of the dyestuffs show poor lightfastness.

Silk and wool cloth from the MODHT project^{63,64} were dyed with 22 early synthetic dyestuffs covering six important early synthetic dye families; xanthene, thiazine, nitro, diphenylmethane, triphenylmethane and azo (Table 5.3). These families are derivatives of coal tar compounds and among the first dye compounds invented following Perkins' accidental discovery of mauveine in 1856 (Section 1.5).

Table 5.3: Early synthetic dye references investigated by DESI-MS on silk and wool. Structures shown in Appendix A5. Year of discovery determined from references.^{62,75–77}

Name (Colour index (CI))	Year of invention	Monoisotopic mass (g mol ⁻¹)	Characteristic ion
<i>Azo dyes</i>			
Aniline Yellow (CI 11000)	1861	197.10	<i>m/z</i> 198.10 [M+H] ⁺
Congo Red (CI 22120)	1883	696.08	<i>m/z</i> 325.18 [M-Na] ²⁻
Crocein Scarlet 7B (CI 27165)	1881	584.04	Not observed
Disperse Orange III (CI 11005)	1878	242.08	Not observed
Methyl Red (CI 13020)	1908	269.11	<i>m/z</i> 268.11 [M-H] ⁻
Orange II Na salt (CI 15510)	1876	350.03	<i>m/z</i> 327.04 [M-Na] ⁻
Ponceau 3R (CI 15155)	1878	494.02	<i>m/z</i> 224.02 [M-2Na] ²⁻
Ponceau S (CI 27195)	1880	759.89	(i) <i>m/z</i> 166.98 [M-4Na] ⁴⁻ (ii) <i>m/z</i> 230.31 [M-3Na] ³⁻ (iii) <i>m/z</i> 356.96 [M-2Na] ²⁻
Xylidine Ponceau (Ponceau 2R) (CI 16150)	1878	480.00	(i) <i>m/z</i> 217.01 [M-2Na] ²⁻ (ii) <i>m/z</i> 457.02 [M-Na] ⁻
<i>Diphenylmethane dye</i>			
Auramine O (CI 41000)	1883	303.15	<i>m/z</i> 268.18 [M-Cl] ⁺
<i>Triphenylmethane dyes</i>			
Basic Fuchsin (CI 42510)	1858	(i) 288.15 (ii) 302.17 (iii) 316.18 (iv) 330.20	(i) <i>m/z</i> 288.15 [M] ⁺ (ii) <i>m/z</i> 302.17 [M] ⁺ (iii) <i>m/z</i> 316.18 [M] ⁺ (iv) <i>m/z</i> 330.20 [M] ⁺
Brilliant Green (CI 42040)	1879	420.23	<i>m/z</i> 385.27 [M-Cl] ⁺
Light Green SF yellowish (CI 42095)	1879	792.12	Not observed
Malachite Green (CI 42000)	1878	364.17	<i>m/z</i> 329.20 [M-Cl] ⁺
Methyl Green (CI 42585)	1871	515.17 422.24?	Not observed

Methyl Violet (CI 42535)	1861	(i) 330.20 (ii) 344.22 (iii) 358.23 (iv) 372.25	(i) m/z 330.20 [M] ⁺ (ii) m/z 344.22 [M] ⁺ (iii) m/z 358.23 [M] ⁺ (iv) m/z 372.25 [M] ⁺
<i>Nitro dyes</i>			
Martius yellow (CI 10315)	1864	234.03	m/z 233.02 [M-H] ⁻
Naphthol Yellow S (CI 13016)	1879	357.948	m/z 155.98 [M-2Na] ²⁻
<i>Xanthene dyes</i>			
Eosin Y (CI Acid Red 87)	1874	687.64	m/z 320.83 [M-2Na] ²⁻
Fluorescein (CI 45350)	1871	333.08	m/z 333.08 [M] ⁻
Rhodamine B (CI 45170)	1887	478.20	m/z 443.23 [M-Cl] ⁺
<i>Thiazine dye</i>			
Methylene Blue (CI 52015)	1876	319.091	m/z 284.12 [M-Cl] ⁺

Before dyeing the silk and wool cloths, conventional ESI-MS was performed on the dye baths as a comparison to the DESI-MS result and to give a guide for which m/z peaks to expect for each sample. The Bruker 7T Solarix FT-ICR-MS instrument used for the DESI-MS analysis was also used for the ESI-MS investigation.

All compounds except aniline yellow and Martius yellow are commercially sold as salts, meaning that the characteristic peak seen was $[M-nCl]^{z+}$ for the cationic dyes and $[M-nNa]^{z-}$ for the anionic dyes. The presence of charged species makes the ionisation step more efficient, accounting for the clean spectra seen despite DESI-MS being an ambient technique. However, the applicability of DESI-MS to dyestuffs readily ionized at neutral pH is shown by the equally clean spectra of Martius yellow with m/z 233.02 corresponding to $[M-H]^{-}$.

Both positive and negative mode were utilised for the analyses depending on the structure. All xanthene, thiazine, diphenylmethane, triphenylmethanes and aniline yellow (azo) were analysed in positive mode while the nitro dyes and all remaining azo dyes were analysed in negative mode. Consistently, DESI-MS analysis in positive ion mode gave higher ion abundances than analysis in negative ion mode, and the analyses of the dyed reference samples on both silk and wool show little background interference despite being performed under ambient conditions (Fig 5.26).

Dyes from all dye families could be analysed using the DESI-MS set-up although no signal was obtained from four of the dyestuffs tested: crocein scarlet, disperse orange

III, light green SF yellowish and methyl green. Two dyes: methyl red, and eosin Y could only be obtained on their silk samples and not wool. It is unknown what these dye samples have in common that resulted in no signal in the DESI-MS spectra as other dyes with similar structures and masses were easily obtained from the DESI-MS analysis and they were not all analysed using the same ionisation mode. A possibility could be a lower quality dyeing of the samples, mislabelled references or that the compounds were not ionised at the pH used. However, crocein scarlet 7B and light green SF yellowish are both sulfonated, disperse orange III contain aniline groups and methyl green is closely related to easily ionised triphenylmethanes, so it is likely that they would be as ionisable as the other synthetic dye references tested. Re-dyeing of references and further study is required to determine the reason for the lack of result from these compounds.

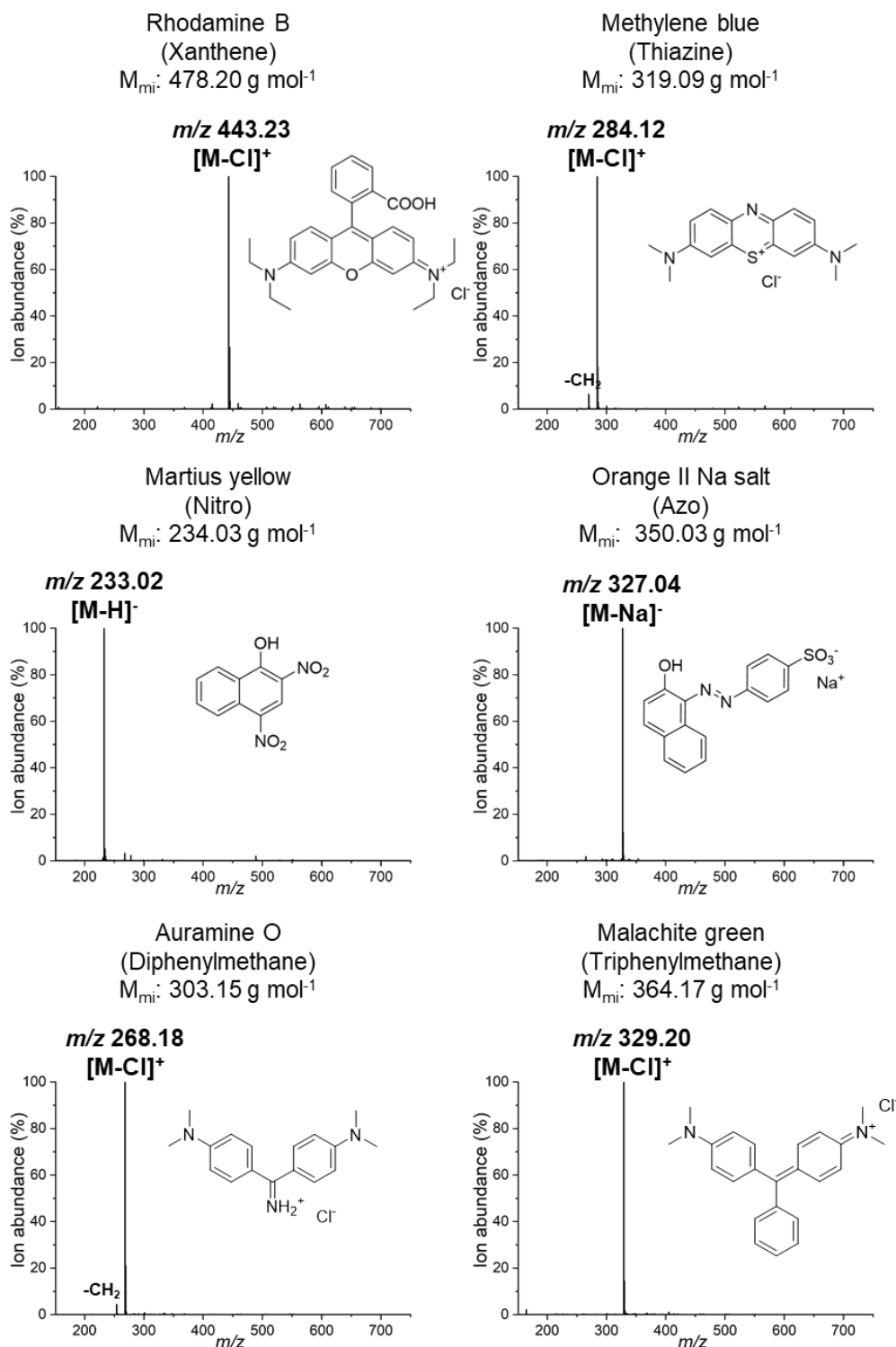


Figure 5.26: Top: DESI-MS spectra of xanthene rhodamine B ([M-Cl]⁺ (m/z 443.23)) and thiazine methylene blue ([M-Cl]⁺ (m/z 284.12)) dyed on silk. **Centre:** DESI-MS spectra of nitro dye Martius yellow ([M-H]⁻ (m/z 233.02)) and azo dye orange II sodium salt ([M-Na]⁻ (m/z 327.04)) dyed on silk. **Bottom:** DESI-MS spectra of diphenylmethane auramine O ([M-Cl]⁺ (m/z 268.18)) and triphenylmethane malachite green ([M-Cl]⁺ (m/z 329.20)) dyed on silk. Sum of two mass spectra shown.

For the 20 samples from which a signal was obtained, the lowest signal-to-noise ratio was seen for the azo dyes and naphthol yellow S (Fig 5.27). One hypothesis for this observation was that the lower ion abundance detected was mass dependent since most of the dyestuffs investigated were below 500 g mol⁻¹ (Table 5.3) while the lower ion abundances were particularly prominent for the azo dyes with masses close to 700 g mol⁻¹ (Congo Red, Ponceau S).

This is likely not the case as naphthol yellow S has a monoisotopic mass of 357.948 g mol⁻¹ which is similar in mass to dyes with higher abundance DESI-MS signal such as malachite green (364.17 g mol⁻¹). Additionally, DESI-MS is used with success in biological imaging where the molecular targets repeatedly^{36,37,50} are of larger mass than the dye molecules analysed in this study.

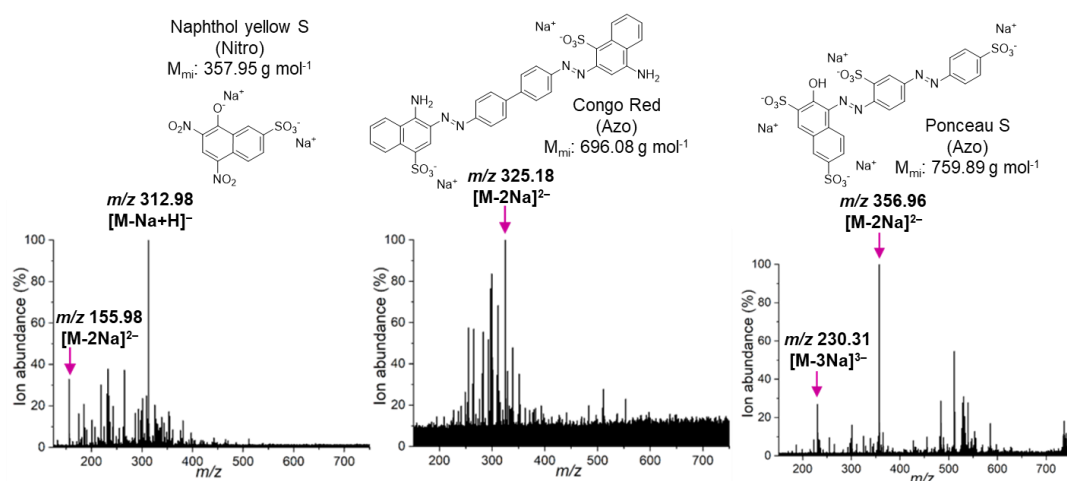


Figure 5.27: DESI-MS spectra of nitro dye naphthol yellow S ($[M-Na+H]^-$ (m/z 312.98), $[M-2Na]^{2-}$ (m/z 155.98)), azo dye Congo red ($[M-2Na]^{2-}$ (m/z 325.18)), and azo dye Ponceau S ($[M-2Na]^{2-}$ (m/z 356.95) and $[M-3Na]^{3-}$ (m/z 230.31)) dyed on silk.

Another explanation for the difference in signal abundance between the tested dyes could be a lower abundance of multiple charged species formed under the conditions used for this DESI-MS project. Naphthol yellow S, Congo red and ponceau S have $[M-2Na]^-$ peaks and both naphthol yellow S and ponceau S display more than one ion. The spreading of the molecular signal across multiple charge states might thus result in the lower signal-to-noise ratios seen for these compounds.

However, despite the decreased target ion abundance for the dyes discussed in comparison to the rest, clear ion signal from these dye molecules can be seen. Hence, it can be concluded that DESI-MS and the constructed set-up can be efficiently

applied to early synthetic dyestuffs in both positive and negative mode. To support this conclusion, the set-up was used on historical early synthetic dye samples.

5.9 Application of DESI-MS analysis to historical dye samples

5.9.1 Lehne's handbook (1893)

Next step was to evaluate the technique on historical samples for future applications on museum's collections. As this technique is still in its development, it was not possible to apply it to an object from the museum collection. Therefore, other historical materials were sought for analysis and a copy of Lehne's handbook dated from 1893 in the personal possession of Lore Troalen was kindly supplied for the study. As this material is historical but not registered in a museum's collection, it provides an opportunity for experimental research, allowing to both test the method on a range of chemical dyes but also to evaluate possible damages to the dye textile samples, which is of utmost importance for future study of museum's collections.

Adolf Lehne (1856 – 1930) was a prominent German dye chemist who held multiple official roles as well as started a textile industry school and a scientific journal for dyes.^{78,79} Much of his work was focussed on the standardisation of the emerging dye industry. He held many official positions as a representative for the textile industry including as an expert advisor of the textile industry by the Berlin council in 1888 and for the Royal Patent Office for textile chemical applications from 1891. He was also chairman of "Fachgruppe für Chemie der Farben- und Textilindustrie" [the focus group of dyeing and textile industry chemistry], for which he developed a German national standardisation of dyeing and printing as part of the "Deutsche Echtheitkommission" [German authenticity commission]. This commission was used as a model for the European international equivalent founded as part of ISO in 1951.

He was an active publisher and founded the scientific journal "die Färber-Zeitung" [the colour journal] in 1889 which in 1920 became the "Melliand Textilberichte" [Melliand textile reports] still published today. Among his most significant works is the *Tabellarische Übersicht über die künstliche organischen Farbstoffe und ihre Anwendung in Färberei und Zeugdruck* [Tabular overview of the synthetic organic dyestuffs and their use in dyeing and printing] (Lehne's handbook).^{78,79}

This book was printed in three editions (1893, 1899, 1906) and in these books he attempted to summarize the most important dyestuffs on the market. Similar synthetic

dye reference books exist but only a few have been studied.⁷⁷ Lehne's handbook (1893) contains 324 dyestuffs divided in 16 dye families. For each of these dyes, the commercial name(s), dyeing details including common uses, solubility and authenticity and one or more dyed sample(s) are presented (Fig 5.28). 12 synthetic dye samples in Lehne's handbook were analysed (Appendix A5), including ethyl violet and picric acid for which no modern references were analysed.

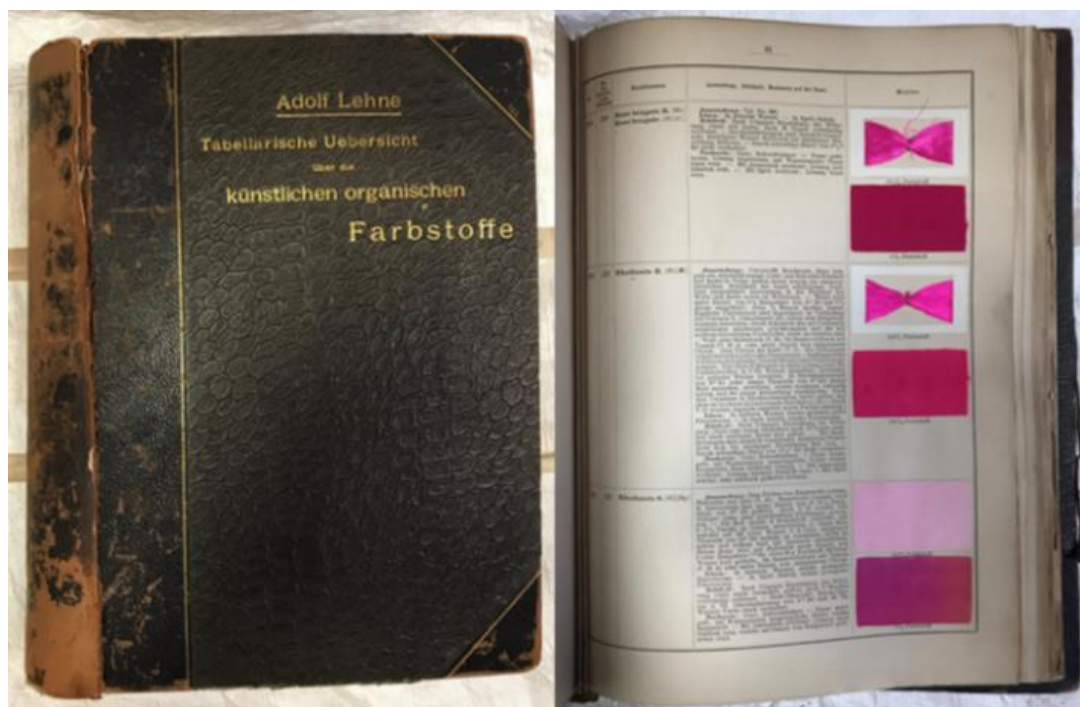


Figure 5.28: *Tabellarische Übersicht über die künstliche organischen Farbstoffe und ihre Anwendung in Färberei und Zeugdruck [Tabular overview of the synthetic organic dyestuffs and their use in dyeing and printing], Adolf Lehne, 1893. Page including rhodamine B shown on the right to demonstrate the tabular layout of the book with index on the far left of the page followed by the commercial name(s). The column adjacent to the samples include the dyeing procedure, common uses of the dye, authentication and verification of the dye on the fibre. L. Troalen, private collection.*

Identifying early synthetic dyestuffs is challenging from a scientific point-of-view by the large number of synthetic dyestuffs introduced during a short time period, often with closely related molecular structures. The wide variety in molecular structure of dye families, the commercialisation of the same dyestuff with different names in different countries as well as the occurrence of dye mixtures in dyestuffs thought of as pure further complicates the analysis. Additionally, photodegradation and inefficient synthetic routes supplying unknown by-products will also add to the challenge of analysis.

Understanding the original dye recipes and how the early synthetic dyestuffs were used and referred to is an important part of deconvoluting some of this complexity.⁸⁰ Lehne's handbook provides authentic and naturally aged reference samples of early synthetic dyes and the corresponding contemporary name, which makes it an important source for understanding original dye recipes and degradation pathways.

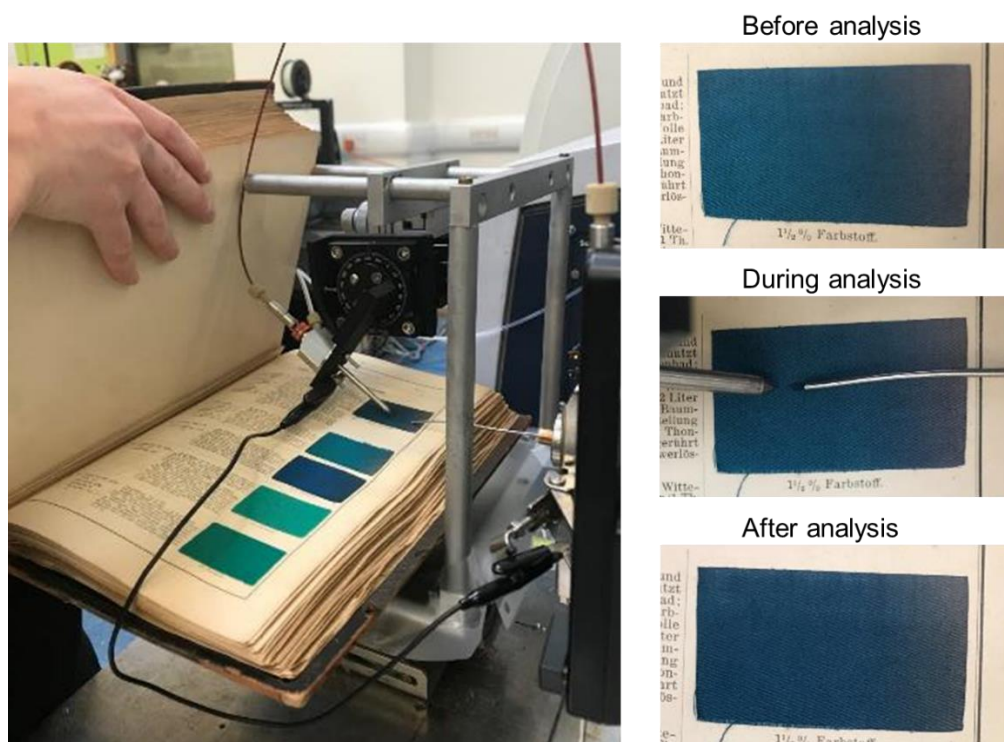


Figure 5.29: **Left:** *In-situ* analysis of malachite green in Lehne's handbook, 1893 for which the object could be manually held in place. **Right:** The sample of malachite green in Lehne's handbook, 1893 is shown before, during and after DESI-MS analysis to demonstrate that no visual damage on the samples could be seen after analysis. The wetted spot analysed can be seen in the middle image.

The advantage of DESI-MS analysis of historical objects was supported by the practical ease of the analysis. The book was manually held open and in place on the stage during the two minutes the analysis took (Fig 5.29). The same procedure and settings as for the optimisation experiment was used for all the analyses which included one minute of wetting the surface before one minute of recording. After evaporation of the applied solvent, no visual damage could be seen (Fig 5.29). Consistently and unsurprisingly, the historical samples show lower concentrations of the dyestuffs in comparison to the modern dyed references demonstrated by the more intense background peaks (Fig 5.30). Regardless of the increased background, the m/z of the dyestuffs can still be clearly identified in the historical Lehne samples.

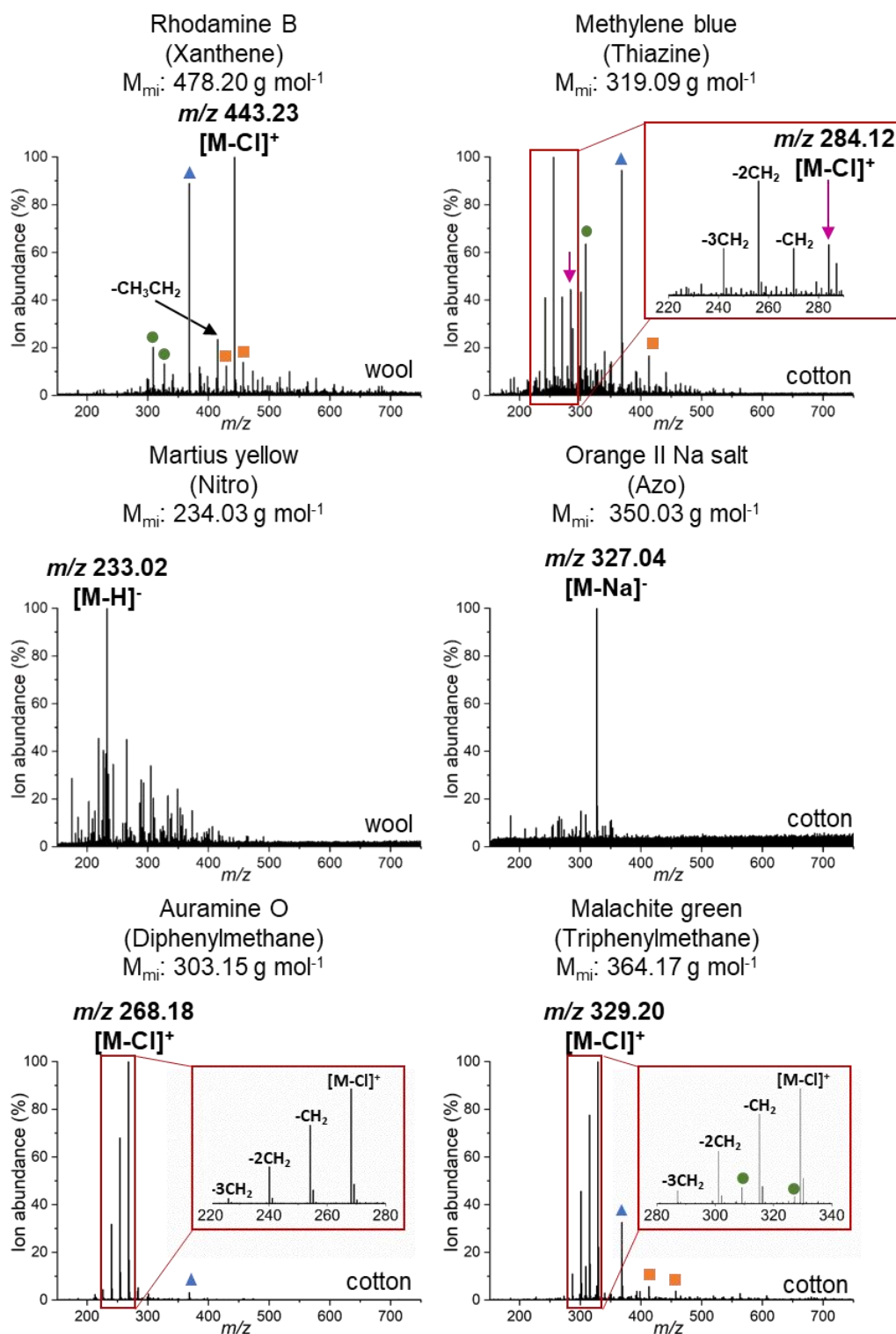


Figure 5.30: Top: DESI-MS spectra of xanthene rhodamine B ([M-Cl]⁺ (m/z 443.23)) and thiazine methylene blue ([M-Cl]⁺ (m/z 284.12)) from Lehne's handbook, 1893. **Centre:** DESI-MS spectra of nitro dye Martius yellow ([M-H]⁻ (m/z 233.02)) and azo dye orange II sodium salt ([M-Na]⁻ (m/z 327.04)) from Lehne's handbook, 1893. **Bottom:** DESI-MS spectra of diphenylmethane auramine O ([M-Cl]⁺ (m/z 268.18)) and triphenylmethane malachite green ([M-Cl]⁺ (m/z 329.20)) from Lehne's handbook, 1893. Sum of two mass spectra shown.

The DESI-MS analyses were sensitive enough that *N*-demethylation products were seen for the di- and triphenylmethane, xanthene and thiazine dye samples tested in the Lehne book (Fig 5.30). This pattern can be seen for auramine O, malachite green and brilliant green as well as xanthene rhodamine B and thiazine methylene blue. *N*-demethylation is a known degradation pathway for these dyes,^{81–84} which indicates the level of degradation of these samples in the Lehne book. The presence of these ions could also be a result of the dye recipes used as it has been established that early synthetic routes and starting material resulted in impure mixtures of related compounds to a larger extent compared to modern synthesis.⁸⁵ The observation of these de-methylated products thus also authenticates the samples and with future work might give an indication of the synthetic route used.

5.9.2 DESI-MS-MS investigation of historical triphenylmethane dyes

The applicability of DESI-MS for tandem MS studies of synthetic dyes was also investigated with the focus on triphenylmethane dyes. The samples of brilliant green and ethyl violet in Lehne's handbook (Fig 5.31) were used.

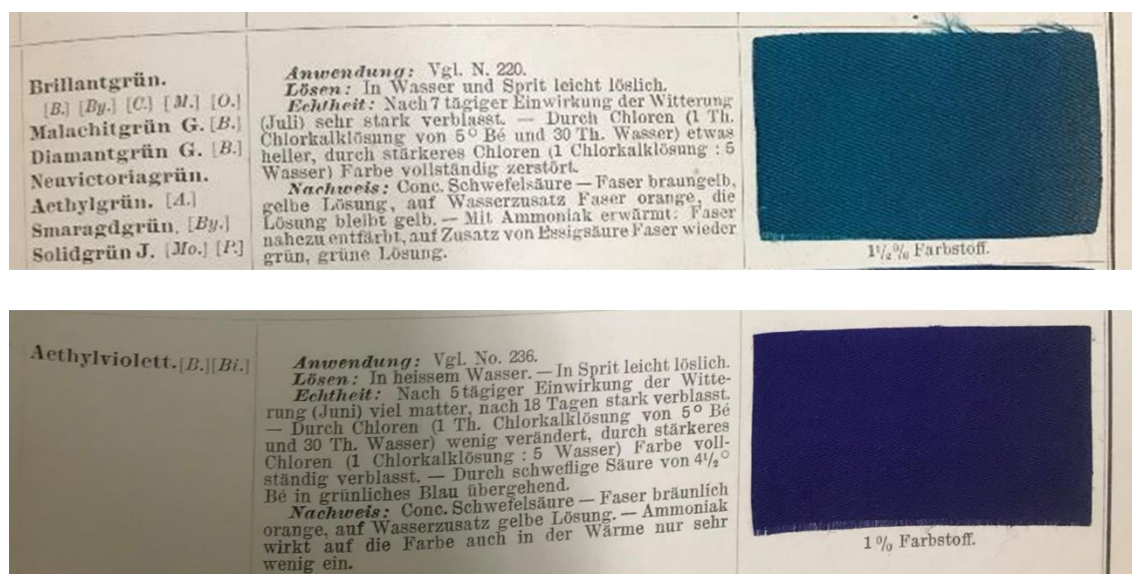


Figure 5.31: Brilliant green and ethyl violet in Lehne's handbook (1893).

The historical samples in Lehne's handbook were wetted for one minute and the molecular ion peaks for brilliant green (m/z 385.27) and ethyl violet (m/z 456.34) isolated. Collision-induced dissociation (CID) used to induce fragmentation for confirmation of the molecular structures. Brilliant green and ethyl violet were chosen due to their high signal-to-noise ratio of the monoisotopic peaks (Appendix A5) and because both follow studied fragmentation pathways for triphenylmethane dyes.^{83,86}

The stable nature of triphenylmethane dyes is demonstrated by the fairly high CID voltage required for both brilliant green and ethyl violet to induce fragmentation. Brilliant green needed 32 V and ethyl violet 35.5 V.

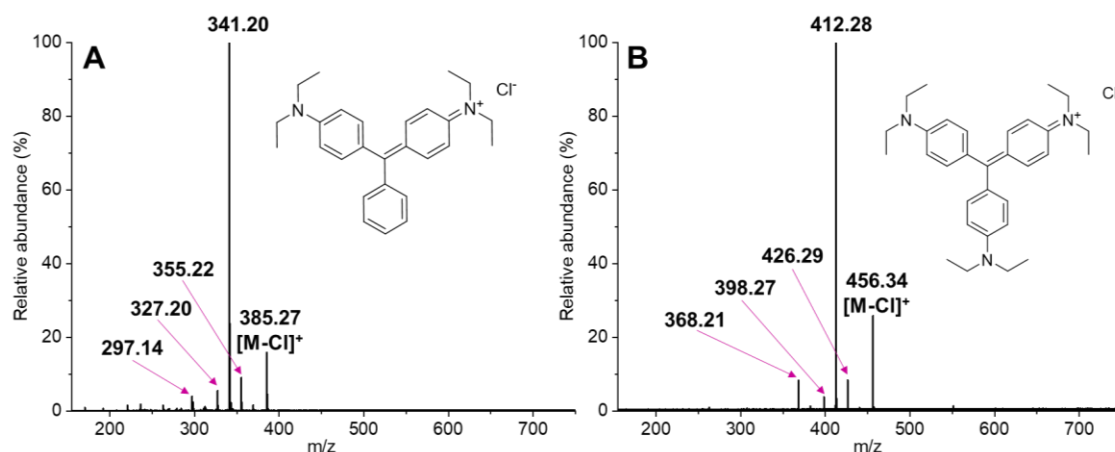


Figure 5.32: **A:** DESI-MS-MS spectrum (CID voltage: 32 V) of the isolated brilliant green [M-Cl]⁺ peak (*m/z* 385.27) with chemical structure inserted. **B:** DESI-MS-MS spectrum (CID voltage: 35.5 V) of the isolated ethyl violet [M-Cl]⁺ peak (*m/z* 456.34) with chemical structure inserted.

Brilliant green and ethyl violet fragment in a series of de-alkylation reactions, as common for di- and triphenylmethane dyes.^{82,84} The main fragment for both brilliant green (Fig 5.32A) and ethyl violet (Fig 5.32B) was a loss of 44 Da corresponding to a -C₃H₈ fragment. Three smaller fragments were seen for both dyes investigated with losses of 30 Da (-C₂H₆), 58 Da (-C₃H₈) and 88 Da (-2×C₃H₈). Proposed structures of the fragment ions recorded are shown in Figure 5.33 using brilliant green as an example. Each fragmentation product except **iv** follow the fragmentation series of C_nH_{2n+2} from a subsequent loss of methyl groups. Fragment **iv** instead likely corresponds to a loss of two C₃H₈ molecules rather than a hexane alkyl chain.

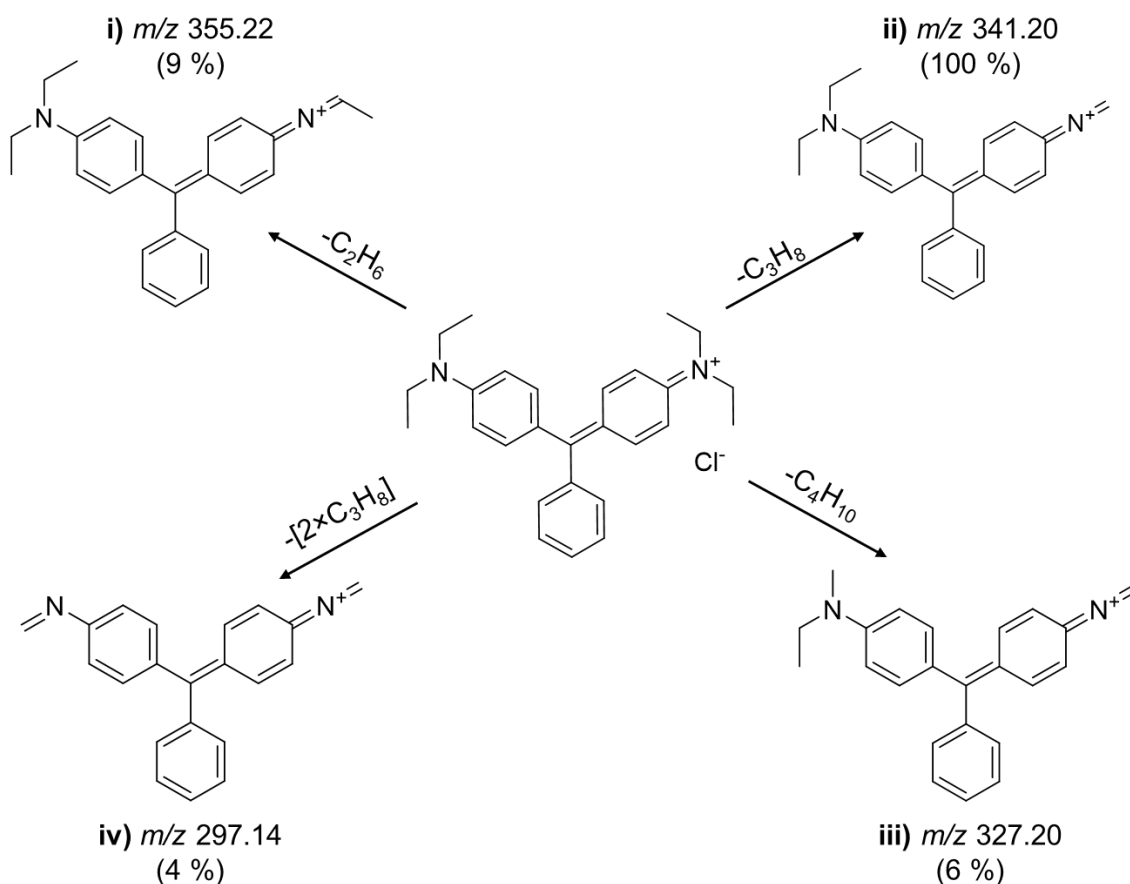


Figure 5.33: Proposed fragmentation structures of brilliant green including the relative intensities of each fragment seen in the DESI-MS-MS spectrum of the isolated brilliant green peak (m/z 385.27).

Worthy of note for brilliant green and ethyl violet is the lack of fragmentation products as a result of a continued de-alkylation of all three nitrogens. No loss of 102 Da from a loss of fragment **iv** + CH_2 is seen, suggesting that after fragment **iv** it is likely that the triphenylmethane compounds fragment into only neutral molecules.

The successful application of DESI-MS to tandem MS studies of synthetic dyes demonstrates the possibility to use DESI-MS to identify unknown dye samples in a similar way to LC-MS-MS techniques. However, the disadvantage of a lack of separation of components in complex mixtures, in common with all techniques not coupled to LC, needs to be remembered. Regardless, the possibility of conducting tandem MS experiments widens the use of DESI-MS to other historical samples and not only samples where the target ion is known.

5.10 Conclusions

A desorption electrospray ionisation (DESI) source was constructed for historical dye analysis for the first time. The source sprayer holder was designed with purchased x-, y- and z-positioners, an angle rotation mount and components 3-D printed in polylactic acid. After exploratory studies, the sprayer angle and solvent system used were determined as the main parameters affecting DESI-MS analysis of textile samples.

Lower sprayer angles was shown for both silk and wool to give higher absolute ion abundance of rhodamine B cation peak in comparison to higher angles. This is likely due to the larger spot area achieved resulting in a larger tolerance of the geometrical parameters of the source. The optimised sprayer angle was determined to be 35° for both silk and wool. ACN-containing systems obtained ten-fold absolute ion abundances in comparison to MeOH-containing system. The optimised solvent system was found to be 3:1 v/v ACN:H₂O for both silk and wool.

The optimised set-up was applied to both natural and early synthetic dye references. No chromophore signal was obtained from mordanted natural dye references while it was possible to obtain the chromophores from direct dyes such as turmeric. However, the response was unreliable in reproducibility. Reliable result were obtained from 20 early synthetic dye references covering six dye families, showcasing the applicability of DESI-MS to early synthetic dyes.

12 historical samples from *Tabellarische Übersicht über die künstliche organischen Farbstoffe und ihre Anwendung in Färberei und Zeugdruck [Tabular overview of the synthetic organic dyestuffs and their use in dyeing and printing]*, Adolf Lehne, 1893 (Lehne's handbook) were analysed with success. DESI-MS-MS studies of two triphenylmethane dyes could also be conducted, highlighting the applicability of DESI-MS to studies of unknown target ions. All of the analysed samples gave expectant result, showing the high quality of Lehne's synthetic work and indicating the importance of the reference book for the study of original dye recipes and degradation pathways.

Exciting future work is required for the full incorporation of DESI-MS into the field of dye analysis, but this initial study has shown that DESI-MS is a technique with large potential and advantages for the field of heritage science.

5.11 References

- 1 I. Degano and J. La Nasa, *Top. Curr. Chem.*, 2016, **374**, 263–290.
- 2 I. Degano, E. Ribechini, F. Modugno and M. P. Colombini, *Appl. Spectrosc. Rev.*, 2009, **44**, 363–410.
- 3 R. G. Cooks, Z. Ouyang, Z. Takats and J. M. Wiseman, *Science*, 2006, **311**, 4894–4895.
- 4 A. E. Kramell, A. O. Brachmann, R. Kluge, J. Piel and R. Csuk, *RSC Adv.*, 2017, **7**, 12990–12997.
- 5 C. Selvius Deroo and R. A. Armitage, *Anal. Chem.*, 2011, **83**, 6924–6928.
- 6 A. Kramell, F. Porbeck and R. Kluge, *J. Mass Spectrom.*, 2015, **50**, 1039–1043.
- 7 K. H. Cochran, J. A. Barry, G. Robichaud and D. C. Mussiman, *Anal Bioanal Chem*, 2015, **407**, 813–820.
- 8 N. Wyplosz, PhD Thesis, Amsterdam University, 2003.
- 9 Z. Takats, J. M. Wiseman, B. Gologan and R. G. Cooks, *Science*, 2004, **306**, 471–473.
- 10 W. M. A. Niessen and D. Falck, in *Analyzing Biomolecular Interactions by Mass Spectrometry*, eds. J. Kool and W. M. A. Niessen, Wiley-VCH Verlag, Weinheim, 2015.
- 11 M. Z. Huang, C. H. Yuan, S. C. Cheng, Y. T. Cho and J. Shiea, *Annu. Rev. Anal. Chem.*, 2010, **3**, 43–65.
- 12 R. B. Cody, J. A. Laramée and H. D. Durst, *Anal. Chem.*, 2005, **77**, 2297–2302.
- 13 J. H. Gross, *Anal. Bioanal. Chem.*, 2014, **406**, 63–80.
- 14 A. Alvarez-Martin, T. P. Cleland, G. M. Kavich, K. Janssens and G. A. Newsome, *Anal. Chem.*, 2019, **91**, 10856–10863.
- 15 R. A. Armitage, C. Day and K. A. Jakes, *Sci. Technol. Archaeol. Res.*, 2015, **1**, 1–10.
- 16 R. A. Armitage, K. Jakes and C. Day, *Sci. Technol. Archaeol. Res.*, 2015, **1**, 60–69.
- 17 R. A. Armitage, D. Fraser, I. Degano and M. P. Colombini, *Herit. Sci.*, 2019, **7**, 1–23.
- 18 G. A. Newsome, I. Kayama and S. A. Brogdon-Grantham, *Anal. Methods*, 2018, **10**, 1038–1045.
- 19 T. T. Häbe and G. E. Morlock, *Rapid Commun. Mass Spectrom.*, 2015, **29**, 474–484.
- 20 C. N. McEwen, R. G. McKay and B. S. Larsen, *Anal. Chem.*, 2005, **77**, 7826–7831.
- 21 E. C. Horning, M. G. Horning, D. I. Carroll, I. Dzidic and R. N. Stillwell, *Anal. Chem.*, 1973, **45**, 936–943.
- 22 B. Munson in *Encyclopedia of Analytical Chemistry*, John Wiley & Sons, Ltd, Hoboken, 2006.
- 23 J. Chen, F. Tang, C. Guo, S. Zhang and X. Zhang, *Anal. Methods*, 2017, **9**, 4908–4923.
- 24 D. Calligaris, D. Caragacianu, X. Liu, I. Norton, C. J. Thompson, A. L. Richardson, M.

- Golshan, M. L. Easterling, S. Santagata, D. A. Dillon, F. A. Jolesz and N. Y. R. Agar, *PNAS*, 2014, **111**, 15184–15189.
- 25 S. A. R. Bogdan, N. Talaty, J. W. Sawicki, A. R. Bogdan, N. Talaty and S. W. Djuric, *React. Chem. Eng.*, 2019, **4**, 1589–1594.
- 26 Z. Zhou and R. N. Zare, *Anal. Chem.*, 2017, **89**, 1369–1372.
- 27 J. Newton, PhD Thesis, University of Glasgow, 2019.
- 28 Z. Takáts, J. M. Wiseman and R. G. Cooks, *J. Mass Spectrom.*, 2005, **40**, 1261–1275.
- 29 T. L. Maser, E. Honarvar and A. R. Venter, *J. Am. Soc. Mass Spectrom.*, 2020, **31**, 803–811.
- 30 W. M. A. Niessen and A. E. Tinke, *J. Chromatogr. A*, 1995, **703**, 37–57.
- 31 P. Kebarle and U. H. Verkerk, *Mass Spectrom. Rev.*, 2009, **28**, 898–917.
- 32 L. Konermann, E. Ahadi, A. D. Rodriguez and S. Vahidi, *Anal. Chem.*, 2013, **85**, 2–9.
- 33 A. B. Costa and R. G. Cooks, *Chem. Commun.*, 2007, 3915–3917.
- 34 A. B. Costa and R. G. Cooks, *Chem. Phys. Lett.*, 2008, **464**, 1–8.
- 35 M. S. Bereman and D. C. Muddiman, *J. Am. Soc. Mass Spectrom.*, 2007, **18**, 1093–1096.
- 36 J. Tillner, V. Wu, E. A. Jones, S. D. Pringle, T. Karancsi, A. Dannhorn, K. Veselkov, J. S. McKenzie and Z. Takats, *J. Am. Soc. Mass Spectrom.*, 2017, **28**, 2090–2098.
- 37 N. Abbassi-Ghadi, E. A. Jones, K. A. Veselkov, J. Huang, S. Kumar, N. Strittmatter, O. Golf, H. Kudo, R. D. Goldin, G. B. Hanna and Z. Takats, *Anal. Methods*, 2015, **7**, 71–80.
- 38 A. Bodzon-Kulakowska, A. Drabik, J. Ner, J. H. Kotlinska and P. Suder, *Rapid Commun. Mass Spectrom.*, 2014, **28**, 1–9.
- 39 F. Bianchi, M. Mattarozzi and M. Careri, *Anal. Bioanal. Chem.*, 2020, **412**, 3967–3973.
- 40 L. Konermann, A. D. Rodriguez and J. Liu, *Anal. Chem.*, 2012, **84**, 6798–6804.
- 41 E. Ahadi and L. Konermann, *J. Phys. Chem. B*, 2012, **116**, 104–112.
- 42 J. V. Iribarne and B. A. Thomson, *J. Chem. Phys.*, 1976, **64**, 2287–2294.
- 43 M. Gamero-Castano and J. Fernandez de la Mora, *J. Mass Spectrom.*, 2000, **35**, 790–803.
- 44 I. G. Loscartales and J. Fernandez de la Mora, *J. Chem. Phys.*, 1995, **103**, 5041–5060.
- 45 M. Gamero-Castano and J. Fernandez de la Mora, *J. Chem. Phys.*, 2000, **113**, 815–832.
- 46 M. L. L. Dole and R. L. Hines, *J. Chem. Phys.*, 1968, **49**, 2240.
- 47 K. A. Douglass, S. Jain, W. R. Brandt and A. R. Venter, *J. Am. Soc. Mass Spectrom.*, 2012, **23**, 1896–1902.
- 48 A. Venter, P. E. Sojka and R. G. Cooks, *Anal. Chem.*, 2006, **78**, 8549–8555.

- 49 S. Muramoto, *Analyst*, 2014, **139**, 5868–5878.
- 50 V. Wu, J. Tillner, E. Jones, J. S. Mckenzie, D. Gurung, A. Mroz, L. Poynter, D. Simon, C. Grau, X. Altafaj, M. E. Dumas, I. Gilmore, J. Bunch and Z. Takats, *Anal. Chem.*, 2022, **94**, 10035–10044.
- 51 A. Wójtowicz and R. Wietecha-Posłuszny, *Appl. Phys. A*, 2019, **125**, 312.
- 52 F. M. Green, P. Stokes, C. Hopley, M. P. Seah, I. S. Gilmore and G. O'Connor, *Anal. Chem.*, 2009, **81**, 2286–2293.
- 53 D. Lostun, C. J. Perez, P. Licence, D. A. Barrett and D. R. Ifa, *Anal. Chem.*, 2015, **87**, 3286–3293.
- 54 N. Talaty, H. Chen and R. G. Cooks, 2005, **77**, 6755–6764.
- 55 M. B. Comasirov and A. G. Marshall, *Chem. Phys. Lett.*, 1974, **25**, 282–283.
- 56 A. G. Marshall, C. L. Hendrickson and G. S. Jackson, *Mass Spectrom. Rev.*, 1998, **17**, 1–35.
- 57 A. G. Marshall and B. Peter, *Anal. Chem.*, 1991, **63**, 215–229.
- 58 A. G. Marshall and F. R. Verdun, *Fourier Transforms in NMR, Optical and Mass Spectrometry*, Elsevier B.V., Amsterdam, 1990.
- 59 K. J. Zemaitis and T. D. Wood, *Rev. Sci. Instrum.*, 2020, **91**, 104102.
- 60 S. Yang, J. Han, Y. Huan, Y. Cui, X. Zhang, H. Chen and H. Gu, *Anal. Chem.*, 2009, **81**, 6070–6079.
- 61 J. Tillner, J. S. Mckenzie, E. A. Jones, A. V. M. Speller, J. L. Walsh, K. A. Veselkov, J. Bunch, Z. Takats and I. S. Gilmore, *Anal. Chem.*, 2016, **88**, 4808–4816.
- 62 C. J. Cooksey, *Biotech. Histochem.*, 2016, **91**, 71–76.
- 63 A. Quye, K. Hallett and C. Herrero Carretero, *Wrought in Gold and Silk: Preserving the Art of Historic Tapestries*, NMS Enterprises Limited, Edinburgh, 2009.
- 64 M. Hacke, PhD Thesis, University of Manchester, 2006.
- 65 E. Steven, J. G. Park, A. Paravastu, E. Branco Lopes, J. S. Brooks, O. Englander, T. Siegrist, P. Kaner and R. G. Alamo, *Sci. Technol. Adv. Mater.*, 2011, **12**, 055002.
- 66 J. Torrenblanca Gonzalez, R. Garcia Ovejero, A. Lozano Murciego, V. Gonzalez and J. F. De Paz, *Sensors*, 2019, **19**, 5145.
- 67 L. Rafaëly, S. Héron, W. Nowik and A. Tchapla, *Dye. Pigment.*, 2008, **77**, 191–203.
- 68 M. R. van Bommel, I. Vanden Berghe, A. M. Wallert, R. Boitelle and J. Wouters, *J. Chromatogr. A*, 2007, **1157**, 260–272.
- 69 A. Timar-Balazsy and D. Eastop, *Chemical principles of textile conservation*, Butterworth-Heinemann, Oxford, 1998.
- 70 Common Background Contamination Ions in Mass Spectrometry, https://beta-static.fishersci.ca/content/dam/fishersci/en_US/documents/programs/scientific/brochures-and-catalogs/posters/fisher-chemical-poster.pdf, accessed December 2022.
- 71 Background Ion List, https://www.waters.com/webassets/cms/support/docs/bkgrnd_ion_mstr_list.pdf,

accessed December 2022.

- 72 C. Mouri and R. Laursen, *Microchim. Acta*, 2012, **179**, 105–113.
- 73 E. S. B. Ferreira, A. N. Hulme, H. McNab and A. Quye, *Chem. Soc. Rev.*, 2004, **33**, 329–336.
- 74 J. H. Hofenk de Graaff, *Colourful Past*, Archetype Books, London, 2007.
- 75 H. Hurst, George, *Dictionary of the coal tar colours*, Heywood and Co Ltd, London, 1892.
- 76 C. J. Cooksey and A. T. Dronsfield, *Biotech. Histochem.*, 2015, **90**, 288–293.
- 77 D. Tamburini, C. M. Shimada and B. McCarthy, *Dye. Pigment.*, 2021, **190**, 109286.
- 78 O. Stolberg-Wernigerode, *Neue deutsche Biographie [New German biography]*, Duncker & Humblot, Berlin, 1985.
- 79 M. De Keijzer and R. Hofmann-De Keijzer, in *Dyes in History and Archaeology 28*, 2009.
- 80 J. C. Barnett, *Stud. Conserv.*, 2007, **52**, 67–77.
- 81 D. F. Duxbury, *Chem. Rev.*, 1993, **93**, 381–433.
- 82 C. G. Kumar, P. Mongolla, J. Joseph and V. U. Maheshwara, *Process Biochem.*, 2012, **47**, 1388–1394.
- 83 F. Sabatini, I. Degano and M. Van Bommel, *Color. Technol.*, 2021, **137**, 456–467.
- 84 D. Confortin, H. Neevel, M. Brustolon, L. Franco, A. J. Kettelarij, R. M. Williams and M. R. Van Bommel, *J. Phys. Conf. Ser.*, 2010, **231**, 012011.
- 85 T. F. G. G. Cova, A. A. C. C. Pais and J. S. Seixas de Melo, *Sci. Rep.*, 2017, **7**, 6806.
- 86 I. Degano, F. Sabatini, C. Braccini and M. P. Colombini, *Dye. Pigment.*, 2019, **160**, 587–596.

Chapter 6 Summary and Future Work

In this thesis, two analytical approaches focussing on minimising the physical impact on the object studied have been developed. A more reproducible high-throughput small-scale sample preparation workflow for UHPLC-PDA(-MS) analysis requiring less sample ($< 0.02 \pm 0.005$ mg) was developed and used for the analysis of a collection of Renaissance embroideries. The dye analysis of the embroideries showed that already by the 17th century, embroidery was a domestic art dependent on global trade. A DESI source was designed, constructed, optimised, and applied to early synthetic dye references and historical samples from 1893. This first successful introduction of DESI-MS into the dye analysis field showed the possibility of ambient mass spectrometry approaches to acquire similar levels of information from textiles as invasive methods, without the requirement of a physical sample.

Future work specifically connected to the studies presented in this thesis could include combining the results presented in Chapter 4 with dye analysis of contemporary English and continental European tapestry and carpet samples to give a needed overview of the textile culture in Scotland and England during the Renaissance. Such thorough studies, with a focus on domestic textile production in Scotland and England have not yet been conducted and it would aid our understanding of the early modern time period. The ability to produce larger datasets using the developed workflow and UHPLC-PDA method in Chapter 3 would facilitate such a study.

The results presented in Chapter 4 also suggest that the dye bath conditions for dyeing with weld could be elucidated in a similar fashion to anthraquinone dye preparations.^{1,2} Such investigations would require dyeing experiments to be conducted at different temperatures and pH values, as well as on different cloth. The effect of the natural environment on the flavonoid ratios would also be interesting to explore, which might require stable isotope mass spectrometry studies similar to ancient diet investigations.³

Chapter 5 presented the construction, optimisation, and application of a DESI source for the analysis of early synthetic dyes. The exploratory nature of the project highlighted the need for a quantifiable method of damage assessment before the method can be applied to museum collections. The spot shape and size obtained from the use of different solvents show that although DESI-MS is non-invasive, it will affect the object on a molecular level.

Future work would also involve optimisation of DESI-MS for natural dyes, particularly mordant dyes. A similar study to tha conducted on rhodamine B, varying geometry parameters, solvent systems and sprayer angles, should be undertaken with focus on a natural dye standard. Investigations into improving the design of the DESI source, such as constructing a sprayer

capillary^{4,5} shown to increase ionisation efficiency could also be of benefit during such a project. The number of synthetic dye structures analysed would also need to be expanded to understand the full possibility of incorporating DESI-MS into the field of dye analysis.

In a broader context, the research presented here highlights the growing interest in developing and introducing more advanced analytical techniques into heritage science. The increased visibility of heritage science as a field seen in recent years, gives a larger financial opportunity to fund instrument development and access to sophisticated instrumentation. Such research will be needed to answer currently inaccessible questions about degradation processes, provenance and species differentiation. For example, the development of two-dimensional liquid chromatography combined with a photodegradation cell make it possible to study photodegradation⁶ in real-time. Similarly innovative, microscale and compound specific radiocarbon research has been developed to date dyestuffs and pigments, helping to contextualise the history of artworks.⁷⁻⁹

However, the main analytical techniques likely to be the focus for research in coming years are sophisticated mass spectrometry techniques, such as the development of the DESI source presented here. Similar studies that are on-going with exciting results, focus on both improving already established methods, such as the development of DART-MS without heat damage,¹⁰ and introducing techniques new to heritage science, such as Direct Infusion-Electrospray Ionisation Mass Spectrometry (DI-ESI-MS)¹¹ and high-resolution MS.¹² A focus on ambient MS techniques can be seen,^{13,14} but also the emergence of MS imaging (MSI) for the study of distribution and degradation products.^{15,16}

A subsection of MS research that is likely to expand in the near future is the use of stable isotope mass spectrometry.^{17,18} Multiple projects currently focus on the application of stable isotope mass spectrometry, targeting questions of provenance,¹⁹ species differentiation²⁰ and manufacturing processes.²¹ Such research will be beneficial for dyestuffs where the chemical fingerprints show little to no source-dependent differences, such as cochineal, indigo and as proposed earlier, weld, giving valuable information on trade routes and availability of raw materials. The development of isotope analysis will hopefully become a staple technique in heritage science similar to its status in archaeology.²² Similarly, the application of proteomics-based methods to heritage objects is likely to grow substantially in the coming years, answering questions about animal breeds in textile fibres,^{23,24} parchment²⁵ and leather.²⁶

Alongside these instrumental developments is a need for a simultaneous focus on computational and chemometric approaches. The development of such methods are likely to increase in popularity as part of the expansion of digital heritage and public access to heritage research.²⁷ For example, introduction of multivariate data analysis, such as principal

component analysis (PCA),^{28,29} and machine learning³⁰ have been used to differentiate cochineal and indigo species. Such studies need access to large, reproducible datasets, which means that research similar to the project presented in Chapter 3 is imperative for the development of computational methods.

The field of heritage science is currently entering an exciting stage, where the increase in interest and realisation of its importance result in greater access to funding opportunities and advanced analytical techniques. Important questions regarding provenance, species differentiation and degradation processes are potentially the main focuses of the field during the current expansion, leading to an increased understanding of objects and collections, and ultimately, our collective heritage.

References

- 1 R. S. Blackburn, *Color. Technol.*, 2017, **133**, 449–462.
- 2 C. Mouri and R. Laursen, *Microchim. Acta*, 2012, **179**, 105–113.
- 3 D. M. Freund and A. D. Hegeman, *Curr. Opin. Biotechnol.*, 2017, **43**, 41–48.
- 4 V. Wu, J. Tillner, E. Jones, J. S. Mckenzie, D. Gurung, A. Mroz, L. Poynter, D. Simon, C. Grau, X. Altafaj, M. E. Dumas, I. Gilmore, J. Bunch and Z. Takats, *Anal. Chem.*, 2022, **94**, 10035–10044.
- 5 J. Tillner, J. S. Mckenzie, E. A. Jones, A. V. M. Speller, J. L. Walsh, K. A. Veselkov, J. Bunch, Z. Takats and I. S. Gilmore, *Anal. Chem.*, 2016, **88**, 4808–4816.
- 6 M. J. Den Uijl, Y. J. H. L. Van Der Wijst, I. Groeneveld, P. J. Schoenmakers, B. W. J. Pirok and M. R. Van Bommel, *Anal. Chem.*, 2022, **94**, 11055–11061.
- 7 L. Hendriks, PhD Thesis, ETH Zurich, 2019.
- 8 L. Hendriks and C. Portmann, *Helv. Chim. Acta*, 2023, **106**, e202200134.
- 9 G. D. Smith, V. J. Chen, A. Holden, N. Haghypour and L. Hendriks, *Herit. Sci.*, 2022, **10**, 0–14.
- 10 G. A. Newsome, I. Kayama and S. A. Brogdon-Grantham, *Anal. Methods*, 2018, **10**, 1038–1045.
- 11 A. Alvarez-Martin, T. P. Cleland, G. M. Kavich, K. Janssens and G. A. Newsome, *Anal. Chem.*, 2019, **91**, 10856–10863.
- 12 A. Alvarez-Martin, G. A. Newsome and K. Janssens, *Anal. Chem.*, 2021, **93**, 14851–14858.
- 13 A. E. Kramell, A. O. Brachmann, R. Kluge, J. Piel and R. Csuk, *RSC Adv.*, 2017, **7**, 12990–12997.
- 14 A. Kramell, F. Porbeck and R. Kluge, *J. Mass Spectrom.*, 2015, **50**, 1039–1043.

- 15 A. E. Kramell, M. García-Altare, M. Pötsch, R. Kluge, A. Rother, G. Hause, C. Hertweck and R. Csuk, *Sci. Rep.*, 2019, **9**, 1–9.
- 16 University of Antwerp, Research Alba Alvarez Martin, <https://www.uantwerpen.be/en/staff/alba-alvarezmartin/research/>, accessed March 2023.
- 17 A. G. Nord and K. Billström, *Herit. Sci.*, 2018, **6**, 1–13.
- 18 E. Geddes da Filicaia, R. Evershed and D. Peggie, *Anal. Chim. Acta*, 2022, **1246**, 340575.
- 19 University of Bristol, Mr Samuel Johns, PhD Candidate, <https://research-information.bris.ac.uk/en/persons/samuel-johns>, accessed March 2023.
- 20 The National Gallery, New research on the history and technology of materials in paintings and other cultural heritage artefacts using the enhanced sensitivity and specificity of advanced mass spectrometry techniques, <https://www.nationalgallery.org.uk/research/research-partnerships/new-research-on-the-history-and-technology-of-materials-in-paintings-and-other-cultural-heritage-artefacts-using-the-enhanced-sensitivity-and-specificity-of-advanced-mass-spectrometry-techn>, accessed March 2023.
- 21 C. Messenger, L. Beck, D. Blamart, P. Richard, T. Germain, K. Batur, V. Gonzalez and E. Foy, *J. Archaeol. Sci. Reports*, 2022, **46**, 103685.
- 22 R. P. Evershed in *Organic Mass Spectrometry in Art and Archaeology*, ed. M. P. Colombini, F. Modugno, John Wiley & Sons, Ltd, Hoboken, 2009, ch. 14, pp. 391–432.
- 23 C. Solazzo, *Conserv. Patrim.*, 2019, **31**, 97–114.
- 24 C. Solazzo, J. M. Dyer, S. Clerens, J. Plowman, E. E. Peacock and M. J. Collins, *Int. Biodeterior. Biodegrad.*, 2013, **80**, 48–59.
- 25 M. D. Teasdale, N. L. van Doorn, S. Fiddymment, C. C. Webb, T. O'Connor, M. Hofreiter, M. J. Collins and D. G. Bradley, *Philos. Trans. R. Soc. B*, 2015, **370**, 20130379.
- 26 C. Solazzo and T. Niepold, *J. Proteomics*, 2023, **274**, 104821.
- 27 Š. Mudička and R. Kapica, *Heritage*, 2022, **6**, 112–131.
- 28 R. Santos, J. Hallett, M. C. Oliveira, M. M. Sousa, J. Sarraguça, M. S. J. Simmonds and M. Nesbitt, *Dye. Pigment.*, 2015, **118**, 129–136.
- 29 A. Serrano, A. van den Doel, M. van Bommel, J. Hallett, I. Joosten and K. J. Van den Berg, *Anal. Chim. Acta*, 2015, **897**, 116–127.
- 30 V. Pauk, J. Michalčáková, K. Jagošová and K. Lemr, *Dye. Pigment.*, 2022, **197**, 109943.

Appendices

Appendix A1 Sample preparation workflow and UHPLC-PDA method specifications

Percentage recoveries of compounds in standard mixture 1

Average percentage recoveries of the filtration step for all tested concentrations (n = 5).

Chromophore	20 µg ml ⁻¹		10 µg ml ⁻¹		5 µg ml ⁻¹		2.5 µg ml ⁻¹		1 µg ml ⁻¹		0.5 µg ml ⁻¹		0.1 µg ml ⁻¹	
	% Recovery	std dev	% Recovery	std dev	% Recovery	std dev	% Recovery	std dev	% Recovery	std dev	% Recovery	std dev	% Recovery	std dev
Fisetin	93.10	4.17	96.08	6.07	96.50	9.47	97.22	8.79	87.83	6.96	99.71	13.04	87.21	17.65
Sulfuretin	94.90	4.37	96.57	6.95	97.29	6.87	100.11	4.57	86.25	7.15	87.74	4.77	103.29	17.33
Luteolin	95.83	5.18	97.76	6.39	97.77	6.42	97.57	6.49	87.39	6.37	90.11	5.93	102.86	13.19
Genistein	94.64	6.40	95.24	6.17	98.93	6.70	101.27	6.71	86.56	6.95	91.64	7.77	106.16	17.38
Apigenin	91.41	8.26	97.63	6.73	98.54	6.80	100.38	7.24	89.40	6.87	89.47	8.16	100.26	14.38
Chrysoeriol	97.67	8.63	96.00	8.85	99.35	7.80	100.09	8.00	87.11	6.58	86.62	6.44	103.50	15.06
Diosmetin	98.14	7.95	98.36	6.86	97.26	6.32	96.93	7.11	85.56	7.26	88.44	3.75	106.66	18.06
Alizarin	92.17	7.90	96.33	5.06	90.08	9.35	89.52	9.87	85.06	8.66	90.67	12.42	79.77	28.38
Prunetin	97.98	12.54	88.77	12.68	108.20	17.08	111.70	17.13	94.48	8.35	92.95	9.97	108.86	19.63

Linearity graphs of compounds in standard mixture 1

Equation and calculated slope error (n = 5) for the Peak Area_{unfiltered} vs Peak Area_{filtered} graphs.

Chromophore	Equation	slope std error (n = 5)
Fisetin	$y = 0.9405x$	0.0140
Sulfuretin	$y = 0.9306x$	0.0193
Luteolin	$y = 0.9449x$	0.0168
Genistein	$y = 0.9452x$	0.0165
Apigenin	$y = 0.9469x$	0.0175
Chrysoeriol	$y = 0.9473x$	0.0224
Diosmetin	$y = 0.9236x$	0.0203
Alizarin	$y = 0.9144x$	0.0171
Prunetin	$y = 0.9998x$	0.0313

(3) : (3)-7-O ratios

(3) : (3)-7-O ratios found for filtered and unfiltered standard mixture 1 with added (3)-7-O.

Run	Filtered sample	Unfiltered sample
1	3.18	3.19
2	3.28	3.18
3	3.39	3.19

Solubility graphs of compounds in standard mixture 1

Average Peak Area of the reconstitution solvents for all chromophores using reconstitution volume of 25 μ l (n = 3)

Chromophore	DMSO		10 % DMSO		MeOH:H ₂ O 1:1 v/v		0.1 % FA		Control	
	Peak Area	std dev	Peak Area	std dev	Peak Area	std dev	Peak Area	std dev	Peak Area	std dev
Fisetin	584956	21910	740851	19413	646132	2321	813981	21781	322012	3870
Sulfuretin	474759	18653	601883	21878	535500	2609	667076	17748	258619	3111
Luteolin	910957	33087	1079223	42854	982944	8686	1237990	34310	478773	6975
Genistein	1760157	49858	2059121	81172	1945549	13517	2416550	63178	924830	12426
Apigenin	649227	25129	591372	7930	497595	12373	618152	15205	302260	9060
Chrysoeriol	789194	30867	595086	914	537781	7445	644735	13489	274915	5522
Diosmetin	821619	31000	1033167	55532	850510	14048	1010157	26199	444557	8377
Alizarin	1391289	51705	1827053	79932	1526886	9881	1920672	51500	747887	6731
Prunetin	1448874	18871	1114907	51880	1061709	6358	1207820	25844	611611	19195

Average Peak Area of the reconstitution solvents for all chromophores using reconstitution volume of 50 μ l (n = 3)

Chromophore	DMSO		10 % DMSO		MeOH:H ₂ O 1:1 v/v		0.1 % FA		Control	
	Peak Area	std dev	Peak Area	std dev	Peak Area	std dev	Peak Area	std dev	Peak Area	std dev
Fisetin	268308	20272	301611	1647	314650	6521	383581	8149	322012	3870
Sulfuretin	234928	3873	254295	832	263701	5004	320314	6207	258619	3111
Luteolin	458603	13610	476975	1417	491980	6924	594654	12891	478773	6975
Genistein	860323	15962	952866	2356	986156	15996	1173186	24731	924830	12426
Apigenin	318031	4897	321043	2818	275524	10245	299474	6020	302260	9060
Chrysoeriol	511751	16059	358602	3640	276197	3468	316876	6894	274915	5522
Diosmetin	288485	4546	439253	1063	441505	5945	504929	11750	444557	8377
Alizarin	706257	13721	737333	1716	766978	13122	927362	18622	747887	6731
Prunetin	735502	23671	645643	11944	544794	10067	604329	14086	611611	19195

Defined noise and calibration curves of compounds in standard mixture 1




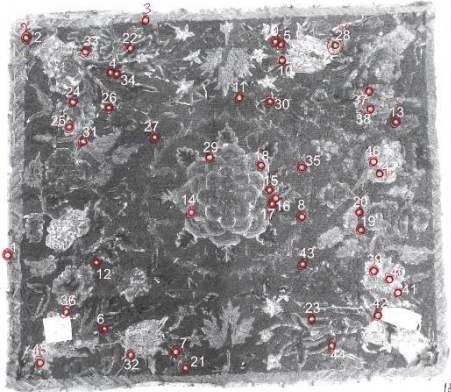
Equation, calculated slope error and R² values of the calibration curves (Peak Height (AU) vs Concentration (µg ml⁻¹), (7 concentrations used, n = 5)

Chromophore	Equation	slope std error	R ² value
Fisetin	y = 0.0143x	3.51E-04	0.9958
Sulfuretin	y = 0.0124x	8.84E-05	0.9997
Luteolin	y = 0.0226x	1.95E-04	0.9995
Genistein	y = 0.0460x	1.71E-04	0.9999
Apigenin	y = 0.0121x	7.60E-04	0.9729
Chrysoeriol	y = 0.0148x	1.06E-03	0.9653
Diosmetin	y = 0.0203x	4.93E-05	0.9999
Alizarin	y = 0.0328x	9.98E-04	0.9935
Prunetin	y = 0.0278x	1.33E-03	0.9842

Average signal (peak height) of retention time ± 0.25 min in blank runs (n = 3) used as noise in LoD and LoQ calculations.

Chromophore	Peak height	std dev
Fisetin	1.25E-03	2.24E-05
Sulfuretin	1.50E-03	4.94E-05
Luteolin	1.46E-03	4.55E-05
Genistein	1.48E-03	4.34E-05
Apigenin	1.61E-03	3.44E-05
Chrysoeriol	1.67E-03	3.64E-05
Diosmetin	1.69E-03	3.70E-05
Alizarin	1.92E-03	9.16E-05
Prunetin	2.29E-03	8.99E-05

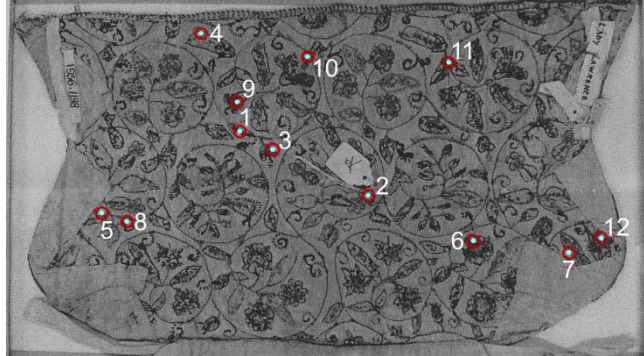


Appendix A2 Sampled objects and sample locations


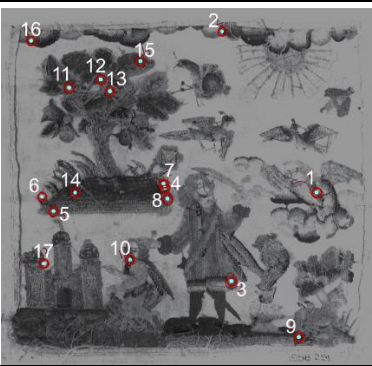


Accession number	Type (age)	Number of samples	Image ©NMS	Sample location
A.1894.125	Stomacher (1650-1700)	3		
A.1894.234	Seat cover (1710-1720)	47		

A.1925.418	Silk purl picture	1		Sample location unknown – sample fallen off
A.1926.168	Book cover (1600-1650)	23		
A.1929.152	Blackwork (c. 1580)	5		

A.1938.580	Blackwork (1550-1600)	3		
A.1938.584 A	Crewel work (c. 1700)	18		
A.1949.220	Book cover	1		Sample location unknown – sample fallen off

A.1949.224	Crewel work (cover) (c. 1700)	17		
A.1955.120	Crewel work (curtain) (1650-1700)	19		 <p data-bbox="1467 1072 1921 1096">Sample 3 locatioin unknown – sample fallen off</p>

A.1956.1198	Woman's coif (Late 1600)	12		
A.1956.1484	Panel (Early 1700)	10		
A.1958.85	Picture (c. 1650)	3		

A. 1958.291	Picture (1650-1700)	17		
A.1960.231	Picture (c. 1650)	10		

<p>A.1962.1067</p>	<p>Stomacher (embroidery c. 1600, stomacher late 1600)</p>	<p>25</p>		
<p>A.1965.722</p>	<p>Woman's coif Prob Italian or French (1568-1600)</p>	<p>16</p>		
<p>A.1989.202</p>	<p>Panel Portuguese (c. 1620)</p>	<p>2</p>		






K.2001.637	Altar frontal Italian, French or English (late 1500- early 1600)	19		
RHB.25.1	Bed valances (1632)	1		



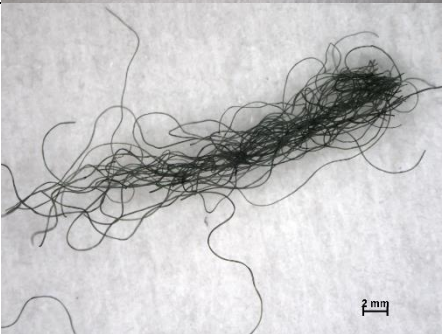


RHB.25.4	Bed valances (1632)	1		Sample locatioin unknown – sample fallen off
RHB.25.5	Bed valances (1632)	3		


RHB.25.6	Bed valances (1632)	3		
RHB.25.7	Bed valances (1632)	3		

RHB.25.9	Bed valances (1632)	4		
RHB.25.10	Bed valances (1632)	4		


Appendix A3 Collected samples and identified dye sources





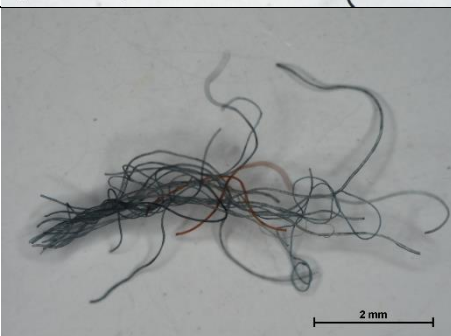
Sample number	Assigned colour	Stereomicroscope image	Identified dyestuff
1894.125 – 1	Yellow		Weld
1894.125 – 2	Dull pink a		Soluble redwood
1894.125 – 3	Metal thread (Ag)		
1894.234 – 1	Orange b		Young fustic, Madder, Soluble redwood
1894.234 – 2	Orange c		Young fustic, Madder, Soluble redwood

1894.234 – 3	Orange a		Weld, Old fustic
1894.234 – 4	Green c		Weld, Indigo
1894.234 – 5	Green b		Weld, Indigo
1894.234 – 6	Green b		Weld, Indigo
1894.234 – 7	Grey green a		Weld, Indigo






1894.234 – 8	Grey green a		Weld, Indigo
1894.234 – 9	Green c		Weld, Indigo
1894.234 – 10	Green a		Weld, Indigo
1894.234 – 11	Green a		Weld, Indigo
1894.234 – 12	Red background		Madder, Soluble redwood


1894.234 – 13	Red background		Madder, Soluble redwood
1894.234 – 14	Brown pink a		Orchil, Madder, Soluble redwood
1894.234 – 15	Brown pink a		Orchil, Madder, Soluble redwood
1894.234 – 16	Pink a		Weld, Cochineal
1894.234 – 17	Pink b		Weld, Cochineal






1894.234 – 18	Pink c		Madder, Cochineal
1894.234 – 19	Pink a		Cochineal
1894.234 – 20	Pink c		Madder, Cochineal
1894.234 – 21	Pink b		Madder, Soluble redwood, Cochineal
1894.234 – 22	Purple b		Indigo, Orchil






1894.234 – 23	Purple c		Indigo, Orchil
1894.234 – 24	Purple a		Orchil
1894.234 – 25	Purple b		Indigo, Orchil
1894.234 – 26	Blue c		Indigo
1894.234 – 27	Blue b		Indigo





1894.234 – 28	Grey		
1894.234 – 29	Undyed		
1894.234 – 30	Yellow		Weld
1894.234 – 31	Yellow		Weld
1894.234 – 32	Grey a		






1894.234 – 33	Grey b		
1894.234 – 34	Olive green		Young fustic, Saxon blue
1894.234 – 35	Brown b		Old fustic
1894.234 – 36	Peach		Tannins
1894.234 – 37	Grey brown b		






1894.234 – 38	Grey brown c		
1894.234 – 39	Sea green a		
1894.234 – 40	Sea green b		
1894.234 – 41	Sea green b		
1894.234 – 42	Green c		Weld





1894.234 – 43	Blue a		Indigo
1894.234 – 44	Purple c		Indigo, Soluble redwood
1894.234 – 45	Yellow		Weld
1894.234 – 46	Orange b		Weld, Young fustic, Soluble redwood
1894.234 – 47	Orange c		Weld, Young fustic, Soluble redwood






1925.418 – 1	Silk purl		
1926.168 – 1	Green		Weld, Indigo
1926.168 – 2	Acid green		Weld, Indigo
1926.168 – 3	Green		Weld, Indigo
1926.168 – 4	Green		Weld, Indigo






1926.168 – 5	Pink		Tannins, Weld, Soluble redwood
1926.168 – 6	Dark pink		Soluble redwood
1926.168 – 7	Mid pink		Old fustic, Madder
1926.168 – 8	Mid pink		Soluble redwood
1926.168 – 9	Light pink		Soluble redwood






1926.168 – 10	Pink		tannins
1926.168 – 11	Yellow		Weld
1926.168 – 12	Yellow		Weld
1926.168 – 13	Blue c		Indigo
1926.168 – 14	Pink c, Blue c		Indigo, Soluble redwood






1926.168 – 15	Pink a, Blue b		Indigo, Soluble redwood
1926.168 – 16	Light brown		Young fustic
1926.168 – 17	Light brown		Young fustic
1926.168 – 18	Blue c		Weld, Indigo
1926.168 – 19	Pink c, Blue c		Indigo






1926.168 – 20	Acid green		Weld, Indigo
1926.168 – 21	Dark green		Weld, Indigo
1926.168 – 22	Dark green		Weld, Indigo
1926.168 – 23	Dark green		Weld, Indigo
1929.152 – 1	Metal thread		






1929.152 – 2	Metal thread		
1929.152 – 3	Black		Tannins
1929.152 – 4	Black		Tannins
1929.152 – 5	Black		Tannins
1938.580 – 1	Dark brown		Old fustic






1938.580 – 2	Dark brown		Old fustic
1938.580 – 3	Dark brown		Old fustic
1938.584 A – 1	Green a		Weld, Indigo
1938.584 A – 2	Green a		Weld, Indigo
1938.584 A – 3	Green b		Weld, Indigo




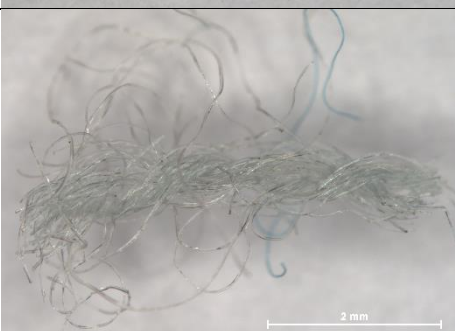

1938.584 A – 4	Green c		Weld, Indigo
1938.584 A – 5	Green c		Weld, Indigo
1938.584 A – 6	Green d		Weld, Indigo
1938.584 A – 7	Green d		Weld, Indigo
1938.584 A – 8	Green e		Weld, Indigo






1938.584 A – 9	Green e		Weld, Indigo
1938.584 A – 10	Yellow		Weld
1938.584 A – 11	Yellow		Weld
1938.584 A – 12	Brown b		Weld, Madder
1938.584 A – 13	Brown b		Weld, Madder






1938.584 A – 14	Brown c		Weld, Indigo, Madder
1938.584 A – 15	Brown c		Weld, Indigo, Madder
1938.584 A – 16	Brown c		Weld, Indigo, Tannins
1938.584 A – 17	Brown d		Weld, Tannins
1938.584 A – 18	Brown d		Weld, Tannins






1949.220 – 1	Metal sequin		
1949.224 – 1	Red c		Madder
1949.224 – 2	Red d		Weld, Indigo
1949.224 – 3	Green b		Weld, Indigo
1949.224 – 4	Green c		Weld, Indigo






1949.224 – 5	Green a		Weld, Indigo
1949.224 – 6	Green d		Weld
1949.224 – 7	Yellow a		Weld
1949.224 – 8	Yellow b		Weld
1949.224 – 9	Blue c		Weld, Tannins






1949.224 – 10	Brown c		Madder, Tannins
1949.224 – 11	Brown a		Madder
1949.224 – 12	Blue b		Indigo
1949.224 – 13	Blue a		Indigo
1949.224 – 14	Red a		Cochineal






1949.224 – 15	Red b		Cochineal
1949.224 – 16	Red e		Madder, Tannins
1949.224 – 17	Green b		Weld, Indigo
1955.120 – 1	Brown a		Madder
1955.120 – 2	Green b		Weld, Indigo

1955.120 – 3	Brown e		
1955.120 – 4	Brown a		Weld, Madder
1955.120 – 5	Brown c		Weld, Madder
1955.120 – 6	Green c		Weld, Indigo
1955.120 – 7	Green b		Weld, Indigo





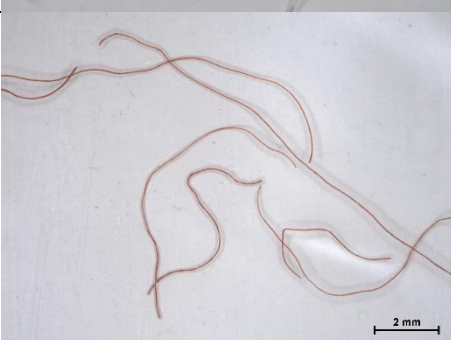
1955.120 – 8	Brown a		Madder
1955.120 – 9	Green a		Weld, Indigo
1955.120 – 10	Blue green b		Weld, Indigo
1955.120 – 11	Green c		Weld, Indigo
1955.120 – 12	Blue green a		Weld, Indigo






1955.120 – 13	Red d		Madder, Cochineal
1955.120 – 14	Brown e		Weld, Soluble redwood
1955.120 – 15	Brown b		Madder
1955.120 – 16	Blue green a		Weld, Indigo
1955.120 – 17	Blue green c		Weld, Indigo






1955.120 – 18	Red d		Weld, Indigo, Madder, Cochineal
1955.120 – 19	Yellow b		Weld
1956.1198 – 1	Red		Cochineal
1956.1198 – 2	Red		Cochineal
1956.1198 – 3	Dark green		Weld, Indigo






1956.1198 – 4	Yellow		Weld
1956.1198 – 5	Au metal core		
1956.1198 – 6	Au metal core		
1956.1198 – 7	Au metal core		
1956.1198 – 8	Au metal thread		






1956.1198 – 9	Dark pink		
1956.1198 – 10	Light green		Weld, Indigo
1956.1198 – 11	Light brown		Young fustic
1956.1198 – 12	Ag metal thread		
1956.1484 – 1	Dark green		Weld, Indigo




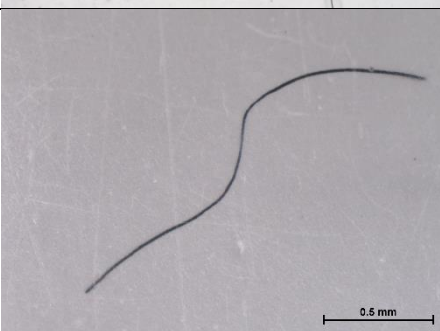

1956.1484 – 2	Dark green		Weld, Indigo
1956.1484 – 3	Yellow		Weld
1956.1484 – 4	Fluorescent pink		Cochineal
1956.1484 – 5	Light pink		Cochineal
1956.1484 – 6	Dark pink		Madder, Soluble redwood






1956.1484 – 7	Brown		Young fustic, Old fustic, Madder, Soluble redwood
1956.1484 – 8	Brown		Old fustic, Madder, Soluble redwood
1956.1484 – 9	Dark brown		Madder
1956.1484 – 10	Purple		Orchil
1958.85 – 1	Red		Madder, Cochineal

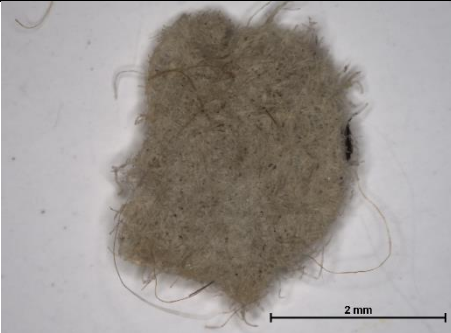


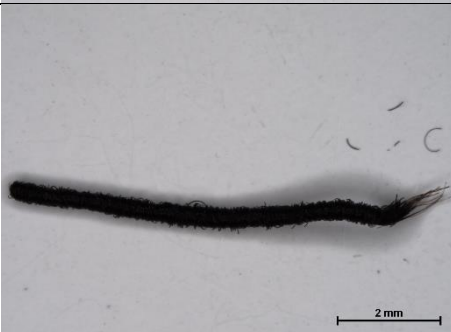

1958.85 – 2	Red		Madder, Cochineal
1958.85 – 3	Red		Madder, Cochineal
1958.291 – 1	Dark pink		Cochineal
1958.291 – 2	Purply pink c		Lichen
1958.291 – 3	Purply pink b		Lichen






1958.291 – 4	Yellow		Weld
1958.291 – 5	Acid green a		Weld, Indigo
1958.291 – 6	Acid green b		Weld, Indigo
1958.291 – 7	Acid green c		Weld, Indigo
1958.291 – 8	Acid green d		Weld, Indigo

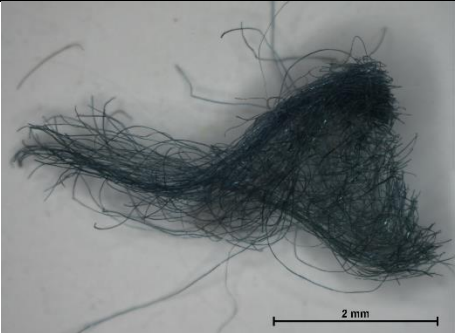




1958.291 – 9	Sea green b		Weld, Indigo
1958.291 – 10	Light pink		
1958.291 – 11	Brown a		Weld
1958.291 – 12	Unidentified object?		
1958.291 – 13	Brown a		Weld






1958.291 – 14	Yellow		Weld
1958.291 – 15	Olive green		
1958.291 – 16	Greyish blue a		Indigo
1958.291 – 17	Bright blue c		
1960.231 – 1	Pink b		Madder, Tannins


1960.231 – 2	Pink b		Madder, Tannins
1960.231 – 3	Mid green		Weld, Indigo
1960.231 – 4	Mid brown		Young fustic
1960.231 – 5	Light brown		Madder
1960.231 – 6	Mid brown		Old fustic, Madder



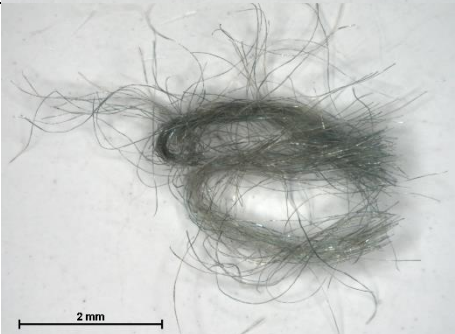
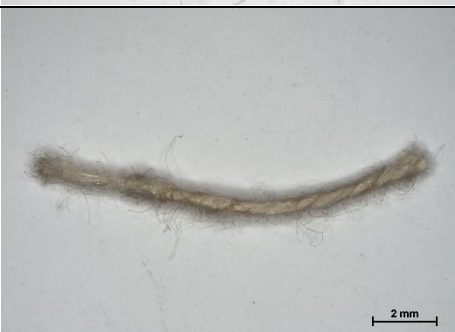
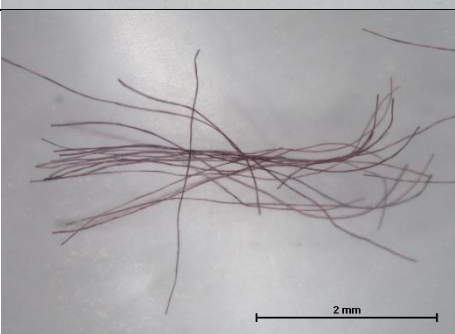
1960.231 – 7	Paper		
1960.231 – 8	Light brown		
1960.231 – 9	Dark brown		Tannins
1960.231 – 10	Dark brown		Tannins
1962.1067 – 1	Au metal thread		



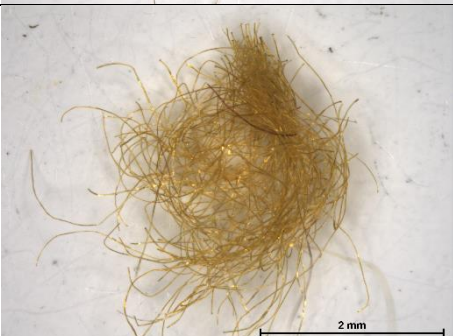
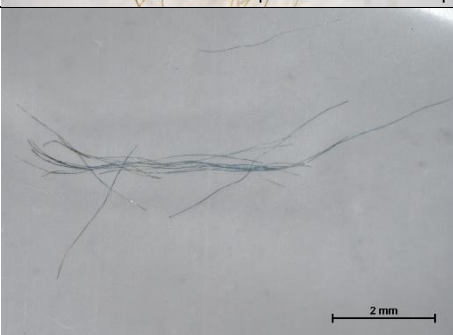
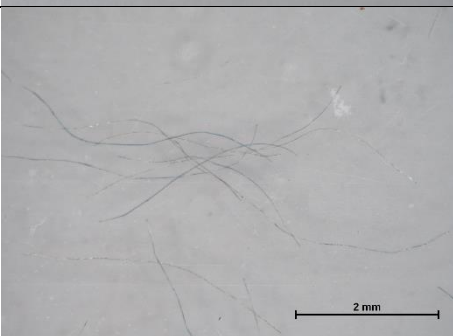
1962.1067 – 2	Ag metal thread		
1962.1067 – 3	Light brown		Young fustic, Madder
1962.1067 – 4	Green c		Weld, Indigo
1962.1067 – 5	Green c		Weld, Indigo
1962.1067 – 6	Green b		Weld, Indigo

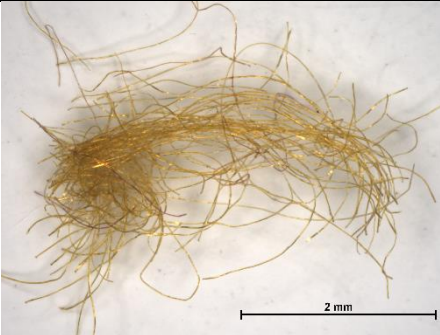
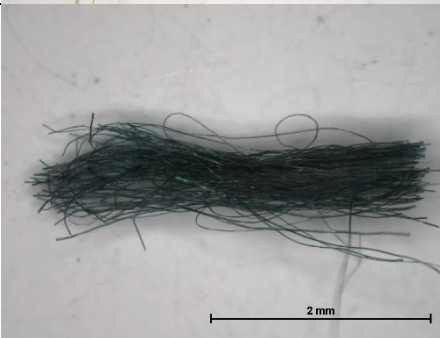
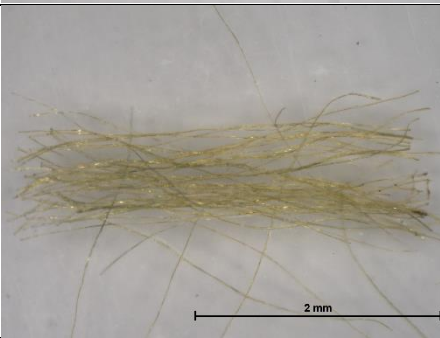


1962.1067 – 7	Green d		Weld, Indigo
1962.1067 – 8	Green d		Weld, Indigo
1962.1067 – 9	Green b		Weld, Indigo
1962.1067 – 10	Green a		Weld, Indigo
1962.1067 – 11	Green a		Weld, Indigo



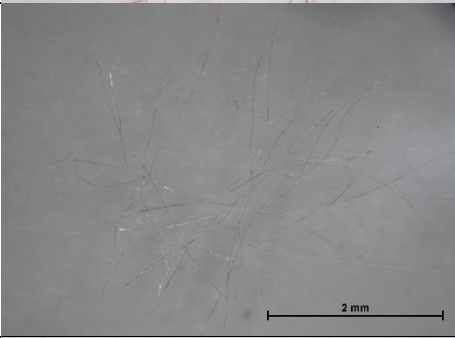


1962.1067 – 12	Yellow		Weld
1962.1067 – 13	Yellow		Weld
1962.1067 – 14	Pink e		Madder, Cochineal
1962.1067 – 15	Pink e		Cochineal
1962.1067 – 16	Pink d		Madder, Cochineal






1962.1067 – 17	Pink d		Cochineal
1962.1067 – 18	Pink c		Safflower
1962.1067 – 19	Pink c		
1962.1067 – 20	Grey		
1962.1067 – 21	Blue b		Indigo

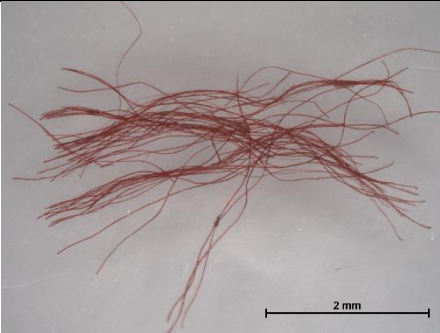



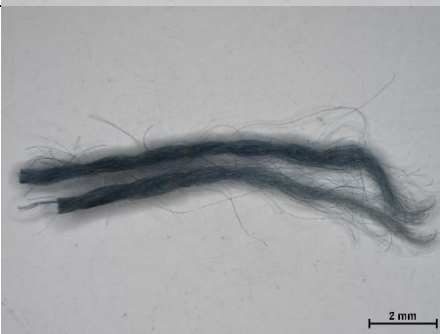
1962.1067 – 22	Sea green b		Indigo
1962.1067 – 23	Sea green a		
1962.1067 – 24	Sea green b		Indigo
1962.1067 – 25	Sequin thread (undyed)		
1965.722 – 1	Purple		Indigo, Cochineal

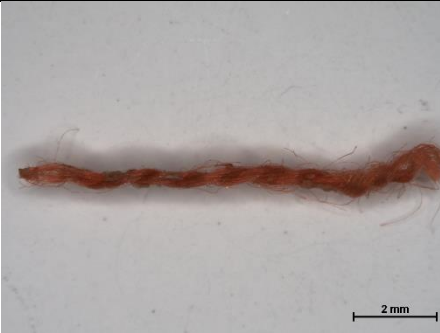




1965.722 – 2	Purple		Indigo, Cochineal
1965.722 – 3	Olive green		Weld, Indigo
1965.722 – 4	Yellow		Weld
1965.722 – 5	Light blue		Indigo
1965.722 – 6	Light blue		Indigo





1965.722 – 7	Yellow		Weld
1965.722 – 8	Dark green		Weld, Indigo
1965.722 – 9	Light green		Weld, Indigo
1965.722 – 10	Purple		Indigo, Cochineal
1965.722 – 11	Dark pink		Madder, Cochineal






1965.722 – 12	Light pink		
1965.722 – 13	Mid pink		Cochineal, Safflower
1965.722 – 14	Lightest pink		Cochineal
1965.722 – 15	Mid green		Weld, Indigo
1965.722 – 16	Yellow		Weld






1989.202 – 1	Green		Weld, Indigo
K.2001.637 – 1	Blue		Indigo
K.2001.637 – 2	Red velvet		Cochineal
K.2001.637 – 3	Green velvet		Weld, Indigo
K.2001.637 – 4	Green velvet		Weld, Indigo





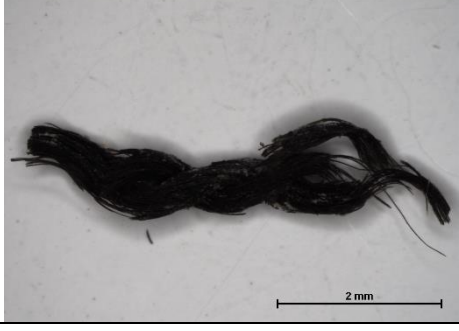
K.2001.637 – 5	Red velvet		Cochineal
K.2001.637 – 6	Acid green		Weld, Indigo
K.2001.637 – 7	Ag metal thread		
K.2001.637 – 8	Ag metal thread		
K.2001.637 – 9	Blue		Indigo



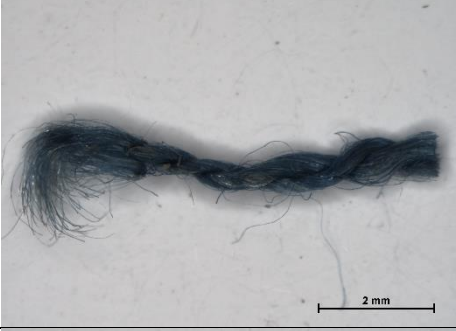


K.2001.637 – 10	Orange		Safflower
K.2001.637 – 11	Orange 2		Safflower
K.2001.637 – 12	Acid green 2		Weld, Indigo
K.2001.637 – 13	Au metal thread		
K.2001.637 – 14	Dark brown		Tannins

K.2001.637 – 15	Peach		Soluble redwood
K.2001.637 – 16	Dark brown		Weld, Young fustic
K.2001.637 – 17	Peach		Soluble redwood
K.2001.637 – 18	Undyed thread		
K.2001.637 – 19	Green velvet		Weld, Indigo

K.2001.637 – 20	Red velvet		Cochineal
RHB.25.1 – 1	Yellow		Weld
RHB.25.4 – 1	Blue		Indigo
RHB.25.5 – 1	Red		Orchil, Cochineal
RHB.25.5 – 2	Green		Weld, Indigo

RHB.25.5 – 3	Beige		Weld, Young fustic
RHB.25.6 – 1	Yellow		Weld
RHB.25.6 – 2	Pink		Soluble redwood, Tannins
RHB.25.6 – 3	Brownish pink		Young fustic
RHB.25.7 – 1	Green		Weld, Indigo

RHB.25.7 – 2	Pink		Soluble redwood
RHB.25.7 – 3	Blue		Indigo
RHB.25.9 – 1	Pink		Soluble redwood, Tannins
RHB.25.9 – 2	Blue		Indigo
RHB.25.9 – 3	Black		Tannins

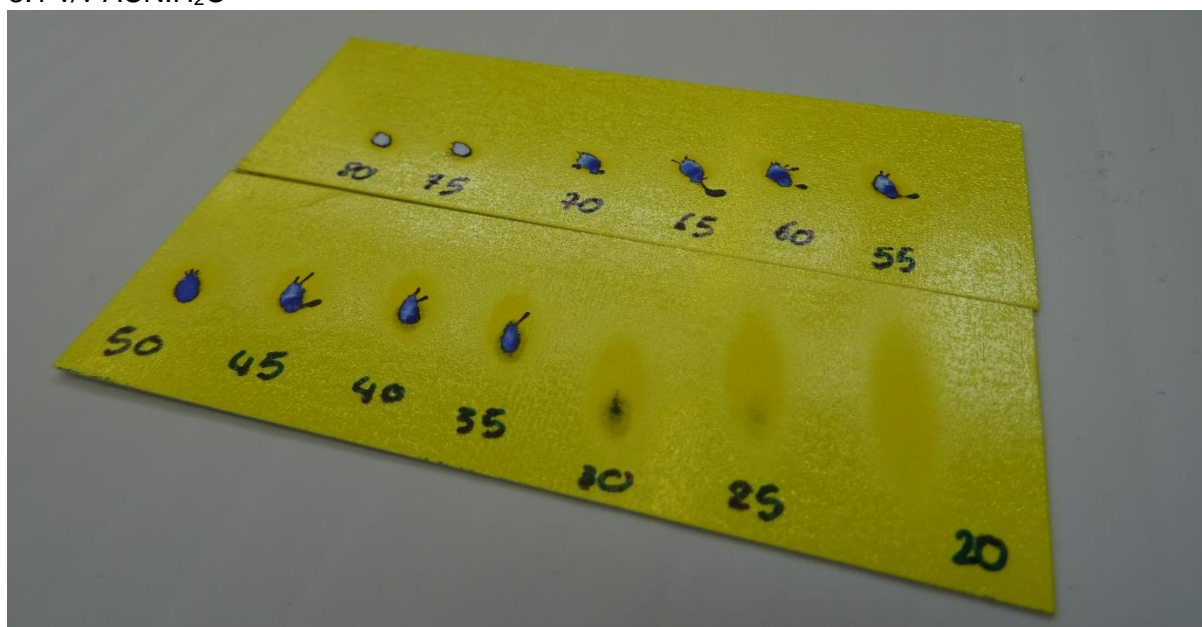
RHB.25.9 – 4	Blue		Indigo
RHB.25.10 – 1	Dark blue		Indigo
RHB.25.10 – 2	Dark blue		Indigo
RHB.25.10 – 3	Orange pink		Young fustic, Soluble redwood
RHB.25.10 – 4	Orange pink		Young fustic, Soluble redwood

Appendix A4 DESI-MS solvent spot and shape of tested solvent systems

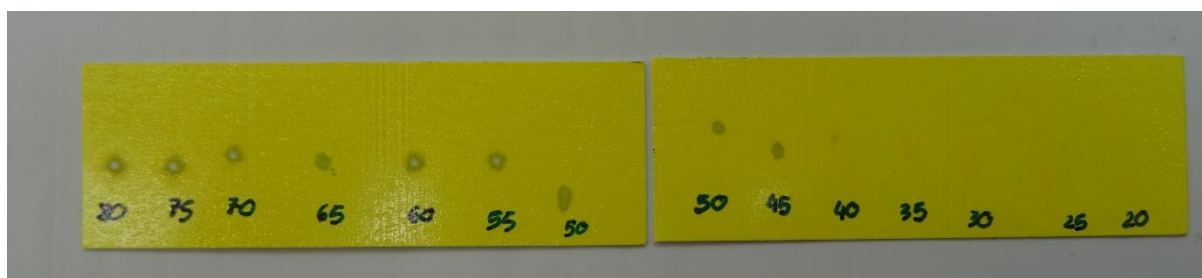
3:1 v/v MeOH:H₂O



3:1 v/v ACN:H₂O



ACN

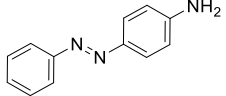
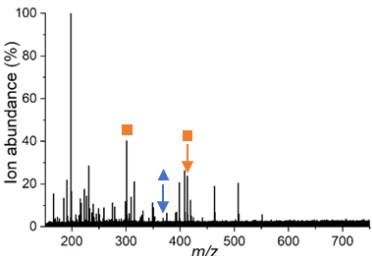
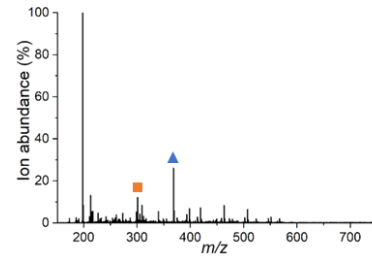
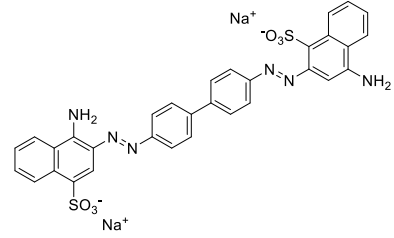
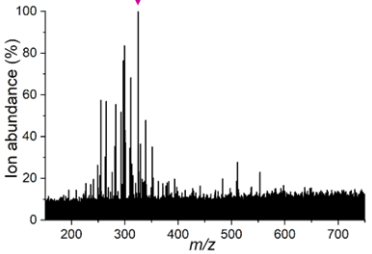
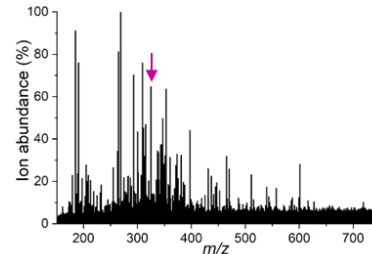
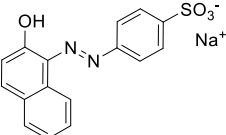
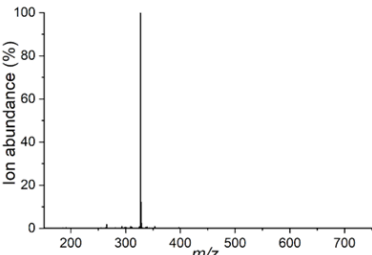
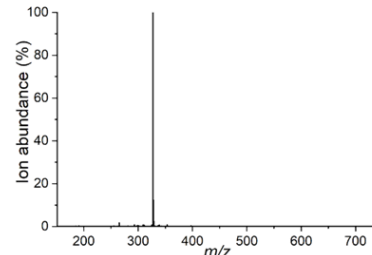
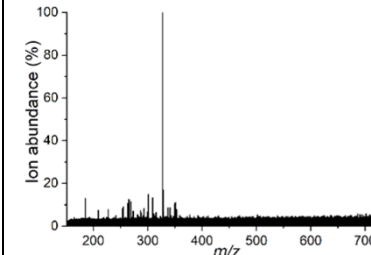


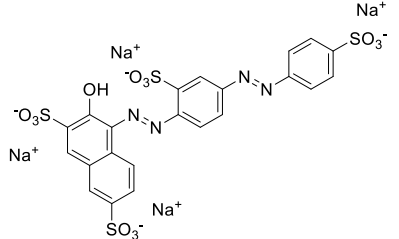
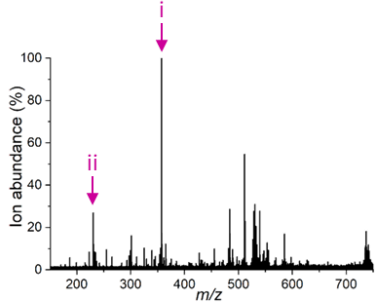
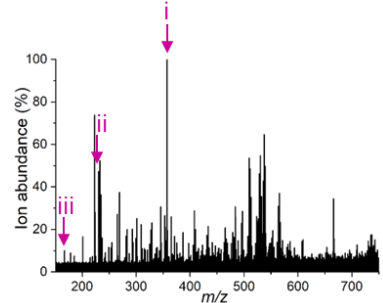
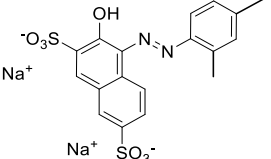
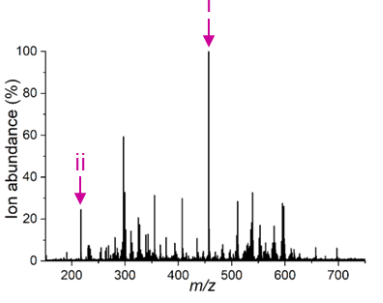
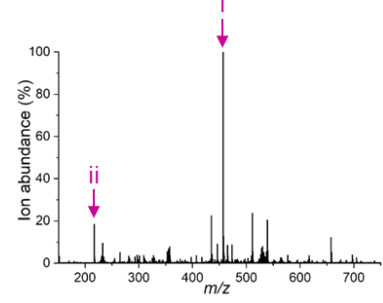
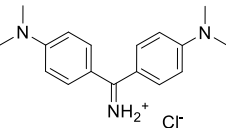
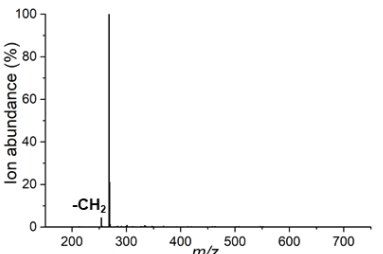
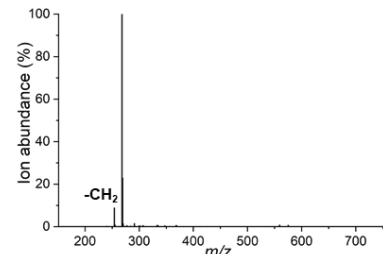
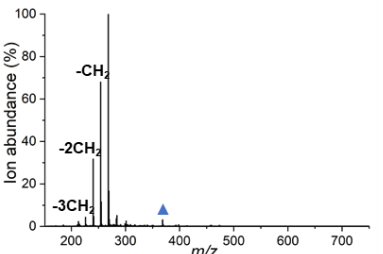
MeOH



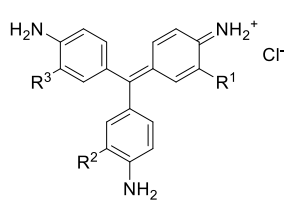
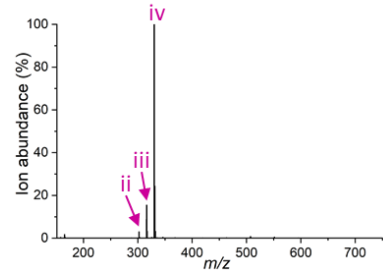
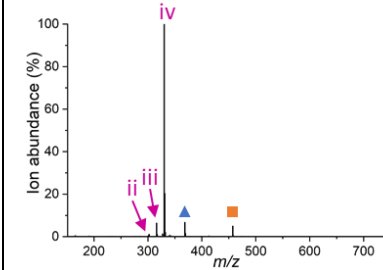
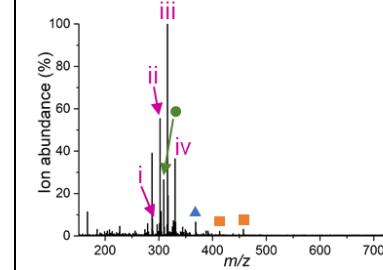
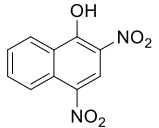
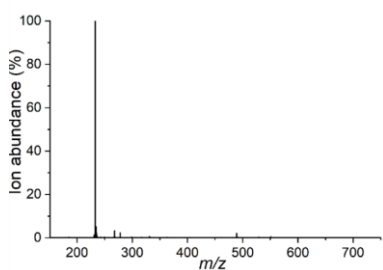
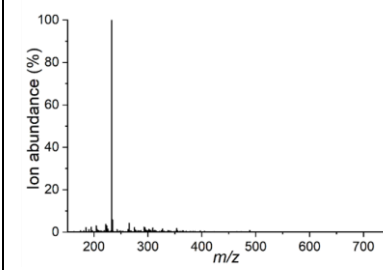
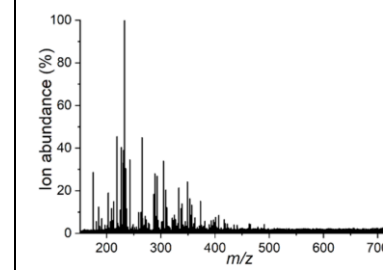
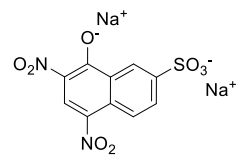
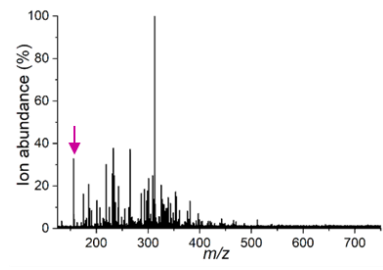
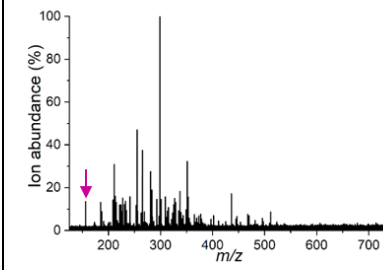

Appendix A5 DESI-MS spectra of early synthetic and historical dyes

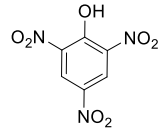
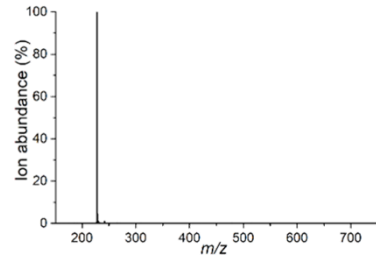
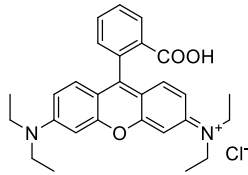
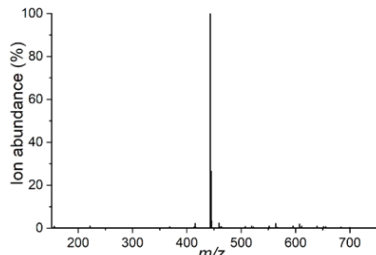
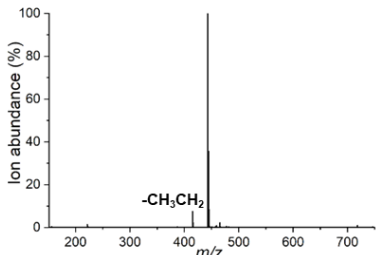
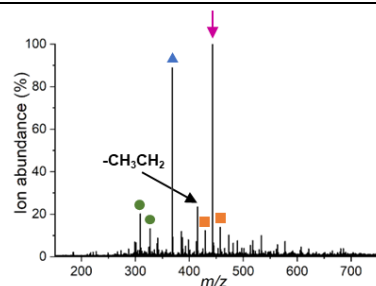
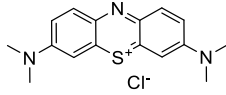
Marked with a blue triangle is m/z 368.43 (BTAC-228), green circle is m/z 309.21 (PPG) and m/z 327.18 (PEG). An orange square marks phthalates at m/z 301.07, 413.26, 429.24, 457.27.

Compound (CI number) Family	Structure	M_{mi} (g mol^{-1})	Characteristic ion	DESI-MS spectrum Silk	DESI-MS spectrum Wool	DESI-MS spectrum Lehne sample
Aniline Yellow (CI 11000) Azo		197.10	m/z 198.10 [M+H] ⁺			
Congo Red (CI 22120) Azo		696.08	m/z 325.18 [M-Na] ²⁻			
Orange II Na salt (CI 15510) Azo		350.03	m/z 327.04 [M-Na]			

Compound (CI number) Family	Structure	M _{mi} (g mol ⁻¹)	Characteristic ion	DESI-MS spectrum Silk	DESI-MS spectrum Wool	DESI-MS spectrum Lehne sample
Ponceau S (CI 27195) Azo		759.89	(i) <i>m/z</i> 166.98 [M-4Na] ⁴⁺ (ii) <i>m/z</i> 230.31 [M-3Na] ³⁺ (iii) <i>m/z</i> 356.96 [M-2Na] ²⁺			
Xylidine Ponceau (Ponceau 2R) (CI 16150) Azo		480.00	(i) <i>m/z</i> 217.01 [M-2Na] ²⁺ (ii) <i>m/z</i> 457.02 [M-Na] ⁻			
Auramine O (CI 41000) Diphenyl- methane		303.15	<i>m/z</i> 268.18 [M-Cl] ⁺			

Compound (CI number) Family	Structure	M_{mi} (g mol ⁻¹)	Characteristic ion	DESI-MS spectrum Silk	DESI-MS spectrum Wool	DESI-MS spectrum Lehne sample
Brilliant Green (CI 42040) Triphenylmethane		420.23	m/z 385.27 [M-Cl] ⁺			
Malachite Green (CI 42000) Triphenylmethane		364.17	m/z 329.20 [M-Cl] ⁺			
Methyl Violet (CI 42535) Triphenylmethane	 (i) R ¹ = H, R ² = H, R ³ = H (ii) R ¹ = H, R ² = CH ₃ , R ³ = H (iii) R ¹ = H, R ² = CH ₃ , R ³ = CH ₃ (iv) R ¹ = CH ₃ , R ² = CH ₃ , R ³ = CH ₃	(i) 365.17 (ii) 379.19 (iii) 393.20 (iv) 407.22	(i) m/z 330.20 [M-Cl] ⁺ (ii) m/z 344.22 [M-Cl] ⁺ (iii) m/z 358.23 [M-Cl] ⁺ (iv) m/z 372.25 [M-Cl] ⁺			

Compound (CI number) Family	Structure	M _{mi} (g mol ⁻¹)	Characteristic ion	DESI-MS spectrum Silk	DESI-MS spectrum5 Wool	DESI-MS spectrum Lehne sample
Basic fuchsin (CI 42510) Triphenylmethane	 <p>(i) R¹ = H, R² = H, R³ = H (ii) R¹ = H, R² = CH₃, R³ = H (iii) R¹ = H, R² = CH₃, R³ = CH₃ (iv) R¹ = CH₃, R² = CH₃, R³ = CH₃</p>	(i) 323.12 (ii) 337.14 (iii) 351.15 (iv) 365.17	(i) <i>m/z</i> 288.15 [M-Cl] ⁺ (ii) <i>m/z</i> 302.17 [M-Cl] ⁺ (iii) <i>m/z</i> 316.18 [M-Cl] ⁺ (iv) <i>m/z</i> 330.20 [M-Cl] ⁺			
Martius yellow (CI 10315) Nitro		234.03	<i>m/z</i> 233.02 [M-Na] ⁻			
Naphthol Yellow S (CI 10316) Nitro		357.95	<i>m/z</i> 155.98 [M-2Na] ²⁻			

Compound (CI number) Family	Structure	M_{mi} (g mol ⁻¹)	Characteristic ion	DESI-MS spectrum Silk	DESI-MS spectrum Wool	DESI-MS spectrum Lehne sample
Picric acid (CI 10305) Nitro		229.00	m/z 227.99 [M-H] ⁻			
Rhodamine B (CI 45170) Xanthene		478.20	m/z 443.23 [M-Cl] ⁺			
Methylene Blue (CI 52015) Thiazine		319.09	m/z 284.12 [M-Cl] ⁺	